



HAL
open science

Decarbonizing energy consumption in the residential sector in France in the context of climate change

Qiqi Tao

► **To cite this version:**

Qiqi Tao. Decarbonizing energy consumption in the residential sector in France in the context of climate change. Engineering Sciences [physics]. Institut Polytechnique de Paris, 2024. English. NNT : 2024IPPAX034 . tel-04861184

HAL Id: tel-04861184

<https://theses.hal.science/tel-04861184v1>

Submitted on 2 Jan 2025

HAL is a multi-disciplinary open access archive for the deposit and dissemination of scientific research documents, whether they are published or not. The documents may come from teaching and research institutions in France or abroad, or from public or private research centers.

L'archive ouverte pluridisciplinaire **HAL**, est destinée au dépôt et à la diffusion de documents scientifiques de niveau recherche, publiés ou non, émanant des établissements d'enseignement et de recherche français ou étrangers, des laboratoires publics ou privés.



INSTITUT
POLYTECHNIQUE
DE PARIS

NNT : 2024IPPAX034

Thèse de doctorat



Decarbonizing energy consumption in the residential sector in France in the context of climate change

Thèse de doctorat de l'Institut Polytechnique de Paris
préparée à École Polytechnique

École doctorale n°626 Dénomination (EDIPP)
Spécialité de doctorat : Sciences et technologies industrielles

Thèse présentée et soutenue à Palaiseau, le 04/06/2024, par

QIQI TAO

Composition du Jury :

Patricia CRIFO Professeure, École Polytechnique (CREST)	Présidente
Louis-Gaëtan GIRAUDET HDR, École des Ponts ParisTech (CIRED)	Rapporteur
Jairo CUGLIARI HDR, Université Lumière 2 (ERIC)	Rapporteur
Roberta QUADRELLI Cadre scientifique, IEA	Examinatrice
Victor HOMAR Professeur, Université des Baléares (Meteorology Group, Physics Department)	Examineur
Anne MIGAN-DUBOIS Professeure, Centrale Supélec (GeePs)	Examinatrice
Philippe DROBINSKI Directeur de recherche, École polytechnique (LMD)	Directeur de thèse
Alexis TANTET Professeur assistant, École polytechnique (LMD)	Co-encadrant de thèse
Marc STEFANON Head of Data Product, NamR	Invité

Dedicated to my grandparents, Guobin Li and Qiuying Jiang, and my mother, Yun Li.

Acknowledgements

I would like to thank many people who helped me to complete my Ph.D. thesis during these four years. First of all, I would like to thank my supervisors, Philippe Drobinski and Alexis Tantet. Philippe, thank you for always being available despite your busy schedule as lab director and director of the E4C center. Thank you for always being interested in my research topics and results, even if it was not your area of expertise. Every time we had discussions, the ideas you suggested were always insightful. Your strong curiosity in different research areas and your competence in presenting the research to different audiences inspire me greatly. I can never become the same person as you, but you are the idol of my future path. Alexis, thank you for always helping me with my technical and scientific problems. I am not a good math student, but you were patient and systematically introduced me to the mathematical tools while sincerely wishing me to master them. You taught me that mathematical rigor is very important for all kinds of research, especially for the statistical problems I worked on. I will always remember this for my future work. Both of you patiently guided me from beginning to end, whether it was writing or oral presentation. Philippe taught me how to tell a good story to connect different results, while Alexis helped me build the competence to present the methodology clearly and scientifically. You both showed me the academic rigor of interpreting the results and the importance of conveying the key messages. Without the support of both of you, it would not have been possible to complete this thesis. I must thank Jordi Badosa and Sylvain Cros for their contributions and expertise in the PV field, which greatly expanded the scope of this study. I also would like to thank Marie Naveau, the second author of my first article, for building the original code for the model. The old Chinese saying goes, "One generation plants the trees, and the next enjoys the shade." Thanks to your dedication and help, my internship and early Ph.D. studies went smoothly.

I would also like to thank my thesis committee members, Vincent Vigi   and Hiba Omrani, who gave me valuable advice during the mini-defenses. Thank you, Louis-Gaetan Giraudet and Jairo Gugliari, for your valuable comments and constructive criticism, which greatly improved the quality of this thesis. I am honored to have you as my thesis reviewers. I would also like to thank Patricia Crifo, Roberta Quadrelli, Victor Homar, and Anne Migan-Dubois for being my jury members. The discussion during the defense was interesting and valuable for my future work.

More generally, I would like to thank all the faculty, staff, graduate students, and postdocs

at LMD who have made these years very enjoyable. Thank you to all the young researchers and engineers for the nice moments we spent together at lunch and around the Wednesday cakes. Thanks to my co-office Samouro Dansokho, Julie Collignan, and Joan Delort Ylla for our time together. And thanks to Maryam Kadkhodaei and Moira Itzel Torres for the multicultural discussions. Thank you to Douglas Keller for sharing the time of MEC101 with me, and thank you to Assia Arouf, Milena Corcos, and other senior doctors for sharing your experiences to help us debut. I would also like to thank Xiaofei Ju and Silin Fu for our time together at traditional Chinese festivals. Thank you to the INTRO group for the monthly meeting. I had the chance to practice my presentation while learning what and how other researchers from different domains work. Thank you to CIRED for the opportunity to present my work and for the questions that people working in the same field have. I thank my closest friends, Yifan Wei, Xiaoxi Zhao, Chunyang Xu, Siying Jiang, and Céline Gault, for their companionship and emotional support. Finally, I thank my grandparents, Guobin Li and Qiuying Jiang, and my mother, Yun Li, for their unconditional support. I thank my boyfriend, Xinyuan Zhai, for his constant companionship, support, and interesting scientific discussions. I would also like to thank my two cats, Sunny and Sven, for helping me relieve stress and maintain my mental health.

Résumé en français

Le secteur résidentiel est important pour la transition énergétique visant à lutter contre le réchauffement climatique. En raison de la variabilité géographique des facteurs socio-économiques, la consommation d'électricité du secteur résidentiel (REC pour Residential Electricity Consumption), très dépendante, doit être étudiée localement. La première partie de cette étude vise à projeter les futures REC françaises, en considérant les scénarios de changement climatique et de climatisation (AC) et en quantifiant leur variabilité spatiale. Pour ce faire, un modèle linéaire de sensibilité à la température adapté aux données annuelles de consommation d'électricité observées et à la température historique est appliqué à l'échelle intrarégionale. Les futures REC sensibles à la température sont calculées en utilisant le modèle pour les projections de température dans le cadre du changement climatique RCP8.5. Trois scénarios de climatisation sont envisagés : (1) un scénario de taux de climatisation de 100% supposant que toute région partiellement équipée de systèmes de climatisation aujourd'hui verra tous ses ménages équipés de climatisation, mais que la sensibilité locale à la température ne progressera plus ; (2) un scénario de diffusion progressive imitant le comportement « faire comme mon voisin » ; (3) une combinaison des deux scénarios. L'augmentation des températures entraîne une diminution globale des REC (-8 TWh d'ici 2040 et jusqu'à -20 TWh d'ici 2100) avec une variabilité spatiale significative. L'évolution des REC est modulée par l'évolution des besoins de refroidissement et le déploiement des systèmes de climatisation pour répondre à ces besoins. Dans les deux premiers scénarios AC, la diminution des REC due au changement climatique pourrait être compensée dans le sud de la France, qui afficherait alors une augmentation des REC. Lorsque les deux scénarios CA sont combinés, une augmentation des REC pourrait être observée dans l'ensemble du pays. Le scénario AC le plus extrême montre une augmentation potentielle des REC due à l'utilisation de l'AC de 2% d'ici 2040 et de 32% d'ici 2100.

Nous voulons décarboniser le secteur résidentiel une fois que nous aurons finalisé la projection de la consommation d'électricité résidentielle. Deux axes principaux sont étudiés : le premier vise à étudier la performance des rénovations. Pour ce faire, un modèle linéaire modifié de sensibilité à la température basé sur l'étude précédente est utilisé en incluant les variables des âges de construction de sorte que la consommation sensible à la température par groupes de périodes de construction est estimée pour chaque région administrative. Ces consommations sensibles à la température estimées sur la base de la consommation réelle sont dominées par le chauffage et peuvent être comparées à la consommation théorique de chauffage calculée par le calcul standard

du certificat de performance énergétique (EPC). La comparaison fait apparaître une nette différence ; cette différence entre la consommation réelle et la consommation conventionnelle est également connue sous le nom d'écart de performance énergétique. La France a introduit sa première réglementation en matière de performance thermique en 1974 (RT1974), dans le but de réduire la consommation d'énergie de 25% par rapport aux logements anciens. Elle a été suivie d'une nouvelle réglementation en 1982 (RT1982), visant à réduire la consommation d'énergie de 20% par rapport à la RT1974. Puis est venue la RT2005, dont l'objectif était de réduire la consommation d'énergie de 15% supplémentaires. Cependant, nos résultats montrent que pour la plupart des régions administratives, la performance thermique n'est pas améliorée par la mise en œuvre des réglementations thermiques RT1974 et RT2005 comme prévu. Le gain attendu de la rénovation en utilisant le calcul conventionnel est d'environ 60%, si tous les bâtiments doivent avoir la même performance thermique que les nouveaux bâtiments construits après 2006. Mais avec nos résultats, plus de 30% des bâtiments consommeront plus qu'avant la rénovation, ce qui sera problématique pour l'objectif net zéro.

Le deuxième axe consiste à décarboniser le secteur résidentiel en mettant en œuvre l'autoconsommation par l'installation de panneaux photovoltaïques sur les toits. Nous nous concentrons sur les bénéfices mutuels de la production d'énergie photovoltaïque entre la ville et la campagne et entre le réseau et le consommateur pour la métropole du Grand Paris. Nous explorons différentes échelles de périmètre d'autoconsommation contractuelle afin de maximiser l'autoconsommation photovoltaïque et les taux d'autosuffisance. Pour pouvoir évaluer la performance avec plus de précision, les profils de consommation d'électricité en temps réel et la production d'énergie solaire sont importants. Nous utilisons une méthode de sensibilité à la température basée sur des études antérieures pour estimer l'évolution horaire de la consommation d'électricité par consommateur pour le secteur résidentiel et le secteur commercial. Les principales conclusions soulignent que le partage de l'énergie entre les secteurs résidentiel et commercial réduit considérablement les pertes excédentaires de l'énergie photovoltaïque et améliore la stabilité du réseau, les avantages augmentant au fur et à mesure que le périmètre de partage s'accroît. Après avoir combiné les secteurs résidentiel et commercial, l'amélioration de la SSR et de la SCR due à la complémentarité des secteurs atteint 6,5%. Après avoir combiné différents sous-domaines de la métropole (centre-ville et périphérie semi-urbaine), l'amélioration de la SSR et de la SCR due à l'extension du périmètre de partage de l'énergie est de 10%. En outre, l'amélioration du bilan énergétique est plus significative pour la périphérie. En termes économiques, les installations photovoltaïques en toiture permettent des économies plus importantes pour les habitants et les entreprises de la périphérie que pour ceux du centre de Paris. L'extension du périmètre permet ensuite un bénéfice plus important pour les usagers du centre de Paris. L'étude conclut que l'extension du périmètre de partage de l'énergie dans les zones urbaines optimise l'utilisation de la production photovoltaïque et contribue à des systèmes énergétiques urbains plus durables et plus résistants. Lorsque l'ensemble de la métropole du Grand-Paris est considéré comme une communauté énergétique qui permet le

partage, le bénéfice potentiel est le plus important avec 22,4% de la consommation couverte par la production photovoltaïque en toiture.

Mots clés: Consommation d'énergie résidentielle ; Changement climatique ; Décarbonisation ; Rénovation des bâtiments ; PV en toiture

Contents

List of Figures	xv
List of Tables	xxi
Nomenclature	xxiii
1 Introduction	1
1.1 Building energy consumption	1
1.1.1 Residential Energy Consumption	3
1.1.2 The Case of France	3
1.1.3 Climate change effect	4
1.2 Buildings decarbonization	5
1.2.1 Net-Zero Objectives	5
1.2.2 Energy Assessment Tools	6
1.2.3 Photovoltaic (PV) in the residential sector	6
1.2.4 The case of France	7
1.3 Challenges and Delays in Achieving Net-Zero Objectives	8
1.3.1 Energy performance gap	9
1.4 Study Objectives and thesis structure	10
2 Assessing residential electricity consumption under climate-change and air-conditioning scenarios	13
2.1 Introduction	14
2.2 Methodology and data	18
2.2.1 Temperature sensitivity statistical model	18
2.2.2 Training the temperature sensitivity model for the French REC	20
2.2.3 Projection data and scenarios definitions	27
2.2.4 Quantifying the uncertainty in the projected REC change	31
2.3 Results and discussion	36
2.3.1 Projected REC change without change in AC use	36
2.3.2 Projected REC change with change in AC use	37

2.3.3	Spatial heterogeneity	38
2.3.4	REC change error estimates	39
2.4	Conclusions and policy implications	48
3	Decarbonizing the residential sector by retrofitting buildings	51
3.1	Introduction	52
3.2	Methodology and data	52
3.2.1	Modified temperature sensitivity model	53
3.2.2	Data for the French case	54
3.2.3	Training the model for the French case	57
3.2.4	Future retrofitting projection	62
3.3	Results and discussion	63
3.3.1	Temperature sensitivities	63
3.3.2	Energy performance gap (EPG)	70
3.3.3	Retrofitting projection	72
3.3.4	Impact of socio-economic factors	74
3.4	Conclusion	75
	Appendix 3.A Bayesian Ridge analysis	77
	Appendix 3.B Impact of income results	79
4	Decarbonizing the residential sector by implementing self-consumption with rooftop photovoltaic (PV)	83
4.1	Introduction	84
4.2	Methodology and materials	87
4.2.1	Energy balance indicators	87
4.2.2	Economic evaluation	89
4.2.3	Hourly electricity consumption model	89
4.2.4	Grand Paris metropolis case study data	92
4.3	Results	96
4.3.1	Supply-demand balance analysis	96
4.3.2	Economic impacts	101
4.4	Conclusion	103
5	Conclusion and Perspectives	105
5.1	Conclusion	105
5.1.1	Main results and messages	105
5.1.2	Reflexion around limits of the thesis	107
5.2	Perspectives	108
	Appendix A Article published in <i>Climate Services</i>	125

List of Figures

- 1.1 Largest end uses of energy by sector in selected IEA countries (Refers to 2019 data for nineteen IEA countries for which data are available for most end uses: Australia, Austria, Canada, Czech Republic, Finland, France, Germany, Hungary, Japan, Italy, Korea, Luxembourg, New Zealand, Poland, Portugal, Spain, Switzerland, the United Kingdom and the United States; to 2018 data for Canada and Italy). Source: IEA Energy Efficiency Indicators database, 2021 (IEA and Birol, 2021) 2
- 1.2 Timeline of thermal regulations in France with their brief objectives and application scope. 7
- 2.1 Map of 12 administrative regions of metropolitan France, with thicker white lines representing 94 departments and thinner white lines representing more than 48000 IRIS cells. (Plate carrée projection, same projection used in the presented study) 16
- 2.2 Flow chart of the present study. 17
- 2.3 Top: Estimates of α^H (left) and α^C (middle) obtained by training the model (2.2) on the observational data (Section 2.2.2). Projections of α^C (right) by gradual spreading (Section 2.2.3.2). Bottom: Corresponding values of β^H (left) and β^C (middle), and projections of β^C (right) for the AC2018 scenario (Section 2.2.3.2). 25
- 2.4 Temperature-sensitive REC per year averaged over departments estimated from (a) the Enedis β^H estimates for 2018 (for 50% of the cells only, Section 2.2.2.1), (b) the model (2.2) applied to the E-OBS temperatures for 2018 and (c) the model (2.2) applied to the CORDEX historical temperatures over the 1975–2005 period and averaged over the period and over the climate-model simulations (Section 2.2.3.1). 26
- 2.5 Total temperature-sensitive REC reference aggregated at the department level, estimated with our model using the temperature of 1975–2005 from CORDEX simulations on all valid cells (60% of the cells). 26
- 2.6 Comparison between linear regression methods of R^2 score distribution for all valid IRIS. 27

2.9	Flowchart for determination of cooling needs for each IRIS with our hypothesis, α_i^C refers to the cooling temperature sensitivity estimated with observational consumption data and α_f^C refers to the future temperature sensitivity.	32
2.7	Mean over 1975–2005, mean change over 2025–2055 wrt. 1975–2005 (CC2040), and mean change over 2070–2100 wrt. 1975–2005 (CC2085) for the HDDs (top) and CDDs (bottom) computed according to Eq. (2.1). The temperature data for 1975–2005 is from the historical CORDEX simulations, while that for 2025–2055 and 2070–2100 is from the RCP8.5 CORDEX simulations. The results are spatially averaged over the departments and averaged over the climate-model simulations listed in Table 2.4. Warm colors represent situations associated with warm temperatures (i.e. to a decrease in heating REC and to an increase in cooling REC).	34
2.8	Test R^2 score between estimated α_i^C with Gradual Spreading method and regression model estimation as a function of the chosen number of neighbors J taken into account for the calculation of average (Gradual Spreading).	35
2.10	Relative change (%) in REC wrt. to the historical period (1975–2005) for CC2040 and for different AC scenarios: AC18-NOGS (a), ACall-NOGS (b), AC18-GS (c) and ACall-GS (d).	42
2.11	Relative change (%) in REC wrt. to the historical period (1975–2005) for CC2085 and for different AC scenarios: AC18-NOGS (a), ACall-NOGS (b), AC18-GS (c) and ACall-GS (d).	43
2.12	Boxplots over the cells of the relative change in temperature-sensitive REC corresponding to Fig. 2.10 and Fig. 2.11. The whiskers here show the minimum on the left and the 99% quantile on the right.	44
2.13	Same as Fig. 2.10 but for the cooling REC.	45
2.14	Same as Fig. 2.11 but for the cooling REC.	46
2.15	The global uncertainty of estimation of evolution in temperature-sensitive REC by combining all possible estimated coefficients with the leave-one-out cross-validation method and the 5 CORDEX simulations, represented by the Relative Standard Deviation (RSD) for the CC2040-AC18-NOGS (left) and the CC2085-AC18-NOGS (right) scenarios.	47
3.1	Pearson correlation between construction period distribution and median income at the IRIS level for all French metropolitan administrative regions. The table in the first row shows the representative percentage of IRIS from the income dataset compared to the total number of Enedis.	56
3.2	Distribution of estimated temperature sensitivities related to different construction periods α_a^H of the region Ile-de-France using different test sampling scenarios.	59

3.3	Example of distribution matching to retrofit EPC class G to EPC class C. The orange is the current distribution of heating consumption of households with category G, the blue is the current distribution of category D, and the green is the distribution of the category G sample after the retrofit.	62
3.4	25%-75% distribution of estimated temperature sensitivities related to different construction periods α_a^H of different administrative regions using different test sampling scenarios.	64
3.4	25%-75% distribution of estimated temperature sensitivities related to different construction periods α_a^H of different administrative regions using different test sampling scenarios. (cont.)	65
3.4	25%-75% distribution of estimated temperature sensitivities related to different construction periods α_a^H of different administrative regions using different test sampling scenarios. (cont.)	66
3.5	Comparison of the relative coefficients uncertainty with the explicit sources as described in Eq. (3.8) between other administrative regions and Ile-de-France as ratios (Ile-de-France has the smallest relative coefficients uncertainty and is used as the reference for the comparison).	68
3.6	Stacked bar chart of uncertainty sources represented by Mean-Squared-Error (MSE) for all 12 administrative regions in France.	69
3.7	Energy Performance Gap (EPG) distribution, which compares the heating consumption between 3CL calculation and model estimation based on actual consumption of France with 1.46 million housing observations.	70
3.8	Map of percentage of negative EPG for French 12 administrative regions for different groups of construction periods (negative EPG indicates lower actual heating consumption compared to expected heating consumption).	71
3.9	Comparison of the distribution of potential savings under four different scenarios using EPCs and one scenario using the estimation of our model for the case of France.	72
3.10	Map of 12 French administrative regions with (a) the median expected retrofit gains (in kWh/m ²) based on EPC estimates; (b) the median expected retrofit gains (in kWh/m ²) based on our model estimates, and (c) the percentage likelihood that energy savings are lower than expected.	73
3.11	Distribution of estimated temperature sensitivities related to different construction periods α_a^H of the region Auvergne-Rhône-Alpes using test sampling size as the income input, blue dots represent estimated coefficients for the sample of income as input and orange dots represent the estimated coefficients with input corrected.	74

3.12	Distribution of estimated temperature sensitivities related to different construction periods α_a^H using test sampling size as the income input, blue dots represent estimated coefficients for the income sample as input, and orange dots represent the estimated coefficients with input corrected.	80
3.12	Distribution of estimated temperature sensitivities related to different construction periods α_a^H using test sampling size as the income input, blue dots represent estimated coefficients for the income sample as input, and orange dots represent the estimated coefficients with input corrected. (cont.)	81
3.12	Distribution of estimated temperature sensitivities related to different construction periods α_a^H using test sampling size as the income input, blue dots represent estimated coefficients for the income sample as input, and orange dots represent the estimated coefficients with input corrected. (cont.)	82
4.1	(a) Map of the ratios between residential electricity consumption E^{RES} over the sum of residential and commercial electricity consumptions $E^{RES} + E^{PRO}$ for the Grand Paris metropolis with white lines representing more than 2700 IRIS cells. The thick black line outlines Paris, surrounded by its periphery. During the present study, the smaller center is named Paris center, and the periphery is named Paris surroundings. The inset map shows in blue an example of rooftop areas identified by APUR (2019). (b) Ratios between the favorable rooftop surfaces for PV installation (i.e. for which the radiation potential is greater than 1000 kWh/m ² per year) and the inhabitable housing surfaces estimated using the APUR data. (Both maps and the subsequent ones are produced for a plate carrée projection.)	85
4.2	Daily consumption evolution summed over the Grand Paris metropolis with $P \leq 36$ kVA during the 2020/04/02–2022/01/01 period. The blue line (resp. the orange line) represents daily (resp. weekly) running averages. (a) Residential electricity consumption (RES) and the blue dots represent daily consumption on weekends and public holidays. (b) Small businesses' electricity consumption (PRO) and the blue dots represent daily consumption on Sundays and public holidays.	90
4.3	Average of the base electricity consumption for each hour of the day and for each season over the period between April 2020 and January 2022. Separate profiles are given for RES (top) and PRO (bottom) and for the weekdays (left) and for the weekends and holidays (right). The Central European Time (CET) standard is used.	95

- 4.4 Map at the IRIS level, the first row (a, b, c) is of self-consumption rate (SCR) and the second row (d, e, f) is of self-sufficiency rate (SSR). The first column (a, d) is for residential consumption only, the middle column (b, e) is for small businesses only, and the right column (c, f) is for the sum of both sectors. . . . 97
- 4.5 IRIS map of average electricity cost (Euro cents per kWh c€/kWh) at the IRIS level after energy sharing between the residential and the commercial sectors with each IRIS as a microgrid. 102
- 4.6 Distribution of IRIS normalized cost compared to the regional value of 15.4 c€/kWh with energy sharing in the Grand Paris metropolis between all residential and commercial users (dashed red line) and the initial electricity buying price of 20 c€/kWh (dashed black line). 103

List of Tables

2.1	Summary of variables and their physical meanings presented in Eq. (2.2). . . .	19
2.2	Heating setpoints T_r^H for all regions of metropolitan France computed according to Section 2.2.2.3.	22
2.3	AC adoption rates (%) for 2011 and 2018.	23
2.4	Institute, GCM name and RCP name for the 5 climate change simulations used in this study.	29
2.5	Definition of the four AC scenarios in terms of AC adoption rate and α^C spreading strategy. XXXX is either 2040 or 2085, corresponding to the central year of the climate change projection window considered.	30
2.6	Decomposition of variability into different geographical scales for different studied variables in terms of proportion (%).	39
2.7	Average values with uncertainty for all possible combinations, the uncertainty is converted to the same magnitude by averaging over the number of cells. A t-test shows that mean values of REC change under all scenarios are significant. . . .	40
2.8	Comparison of uncertainty due to model or CORDEX for scenario AC18-NOGS in the form of standard deviation (GWh/cell).	41
3.1	Summary of variables and their physical meanings presented in Eq. (3.1). . . .	53
3.2	Data information for training the modified temperature sensitivity model for the French case.	58
3.3	Notations and definitions of variables used for the error analysis.	59
4.1	Annual electricity consumption and PV production (all in TWh) for the Grand Paris metropolis and its two subdomains (center and surroundings) for different sectors.	93
4.2	Annual self-sufficiency rate (SSR) and self-consumption rate (SCR) for the Grand Paris metropolis and its two subdomains (center and surroundings) compared to the weighted average of IRIS values for different sectors.	98

- 4.3 Self-sufficiency rate (SSR) and self-consumption rate (SCR) for the region Grand Paris and its two subdomains (center and surroundings) compared to the weighted average of IRIS values under different seasons for the sum of RES and PRO sectors. [99](#)

Nomenclature

List of abbreviations

AC	Air conditioning
CDD	Cooling Degree Days
DD	Degree Days
EPC	Energy Performance Certificate
EPG	Energy Performance Gap
HDD	Heating Degree Days
IRIS	Ilots Regroupés pour l'Information Statistical
OLS	Ordinary Least Squares
PRO	Small businesses sector
PV	Photovoltaic
REC	Residential Electricity Consumption
RES	Residential sector
SCR	Self-Consumption Rate
SSR	Self-Sufficiency Rate

Chapter 1

Introduction

Contents

1.1 Building energy consumption	1
1.1.1 Residential Energy Consumption	3
1.1.2 The Case of France	3
1.1.3 Climate change effect	4
1.2 Buildings decarbonization	5
1.2.1 Net-Zero Objectives	5
1.2.2 Energy Assessment Tools	6
1.2.3 Photovoltaic (PV) in the residential sector	6
1.2.4 The case of France	7
1.3 Challenges and Delays in Achieving Net-Zero Objectives	8
1.3.1 Energy performance gap	9
1.4 Study Objectives and thesis structure	10

1.1 Building energy consumption

The building sector, including residential, commercial, and public buildings, is one of the global final energy consumers (Lu and Lai, 2019; Mastouri et al., 2020). It accounted for 34 % of total global final energy consumption in 2019, highlighting its significant impact on energy demand and carbon emissions (IEA, 2020). The residential sector is particularly important, accounting for 20% of total energy consumption (International Energy Agency, 2023). Projections by the International Energy Agency (IEA) suggest that the importance of buildings, particularly residential buildings, in global energy consumption and CO₂ emissions will continue to grow (International Energy Agency, 2023). This continuing trend highlights the urgent need for sustainable energy practices and efficiency improvements in the building sector to reduce environmental impacts and support global energy sustainability goals.

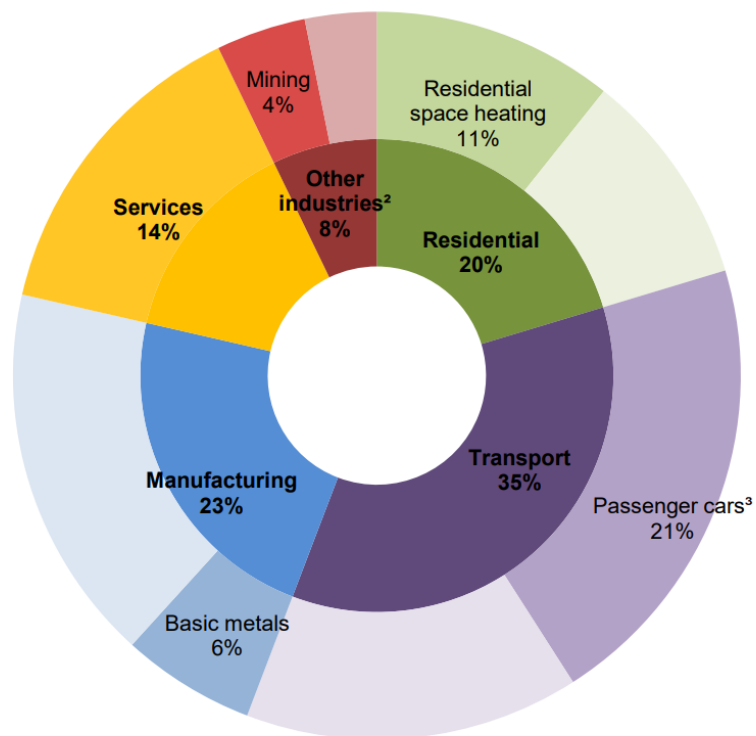


Figure 1.1 Largest end uses of energy by sector in selected IEA countries (Refers to 2019 data for nineteen IEA countries for which data are available for most end uses: Australia, Austria, Canada, Czech Republic, Finland, France, Germany, Hungary, Japan, Italy, Korea, Luxembourg, New Zealand, Poland, Portugal, Spain, Switzerland, the United Kingdom and the United States; to 2018 data for Canada and Italy). Source: IEA Energy Efficiency Indicators database, 2021 (IEA and Birol, 2021)

1.1.1 Residential Energy Consumption

A closer look at residential energy consumption reveals the many factors that influence its evolution (Frederiks et al., 2015; Mashhoodi and van Timmeren, 2018; Yan and Lifang, 2011; Yun and Steemers, 2011). The interaction of socio-demographic, economic and psychological factors is crucial in shaping residential energy consumption patterns. An important aspect of residential energy consumption is its dependence on household income, the thermal quality of the dwelling and the relative cost of energy in relation to the household's purchasing power (Branger et al., 2015; Frederiks et al., 2015; Giraudet et al., 2012). This relationship highlights the multifaceted nature of energy consumption and the importance of considering affordability alongside energy efficiency measures in the residential sector. Studies in many countries have shown considerable variation in household energy use due to differences in income levels, dwelling type, household composition and geographical location. In the UK, for example, the relationship between household energy use and carbon emissions and socio-economic factors such as income level, dwelling type, tenure, household composition and rural/urban location has been well documented (Druckman and Jackson, 2008). This variability is also reflected in the Netherlands, where dwelling characteristics have a strong influence on natural gas consumption, while electricity consumption is closely related to household composition, income and structure (Brounen et al., 2012).

The residential energy consumption, therefore, displays a very large spatial variability, especially in urban areas, which are characterized by the heterogeneity of their demographic, socio-economic, environmental, and cultural characteristics (Li and Kwan, 2018; Pickett et al., 2017) underlying urban resource demands (Rosales Carreón and Worrell, 2018; Voskamp et al., 2020). As our specific case study, France confirms the findings of other countries and illustrates how geographical and economic differences can significantly impact residential energy consumption patterns. This highlights the need for policies to be comprehensive and sensitive to the uniqueness of different regions and communities (Lévy and Belaïd, 2018). This spatial variation illustrates the complexity of addressing energy consumption through policy due to the different needs and characteristics of the population. The significant influence of socio-demographic and psychological factors on residential energy use requires a targeted approach to policy development. Evidence suggests that effective energy efficiency policies must navigate the complexity of these influences and consider the nuances between different geographical contexts. These policies should not only aim to improve the thermal quality of dwellings and make energy more affordable. Still, they should also consider different population groups' unique socio-economic and cultural characteristics to ensure they are inclusive and effective.

1.1.2 The Case of France

From the consumption perspective, the French building sector (residential and service) contributes significantly to energy consumption, accounting for about 44% of total final energy

consumption. With a population of 65 million people residing within a metropolitan territory spanning 333,691 km², France's energy mix and policies present a unique situation that is shaped by a history of energy crises and a strong focus on nuclear energy ([International Energy Agency, 2021](#); [Taylor et al., 1998](#)). France's ambitious nuclear energy program highlights the complexity of the French energy landscape. France's reliance on nuclear power has historically set it apart from many other countries as a leader in low-carbon energy production. However, the current increased focus on electrification and nuclear energy's gradual reduction in its share of the energy mix presents France with a complex challenge. The residential sector, which accounts for over 30% of final energy consumption and 20% of CO₂ emissions in France, is emerging as a critical area of focus. Addressing this sector's energy needs through renewable energy sources and energy efficiency measures, such as deep energy retrofits or renovations, is essential. These measures contribute to France's environmental goals and demonstrate the potential for sustainable energy practices within the existing infrastructural and societal framework. Therefore, key strategies include improving building energy efficiency, promoting thermal renovation, and encouraging the construction of high-performance buildings. These initiatives aim to limit electricity consumption in the residential sector, representing a major environmental challenge and a significant opportunity to mitigate global warming.

1.1.3 Climate change effect

In France, outdoor temperature increase could reach up to 3.8°C by 2100 with regards to 1900-1930 if no policy is in place to reduce greenhouse gas emissions ([Ribes et al., 2022](#)). [Pilli-Sihvola et al. \(2010\)](#) have investigated the impact of climate change on building energy demand for heating and cooling and the associated energy cost using climate simulations of the 3rd Coupled Model Intercomparison Project (CMIP3). More recently, [Larsen et al. \(2020\)](#) find in downscaled CMIP5-climate simulations that when temperature evolution is considered as the only factor of change, needs for cooling increase by 33% to 204% between 2050 and 2010 and needs for heating decrease by -31% to -6% while [Damm et al. \(2017\)](#) predict the impact of a +2°C global temperature change on European electricity demand, with for France, an estimated decrease in total electricity consumption between -10 TWh and -16 TWh. The optimistic reduction in electricity projection is due to France's current heating-dominated state. All households in the country utilize specific heating systems such as gas, oil, wood, or district heating, among which 37% employ electric heating. In contrast, the national adoption of air-conditioning (AC) remains relatively low, standing at only approximately 22% when considering all types and sizes of air conditioners, including mobile and heat pump units.

Rising temperatures and temperature extremes, in particular, imply increased use of air conditioners, both in hot and humid emerging economies where incomes are rising and in industrialized economies where consumer expectations in terms of thermal comfort are constantly growing ([Van Ruijven et al., 2019](#)). Previous studies ([Colelli et al., 2023](#); [Randazzo](#)

[et al., 2020](#); [Van Ruijven et al., 2019](#)) suggest that climatic conditions will encourage more households to adopt AC systems, therefore affecting electricity expenditures. On a global scale, the final energy consumption for AC in residential and commercial buildings has more than tripled between 1990 and 2016. The share of cooling in Residential Electricity Consumption (REC) increased from around 2.5% to 6% during the same period. The use of AC equipment is expected to increase dramatically, becoming one of the main drivers of global electricity demand ([International Energy Agency, 2018](#)).

In France, as heat waves are more and more frequent and long, many households and businesses are equipped with AC for more comfort ([Lemonsu et al., 2015](#)). In 2020, for the first time, the number of equipment sold exceeded 800,000 units, whereas it had stabilized at around 350,000 per year previously. In 2020, 25% of individuals are equipped compared to 14% in 2016, with disparities linked to the type of dwelling (31% of owners of individual houses compared to 20% of households living in collective housing), socio-professional category (37% of liberal professions, executives and higher intellectual professions against only 19% of households whose reference person is unemployed or inactive) and place of residence (e.g. 47% of inhabitants of the South-East and Corsica against only 11% in Brittany) ([ADEME, CODA STRATEGIES, 2021](#)).

1.2 Buildings decarbonization

1.2.1 Net-Zero Objectives

Globally, the transition towards net-zero energy buildings and carbon neutrality is an environmental imperative and a crucial pivot towards sustainable living. The quest for net-zero energy buildings is central to global efforts to combat climate change, in line with the [Paris Agreement](#) and the [Kyoto Protocol](#). Transitioning to net-zero energy buildings is crucial for meeting the targets for reduction of greenhouse gas (GHG) emissions and promises significant energy efficiency enhancements.

The Energy Performance of Buildings Directive (EPBD) ([Council of European Union, 2018](#)) requires EU Member States to ensure that all new buildings meet near-zero energy standards by the end of 2020. In addition, starting at the end of 2018, all new public buildings must comply with these near-zero energy guidelines. Near-zero-emission buildings (NZEB) are characterized by very high energy efficiency and their minimum energy requirements should come mainly from renewable sources. At the end of 2021, the European Commission proposed an amendment to the Directive, marking a significant evolution from the existing NZEB standards to Zero Emission Buildings (ZEB). The revision aligns energy efficiency standards for new buildings with the broader goal of achieving climate neutrality and follows the principle of "energy efficiency first." Under the proposed revisions, a zero-emission building (ZEB) is described as a building with superior energy performance, whose minimum energy needs are met entirely by renewable

energy sources and which does not require burning fossil fuels to produce carbon emissions. The proposed ZEB guidelines will become effective in 2027 for buildings occupied or owned by public authorities and in 2030 for all new buildings.

1.2.2 Energy Assessment Tools

Efforts to enhance the energy efficiency of buildings in Europe have been ongoing, employing a range of legislative, regulatory, and financial mechanisms ((Zuhaib et al., 2022); (Economidou et al., 2020)). Among these mechanisms, Energy Performance Certificates (EPCs) have emerged as an essential tool in driving progress ((Khazal and Sønstebo, 2020)). Initially introduced by the EPBD in 2002, EPCs were designed to enhance transparency regarding the energy performance of individual buildings and facilitate the transition to low-carbon residential sectors. The widespread adoption of EPC regimes by all European Union countries and the United Kingdom by 2015 attests to their growing significance ((Semple and Jenkins, 2020)). Typically, an EPC provides a rating, ranging from A (most efficient) to G (least efficient), that conveys information on the energy and climate performance of a home or building. At the Member State level, the EPC develops standards adapted to national regulations and financial incentives, as in the cases in France, the United Kingdom, the Netherlands, and Italy. France and the UK use the EPC to create a new minimum energy performance for housing by banning rentals of the lowest-performance housing. At the same time, the Netherlands applies a similar standard for office buildings. The Netherlands also offers companies a financial incentive of tax reduction to improve their energy performance, while Italy provides tax reduction for individuals who improve their EPC.

1.2.3 Photovoltaic (PV) in the residential sector

Another key initiative to reduce carbon emissions from residential energy consumption is to increase the share of distributed PV (e.g., rooftop PV). NZEB can be realized by generating electricity on-site so that the net energy purchased from the grid is no longer needed (Babu and Vyjayanthi, 2017; Singh and Verma, 2014). National and local policies have introduced subsidies, such as feed-in tariffs, to promote distributed PV, such as rooftop PV, and it is believed that rooftop PV has a bright market. IEA projects that the number of households relying on solar PV will grow from 25 million today to more than 100 million by 2030 in the Net-Zero Emissions by 2050 Scenario (NZE Scenario). At least 190 GW will be installed from 2022 each year and this number will continue to rise due to increased competitiveness of PV and the growing appetite for clean energy sources (IEA, 2022).

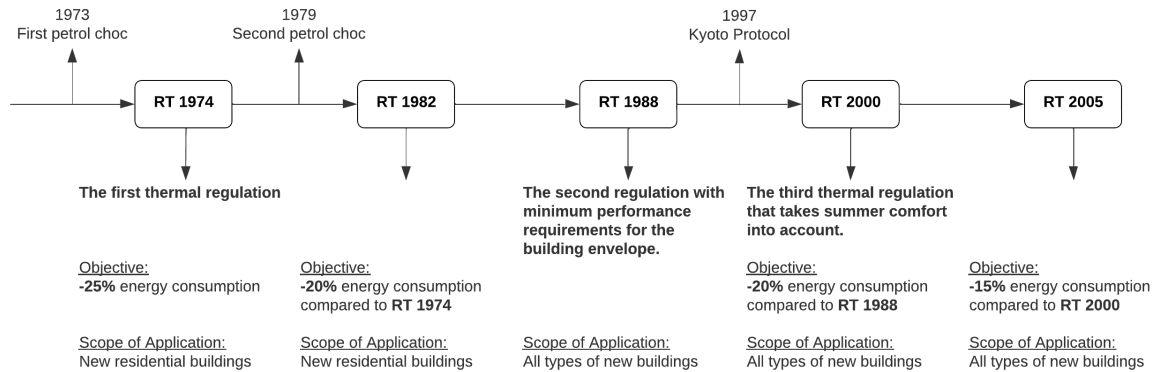


Figure 1.2 Timeline of thermal regulations in France with their brief objectives and application scope.

1.2.4 The case of France

France is actively pursuing a transition to more sustainable energy sources, underlined by *Law for the ecological transition and green growth*¹. This law underlines France's commitment to reducing greenhouse gas emissions by 40% by 2030 and divided by four by 2050. It also sets ambitious targets for reducing fossil fuel consumption by 30% by 2030 and halving final energy consumption by 2050 compared to 2012. These efforts align with the [Paris Agreement](#)'s goal of limiting the global temperature increase to below 2°C, with further efforts towards 1.5°C. The legislation is part of a broader strategy embodied in the European Green Deal ([European Commission, 2021](#)) to achieve sustainability and decarbonization across the continent. Before the EPC was enforced in France, the French government had already formulated the calculation standard for the thermal performance of new housings to limit fossil consumption. The first thermal building code (RT) was implemented in 1974 to reduce energy consumption by 25% compared with older housings. This was followed by a new regulation in 1982 (RT1982), aimed at reducing energy consumption by 20% compared with RT1974. Then came RT2005, to reduce energy consumption by a further 15%. One of France's goals for achieving the Paris Agreement is to retrofit 500,000 existing homes per year because of the building sector's huge potential for energy savings. The retrofitting process starts with creating an EPC for all buildings, again emphasizing the importance of the EPC.

The French government has also set ambitious targets to increase the share of renewable energy in the national energy mix, aiming to achieve a 40% share of renewable energy by 2030. Rooftop photovoltaics (PV) could play an important role in achieving this goal. For example, the French Electricity Transmission System Operator (known as RTE) has proposed several future energy scenarios, of which Scenario M1 emphasizes distributed PV (i.e., rooftop PV) and predicts that 35 GW of residential rooftop PV will be installed in France by 2050 (about half of all individual houses) ([RTE, 2021](#)). According to [International Energy Agency \(2023\)](#), solar power will dominate future electricity generation technologies. By 2050, solar power will

¹<https://www.legifrance.gouv.fr/loda/id/JORFTEXT000031044385>

account for 30% of global electricity generation, among which distributed rooftop PV power generation is strongly promoted by subsidies in many countries ([Avril et al., 2012](#); [Nousdilis et al., 2018](#); [The European Commission, 2016](#)).

In 2017, France implemented a "self-consumption package" which included several measures to facilitate the deployment of small-scale renewable energy systems and promote self-consumption. This package included changes to the legal framework to facilitate self-consumption, financial incentives such as tax credits and low-interest loans, and regulatory measures such as simplifying administrative procedures for small PV installations ([France, 2017](#)).

1.3 Challenges and Delays in Achieving Net-Zero Objectives

Achieving the ambitious goals set by international agreements such as the Kyoto Protocol and the Paris Agreement, as well as national strategies such as France's, has proven to be a complex and challenging task. Despite the global commitment to decarbonization and the transition to net-zero energy buildings, significant delays and obstacles have emerged ([Brian and John, 2016](#)). These challenges highlight the mismatch between established targets and the current pace of progress in residential decarbonization ([Rockström et al., 2017](#)).

The complexity of accurately forecasting energy consumption in net-zero buildings is a significant challenge ([Becchio et al., 2016](#); [Kneifel and Webb, 2016](#); [Mukherjee, 2011](#)). This is due to the need for sophisticated technologies and control strategies and the influence of occupant behavior ([Becchio et al., 2016](#); [Mukherjee, 2011](#)). [Kneifel and Webb \(2016\)](#) highlights the prominent issues due to capability limits in physical simulation models during net-zero building design and that accurate energy consumption forecasts are critical to meeting net-zero targets. The development of nearly-zero energy buildings and the transition towards post-carbon cities further emphasize the need for accurate energy consumption forecasting ([Becchio et al., 2016](#)).

The path toward building decarbonization also suffers from a lack of consensus on definitions and strategies ([Kibert and Fard, 2012](#); [Moghaddasi et al., 2021](#)). [Moghaddasi et al. \(2021\)](#) highlights this issue, noting how disagreement on fundamental principles can block the adoption of effective policies and delay progress toward net-zero goals. Efforts to address this issue also include differentiating between different building strategies in policy development [Kibert and Fard \(2012\)](#). In addition, the concept of net-positive energy buildings has been introduced, which emphasizes a systems-based approach to maximizing energy performance [Cole and Fedoruk \(2014\)](#). These discussions highlight the need for a more comprehensive and unified approach to defining and realizing the decarbonization of buildings.

1.3.1 Energy performance gap

Some of the barriers to the implementation of the net-zero goal have already been studied. For example, even though the EPC has had great success, its correct representation of energy consumption faces many doubts. Many studies have been conducted to measure the difference between the actual energy consumption and the theoretical demand calculated by EPC (Calì et al., 2016; Cayre et al., 2011; Cozza et al., 2020a; Majcen et al., 2013; Raynaud, 2014). Such difference is known as the Energy Performance Gap (EPG), commonly defined as the deviation from the theoretical consumption expressed as a percentage. While there are different methods to analyze the EPG, the definition of the difference in consumption relative to the theoretical consumption is widely accepted.

$$EPG[\%] = \frac{\text{Actual energy consumption} - \text{Theoretical energy consumption (EPC)}}{\text{Theoretical energy consumption (EPC)}} \quad (1.1)$$

(Cozza et al., 2020a) analyzed a subsample of 1172 buildings from the Swiss national database and found that conventional energy consumption calculation overestimates actual consumption, and the gap increases with the EPC label. Similar results are also found in the Netherlands (Majcen et al., 2013) and in Germany (Calì et al., 2016).

The reason why EPG has been widely studied is to check whether potential energy savings are achieved after renovation works. check if the potential energy savings have been reached. Cayre et al. (2011) studied EPC for 923 French residential buildings and indicated that the actual renovation savings are less than expected since EPC tends to overestimate the potential energy gains by 40%. This is similar to the case of Swiss, where an overestimation of 37% of the achievable savings is found due to calculations based on EPC. All these studies share the same finding that conventional calculations of EPC strongly overestimate the potential energy savings after retrofit due to the overestimate of space heating consumption, especially in older housings (Cozza et al., 2020a).

Improving energy efficiency in the building sector requires accurate energy assessment tools, which was the original goal of constructing EPCs. However, it is important to acknowledge the limitations of traditional EPCs, as many studies have highlighted the energy performance gap resulting from the disparity between calculated and actual energy consumption. This calls for a shift towards considering actual consumption data rather than relying solely on theoretical models. Additionally, individual preferences are significant factors influencing the energy performance gap. While individual analysis is important, adopting a more efficient tool to provide a comprehensive assessment across a large country is necessary. This is particularly crucial in the context of political proposals for building energy retrofitting and energy planning. Developing an actual consumption diagnostic tool with broad applicability is essential to address these challenges.

1.4 Study Objectives and thesis structure

In France, achieving significant reductions in GHG emissions by 2050 will require an integrated strategy that includes technical, economic, and social dimensions. The French experience underscores the importance of addressing these challenges through multifaceted policies that can navigate the complexities of energy consumption, energy efficiency efforts, and the broader socioeconomic context (Charlier and Risch, 2012; Mathy et al., 2015; Égert, 2011). The IEA's France 2021 Energy Policy Review also highlights the complexity of France's energy transition. The report highlights that France's energy transition goals are still behind schedule despite important reforms. For example, France has yet to meet its 2020 energy efficiency and renewable energy targets. The 2030 emissions targets adopted in 2015 remain unchanged, and a second increase in the carbon budget in 2020 reduces the effort required by 2023 (International Energy Agency, 2021).

The obstacles facing France and the broader international community in achieving net-zero goals underscore the need to reassess current strategies and adopt more effective, integrated approaches. We have seen all the efforts in public policy and work on decarbonization. However, with the constant delays and postponed targets, the situation leads to the main research question of this thesis that interests us:

How would residential energy consumption evolve in the context of climate policies?

This question aims to bridge the gap between ambitious environmental goals and real progress, focusing on the role of the residential sector in the broader context of climate change mitigation efforts. The study is organized into several steps to answer the research question. First, the future of French residential energy consumption (especially electricity consumption) is projected in the context of climate change. We have to precisely estimate the future consumption in order to prepare for the decarbonization under climate change.

- Chapter 2 presents the methodology used to project future French residential electricity consumption, considering climate change and air-conditioning (AC) scenarios and quantifying their spatial variability. For this purpose, a linear temperature sensitivity model fitted by annual observed electricity consumption data and historical temperature is applied at an intra-regional scale. Future temperature-sensitive residential electricity consumption is then computed by using the model to temperature projections under the climate change pathway with a high emission scenario.

We want to evaluate the decarbonization of the residential sector once we finalize the projection for residential electricity consumption. Two principle axes are studied: the first aims to study retrofitting performance.

- Chapter 3 builds on previous research and presents a modified linear temperature sensitivity model that includes a building age variable for estimating temperature-sensitive

consumption for different building age groups within each administrative area. These temperature-sensitive consumption estimates based on actual consumption are mainly heating-based and can be compared with theoretical heating consumption calculated from standard Energy Performance Certificates (EPCs). Our models can also predict future retrofit gains.

The second axis of residential decarbonization is the installation of photovoltaic panels on roofs to increase the share of renewable energy. Sustainable urban development is a serious challenge for climate action, and the increase in photovoltaic generation is expected to help meet this challenge. However, due to the variable nature of PV generation, its integration increases the complexity of grid management and requires careful consideration of the energy balance.

- Chapter 4 focuses on the integration of distributed rooftop PV in the greater Paris metropolis to balance energy supply and demand, emphasizing technical aspects such as self-consumption rate (SCR) and self-sufficiency rate (SSR). Using real-time electricity consumption profiles and solar generation data, the study explores the complementarity of participants of different sizes to maximize SSR and SCR. The study concludes that scaling up energy sharing in urban areas can optimize the use of PV generation and contribute to a more sustainable and resilient urban energy system.

At the end, Chapter 5 gives the summary of the main results obtained during the thesis work and the perspectives for future works.

Chapter 2

Assessing residential electricity consumption under climate-change and air-conditioning scenarios

This chapter is a recent article I published in the journal *Climate Services* (Tao et al., 2024a). The chapter consists mainly of this article, with some details added and reorganized in the methods section for better understanding. The full text of the article can be found in Appendix A.

Contents

2.1	Introduction	14
2.2	Methodology and data	18
2.2.1	Temperature sensitivity statistical model	18
2.2.2	Training the temperature sensitivity model for the French REC	20
2.2.3	Projection data and scenarios definitions	27
2.2.4	Quantifying the uncertainty in the projected REC change	31
2.3	Results and discussion	36
2.3.1	Projected REC change without change in AC use	36
2.3.2	Projected REC change with change in AC use	37
2.3.3	Spatial heterogeneity	38
2.3.4	REC change error estimates	39
2.4	Conclusions and policy implications	48

2.1 Introduction

As presented in the introduction, with the energy transition law for green growth 2015, France is committed to reducing its greenhouse gas emissions by 40% by 2030 and divided by four by 2050. It also plans to reduce its consumption of fossil fuels by 30% by 2030 and to halve its final energy consumption in 2050 compared to 2012. Hence, the residential sector could be a significant opportunity and challenge for policies to combat global warming. Indeed, the law text emphasizes improving building energy efficiency, thermal renovation, and constructing buildings with high energy performance.

Limiting electricity consumption in the residential sector through actions aimed at improving buildings' energy performance is a major environmental challenge for communities. However, residential electricity consumption (REC) highly depends on socio-economic factors. It, therefore, displays a very large spatial variability.

Electricity demand also depends on the outdoor temperature. Demand for cooling rises once the temperature exceeds a cooling setpoint, while electricity demand for heating grows once the temperature drops below a heating setpoint ([Auffhammer and Mansur, 2014](#); [Damm et al., 2017](#); [Kozarcenin et al., 2019](#); [Petrick et al., 2010](#); [Wenz et al., 2017](#)). As a result, a theoretical U-shaped link exists between electricity demand and temperature. Choices made by individuals to utilize heating and cooling systems to maintain a comfortable temperature in their residences directly impact electricity demand ([Emenekwe and Emodi, 2022](#); [Emodi et al., 2018](#)). Substantiated correlations between consumption and climate and weather conditions ([Meng et al., 2020](#)), demographic and economic factors ([Bettignies et al., 2019](#)) and urban and architectural morphological characteristics ([Chen et al., 2020b](#); [You and Kim, 2018](#)) cause the large spatial variability in residential energy demand. Climate, socio-economic and morphological characteristics have proven explanatory variables for energy demand and its spatial pattern ([Chen et al., 2020a](#); [Kennedy et al., 2015](#); [Wiedenhofer et al., 2013](#)).

The link between temperature and electricity demand has been studied using various models (e.g. [Emodi et al., 2018](#); [Narayan et al., 2007](#)). One approach is to model this nonlinear relationship by a smooth but nonlinear function of the temperature. For instance, [Moral-Carcedo and Vicéns-Otero \(2005\)](#) and [Damm et al. \(2017\)](#) used a Logistic Smooth Transition (LSTR) function to model the electricity demand response to temperature variations in European countries. The advantage of such a model is that it adequately captures the rather smooth response of electricity demand summed over a large domain to temperature variations. On the other hand, it is less straightforward to interpret the physical meaning of the parameters of such a model. Another approach is to model the electricity demand as a linear combination of nonlinear functions of the temperature (making it a generalized linear model). For instance, [Sailor and Muñoz \(1997\)](#) studied the monthly electricity and gas consumption for states in the US using a linear model with degree-day (DD) inputs in addition to wind speed and relative humidity.

However, most previous studies of future consumption projection only focus on continental and national scales while not considering the sub-national disparity of temperature changes and non-climatic factors listed above. We aim to fill this gap by examining whether the national results proposed by these earlier studies remain consistent at smaller scales, given that changes in consumption and geographical variations in adaptation can lead to inequalities. We provide valuable information on the local impacts of climate change and building cooling strategies on residential energy demand, which can aid local climate and energy planning and decision-making. Specifically, we focus on the sub-regional variability of changes in residential AC requirements for cooling needs in the context of climate change. To this end, we use a modified temperature sensitivity model to project future REC at a fine scale. The smallest geographic scale used in this study is the so-called *Ilots Regroupés pour l'Information Statistique (IRIS)*, here referred to as cells, which divides the French territory into a collection of about 2000 inhabitants per cell. These cells are defined by respecting geographic and demographic criteria and have recognizable contours without ambiguity and stability over time. France has a total of 50,800 cells (IGN, 2009). In metropolitan France, these cells are distributed among 12 administrative regions represented in Fig. 2.1. This model is designed to distinguish between different aspects of electricity use using data from all residential buildings, irrespective of their heating or cooling equipment. The projection of future residential electricity consumption is based on climate change pathway RCP8.5, using downscaled CMIP5 climate simulations carried out as part of EURO-CORDEX (Jacob et al., 2014) and MEC-CORDEX (Ruti et al., 2016), while considering different scenarios of AC use for cooling - full generalization or saturation.

After the introduction in Section 2.1, the details of the model can be found in Section 2.2, with information about the temperature and REC data that are applied to fit the model as inputs for the case of France and the future temperature projection and AC use scenarios. REC projection results and discussion are presented in Section 2.3, and the conclusion and policy implications are given in Section 2.4. The global flow chart of the total work is shown in Fig. 2.2.

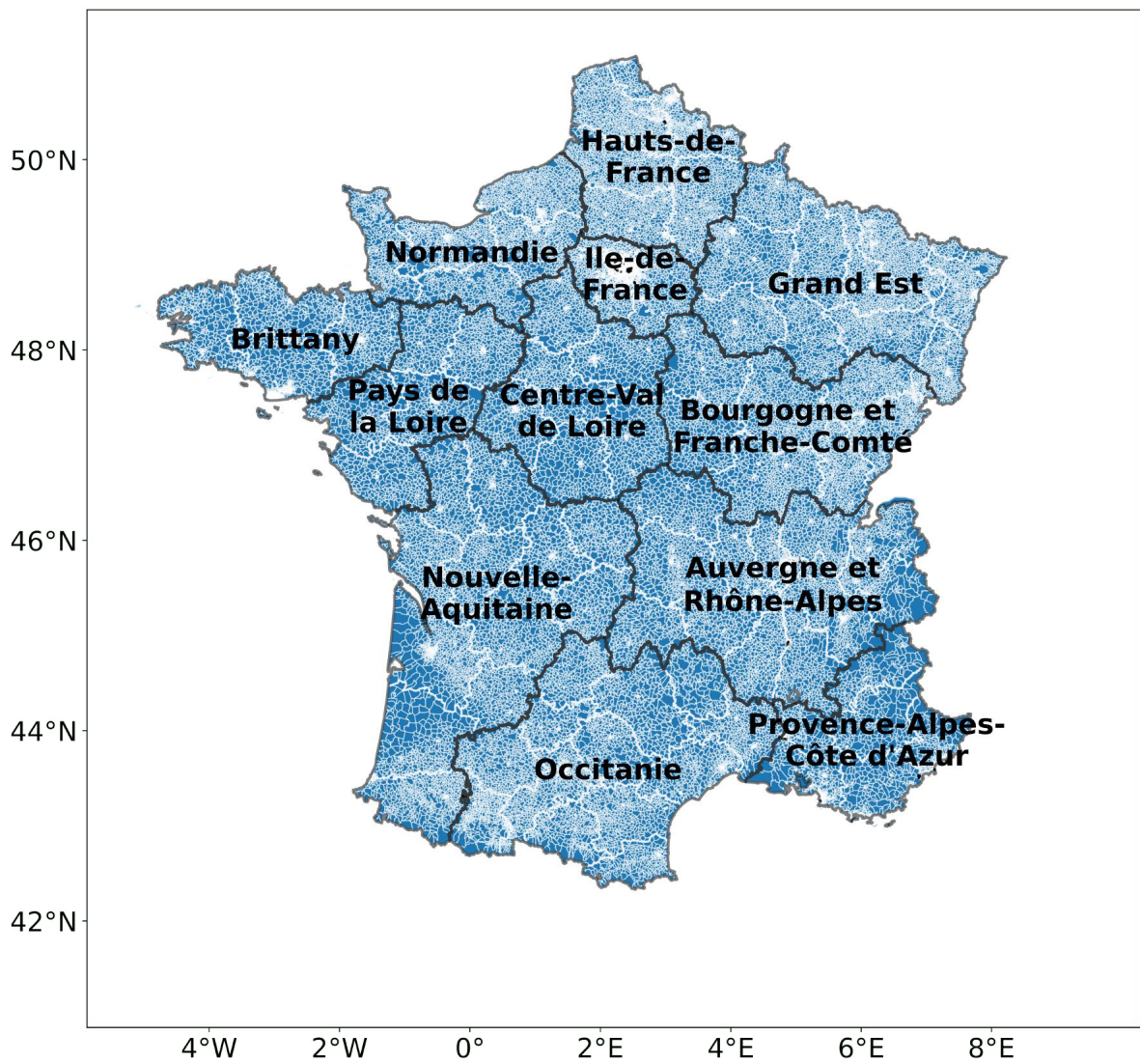


Figure 2.1 Map of 12 administrative regions of metropolitan France, with thicker white lines representing 94 departments and thinner white lines representing more than 48000 IRIS cells. (Plate carrée projection, same projection used in the presented study)

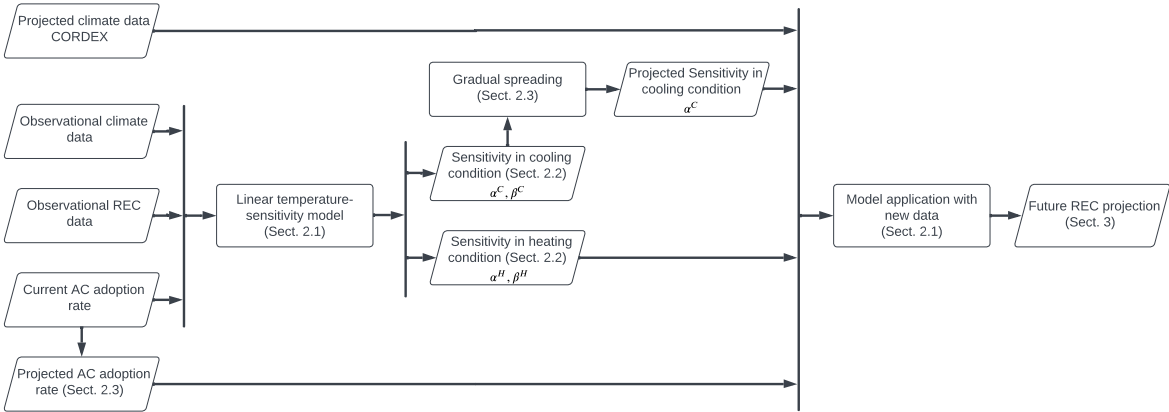


Figure 2.2 Flow chart of the present study.

2.2 Methodology and data

In this section, we explain how the REC is projected at the sub-communal scale by applying a temperature sensitivity model trained on historical data to climate projections. We also present the data for the application to France and define the scenarios used as projections of AC use with widespread adoption or saturation cases.

2.2.1 Temperature sensitivity statistical model

The relationship between the surface air temperature and the energy consumption over a domain is what we call the temperature sensitivity of the consumption. It has been modeled in various ways as presented in the previous section. The advantages of the DD approach are that it is simple to implement as a linear regression model with standard machine learning software and that it is straightforward to interpret the coefficients of the models as temperature sensitivities. For these reasons, we follow the DD approach in this study. The heating degree-days (HDD) (resp. the cooling degree-days (CDD)) for a domain is a positive quantity computed from data for the (weighted-) average temperature of the domain. It is given by the sum over a period of the degrees below (resp. above) a certain setpoint temperature per timestep. Here, the timestep d is a day and the period y a year between 2011 and 2018 (included), while different domains, or cells, i are considered, each corresponding to a different IRIS. The HDD and CDD are thus defined here as (Moral-Carcedo and Vicéns-Otero, 2005),

$$\begin{aligned} \text{HDD}_i(y) &:= \sum_{d=1}^{N_y} \max\left(0; T_i^H - T_i(y, d)\right) \\ \text{CDD}_i(y) &:= \sum_{d=1}^{N_y} \max\left(0; T_i(y, d) - T_i^C\right), \end{aligned} \quad (2.1)$$

where $T_i(y, d)$ is the daily-mean surface air temperature for a day d of year y averaged over cell i , T_i^H and T_i^C with $T_i^C \geq T_i^H$ are respectively the heating and cooling setpoints for cell i , and N_y (365 or 366) is the number of days in year y . The heating and cooling setpoints T_i^H and T_i^C are parameters to be estimated.

The REC scales with the living area in each cell. To leave out this factor, we divide the REC by the living area, giving the normalized annual REC $E_i(y)$ for cell i and year y in kWh/m². For a given scenario (see Section 2.2.3), the general temperature sensitivity model is then expressed as,

$$\begin{aligned} E_i(y) &= \beta_i^H(y) \text{HDD}_i(y) + B_i N_y + \beta_i^C(y) \text{CDD}_i(y) + \epsilon_i(y) \\ &= \alpha_i^H \eta_i^{\text{El}}(y) \text{HDD}_i(y) \\ &\quad + B_i N_y \\ &\quad + \alpha_i^C \eta_i^{\text{AC}}(y) \text{CDD}_i(y) + \epsilon_i(y). \end{aligned} \quad (2.2)$$

Table 2.1 Summary of variables and their physical meanings presented in Eq. (2.2).

Variable	Meaning
$E_i(y)$	Annual REC normalized by surface for cell i and year y (kWh/m ²)
B_i	The basic daily REC for cell i (kWh/m ²)
N_y	The number of days in a year y (365 or 366)
α_i^H	Heating temperature sensitivity for cell i (kWh/(DD m ²))
α_i^C	Cooling temperature sensitivity for cell i and year y (kWh/(DD m ²))
$\eta_i^{\text{El}}(y)$	Rate of electric heating for cell i and year y (%)
$\eta_i^{\text{AC}}(y)$	Rate of AC adoption for cell i and year y (%)
$\beta_i^H(y)$	Coefficient measuring the increase in yearly REC per HDD and unit of area for cell i and year y (kWh/(DD m ²))
$\beta_i^C(y)$	Coefficient measuring the increase in yearly REC per CDD and unit of area for cell i and year y (kWh/(DD m ²))

The first equation in (2.2) relates $E_i(y)$ to a heating, a basic, and a cooling REC (from left to right). The basic daily REC B_i (kWh/m²) is part of the REC that does not depend on temperature. It determines the REC fully when $T_i^H \leq T_i(y, d) \leq T_i^C$. In this study, we focus on the effect of climate change and the rate of air-conditioning (AC) adoption on the REC. Factors affecting the basic REC are thus assumed to remain fixed so that B_i does not depend on time. The temperature-sensitive RECs for a given year are proportional to DD. The coefficients of proportionality $\beta_i^H(y)$ and $\beta_i^C(y)$ (kWh/(DD m²)) measure the increase in yearly REC per DD and unit of area in cell i . Each cell includes residential buildings with and without electric appliances. Thus, other things remain the same, lowering the fraction η_i^{El} of residential buildings in cell i with electric heating lowers β_i^H . To estimate the temperature-sensitive electric consumption restricted to residential buildings with electric heating, β_i^H is developed as the product of η_i^{El} with the heating temperature sensitivity α_i^H (kWh/(DD m²)) of cell i . Factors affecting the heating temperature sensitivity (consumer behavior, thermal efficiency of residential buildings, etc.) are also assumed to remain fixed so that α_i^H is independent of time.

However, the rate of electric heating η_i^{El} may vary in time. Yet, the data used in this study only provides estimates of η_i^{El} for the year 2018 (Section 2.2.2.1). We therefore assume that this rate is fixed to that of 2018, $\eta_i^{\text{El}}(y) = \eta_i^{\text{El}}(2018) := \eta_i^{\text{El}}$, and so $\beta_i^H(y) = \beta_i^H(2018)$, for all years and all cells. This implies that an Ordinary Least-Squares (OLS) regression with β_i^H as coefficient and $\text{HDD}_i(y)$ as input is equivalent to an OLS regression with α_i^H as coefficient and $\eta_i^{\text{El}} \text{HDD}_i(y)$ as input. Similarly, β_i^C is developed as the product of the fraction η_i^{AC} of residential buildings in cell i equipped with AC with the cooling temperature sensitivity α_i^C (kWh/(DD m²)) of cell i . Note, however, that while all residential buildings include some form of heating so that η_i^{El} reflects the choice of heating system, all AC systems are electric, and η_i^{AC} gives the adoption rate of AC equipment. Regarding η_i^{AC} , as presented in the previous

section, the AC adoption rate has increased during the past several years and hence depends on the year during the training (Section 2.2.2.4). For future projection, both α_i^C and η_i^{AC} vary with the choice of AC use scenario, but they are assumed constant during a given period (Section 2.2.3.2).

In summary, all the parameters with their physical meanings are given in Table 2.1. For all pairs (i, y) of cells i and years y , the model inputs are

- $\eta_i^{El}(y)$ HDD $_i(y)$ and
- $\eta_i^{AC}(y)$ CDD $_i(y)$,

where HDD $_i(y)$ and CDD $_i(y)$ depend on the daily-mean temperatures $T_i(y, d)$ for all days d in y . The model coefficients are the temperature sensitivities α_i^H and α_i^C and the hyperparameters are T_i^H and T_i^C . The total number of cells is assumed to remain fixed. In the following sections, we present how this model is trained and applied to climate and AC projections to project the REC.

2.2.2 Training the temperature sensitivity model for the French REC

To apply the temperature sensitivity model to the case of France at the finest spatial scales, one needs (i) pairs of input and target historical data to train and validate the model and (ii) input data from 21st century temperature projections on which to apply the trained model to project the REC. We present the training and validation data set in this subsection while the presentation of the 21st century temperature projections is left for Section 2.2.3.

We thus need data for the inputs of the model: the yearly DD, electric-heating rates, and AC adoption rates. The former is computed from daily surface air temperatures and heating and cooling setpoints. The target $E_i(y)$ is computed from the cell's REC and living surface. Several of these variables used to compute both the inputs and the targets are taken from a dataset provided by the French distribution system operator, Enedis. We first present this dataset and then describe how it is crossed with additional data sources to produce the input and the target training data. The longest training period that the following datasets permit ranges from 2011 to 2018 (included), which is the training period we use.

2.2.2.1 Energy and building characteristics per cell

The Enedis dataset is accessed via their website (Enedis, 2020) and includes the following variables that are relevant to this study:

- longitude and latitude coordinates of the cell centroids used to assign meteorological stations to cells in Section 2.2.2.2;
- yearly REC data per cell from 2011 to 2018 (included) used as the target in Section 2.2.2.5;
- electric-heating rates η_i^{El} for 2018;

- fraction of cell buildings with surfaces in different intervals used to compute the target in Section 2.2.2.5;
- Enedis estimates of β^H using a linear model based on DD akin to the model (2.2) (see below);
- yearly HDDs used in this Enedis model since 2018, but only at the department level, thus not satisfying our needs;
- heating setpoints used to estimate the HDDs used here as described Section 2.2.2.3;

The Enedis estimates of β^H rely on consumption data at higher temporal resolutions (semi-annual, monthly, or daily) than the publicly available data. They thus can fit their temperature sensitivity model at the highest temporal resolution and average over each cell the estimated β^H for the different delivery points in the cell. However, the β^H of a cell is provided only if the estimate is considered sufficiently precise, i.e. if a minimum of 500 delivery points is available in the cell. As a result, around 50 % of the cells are missing, whereas the model (2.2) can be applied to the annual consumption data to provide estimates of the temperature sensitivities for all cells in France.

2.2.2.2 Surface temperatures for training

To train the model (2.2), we use E-OBS version 20.0 (ECA&D, 2020) of the European Climate Assessment & Data (Cornes et al., 2018; Klok and Klein Tank, 2009) (ECA&D for continental gridded surface air temperature (Haylock et al., 2008)). This gridded dataset is available at daily timesteps and a spatial resolution of 0.1° over Europe and the Mediterranean and spans from 1950 to the present. Among the available daily statistics, only the daily mean is retained here. Data observations are aggregated from several weather stations and gridded using an interpolation procedure combining spline interpolation and kriging. This dataset is a reference dataset for regional climate studies (e.g. Haylock and Goodess, 2004; Raymond et al., 2016, 2018; Santos et al., 2007; Stefanon et al., 2012) and the evaluation of regional climate models (e.g. Drobinski et al., 2018; Flaounas et al., 2013a; Frei et al., 2003; Kjellström et al., 2010; Raymond et al., 2018; Räisänen et al., 2004; Stéfanon et al., 2014; Vaittinada Ayar et al., 2016). E-OBS includes some errors and uncertainties (changes in station locations or can induce those interpolation uncertainties, for example). Flaounas et al. (2013b) assessed the E-OBS gridded dataset with temperatures displaying relatively small biases.

The temperature sensitivity model (2.2) requires temperatures for each cell to compute the HDD and CDD, but the cells (i.e. the IRIS in the case of France) do not correspond to the E-OBS grid points. We thus need to adjust E-OBS gridded temperatures to the cells over the French domain. This is done here using a nearest-neighbor interpolation using the Euclidean distance between temperature grid points and the cell centroids from Enedis (Section 2.2.2.1) in a plate carrée projected coordinate system. In order to match the target REC data from

Enedis (Section 2.2.2.1), only the E-OBS data is kept from 2011 to 2018 (included) is kept as training input.

Table 2.2 Heating setpoints T_r^H for all regions of metropolitan France computed according to Section 2.2.2.3.

Region name	T_r^H [°C]
Auvergne-Rhône-Alpes	16.0
Bourgogne-Franche-Comté	16.3
Brittany	14.8
Centre-Val-Loire	15.0
Grand-Est	16.6
Hauts-de-France	16.0
Ile-de-France	15.8
Normandie	15.0
Nouvelle-Aquaine	15.3
Occitanie	16.4
Provance-Alpes-Côte d’Azur (PACA)	17.4
Pays-de-la-Loire	15.0

2.2.2.3 Heating and cooling setpoints estimates

A couple of temperature setpoints T_i^H and T_i^C are required for each cell i in order to compute the HDDs and the CDDs in the temperature sensitivity model (2.2). The estimation of the temperature setpoints is based on those available in the Enedis dataset (Section 2.2.2.1) and which Enedis uses to compute the HDDs in their own temperature sensitivity model. In our case, the model is simplified by identifying T_i^H for each cell i in the given administrative region r of France with the average T_r^H of all the values of T^H provided by Enedis for locations in r . The heating setpoint is thus constant over each region, i.e. $T_i^H = T_r^H$ for all cells i in r , where r runs over all the administrative regions of France. The resulting T_r^H estimates are shown in Table 2.2.

On the other hand, no cooling setpoints are provided by Enedis. Instead, we fix T_i^C for all the cells in France to the value of 21 °C used by EUROSTAT and International Energy Agency.

Another approach to choose T_i^H and T_i^C could be to assume that these temperature setpoints are constant inside each region and to fit them as hyperparameters via a grid search. Doing so, it is found that the prediction error estimated via cross-validation is only marginally improved and that the main conclusions of this study remain unchanged. Considering the higher complexity of this approach, the methodology presented in the previous paragraphs of this subsection is preferred here.

Table 2.3 AC adoption rates (%) for 2011 and 2018.

Region name	η_{2011}^{AC}	η_{2018}^{AC}
Auvergne-Rhône-Alpes	4.3	17.4
Bourgogne-Franche-Comté	3.4	13.9
Brittany	2.5	10.5
Centre-Val-Loire	4.0	16.5
Grand-Est	3.4	13.9
Hauts-de-France	2.5	10.5
Ile-de-France	4.5	18.3
Normandie	2.7	11.3
Nouvelle-Aquitaine	4.3	17.4
Occitanie	5.6	22.6
PACA	10.5	41.7
Pays-de-la-Loire	2.9	12.2

2.2.2.4 AC adoption rates for training

In addition to surface temperatures, the model (2.2) requires as input AC adoption rates η_i^{AC} for each cell in France. However, this information is not available at such a small geographical scale. Based on the evolution of the national AC adoption rate (ADEME, CODA STRATEGIES, 2021) and the regional distribution data in 2019 (Daguenet et al., 2021), we estimated the regional AC adoption rates at the regional level between 2011 and 2020 and assumed that all cells inside one administration region share the same adoption rate, i.e. $\eta_i^{\text{AC}}(y) = \eta_r^{\text{AC}}(y)$. This progression in AC adoption rate during the training period is assumed to be geometric. We calculated the average ratio between different years, which indicates a growth of 20% between two consecutive years. This AC adoption rate progression ratio is assumed constant during training, i.e. $\frac{\eta_i^{\text{AC}}(y+1)}{\eta_i^{\text{AC}}(y)} = \text{constant} = 120\%$. The population-weighted national average is then compared to the reference used in ADEME, CODA STRATEGIES (2021). CODA STRATEGIES uses data from UNICLIMA (the professional union bringing together manufacturers and marketers of AC equipment in France) to estimate the national AC adoption rate from 2004 until 2020, including all types of AC equipment (mobile, heat pump). The national AC rates estimated by CODA STRATEGIES are published by ADEME (the French Agency for Ecological Transition) and are consistent with INSEE (for 2017) and EDF (for 2016 and 2019) data. At a finer scale, a study from Ecole des Ponts (Daguenet et al., 2021) calculated the regional AC adoption rate for 2019 based on data from Likibu (a house rental search engine) for over 800 households. The national population-weighted AC rate is found to be 22% for 2019, which is consistent with the EDF study and CODA STRATEGIES dataset.

These studies show that the cooling equipment market increase is not constant and has accelerated in recent years (ADEME, CODA STRATEGIES, 2021), resulting in a more geometric overall progression of about 20% per year at the country scale. From these studies, we have

regional rates for 2019 only and national rates from 2016 to 2020 from which regional rates from 2011 to 2018 are deduced assuming a spatially homogeneous progression rate. Once estimated, the national rate "population-weighted national average" is deduced from the estimate of the regional rate for the different years and compared to the reference from ADEME (EDF and INSEE). This reconstruction is consistent for 2016–2020. The estimated rate for the years 2011 and 2018 are shown in Table 2.3 with in between a geometric evolution. Errors due to this factor are not studied but should be kept in mind as a limit due to the accessibility of data.

2.2.2.5 Living area to standardize REC

The model (2.2) is trained using as targets the yearly REC data from the Enedis dataset (Section 2.2.2.1). However, we are interested in the consumption per unit of area. Moreover, the number of buildings per cell — also provided by Enedis — varies from year to year. Thus, we need to normalize each cell's REC by the corresponding total living surface. Unfortunately, Enedis does not provide the total living surface but the fraction τ_i^k of buildings in cell i for which the living surface belongs to an interval I_k in $\{(0, 30), (30, 40), (40, 60), (60, 80), (80, 100), (100, +\infty)\}$ (m²). Owing to the data constraints, we cannot get more specific information at the building level and can only present the distribution of intervals at the IRIS level. Thus, for each interval, we approximate the living surface of buildings with a surface in I_k by the center C_k (m²) of the interval, except for the first and last intervals. Due to the legal limitations on small living surfaces, we take the end value of 30 m² for the first interval rather than the median value. For the last interval, we take the finite end of the interval 100 m², primarily because we lack further information on the distribution within the interval and also to counterbalance any potential overestimation for the first interval. It's important to note that these assumptions were made out of necessity due to the data limitations, and the accuracy of these estimates could potentially be improved with data availability at the building level. Then, the average living surface is estimated from the τ_i^k provided by Enedis with the following formula:

$$\bar{S}_i = \sum_k \tau_i^k C_k \quad (\text{m}^2). \quad (2.3)$$

2.2.2.6 Trained temperature sensitivities

As an intermediate methodological result, the maps of the estimated α^H and α^C and corresponding β^H and β^C for cells with statistically significant coefficients at the 5% significance level (60% of all cells) are shown in the left and middle panels of Fig. 2.3. The OLS regression was used with a constraint on coefficients to be positive. Regression methods with regularization (Lasso and Ridge) were also tested, but this led to an increase in the test R² score of less than 10%, so the OLS was preferred to limit the number of parameters of the model. All the test scores are estimated using k-fold cross-validation with one fold per year of data (8 folds in

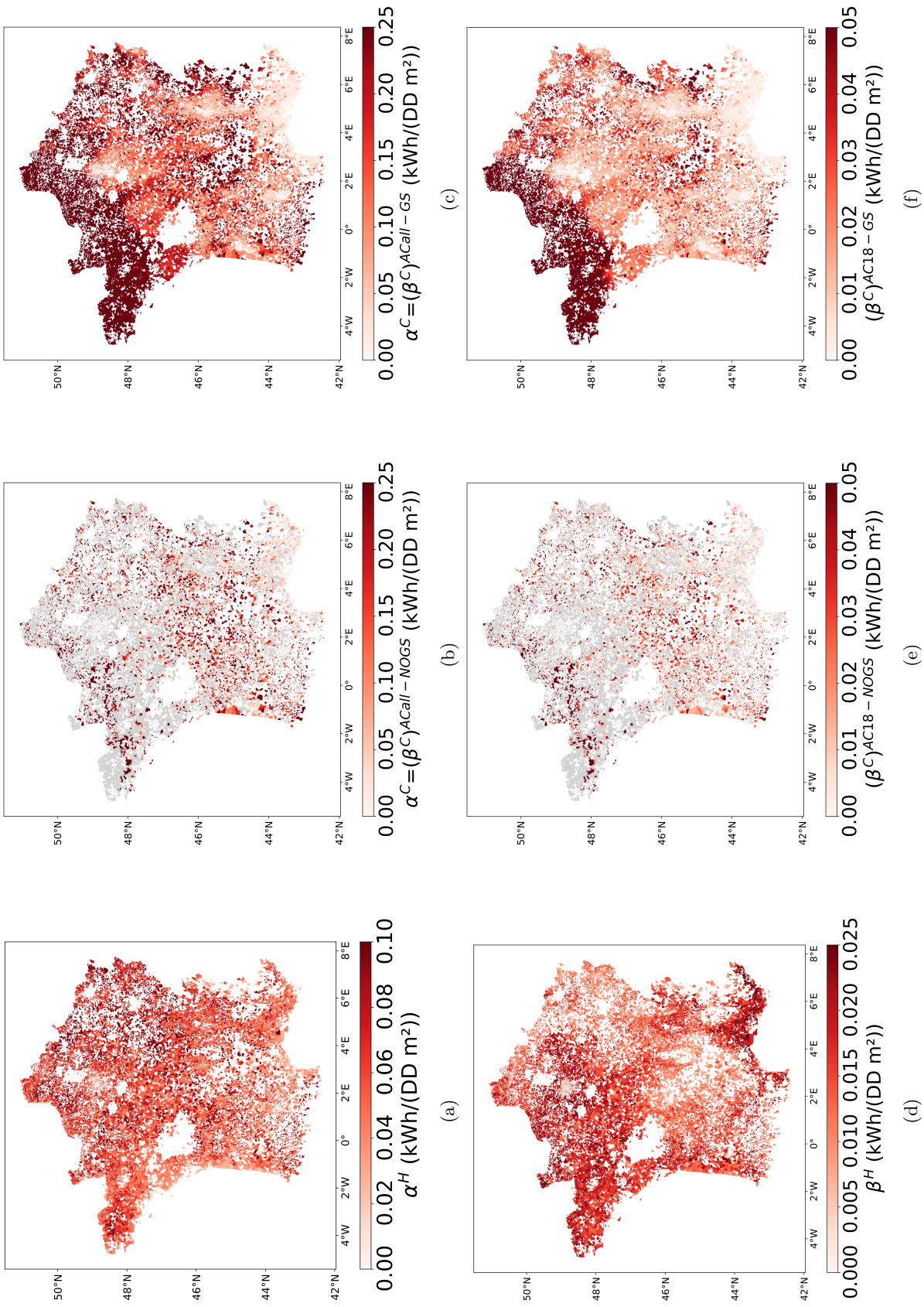


Figure 2.3 Top: Estimates of α^H (left) and α^C (middle) obtained by training the model (2.2) on the observational data (Section 2.2.2). Projections of α^C (right) by gradual spreading (Section 2.2.3.2). Bottom: Corresponding values of β^H (left) and β^C (middle), and projections of β^C (right) for the AC2018 scenario (Section 2.2.3.2).

total). The test R^2 score averaged over all cells is about 0.68 with a 25% quartile of 0.56 and a 75% quartile of 0.79.

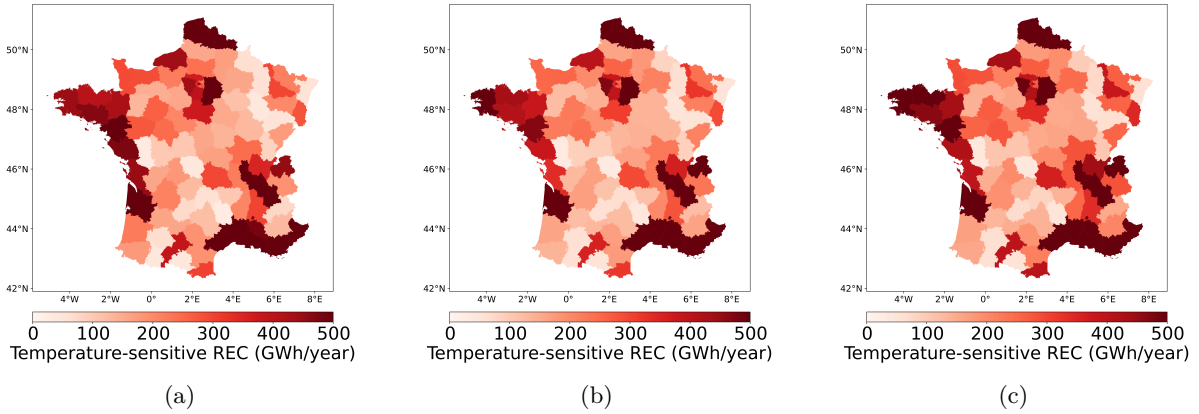


Figure 2.4 Temperature-sensitive REC per year averaged over departments estimated from (a) the Enedis β^H estimates for 2018 (for 50% of the cells only, Section 2.2.2.1), (b) the model (2.2) applied to the E-OBS temperatures for 2018 and (c) the model (2.2) applied to the CORDEX historical temperatures over the 1975–2005 period and averaged over the period and over the climate-model simulations (Section 2.2.3.1).

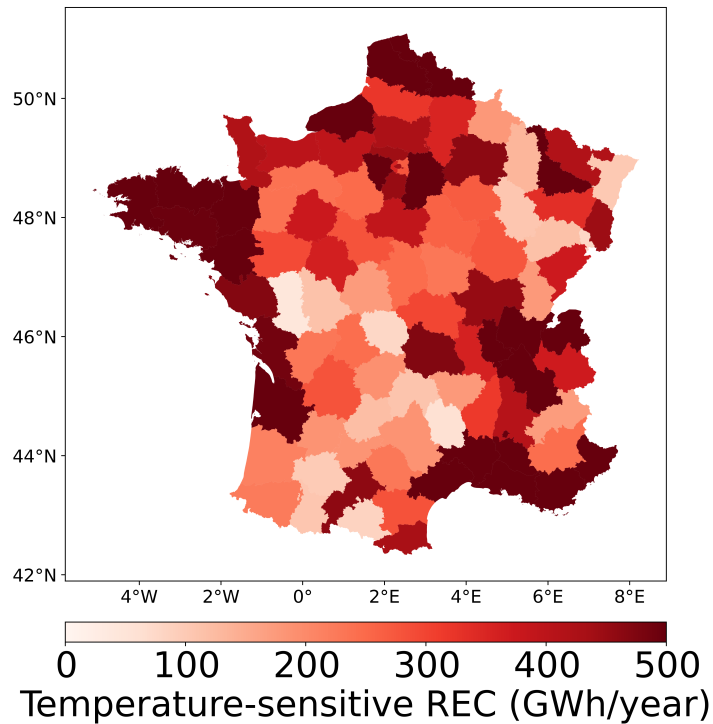


Figure 2.5 Total temperature-sensitive REC reference aggregated at the department level, estimated with our model using the temperature of 1975–2005 from CORDEX simulations on all valid cells (60% of the cells).

Fig. 2.4 shows the temperature-sensitive REC aggregating over the 12 administrative regions

the values at the IRIS where such estimate by Enedis exists from Enedis processing (a), by applying the model (2.2) to temperatures from E-OBS dataset (b) and historical CORDEX simulations (c). Visually, the three show a very similar pattern. Fig. 2.4a and Fig. 2.4b illustrate the quality of the model prediction and quantitatively a R^2 score of 0.77 is found between the common cells. Fig. 2.4c shows how historical climate simulations can satisfactorily reproduce the temperature-sensitive REC for climate projection studies which rely on the climate projections produced in a consistent way with the historical climate simulations.

However, in Section 2.3, the temperature-sensitive REC based on the CORDEX regional climate simulations is estimated over a larger number of IRIS than those of the Enedis subset. At the IRIS kept in the dataset, the estimates of α^H and α^C passed a significance test. The reference REC for the period 1975–2005 used to calculate the change of temperature-sensitive REC is shown in Fig. 2.5.

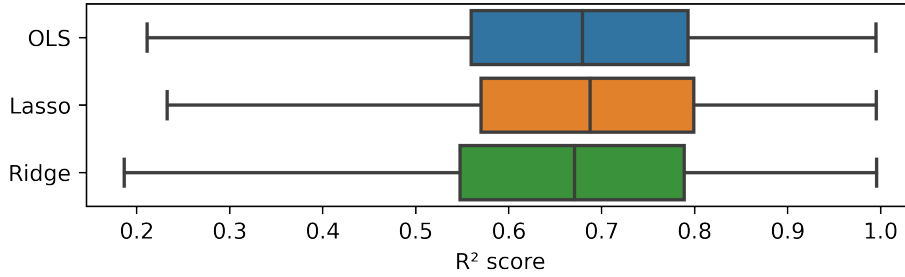


Figure 2.6 Comparison between linear regression methods of R^2 score distribution for all valid IRIS.

During the present study, for each cell we have 8 years of annual REC as inputs to train the model described in Eq. (2.2). The Leave-One-Out cross-validation method has been used to fit the model and to validate the model's performance. Each time we extract one year out as test and train the model with the other 7 years' data and get the prediction using the one test data. And this procedure repeats 8 times. After that, the 8 predicted values with the test data are compared to their initial values, which gives us a test R^2 score. Such test is done for all the cells and a significance test is also performed to get the valid cells. A comparison of different linear regression models has been made with this test method and the distribution of related test R^2 scores are shown in Fig. 2.6.

2.2.3 Projection data and scenarios definitions

As mentioned in Section 2.2.1, the basic consumption, represented by B in (2.2), is assumed to be stationary all the time. As far as the heating REC is concerned, we assume that α^H , T^H and η^{El} are also stationary so that only the HDDs change in response to temperature changes. Regarding the cooling REC, we follow a similar approach as for the heating REC, but η^{AC} and α^C also change in some AC scenarios (T^C is always stationary). We thus need to associate

Info box: Enedis temperature sensitivities.

Enedis provides annual electricity consumption data at different geographical scales such as IRIS, Municipality, Department, and Region. Enedis also provides their estimated electrical temperature sensitivity by sector of activity for these geographical scales. These datasets can be downloaded free from their website in Excel format [Enedis \(2018\)](#). In order to avoid bias linked to seasonal or weekly variations in consumption, Enedis uses an estimation methodology called "Estimation of gradients by difference," which explains a variation in consumption by a variation in temperature. Thus, Enedis estimates the following linear relationship using the least-squares method (OLS):

$$\Delta\text{Consumption} = \textit{Gradient} * \Delta\text{HDD} \quad (2.4)$$

where the gradient is the estimated temperature sensitivity for each delivery point and the calculation of the difference in consumption depends on the type of the statement for the delivery point. Three different types of statements exist semi-annual, monthly, and daily. For delivery points where the majority statement is not daily, the statement is converted to average daily consumption by dividing the total number of days for the specific period. The temperature sensitivity at the IRIS scale is simply the sum of all the temperature sensitivity at delivery points of the IRIS. However, the data related to the temperature sensitivity estimated by Enedis are only published for an IRIS when the estimate is considered sufficiently precise. In order to guarantee precision, Enedis sets a minimum number of delivery points per IRIS of 500. Hence, the temperature sensitivity information is unavailable for all the IRIS by Enedis. Around two third of the IRIS lack such information. During the comparison of the results of our model and the temperature sensitivity parameters given by Enedis, all the IRIS with missing values will be eliminated. However, while the projection of future electricity consumption, estimated coefficients with our model for all the IRIS will be conserved once the training score is positive. It is crucial to notice that the daily datasets that Enedis uses as input for their temperature sensitivity model are not available for our study. In many countries, only the annual energy consumption is captured, and the daily data are not accessible.

each cell with a temperature projection for a given climate change pathway, as well as with projections of η^{AC} and of a^{C} .

2.2.3.1 Temperature projection data under a climate change pathway

In this study, the most severe climate change pathway, the Representative Concentration Pathways (RCP) 8.5, is selected. The corresponding bias-corrected daily-mean temperature change is obtained from multiple regional climate models from the CORDEX program. In this study, these projections are completed with the corresponding historical experiments that serve as a reference to measure the effect of climate change. Due to modeling uncertainty, the projected statistics of the atmosphere may vary significantly with the choice of Regional Climate Model (RCM) and of driving Global Climate Model (GCM). Hence, multi-model ensembles are commonly used in climate studies to provide a partial estimation of the modeling error. This is why the five model combinations listed in Table 2.4 are used in this study. These simulations are accessed via the Copernicus Climate Change Service database (<https://climate.copernicus.eu/>).

Table 2.4 Institute, GCM name and RCP name for the 5 climate change simulations used in this study.

No.	Institute	Driving GCM model	RCM model
1	CNRM	CERFACS-CM5	ARPEGE51
2	CNRM	CERFACS-CM5	RCA4
3	IPSL	CM5A-MR	RCA4
4	IPSL	CM5A-MR	WRF331F
5	ICHEC	EC-EARTH	RACM022E

To associate a cell to a climate-model simulation, the same methodology as for the temperature observations used for training is followed (Section 2.2.2.2). Three climate-simulation periods of 30 years are considered, which are distinct from the training period defined in Section 2.2.2: a historical period from 1975 to 2005 (excluded) — used as reference — and two projection periods, one from 2025 to 2055 and one from 2070 to 2100. Results associated with the latter are respectively referred to as CC2040 and CC2085 (based on the central year of the period).

As intermediate methodological results, mean historical HDD and CDDs, as well as the corresponding projected changes, are represented in Fig. 2.7. One can see that the temperature increase projected over France leads to a general decrease in the HDDs (top panels) and to a general increase in the CDDs. These changes are however not homogeneous since the decrease in the HDDs is strongest in the southern and eastern parts of France, while the increase in the CDDs is largest in the southern part of France.

2.2.3.2 AC use scenarios

In the present framework, two factors are sensitive to the evolution of AC use during the 21st century: the AC adoption rate η_i^{AC} , and the switch of a cell from an α_i^{C} of zero to a positive α_i^{C} , for each cell i . While the former reflects the evolution of AC use within a cell, the latter corresponds to a conversion of a cell from having no AC user at all to having some AC users. Here, we do not attempt to make plausible projections of these factors based on current signals. Instead, as summarized in Table 2.5 and explained below, two extreme cases are considered for both factors and indifferently for the 2025–2055 and the 2070–2100 periods.

Table 2.5 Definition of the four AC scenarios in terms of AC adoption rate and α^{C} spreading strategy. XXXX is either 2040 or 2085, corresponding to the central year of the climate change projection window considered.

Name	Definition	
	η^{AC}	Gradual Spreading of α^{C}
CCXXXX-AC18-NOGS	Same as in 2018	No
CCXXXX-AC18-GS	Same as in 2018	Yes
CCXXXX-ACall-NOGS	100%	No
CCXXXX-ACall-GS	100%	Yes

Regarding η^{AC} , the minimal scenario is that η^{AC} remains fixed to its 2018 cell values (Section 2.2.2.4), corresponding to a situation in which AC installation no longer progresses. The maximal scenario is that η^{AC} has reached 100% in every cell before the beginning of the projection period and remains fixed over the period, corresponding to a situation in which all households are equipped with AC (regardless of the technology).

Regarding α^{C} , the minimal scenario is that cells with no cooling temperature sensitivity remain so. The maximal scenario is that all cells become cooling-sensitive. In this case, further assumptions are needed to determine α^{C} for these cells that were not cooling-sensitive historically. Here, we assume that α^{C} for these cells is the result of interpolation from the α^{C} values of the surrounding cells with a positive α^{C} . A nearest-neighbor interpolation is performed for a given number of neighbors and for the Euclidean distance in the plate carrée projection.

With the historical REC data, around 60% of the cells are estimated with zero current cooling temperature sensitivity (i.e. $\alpha_i^{\text{C}} = 0$). As described in Section 2.2.3.2, so-called Gradual Spreading is our way of estimating future α^{C} based on an interpolation assumption of actual values, especially for cells without current α^{C} . For cells with positive non-null cooling temperature sensitivity, the future cooling temperature sensitivity is assumed to be consistent with the current value (i.e. $(\alpha_i^{\text{C}})^{\text{GS}} = \alpha_i^{\text{C}} > 0$), while for other cells without current α^{C} , a

nearest-neighbor interpolation is performed with the following formula:

$$(\alpha_i^C)^{GS} = \frac{1}{J} \sum_{j=0}^{J-1} \alpha_j^C.$$

For a studied cell i , all the cells with current non-null sensitivity $\alpha_j^C > 0$ are ordered by the Euclidean distance with the given cell in the plate carrée projection, and J is the number of nearest cells taken into account for the calculation of the average.

This assumption has been tested with the group of cells where α^C are estimated non-null in the first place. During the test, 60% of these cells are selected randomly to become zero, conforming to the actual situation, and are given an estimation with the Gradual Spreading method. Then the estimated values with Gradual Spreading are compared with the model's initial estimation α^C . This process repeats 30 times for each J , and the average test R^2 score as a function of the number of neighbors J is given in Fig. 2.8. It can be seen clearly that there exists a local similarity: the test R^2 score is larger when $J \in [10, 60]$. In our study, the optimal value for J is 25. Despite selecting the optimal number of cells per cluster based on evidence of local similarity through a pre-test, the resulting prediction R^2 score remains low (below 0.23). This uncertainty in the future assumption of the coefficient α^C remains a limitation of the scenario study with the Gradual Spreading approach.

We refer to this scenario as the gradual spreading of α^C , and the resulting α^C estimates are shown in Fig. 2.3c. The gradual spreading scenario mimics a "do like my neighbor" behavior.

2.2.4 Quantifying the uncertainty in the projected REC change

For a given cell i , a model m (Table 2.4) and a scenario s (Table 2.5), we define the absolute change in REC, $\Delta \bar{E}_i^{m,s}$, as the difference (Δ) at i between the REC averaged ($\bar{\cdot}$) over the CORDEX historical period and the REC averaged over one of the two CORDEX projection periods, estimated with the model m simulations for the scenario s . In addition, the relative REC change is defined as the absolute REC change divided by the REC averaged over the CORDEX historical period. Given the stationarity assumptions (Section 2.2.3), the absolute REC change is given by

$$\begin{aligned} \Delta \bar{E}_i^{m,s} &= \alpha_i^H \eta_i^{\text{El}} \Delta \left[\overline{\text{HDD}}_i^{m,s} \right] \\ &+ \Delta \left[\left(\alpha_i^C \eta_i^{\text{AC}} \right)^s \overline{\text{CDD}}_i^{m,s} \right]. \end{aligned} \quad (2.5)$$

In the AC18-NOGS scenario, α^C and η^{AC} are also stationary, so that

$$\begin{aligned} \Delta \bar{E}_i^{m,s} &= \alpha_i^H \eta_i^{\text{El}} \Delta \left[\overline{\text{HDD}}_i^{m,s} \right] \\ &+ \left(\alpha_i^C \eta_i^{\text{AC}} \right)^{\text{AC18-NOGS}} \Delta \left[\overline{\text{CDD}}_i^{m,s} \right], \end{aligned} \quad (2.6)$$

in this case.

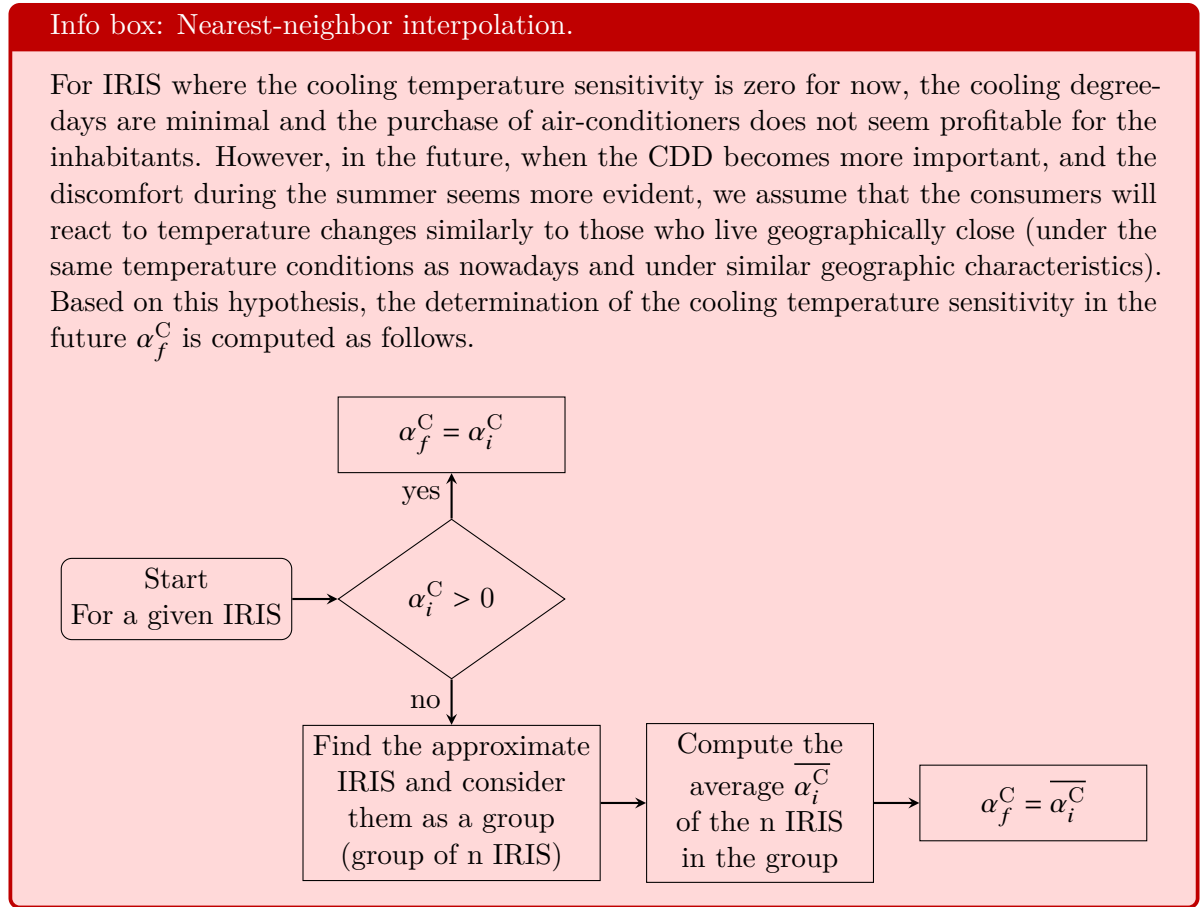


Figure 2.9 Flowchart for determination of cooling needs for each IRIS with our hypothesis, α_i^C refers to the cooling temperature sensitivity estimated with observational consumption data and α_f^C refers to the future temperature sensitivity.

The corresponding multi-model average is

$$\langle \Delta \bar{E}_i^s \rangle := \frac{1}{M} \sum_{m=0}^{M-1} \Delta \bar{E}_i^{m,s}. \quad (2.7)$$

An essential part of this study is quantifying the uncertainty of our estimates of temperature-sensitive REC change $\langle \Delta \bar{E}_i^s \rangle$. From (2.7), we can see that errors may come from

- the temperature sensitivity model design,
- the stationarity assumptions on the model coefficients and on electric appliances adoption rate η_i^{El} and η_i^{AC} during scenarios studies,
- the regression of the coefficients from a particular training dataset,
- the historical estimates of η_i^{El} and η_i^{AC} ,
- the climate models (Jacob et al., 2014; Ruti et al., 2016),
- the choice of climate change pathway and AC use scenario.

Here, only the worst-case climate change pathway is considered (i.e. RCP8.5, Section 2.2.3.1), so that uncertainty in the climate-model pathway is not assessed. On the other hand, a partial estimate of climate-model errors is provided in the results Section 2.3 from the variations of the projected REC change with the choice of the climate model. To estimate the sensitivity of temperature-sensitive REC change to AC adoption rate projections, extreme scenarios are considered (Section 2.2.3), while measurements of the electric-heating rate are assumed to be reliable and representative of other years than the year it is provided for. The assumption of the stationary temperature sensitivity model coefficients restricts the scope of the results of this study. It is not tested in-depth in this work, but a simple analysis is conducted in Section 2.3.2 and further discussed in terms of policy implications in Section 2.4. Finally, the errors from the model design and the regression are estimated using cross-validation (Section 2.3.4).

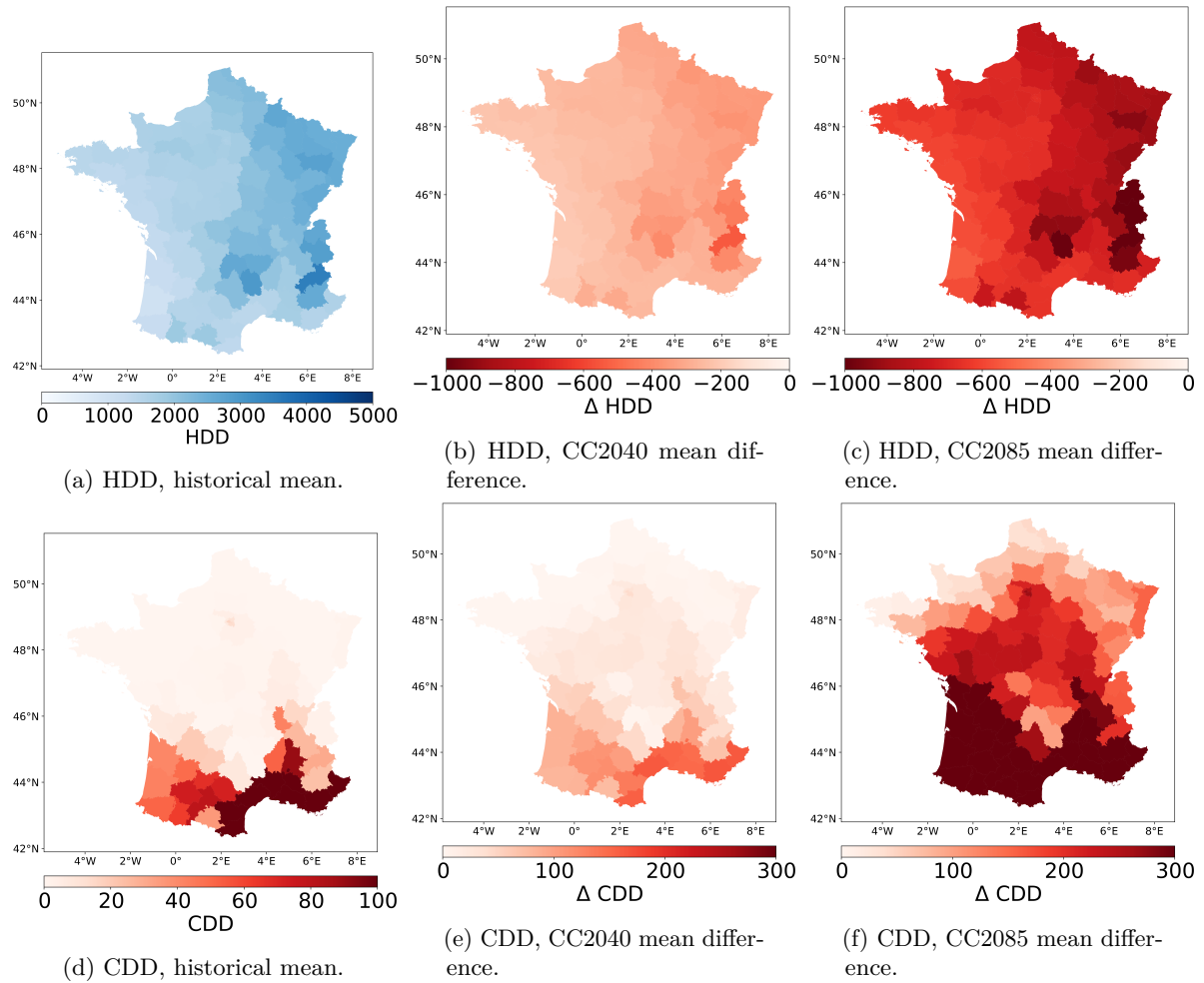


Figure 2.7 Mean over 1975–2005, mean change over 2025–2055 wrt. 1975–2005 (CC2040), and mean change over 2070–2100 wrt. 1975–2005 (CC2085) for the HDDs (top) and CDDs (bottom) computed according to Eq. (2.1). The temperature data for 1975–2005 is from the historical CORDEX simulations, while that for 2025–2055 and 2070–2100 is from the RCP8.5 CORDEX simulations. The results are spatially averaged over the departments and averaged over the climate-model simulations listed in Table 2.4. Warm colors represent situations associated with warm temperatures (i.e. to a decrease in heating REC and to an increase in cooling REC).

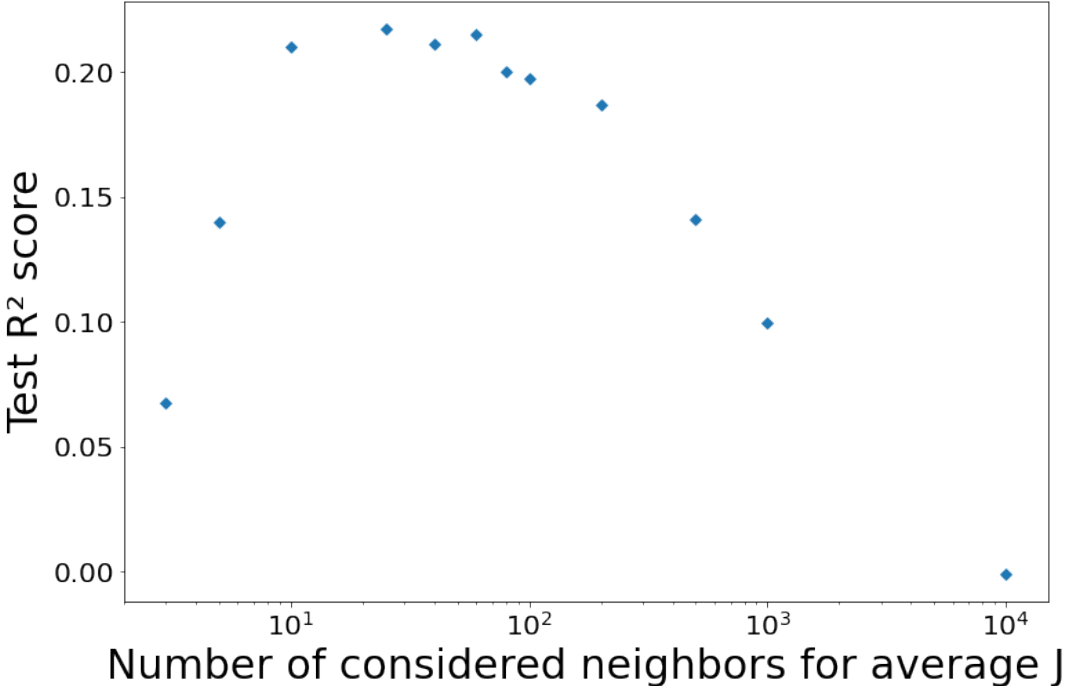


Figure 2.8 Test R² score between estimated α_i^C with Gradual Spreading method and regression model estimation as a function of the chosen number of neighbors J taken into account for the calculation of average (Gradual Spreading).

2.3 Results and discussion

We now analyze the projected changes in the REC, first for the scenarios where the AC uses remain fixed, then for scenarios with AC uses changes. The discussion of the uncertainty in the results is left for the next Section 2.4, the main conclusions from these results being robust.

2.3.1 Projected REC change without change in AC use

The projections of temperature-sensitive REC changes for fixed AC use (AC18-NOGS) are shown in Fig. 2.10a and Fig. 2.11a. In general, the REC decreases between 7% and 16% in all departments for CC2040, down to 20% to 42% for CC2085. Aggregated at the country scale, the REC decreases by about 8 TWh and 20 TWh, respectively. This is consistent with the results of Damm et al. (2017); Spinoni et al. (2018), but significant variations are observed between departments.

For this scenario and for a given cell, according to (2.6), the projected heating and cooling REC changes are proportional to the HDD and CDD changes, respectively, represented in Fig. 2.7. However, the coefficients of proportionality, $\alpha_i^H \eta_i^{El}$ and $(\alpha_i^C \eta_i^{AC})^{AC18-NOGS}$, represented in Fig. 2.3, depend on the cell. From this can be deduced that the REC changes for this scenario are dominated by the large decrease in the HDDs (Fig. 2.7b and Fig. 2.7c) modulated by variations in β^H with the cells (Fig. 2.3d). This effect can for instance be seen in the weaker reduction of the REC in the North-East and the South-West of France.

In addition, the REC decrease is reduced in the south of France due to the significant increase in the cooling REC with the increase in the CDDs (Fig. 2.7e and Fig. 2.7f) in conjunction with the positive β^C there (Fig. 2.3e). This is more obvious from the plots of the cooling REC for the AC18-NOGS scenario in Fig. 2.13a and Fig. 2.14a. One can see that, according to this scenario, the cooling REC increases everywhere, but this is particularly evident along the Atlantic coast and South of 46°N latitude, between the Massif Central and the Alps, especially for the CC2085 period. At these locations, HDDs indeed tend to increase significantly, but the correlation is not perfect, since, for this scenario, the translation of this change in a cooling REC change depends on AC being already in use there (Fig. 2.3e). A substantial increase in the cooling REC is also observed in the Northwest part of France for CC2085 (Fig. 2.14b), even though the increase in CDDs is relatively weak there (Fig. 2.7f). This is explained by the fact that a significant number of cells there have a large β^C (Fig. 2.3e).

The distribution of the temperature-sensitive REC change at the cell level is shown in Fig. 2.12 in the form of box plots. The distribution for scenario CC2040 without AC use changes (AC18-NOGS) is right-skewed, meaning the temperature-sensitive REC is expected to decrease around 15% in most regions. In the longer term, the disparity between IRIS increases with decreasing averaged temperature-sensitive REC. Indeed, some IRIS may display a positive temperature-sensitive REC change (i.e. an increase in temperature-sensitive REC) over 3% of the French territory in the near future and up to 7% by the end of the 21st century.

2.3.2 Projected REC change with change in AC use

The projections of temperature-sensitive REC change with different AC scenarios are shown in Fig. 2.10b-2.10d and Fig. 2.11b-2.11d. Contrary to the results including temperature change only, some regions display an increase of temperature-sensitive REC whose pace and spatial extent depend on the AC scenario.

Results also show that the different factors have diverse effects. In the case where the AC rate is changed without spreading geographically, the temperature-sensitive REC is expected to increase in the South-West of France and in the South along the Mediterranean Sea (Fig. 2.10b and Fig. 2.11b). Indeed, in this region, α^H is relatively low with respect to other regions, and AC systems are already deployed so that α^C is different from zero. But α^C in these regions has a relatively low value, so if the temperature change is only accounted for, increased CDD makes the decline in temperature-sensitive REC less rapid. However, in the considered scenario, the change in AC rate directly multiplies the current cooling demand by four to five times. The electricity savings from heating in the South-West are thus expected to be fully offset by cooling in the near future (Fig. 2.13b). In the far future, this trend should be exacerbated in the South-West and in the South and spread significantly along the Atlantic coast and South of 46°N (Fig. 2.14b). As there is no spatial spreading of AC usage, the geographical patterns of temperature-sensitive REC change are similar between Fig. 2.13a and Fig. 2.14a, and Fig. 2.13b and Fig. 2.14b.

With regards to the AC rate scenario, the gradual spreading of the present AC rate lowers the change of REC for cooling needs, but REC for cooling needs becoming positive spreads geographically (Fig. 2.10c and Fig. 2.11c). Gradual spreading does not change the values instantly in regions where most IRIS cells are already given with non-null estimation for α^C . However, it helps to smooth the map of coefficients as shown in Fig. 2.3b and Fig. 2.3c. Based on observational data, many cells in Ile-de-France, Auvergne-Rhône-Alpes, and along the Atlantic coast have been given null estimates for α^C . However, some nearby cells still received significant values for α^C with high regression scores. Assigned with proximity averages, these areas mixed with sporadic large values are most affected.

Fig. 2.12 shows that a 100% AC rate in already equipped cells (ACall-NOGS) modifies the shape of the distribution, with an increased number of cells with positive evolution. More positive values correspond to the cells currently equipped with AC at which the AC rate is increased from its current value to 100% and where the change of REC for cooling needs exceeds that for heating needs. No change is expected for the cells currently without AC hence the minimal, the first quartile even the median values remain the same as for AC18-NOGS. In the gradual spreading scenario (AC18-GS), the shape of the distribution displays an even larger positive skewness than in the 100% AC rate scenario. Less negative values correspond to the larger number of cells equipped with AC and bring an increase to all cells.

In a scenario combining gradual spreading and 100% AC rate, almost half of the territory,

except the North of France, sees the REC increasing in the near-term future, amounting to a global change of +2%. At the end of the 21st century, this fraction of positive trend increases up to 90%, leading to a global change of +32%.

The results of these scenarios motivate actions allowing at least to prevent AC from inducing an increase in cooling REC. A simple approach, applicable to the whole country, consists at least in the region of South of France with the greatest AC impact to modify in the future climate scenarios only the cooling setpoint in such a way as to maintain the cooling REC unchanged with respect to the present situation. Such an approach leads to the most constraining action as it sets for the whole country the highest cooling setpoint, but it ensures at least unchanged cooling REC in the South of France and in most regions of France a negative cooling REC trend. The cooling setpoint preventing any cooling REC increase over the whole country varies with the time horizon, which is about 23-24°C by 2040 and 26-27°C by 2085.

2.3.3 Spatial heterogeneity

The maps shown in Fig. 2.3 and Fig. 2.10 and Fig. 2.11 show an apparent geographical disparity of temperature sensitivities and temperature-sensitive REC changes. To compare the intra-department variability with the one of inter-department, each studied variable y_i (sensitivity coefficients α_i^H , α_i^C , DD evolution $\langle \Delta \overline{HDD}_i^s \rangle$, $\langle \Delta \overline{CDD}_i^s \rangle$ and the REC evolution $\langle \Delta \overline{E}_i^s \rangle$) can be decomposed as:

$$\begin{aligned}
 y_i &= (y_i - \langle y_i \rangle_d) \\
 &+ (\langle y_i \rangle_d - \langle y_i \rangle_r) \\
 &+ (\langle y_i \rangle_r - \langle y_i \rangle_n) \\
 &+ \langle y_i \rangle_n.
 \end{aligned} \tag{2.8}$$

with $\langle y_i \rangle_d$ the average value of cells inside a given department, $\langle y_i \rangle_r$ the average value of cells inside a given administrative region, and $\langle y_i \rangle_n$ the average value of all cells in France. Hence with the above equation, the variability of all cells can be decomposed into disparities at several stages:

$$\begin{aligned}
 \sigma^2(y_i) &= \sigma^2(y_i - \langle y_i \rangle_d) \\
 &+ \sigma^2(\langle y_i \rangle_d - \langle y_i \rangle_r) \\
 &+ \sigma^2(\langle y_i \rangle_r - \langle y_i \rangle_n).
 \end{aligned} \tag{2.9}$$

where $\sigma^2(y_i - \langle y_i \rangle_d)$ represents the variability of cells inside the department while $\sigma^2(\langle y_i \rangle_d - \langle y_i \rangle_r)$ represents the variability of departments inside a given administration region and $\sigma^2(\langle y_i \rangle_r - \langle y_i \rangle_n)$ the variability between different administrative regions. Table 2.6 shows the proportion of variability at each geographical scale over the whole variability.

Table 2.6 Decomposition of variability into different geographical scales for different studied variables in terms of proportion (%).

Variable y_i	$\frac{\sigma^2(y_i - \langle y_i \rangle_d)}{\sigma^2(y_i)}$	$\frac{\sigma^2(\langle y_i \rangle_d - \langle y_i \rangle_r)}{\sigma^2(y_i)}$	$\frac{\sigma^2(\langle y_i \rangle_r - \langle y_i \rangle_n)}{\sigma^2(y_i)}$
β_i^H	75%	13%	12%
α_i^C	77%	4%	19%
$\langle \overline{\Delta HDD}_i \rangle^{CC2040}$	24%	20%	56%
$\langle \overline{\Delta HDD}_i \rangle^{CC2085}$	29%	23%	48%
$\langle \overline{\Delta CDD}_i \rangle^{CC2040}$	13%	15%	72%
$\langle \overline{\Delta CDD}_i \rangle^{CC2085}$	14%	13%	73%
$\langle \overline{\Delta E}_i \rangle^{AC18-NOGS}$	82%	7%	11%

The regional variability is more important than the local difference for the DD changes. However, the variability of temperature sensitivities between cells within the same department dominates. At the same time, because of the large spatial variability of β^H and α^C within the administrative regions, a larger disparity of temperature-sensitive REC changes is found between cells than between administrative regions. For both temperature sensitivities, β^H and α^C and temperature-sensitive REC changes, it shows that the variability between the cells is more significant than the difference between regions, which justifies our choice of study at a small geographical scale.

2.3.4 REC change error estimates

In this study, public data are used to train the temperature sensitivity model with only eight annual samples applied for the regression. Compared to models with a larger dataset, our model can be easily influenced by outliers and may have coefficients over-fitted.

We did not choose regularized regression because the performance did not improve much, but this method may be more attractive if a more extensive input is available. Nonetheless, the possibility of applying the leave-one-out cross-validation over the training gives us eight possible models and, thus, a range of eight different results of the temperature sensitivities with uncertainty.

At the same time, CORDEX simulations from different models may produce different future temperature projections. Combining the five different simulations and all possible estimated coefficients with the leave-one-out cross-validation method, the global uncertainty of our results, quantified by the Relative Standard Deviation (RSD), is shown in Fig. 2.15. The relative error is large in the South-West, where $\alpha^C > 0$, due to the biased model regressions as the observed temperatures do not largely and frequently exceed the 21°C cooling setpoint.

The global uncertainty for all the scenarios is presented in Table 2.7. The standard deviation is identified after aggregating REC at different levels. For the results to have the same order of

40

magnitude and to be comparable, the REC change is normalized by the average number of IRIS in the desired geographical scale. The method using a REC linear model together with the CORDEX simulations derives robust estimates of future REC with an error of less than 18.4% without assumptions on AC uses. The uncertainty of scenario ACall-GS is the largest among all other scenarios because the results may become less precise with all the assumptions together. We can see clearly that with spatial aggregation, the error decreases because there can be compensation between IRIS within the large scales, and the variation becomes smaller. For the average values of all possible combinations, a t-test shows that the mean values of REC change under all scenarios are significant.

The global error of future REC mainly comes from the multi-model ensemble spread of the projected temperatures and the training bias and variance of the REC linear model. To find the standard deviation due to different sources, we use the average values of the cross-validated coefficients estimated by the model or the average of the five simulations of CORDEX, respectively. The uncertainty due to the simulations of CORDEX and to the model regression can be found in the following Table 2.8.

Table 2.7 Average values with uncertainty for all possible combinations, the uncertainty is converted to the same magnitude by averaging over the number of cells. A t-test shows that mean values of REC change under all scenarios are significant.

Time	Scenario name	Mean (GWh/cell)	Std (GWh/cell)		
			Cell	Department	Country
2040	CC-AC18-NOGS	-0.22	0.037	0.029	0.024
	CC-AC18-GS	-0.16	0.053	0.038	0.031
	CC-ACall-NOGS	-0.16	0.066	0.042	0.032
	CC-ACall-GS	0.08	0.191	0.146	0.125
2085	CC-AC18-NOGS	-0.53	0.085	0.057	0.047
	CC-AC18-GS	-0.28	0.185	0.150	0.136
	CC-ACall-NOGS	-0.26	0.236	0.159	0.138
	CC-ACall-GS	1.26	1.019	0.867	0.790

With the previous tables, we can see clearly that the uncertainty due to the various simulations of CORDEX leads to a more significant error than the one from the regression. This 10% error due to the model is reassuring the basis of a temperature sensitivity model: the temperature sensitivity is quasi-constant under a stable climate. Nevertheless, this error can still be improved if more annual consumption data are available or daily consumption data can be accessible.

Table 2.8 Comparison of uncertainty due to model or CORDEX for scenario AC18-NOGS in the form of standard deviation (GWh/cell).

Time	Cell		Commune		Country	
	Model	CORDEX	Model	CORDEX	Model	CORDEX
2040	0.020	0.034	0.012	0.029	0.010	0.022
2085	0.056	0.066	0.031	0.052	0.026	0.040

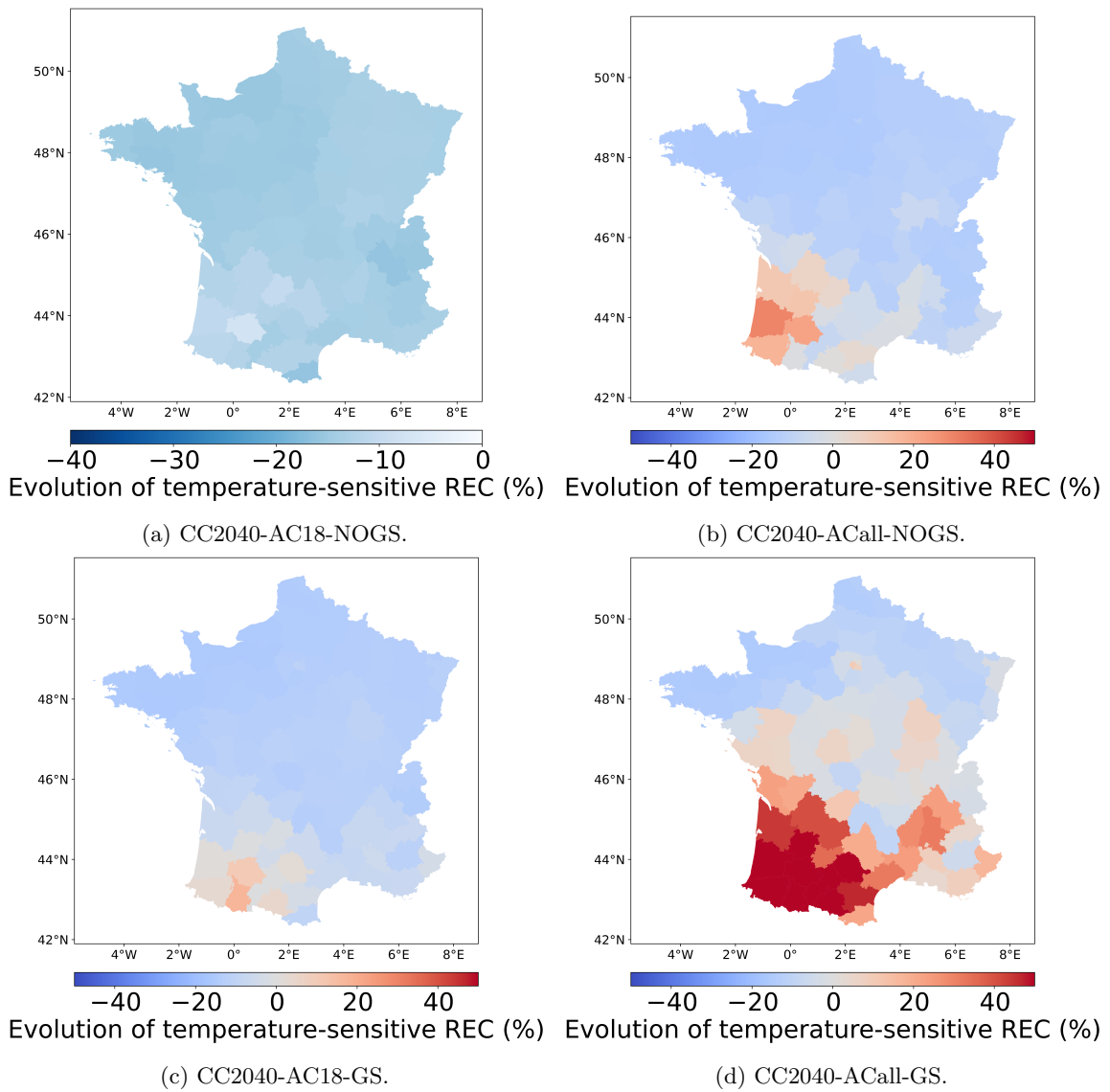


Figure 2.10 Relative change (%) in REC wrt. to the historical period (1975–2005) for CC2040 and for different AC scenarios: AC18-NOGS (a), ACall-NOGS (b), AC18-GS (c) and ACall-GS (d).

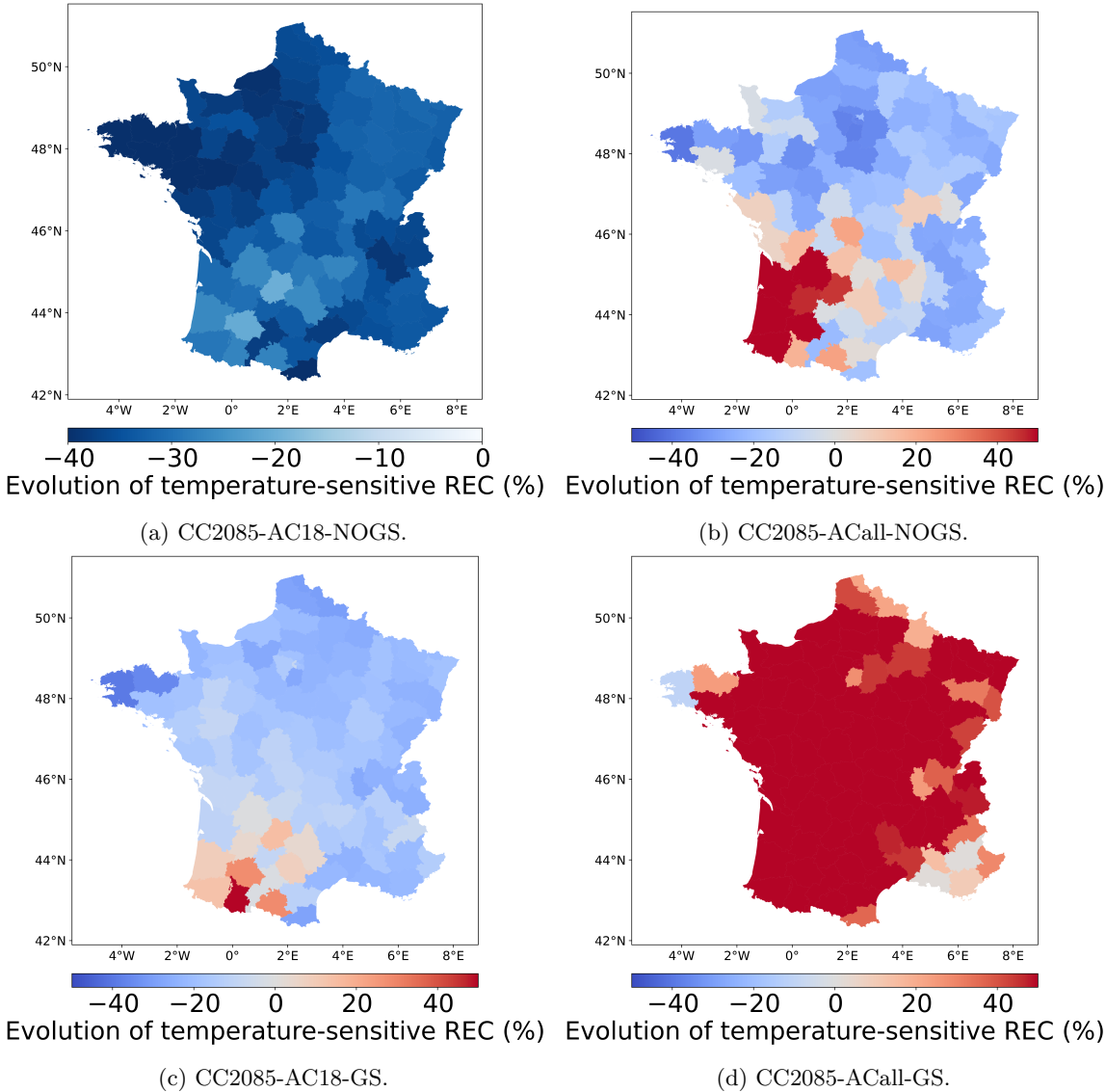
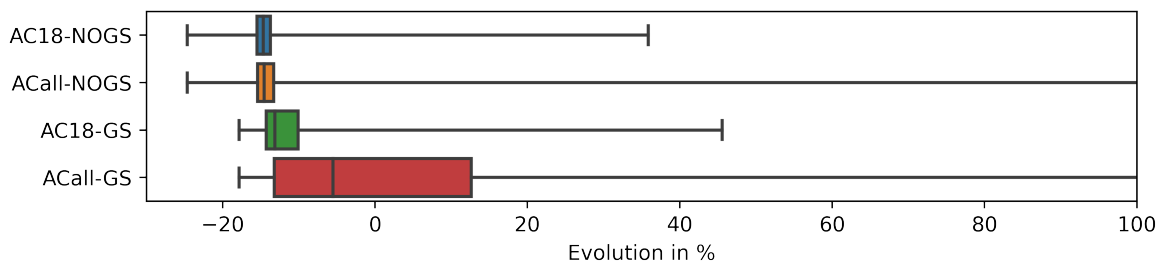
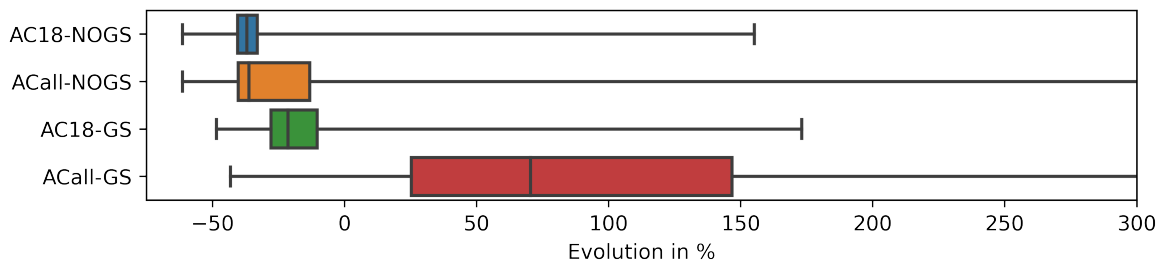


Figure 2.11 Relative change (%) in REC wrt. to the historical period (1975–2005) for CC2085 and for different AC scenarios: AC18-NOGS (a), ACall-NOGS (b), AC18-GS (c) and ACall-GS (d).



(a) CC2040.



(b) CC2085.

Figure 2.12 Boxplots over the cells of the relative change in temperature-sensitive REC corresponding to Fig. 2.10 and Fig. 2.11. The whiskers here show the minimum on the left and the 99% quantile on the right.

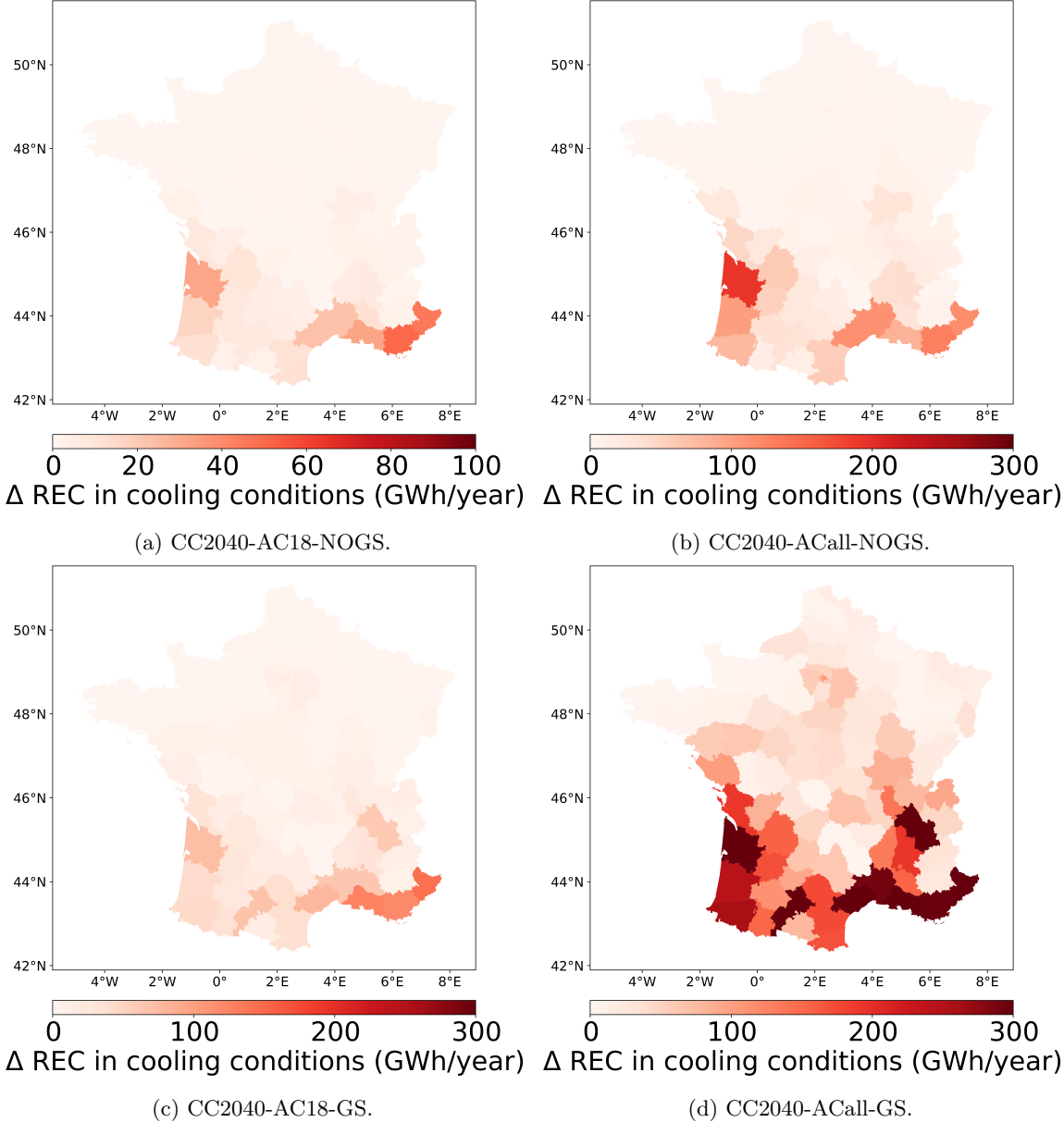


Figure 2.13 Same as Fig. 2.10 but for the cooling REC.

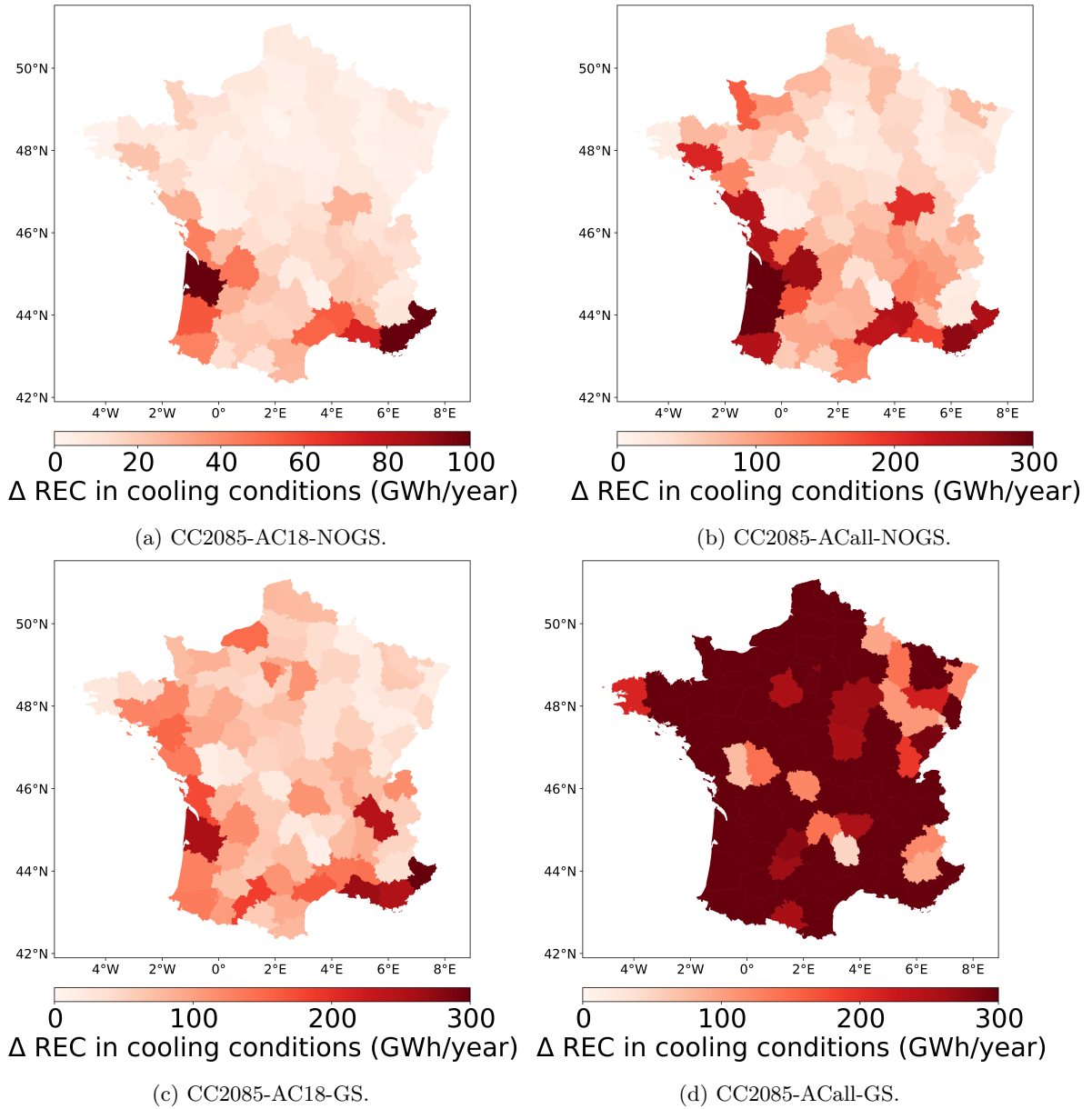


Figure 2.14 Same as Fig. 2.11 but for the cooling REC.

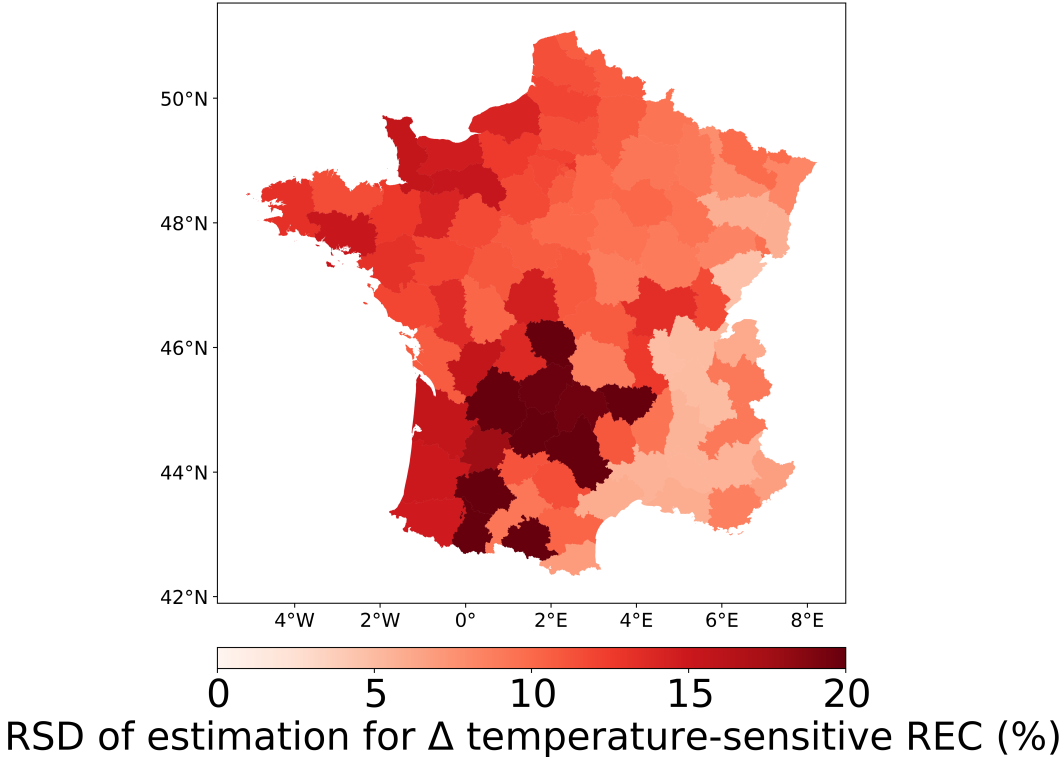
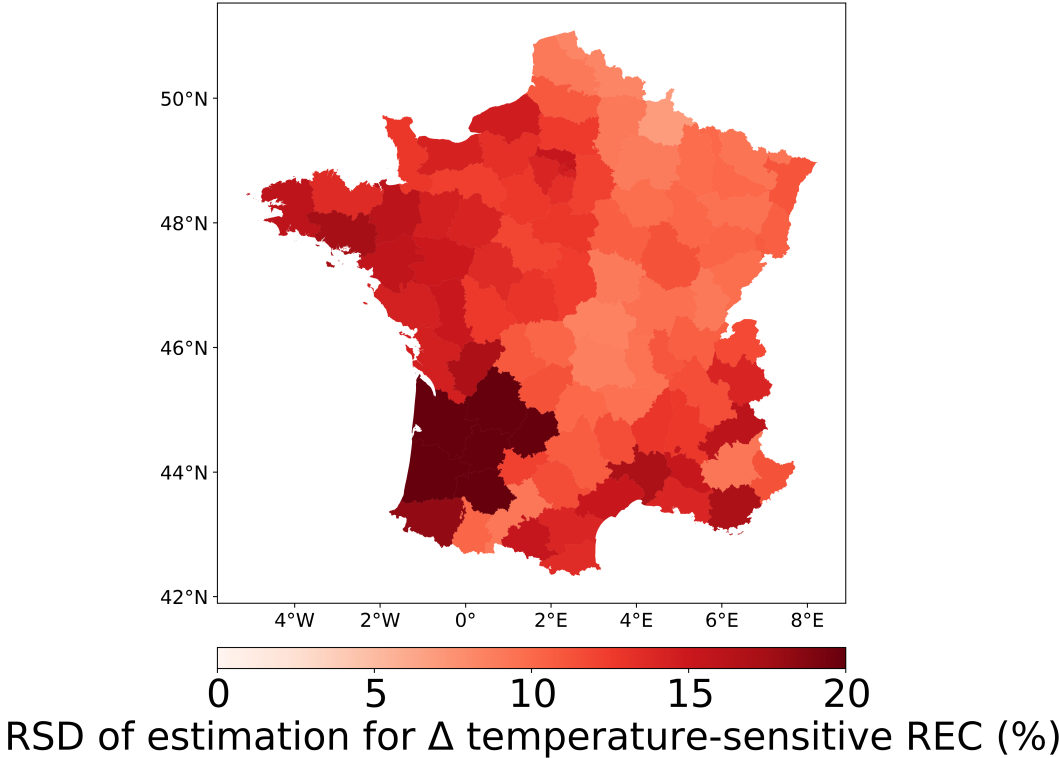


Figure 2.15 The global uncertainty of estimation of evolution in temperature-sensitive REC by combining all possible estimated coefficients with the leave-one-out cross-validation method and the 5 CORDEX simulations, represented by the Relative Standard Deviation (RSD) for the CC2040-AC18-NOGS (left) and the CC2085-AC18-NOGS (right) scenarios.

2.4 Conclusions and policy implications

A number of key messages can be drawn from the results of this study. First, REC varies significantly at very fine spatial scales, from the IRIS size (region of 2,000 inhabitants) to the administrative departments (96 departments on the European continent and 5 overseas) and regions (13 on the European continent and 5 overseas). Such variability had never been quantified and mapped due to a lack of suited methodology and limited available data at the finest scale (IRIS). Such variability which is the largest at the finest spatial scale calls for solutions and policies steered to the local specificities.

With increasing temperatures due to climate change, the heating needs decrease especially in the North-East which displays a continental climate with very hot summers and very cold winters (Köppen, 1936) and thus a strong sensitivity to any heating need reduction. Conversely, the South and Western regions along the Mediterranean Sea and the Atlantic Ocean, respectively, display a smaller trend in heating needs as they display a Mediterranean climate (hot, dry summers and cool, wet winters) and a maritime climate (cool summers and mild winters) (Köppen, 1936), respectively with warmer winters with regards to the North-East of France. At the end of the 21st century, in the worst-case climate scenario (RCP8.5), the spatial variability of the trend decreases as many regions are expected to experience temperatures much more rarely below their heating setpoint. There is a strong link between the heating needs and its evolution with that of REC.

However, the evolution of REC is modulated by the evolution of cooling needs and the deployment of AC systems to meet those needs. Our worst-case scenarios suppose either a 100% AC adoption rate in the IRIS already equipped at present, or a gradual spreading of AC systems, which mimics a "do like my neighbor" behavior. We also consider a combination of the two. In any scenario, the decrease in REC due to climate change could be totally offset in the South of France, which would then display an increase in REC. When the 2 AC scenarios are combined, an increase in REC could be seen over the whole country.

One key message deals with the overall uncertainty of our modeling setup. The uncertainty of our REC trends, including climate change impact and AC system deployment, is dominated by the spread between the climate simulations of our ensemble. The regression-based REC model does not add up much to the overall uncertainty. Such a result was not straightforward as the data available at the IRIS scale was at best limited in time, at worst available on an annual basis only, and sparse in some regions. The level of overall uncertainty therefore allows for drawing some recommendations in terms of practical applications and energy policies.

Takeaways for policy implications can be formulated from these results. In our scenario, AC gradual spreading mimics a "do like my neighbor" behavior. Our results show that such behavior has a major and detrimental impact on REC (more than 100% AC rate scenario). Such results call for targeted and local information actions where the risk of spreading is high (i.e. in areas where households are already equipped with AC systems) to limit the spreading or

mitigate its effect with at least the most energy-efficient AC systems. A more straightforward result is that the South of France is where the REC trend is expected to occur first with possible impacts on the energy system. Therefore there is a need to target actions to prevent any further deployment of AC systems. Especially, the climate of the South of France is expected to become similar to the present climate of countries more to the South, such as Italy or Morocco (Hallegatte et al., 2007). In Morocco, there is no visible impact on REC of AC use (Bouramdane et al., 2021). In Italy, the signal on REC of the use of AC is very limited (Tantet et al., 2019) but locally the evolution of cooling needs can have a significant impact on REC (De Felice et al., 2013; Scapin et al., 2016). Therefore, analyzing the socio-economic drivers, and the energy policies of these countries and drawing inspiration from them to deploy actions adapted to the local specificities of some French regions should be considered. Our worst-case results clearly show the detrimental impact of the increase in AC rate and spreading. Increasing the cooling setpoint T^C (e.g. recommended temperature of 26°C by the US Department of Energy) or maintaining an optimal difference with outdoor air temperature to about 7-8°C to maximize the energy efficiency of the AC equipment, could lower the cooling REC. Based on our model, shifting the cooling setpoint from 21°C at present to 23-24°C by 2040 and 26-27°C by 2085 would prevent any cooling REC increase in our worst-case scenarios. These values are consistent with existing recommendations. Low-tech alternative solutions also exist which are widely implemented in subtropical regions, and can be implemented in France to improve the thermal comfort of buildings and reduce the use of AC equipment and their impact on the environment, such as the reflective white coating on the buildings or roofs (Rawat and Singh, 2022; Vigié et al., 2020).

There are still several limits to this study. The temperature sensitivity results from a regression between REC and temperature, and the model implicitly integrates "human behaviors" related to other factors such as electricity costs and household revenue (Frederiks et al., 2015; Gertler et al., 2016). However, at this stage, no approach to segment the consumption data along multiple socio-economic dimensions (e.g. price, revenue) has been successful with the available data (e.g. time sampling and spatial granularity too coarse and aggregated) which would have been valuable to reduce global uncertainty. It could have been relevant to perform a sensitivity analysis on the temperature sensitivity through η^{El} to account for the further electrification of heating (e.g. fuel oil or gas to heat pumps) or through α^C to account for improved efficiency of AC systems. Regarding α^C , regions of the North-West along the Atlantic coast where the AC rate is on average 14% (versus 22% at the national level in 2019) can display surprisingly large positive α^C values. The causes should be further explored, whether due to statistical processing or behavioral in origin (e.g. residents may be less adapted to extreme heat events and more likely to install AC equipment for use during such extreme events (He et al., 2022)). Finally, the study from Pagliarini et al. (2019) shows that in a warmer climate, the electricity increases faster than linearly because of the efficiency drop of air-cooled chillers at high temperatures. Such a phenomenon should also be considered in the future.

Chapter 3

Decarbonizing the residential sector by retrofitting buildings

This chapter focuses on decarbonizing the residential sector with retrofitting. The temperature sensitivity model from the previous chapter is modified by including more variables about the building's construction ages. The different coefficients obtained with the linear regression allow us to estimate the heating consumption for each household with its given areas, construction period, and location. All the results are compared to the theoretical values under estimations from the standard energy performance certificate. Finally, with the model, we can project future energy gains.

Contents

3.1	Introduction	52
3.2	Methodology and data	52
3.2.1	Modified temperature sensitivity model	53
3.2.2	Data for the French case	54
3.2.3	Training the model for the French case	57
3.2.4	Future retrofitting projection	62
3.3	Results and discussion	63
3.3.1	Temperature sensitivities	63
3.3.2	Energy performance gap (EPG)	70
3.3.3	Retrofitting projection	72
3.3.4	Impact of socio-economic factors	74
3.4	Conclusion	75
Appendix 3.A Bayesian Ridge analysis		77
Appendix 3.B Impact of income results		79

3.1 Introduction

Many studies show that most European countries are heating-dominated, and a potential decrease in energy consumption is expected with global warming (Damm et al., 2017; Larsen et al., 2020). This is also the case for France, as shown in the previous chapter. However, relying only on this potential decrease in residential energy consumption due to temperature increases is insufficient to achieve the objectives. At the same time, as discussed in the previous chapter and shown by other studies, an increase is expected due to air conditioning adoption to climate change (De Cian and Sue Wing, 2016; Obringer et al., 2022). To offset at least the projected increase in cooling needs, it is important to continue improving the energy efficiency of the residential sector.

Improving energy efficiency in the building sector requires accurate energy assessment tools, which was the original goal of constructing Energy Performance Certificates (EPC). However, it is important to acknowledge the limitations of traditional EPCs, as described in the introduction chapter. In this context, this study aims to evaluate future retrofits based on actual electricity consumption, taking into account the behavior of actual users through the EPC-like indicators obtained from actual consumption data using statistical modeling. This statistical modeling allows for more precise quantification of the added value of energy efficiency retrofits across the region. Our model aims to utilize extensive spatial coverage information and apply it to all contained buildings, thus overcoming the limitations of traditional data collection methods. This data-based analytical modeling can complement this research area as mentioned by Zou et al. (2018) and Cozza et al. (2021). Given the decisive role of space heating in the thermal performance of a house, this study only considered this part of the final energy consumption of the house (excluding electricity consumption for other purposes). In the study of the EPG, we similarly focus only on space heating as predicted by the EPC, which is consistent with previous EPG studies. This work could provide valuable new insights for policymakers and local authorities. The study is organized into five sections. Section 3.2 describes the methodology used for the analysis and the data. Section 3.3 presents and discusses the modeling results and the EPG results obtained based on our model; we also discuss the applications of the model for the energy performance gap analysis and future retrofit projections. Finally, conclusions and perspectives are drawn in Section 3.4.

3.2 Methodology and data

For our study objective, which is to project future retrofit gains, we have to study residential actual consumption. The most convenient way is to study buildings' real bills at the dwelling level. However, obtaining French residential energy consumption data at the individual dwelling level is challenging. France has strict data privacy and protection regulations, particularly concerning personal information and energy consumption data. Therefore, access to detailed

residential energy consumption data at the dwelling level is typically restricted. However, some aggregated and anonymized energy consumption data are available for research purposes through authorized channels. These datasets are often aggregated at a higher level to protect individual privacy, such as by geographic regions or building types. This section describes how household consumption is obtained using aggregated data. Once the actual consumption per household is obtained, they can be used for further analysis of retrofit gains.

3.2.1 Modified temperature sensitivity model

Table 3.1 Summary of variables and their physical meanings presented in Eq. (3.1).

Variable	Meaning
$E_i(y)$	Annual REC for cell i and year y (kWh)
$NH_i(y)$	Number of households in cell i and year y
\bar{S}_i	Average living surface for cell i
$HDD_i(y)$	Annual heating degree days
N_y	The number of days in a year y (365 or 366)
B_i	The basic daily REC for cell i (kWh/m ²)
$\eta_i^{El}(y)$	Rate of electric heating for cell i and year y (%)
α_i^H	Heating temperature sensitivity for cell i (kWh/(DD m ²))
$\tau_{i,a}$	The percentage of buildings for period of construction a in cell i
$\eta_{i,a}^{El}(y)$	The rate of electric heating for a specific construction age a
$\alpha_{r,a}^H$	Heating temperature sensitivities for period of construction a of region r

When considering the main determinants of the thermal performance of buildings, the construction period has been reported in previous studies (Carreras et al., 2015; Cozza et al., 2020b). The construction period has long been a main characteristic defining the housing stock (Cuchí Burgos and Sweatman, 2011; Torres-Rivas et al., 2022). Due to regulatory changes and the evolution of construction technology, old buildings may have less or no insulation than newer buildings (Torres-Rivas et al., 2022). This affects the thermal performance of the building envelope, which is the key parameter that influences the energy demand of any building (Carreras et al., 2015).

Since we want to link aggregated consumption data to building characteristics to determine building energy consumption, this construction period variable is chosen because of its impact on thermal performance. Thus, this study examines the impact of buildings' construction age on temperature-sensitive consumption. The temperature sensitivity for different construction ages is determined with the following model by using statistical information at the IRIS level that each IRIS is considered as a uniform cell. Identical to the previous chapter, the first step is to normalize the Residential Electricity Consumption (REC) by the living areas in each cell to remove its impact. We divide the annual REC $E_i(y)$ for cell i and year y by the total living area in the cell $NH_i(y) \bar{S}_i$ with $NH_i(y)$ the number of households signing contracts for electricity

consumptions within the cell i for the year y and \bar{S}_i the average living surface per household, giving the normalized annual REC $E'_i(y)$ in kWh/m². In this study, several assumptions were made:

- The temperature-sensitive part of the model is assumed to be only heating-related as cooling accounts for less than 6% of the total REC.
- Final heating energy consumption does not depend on heating system type.
- The temperature sensitivity of each IRIS is the sum of the temperature sensitivities of all buildings from different construction periods.
- For each region, buildings constructed during the same period have the same final energy sensitivity to temperature $\alpha_{r,a}^H$, whatever their heating type.

With the above assumptions, the modified temperature sensitivity model can be expressed as:

$$\begin{aligned} \frac{E_i(y)}{NH_i(y) \bar{S}_i} &= E'_i(y) = HDD_i(y) \beta_i^H(y) + N_y B_i + \epsilon_i(y) \\ &= HDD_i(y) \eta_i^{El}(y) \alpha_i^H + N_y B_i + \epsilon_i(y) \\ &= HDD_i(y) \sum_a \tau_{i,a} \eta_{i,a}^{El}(y) \alpha_{r,a}^H + N_y B_i + \epsilon_i(y). \end{aligned} \quad (3.1)$$

All the variables presented in Eq. (3.1) and their physical meanings are given in Table 3.1. The first equation in Eq. (3.1) links $E'_i(y)$ to a heating REC and a base REC, with all the definitions similar as before. Each cell comprises buildings of different age distribution hence, the total temperature sensitivity β_i^H can be expressed with the sum of distributions of all construction periods. At the same time, each group of residential buildings from the same construction period comprises buildings with and without electric appliances. Consequently, the production of the previous study $\eta_{i,a}^{El} \alpha_i^H$ can be expressed as the sum of distributions of each construction period $\tau_{i,a} \eta_{i,a}^{El} \alpha_{r,a}^H$. This implies that a linear regression with $\beta_i^H HDD_i(y)$ as input is equivalent to a regression with $\alpha_{r,a}^H$ as coefficient and $HDD_i(y) \sum_a \tau_{i,a} \eta_{i,a}^{El}(y)$ as input.

Once the temperature sensitivity coefficient is determined, for any building with a given location and a given period of construction, its heating consumption is computed with an average HDD as:

$$E_i^H = \overline{HDD_i(y)} \alpha_{r,a}^H \quad (3.2)$$

3.2.2 Data for the French case

The Enedis consumption dataset is accessed via their website (Enedis, 2020) and includes the following variables that are relevant to this study:

- longitude and latitude coordinates of the cell centroids used to assign meteorological stations to cells;
- yearly residential electricity consumption (REC) data per cell from 2011 to 2018 (included);
- electric-heating rates η_i^{El} for 2018;
- fraction of cell buildings with surfaces in different intervals;
- heating setpoints used to estimate the HDDs.

When considering the impact of construction age, another dataset from the French government (Logements ordinaires) shows that the electric heating rate depends on when the buildings were constructed. This is due to changes in heating system preferences resulting from different thermal regulations implemented at different periods. Additionally, the distribution of construction ages may differ across cells, directly influencing each cell's temperature sensitivity. As a result, the coefficient of proportionality $\beta_i^{\text{H}}(y)$ (kWh/(DD m²)), which quantifies the yearly REC increase per HDD and unit area in cell i , can be expressed as the population-weighted average of electric heating temperature sensitivities of different construction ages $\eta_{i,a}^{\text{El}}(y)$ $\alpha_{r,a}^{\text{H}}$, represented by the third equation in Eq. (3.1). This average considers the distribution of construction ages $\tau_{i,a}$ within cell i for the year 2018, assuming that the distribution remains unchanged. As the geographical variability of the distribution is considered explanatory, the coefficients $\alpha_{r,a}^{\text{H}}$, which reflect the age-dependent temperature sensitivities, will have the same values for all cells within the same administrative region r .

However, the dataset providing $\eta_{i,a}^{\text{El}}(y)$ does not fully represent the population presented in Enedis, and the original dataset of Enedis provides only estimates of η_i^{El} for 2018. If the electric rate is only applied to common IRIS, the information on other IRIS will not be included, and the estimated temperature sensitivities might be biased. First, the electric heating rate for different ages must be estimated. A hypothesis is made to correspond data sets together that the dependency of the electric rate over the construction period is constant for each region. This dependency relates the total electric heating rate of each IRIS with the sub-rate of each construction period by the term $\kappa_{r,a}$.

$$\eta_i^{\text{El}} \cdot \kappa_{r,a} = \eta_{i,a}^{\text{El}} \quad (3.3)$$

With the above relationship and the input of the Logements Ordinaires, $\kappa_{r,a}$ is calibrated considering only the common cells with linear regression and is then applied to all IRIS of the Enedis dataset to get $\eta_{i,a}^{\text{El}}$. The outputs of Eq. (3.3) are then used as the new input in Eq. (3.1).

On the other hand, the French Environment and Energy Management Agency (ADEME) provides an EPC database collecting the EPCs resulting from the new EPC reform effective July 1, 2021. This study considers only the EPC established using the 3CL calculation method. The Energy Performance Certificate (EPC) measure in France, as introduced by [Bakaloglou and](#)

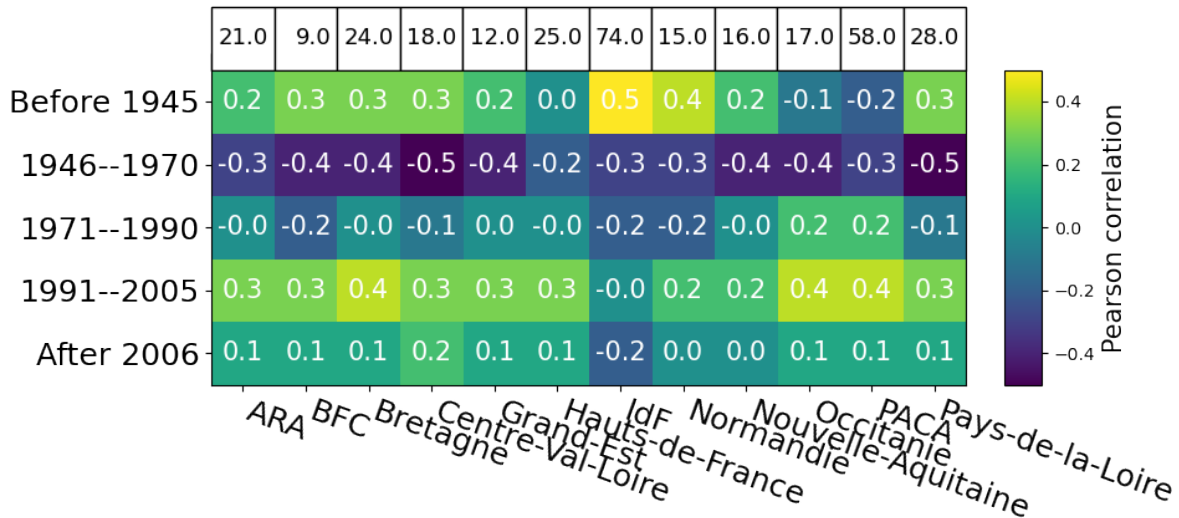


Figure 3.1 Pearson correlation between construction period distribution and median income at the IRIS level for all French metropolitan administrative regions. The table in the first row shows the representative percentage of IRIS from the income dataset compared to the total number of Enedis.

Charlier (2021), is a standardized method implemented by the French government. It involves an energy audit conducted by an approved auditor, which includes a visual inspection and collection of technical data. Theoretical energy consumption is then assessed using engineering models under the assumption of standardized behaviors. This measure considers five energy uses: heating, hot water production, cooling, lighting consumption, and domestic appliances. Various characteristics such as house construction data, window and wall insulation, heating performance, and climate data are collected and combined to obtain an aggregated measure of energy consumption. This method, known as the 3CL calculation, is the standard for EPC measurement in France, with calculation details in the infobox (Bakaloglou and Charlier, 2021, Section 3.1.1). These EPCs concern either an individual house, an apartment, or an entire building. We are only interested in the theoretical estimation of the final energy needs of heating. A filter is applied to preprocess the data to ensure all the housing samples from the EPC reference have the non-zero heating consumption estimation using the 3CL method and non-zero living surfaces. All the information about the data is given in Table 3.2.

The other dataset used was the median income at the IRIS level of the year 2017 ((INSEE, 2017)). Figure 3.1 shows the correlation between the proportion of all building periods in each IRIS and the median income for each IRIS. Globally, for all regions, the income level negatively correlates with the construction distribution of 1946 – 1970. For IRIS, the more buildings constructed during this period, the lower the income of its inhabitants. A positive correlation was found between 1991 and 2005 (except for the administrative region of Ile-de-France) and before 1945 for most administrative regions. However, this dataset represents a lower proportion of the total population, with the common IRIS percentage (in %) shown in the first row of

Info box: French EPC (DPE) calculation.

EPC certification typically involves an energy audit performed by a certified inspector who looks at the building and collects technical details, then calculates how much energy the building is expected to use based on engineering formulas assuming common usage patterns. This audit includes energy for hot water, heating, lighting, air ventilation, and cooling.

Details such as building construction, window and wall insulation quality, heating efficiency, and local weather are collected and used to determine total energy use. Each home's energy needs are calculated using the 3CL method, which predicts energy use for heating, hot water, and cooling as $C = C_{ch} + C_{ecs} + C_{cool}$, where C_{ch} is the predicted energy demand for heating, C_{ecs} is the predicted energy demand for hot water, and C_{cool} is the predicted energy demand for cooling. The calculation for C_{ch} depends on the heating demand of the building (B_{ch}) divided by the efficiency of the heating system (I_{ch}). $C_{ch} = B_{ch} \times I_{ch}$, where B_{ch} takes into account the size of the building, heat loss through walls and ventilation, typical local weather, and how the heating is managed. Key factors in this calculation include using local historical weather data to determine heating needs and setting the default heating temperature to 19 degrees Celsius. The entire house is assumed to be heated throughout the heating season. Hot water needs are also estimated based on the size of the home and its location.

Finally, this engineering modeling estimates the home's primary and useable energy use, expressed in kilowatt-hours per square meter.

Fig. 3.1. Although the model was constructed without first considering economic factors, this effect is examined in the discussion section (see Section 3.3.4) due to the correlation between building distribution and income.

3.2.3 Training the model for the French case

Ridge regression is a popular parameter estimation method used to address the collinearity problem frequently arising in multiple linear regression (McDonald, 2009). In our study, the inputs were constructed using Eq. (3.1). From the physical perspective, they are unrelated between different building ages. However, from a mathematical perspective, collinearity can not be perfectly avoided. Moreover, collinearity is a severe problem when a model is trained on data from one region or time and predicted to another with a different or unknown structure of collinearity, which is also our case (Dormann et al., 2012). To avoid the coefficients' misestimation due to the collinearity problem, we have tested the Ridge linear regression on our model (see Section 3.A for details of error analysis for the case of Bayesian Ridge). The prediction score improvement using Ridge is less than 2% on average compared to the Ordinary Least Squares (OLS) method, and the difference between coefficients is only around 0.9% —8%. Since the difference is negligible, instead of making the model more complex with more variables to estimate (i.e., the regularization coefficient to optimize), we choose to use the simple OLS

Data source	Spatial and resolution	Time period and resolution	Content details	Usage
E-OBS	Grid for each 0.1 degree of latitude or longitude	From 1944 Daily	Daily temperature $HDD_i(t)$	Input
Enedis	IRIS	2011-2018 Annual	Electricity consumption $E_i(y)$	Input
Enedis	IRIS	2018 One single year	Housing ages distributions $\tau_{i,a}$ Electric heating rate by IRIS η_i^{El}	Pre-processing for input
Logements Ordinaires	Housing 10.07 million observations	2016 One single year	Type of heating per dwelling $\eta_{i,a}^{El}$	Pre-processing for input
ADEME	Housing 1.46 million observations	2020 One single year	EPC energy consumption	EPC reference

Table 3.2 Data information for training the modified temperature sensitivity model for the French case.

but carefully analyze the coefficient errors.

3.2.3.1 Coefficient error analysis

Cross-validation is probably the simplest and most widely used method for estimating prediction error (Hastie et al., 2009). Since the inputs are constructed with two levels, year and IRIS, the effect of sampling on both levels has to be studied. We have eight years (2011 to 2018 included) of inputs, so we used Leave-one-out sampling for the input, which gives us eight groups of training-test samples. For the IRIS sampling, the first reflection is to use the same sample size as the one for the year effect (i.e. 1/8 of the population as the test sample). Then, the total effect of both temporal and geographical samplings is considered together. At the same time, we recall the mathematical explicit calculation (what we call the parametric solutions in the study) of estimates of coefficients m ($\alpha_{r,a}^H$ in our case) as well as the estimates of error of the coefficients Σ (or the estimates of the variances of the coefficients) under the OLS case:

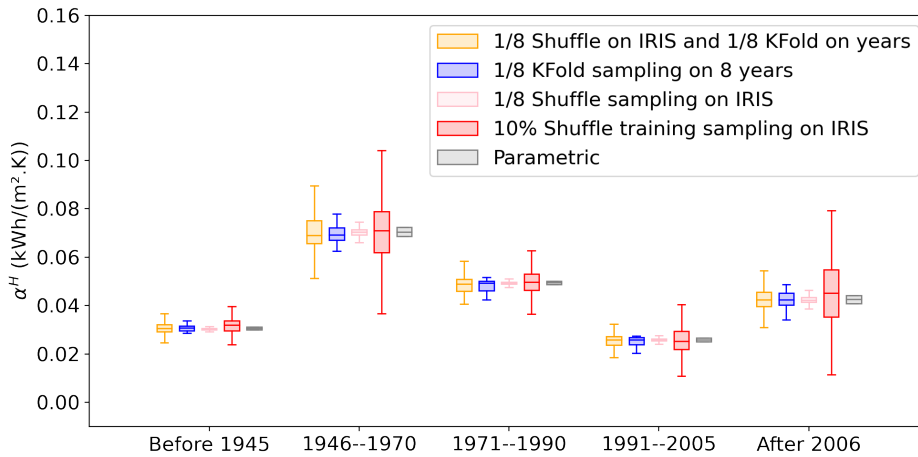
$$\begin{cases} \Sigma &= \hat{\sigma}^2(\mathbf{X}^T \mathbf{X})^{-1} \quad \text{with} \quad \hat{\sigma}^2 = \text{MSE} \frac{N}{N-P-1} \\ m &= (\mathbf{X}^T \mathbf{X})^{-1}(\mathbf{X}^T \mathbf{y}). \end{cases} \quad (3.4)$$

With cross-validation and parametric solutions, the uncertainty of coefficients estimation is given for each administrative region as shown in Fig. 3.4. The interquartile of the parametric solutions is determined assuming a normal distribution. In the study, each box in all the presented boxplots displays the interquartile range, which is the range between the 25th and 75th percentiles, and the median is marked by a darker line in the box with the same color of

Variable	Definition	Details	Dimension
N	The sample size	-	-
P	The number of coefficients	-	-
y	The dependent variable or the response	output	$N \times 1$
\mathbf{X}	The independent or the explanatory variable	input	$N \times P$
m	The vector of regression coefficients	-	$P \times 1$
MSE	Mean Squared Error	$MSE = \frac{1}{N} \sum_N (y_i - \hat{y}_i)^2$	Scalar
σ_t^2	Variance of the response variable	$\sigma_t^2 = \frac{1}{N} \sum_N (y_i - \bar{y}_i)^2$	Scalar
\mathbf{Z}	Principal components of the input \mathbf{X}	-	$N \times P$
$\mathbf{\Sigma}$	Estimate of coefficients variance	-	$P \times 1$
c_{kt}	Correlation between principal components and response	-	$P \times 1$
σ_k^2	Variance of principal components	-	$P \times 1$
λ_k	Eigenvalues of $\frac{\mathbf{X}^T \mathbf{X}}{N}$	-	Scalar
Λ	Matrix of λ_k	-	$P \times 1$

Table 3.3 Notations and definitions of variables used for the error analysis.

the box. Whiskers are extended 1.5 times the interquartile range from both sides, and outliers are not shown. Here, to give an idea of how the distribution of the coefficients looks like, the example of the administrative region of Ile-de-France is shown below in Fig. 3.2, while the results are interpreted later in Section 3.3.

Figure 3.2 Distribution of estimated temperature sensitivities related to different construction periods α_a^H of the region Ile-de-France using different test sampling scenarios.

We are interested in the coefficient errors and their explicit sources. Principal components help us transform the problem into an orthogonal space, which simplifies the relationship between the inputs and the response and helps us find an explicit equation for the error (Hastie et al., 2009). We can transform the inputs \mathbf{X} into an orthogonal matrix \mathbf{Z} with \mathbf{U} which is a P

$\times P$ orthogonal matrix that allows the PCA transformation of \mathbf{X} . We have thus the principal components defined as:

$$\mathbf{Z} := \mathbf{X}\mathbf{U}, \quad (3.5)$$

all the principal components are orthogonal between them. Because of the orthogonality, the coefficient of determination $(R^2)^{PCA}$ equals the sum of the square of the correlation coefficients between the principal components and the response output c_{kt} , so that $(R^2)^{PCA} = \sum_k c_{kt}^2$. With these principal components, we have relations such as:

$$\mathbf{\Sigma} = \hat{\sigma}^2(N\mathbf{U}\mathbf{U}^T)^{-1}, \quad \mathbf{Z}^T\mathbf{Z}^T = \mathbf{U}^T\mathbf{X}^T\mathbf{X}\mathbf{U} = \mathbf{\Lambda}N$$

with $\mathbf{\Lambda}$ the matrix of eigenvalues λ of covariance matrix $\frac{\mathbf{X}^T\mathbf{X}}{N}$ and $tr\{\frac{\mathbf{X}^T\mathbf{X}}{N}\} = tr\{\mathbf{\Lambda}\} = \sum_k \lambda_k$. At the same time, we can determine the estimates of coefficients in the PCA space with:

$$m_k^{PCA} = \frac{c_{kt} \sigma_t}{\sigma_k} \quad (3.6)$$

with $m^T m = m^{PCA T} m^{PCA}$. The standard deviation of the principal components σ_k is the squared root of the eigenvalues so that $\sigma_k^2 = \lambda_k$. On the other hand, we have the definition of coefficient of determination R^2 as:

$$R^2 = 1 - \frac{SSres}{SStot} = 1 - \frac{N \text{MSE}}{N \sigma_t^2} = 1 - \frac{\hat{\sigma}^2}{\sigma_t^2} \frac{N - P}{N}. \quad (3.7)$$

Since we have $tr\{\mathbf{\Sigma}\} = tr\{\frac{\hat{\sigma}^2}{\mathbf{X}^T\mathbf{X}}\} = tr\{\frac{\hat{\sigma}^2}{N} \frac{N}{\mathbf{X}^T\mathbf{X}}\} = \frac{\hat{\sigma}^2}{N} \sum_k \frac{1}{\lambda_k}$, the relative error of the estimated coefficients is therefore:

$$\begin{aligned} \frac{tr\{\mathbf{\Sigma}\}}{m^T m} &= \frac{1}{N} \frac{\hat{\sigma}^2}{\sigma_t^2} \frac{\sum \lambda_k^{-1}}{\sum \frac{c_{kt}^2}{\lambda_k}} \\ &= \frac{1 - R^2}{N - P} \frac{\sum \lambda_k^{-1}}{\sum \frac{c_{kt}^2}{\lambda_k}}. \end{aligned} \quad (3.8)$$

3.2.3.2 Prediction error analysis

With the definitions from the parametric analysis in the previous section, we have the relative errors of the output prediction as:

$$\begin{aligned} \frac{tr\{\mathbf{X}\mathbf{\Sigma}\mathbf{X}^T\}}{\beta^T\mathbf{X}^T\mathbf{X}\beta} &= \frac{\hat{\sigma}^2 P}{N \sigma_t^2 \sum_k c_{kt}^2} \\ &= \frac{1 - R^2}{N - P} \frac{1}{R^2} \\ &= \left(\frac{1}{R^2} - 1\right) \frac{P}{N - P} \end{aligned} \quad (3.9)$$

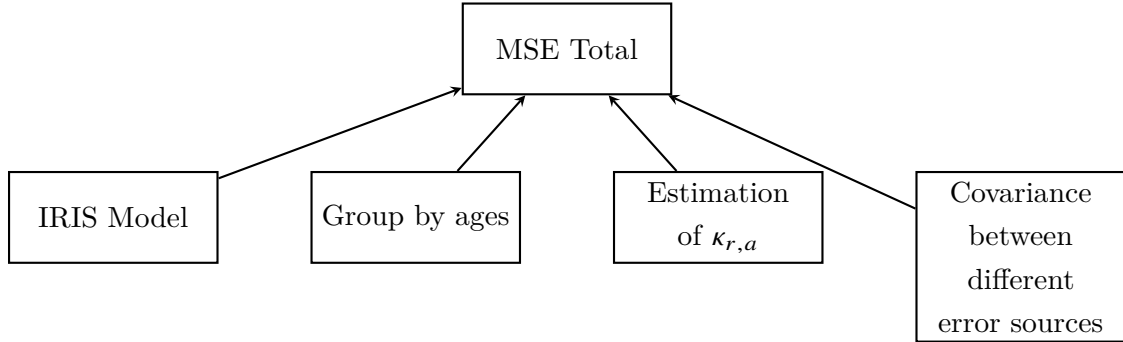
since

$$\begin{aligned} \text{tr}\{\mathbf{X}\boldsymbol{\Sigma}\mathbf{X}^T\} &= \hat{\sigma}^2 \text{tr}\{\mathbf{X}(\mathbf{X}^T\mathbf{X})^{-1}\mathbf{X}^T\} \\ &= \hat{\sigma}^2 \text{tr}\{\mathbf{I}_p\} \\ &= \hat{\sigma}^2 P \end{aligned} \quad (3.10)$$

and

$$\text{MSE} = \sigma_t^2 - \frac{m^T \mathbf{X}^T \mathbf{X} m}{N}. \quad (3.11)$$

The total uncertainty mainly comes from the different assumptions made during the model construction process. The first assumption is that electricity consumption is expressed linearly in terms of temperature sensitivity, temperature, and electric heat rate at the IRIS level using only annual aggregated data. We refer to the first source component of total uncertainty as the "IRIS model" because the temperature sensitivity coefficients can be estimated at the IRIS level using temporal temperature changes. The second assumption focuses on the effect of building age on temperature sensitivity by decomposing the IRIS model into different building ages. We refer to the uncertainty caused by this assumption as the "IRIS effect on age". Finally, the third assumption is to consider the dependence of each IRIS's total electric heating rate on the electric heating rate for each construction period using the coefficient $\kappa_{r,a}$, which is invariant for each region and construction period. Since this variable $\kappa_{r,a}$ is estimated first, the uncertainty introduced by the calibration of the coefficient $\kappa_{r,a}$ is named "Kappa".



The MSE can be thus expressed as:

$$\begin{aligned} \text{MSE Total} &= \frac{1}{N} \sum_i (y_i - \hat{y}_i)^2 \\ &= \frac{1}{N} \sum_i (y_i - y_i^{IRIS})^2 + \frac{1}{N} \sum_i (y_i^{IRIS} - y_i^{age})^2 + \frac{1}{N} \sum_i (y_i^{age} - y_i^{\kappa_a})^2 + \text{Covariance}, \end{aligned} \quad (3.12)$$

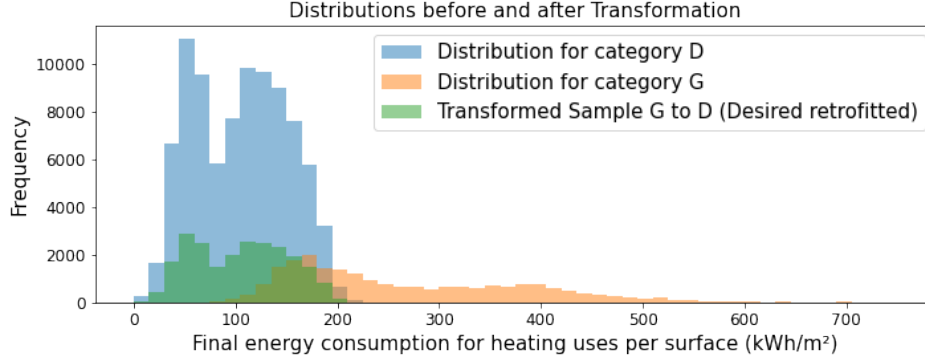


Figure 3.3 Example of distribution matching to retrofit EPC class G to EPC class C. The orange is the current distribution of heating consumption of households with category G, the blue is the current distribution of category D, and the green is the distribution of the category G sample after the retrofit.

with

$$\begin{aligned}
 y_i^{IRIS} &= HDD_i \eta_i^{El} \beta_i^H \\
 y_i^{age} &= HDD_i \sum_a \tau_a \eta_{i,a}^{El} \alpha_a^H \\
 y_i^{\kappa_a} &= HDD_i \sum_a \tau_a \kappa_a \eta_i^{El} \alpha_a^H.
 \end{aligned} \tag{3.13}$$

3.2.4 Future retrofitting projection

One of the purposes of this actual consumption modeling is to predict energy savings from building retrofits. Currently, the most common method of predicting energy savings is using Energy Performance Certificates (EPCs). However, misreporting of actual energy consumption using EPCs can cause energy-saving deficit problems due to rebound and pre-bound effects. Therefore, the advantages of modeling based on actual consumption data may help to address the energy-saving deficit problem. We use the distribution matching method to project future energy consumption and the energy savings after retrofit. The goal is to fit a given sample distribution to the desired distribution. In our case, the desired distribution of the matching destination is the current one of the chosen buildings with better performance, and the sample before transformation is all the buildings that we choose to retrofit. Figure 3.3 shows the example for a better understanding of the method. In the example, we show a retrofit projection with distribution matching from EPC category G to EPC category D. So, both distributions before and after retrofit have the same sample size, while the after retrofit follows the same profile as the desired distribution. It preserves the size of the differences in the different parts of the distribution, and these differences are the potential benefits of retrofitting. And the energy gains due to the retrofitting can be estimated by the difference of the sample before/after the retrofit. For the retrofitting scenarios, first, we use the EPC label to differentiate the pre- and post-retrofit groups for the paired distribution quantification approach, assuming that

buildings with worse energy labels will perform the same after retrofitting as buildings with better-expected labels. Energy savings are projected under three scenarios. The first scenario is to retrofit a building three levels up (i.e., from G to D); the second is to retrofit all buildings currently worse than B to B; and the third is to retrofit all buildings currently worse than C to C. Then, a scenario is considered that differentiates buildings according to their age: All households living in buildings built before 2005 will have the same thermal performance and consumption behavior as buildings built after 2005. This scenario is applied with EPC and temperature-sensitive consumptions estimated with our model. Since the same scenario is applied with different inputs, we can directly compare the retrofit gain of the EPC estimates with our model.

3.3 Results and discussion

In this section, we conducted various analyses in the following order. First, we estimated temperature sensitivities for different building age groups using the model presented in the previous section. We also identified and analyzed sources of uncertainty. Next, we compared these estimates of heating consumption based on current consumption with EPC data to analyze EPG. Finally, based on our results, we projected the effect of retrofitting. We also analyzed confusion caused by a socio-economic factor that has the most impact on energy consumption: income.

3.3.1 Temperature sensitivities

As the first methodological result, the 25%-75% distribution of estimated temperature sensitivities for different periods of construction ages $\alpha_{r,a}^H$ of all the 12 metropolitan administrative regions are shown in Fig. 3.4. The Ordinary Least-Squares (OLS) regression was used with a constraint on coefficients to be positive due to their physical meanings. The coefficients' uncertainty was evaluated by subsampling at the temporal and spatial levels as described in Section 3.2. The combination effect of both temporal and spatial sampling was also tested. Firstly, the coefficient estimates show robustness across different sampling scenarios. The magnitude of the uncertainty comes mainly from the size of the sampling. For all the administrative regions, the temporal samplings show larger uncertainty compared to the spatial sampling when both samplings are the same size (the second and third boxplots). And the scenario combining both samplings (the first boxplots) has the largest uncertainty compared to the former two. The last boxplot using parametric explicit calculation Eq. (3.4) as described in Section 3.2.3.1 also proves the robustness of the results. Secondly, the results show spatial variation. Not all regions have the same pattern of coefficients across construction periods. For example, in the Île-de-France administrative region, the final energy consumption of buildings constructed between 1946 and 1970 (i.e., after World War II and before the first thermal regulation) has a higher sensitivity to

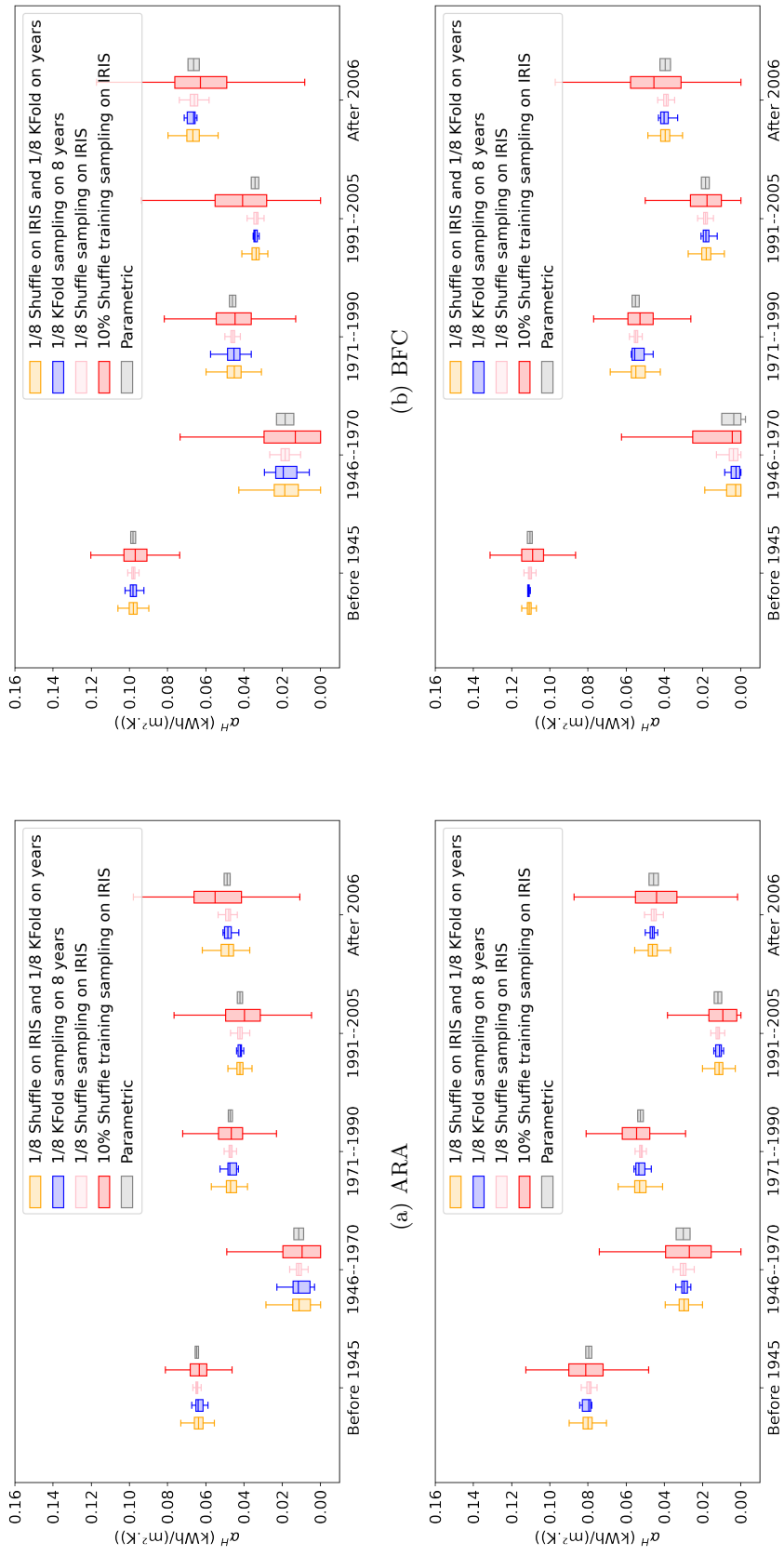


Figure 3.4 25%-75% distribution of estimated temperature sensitivities related to different construction periods α_H^H of different administrative regions using different test sampling scenarios.

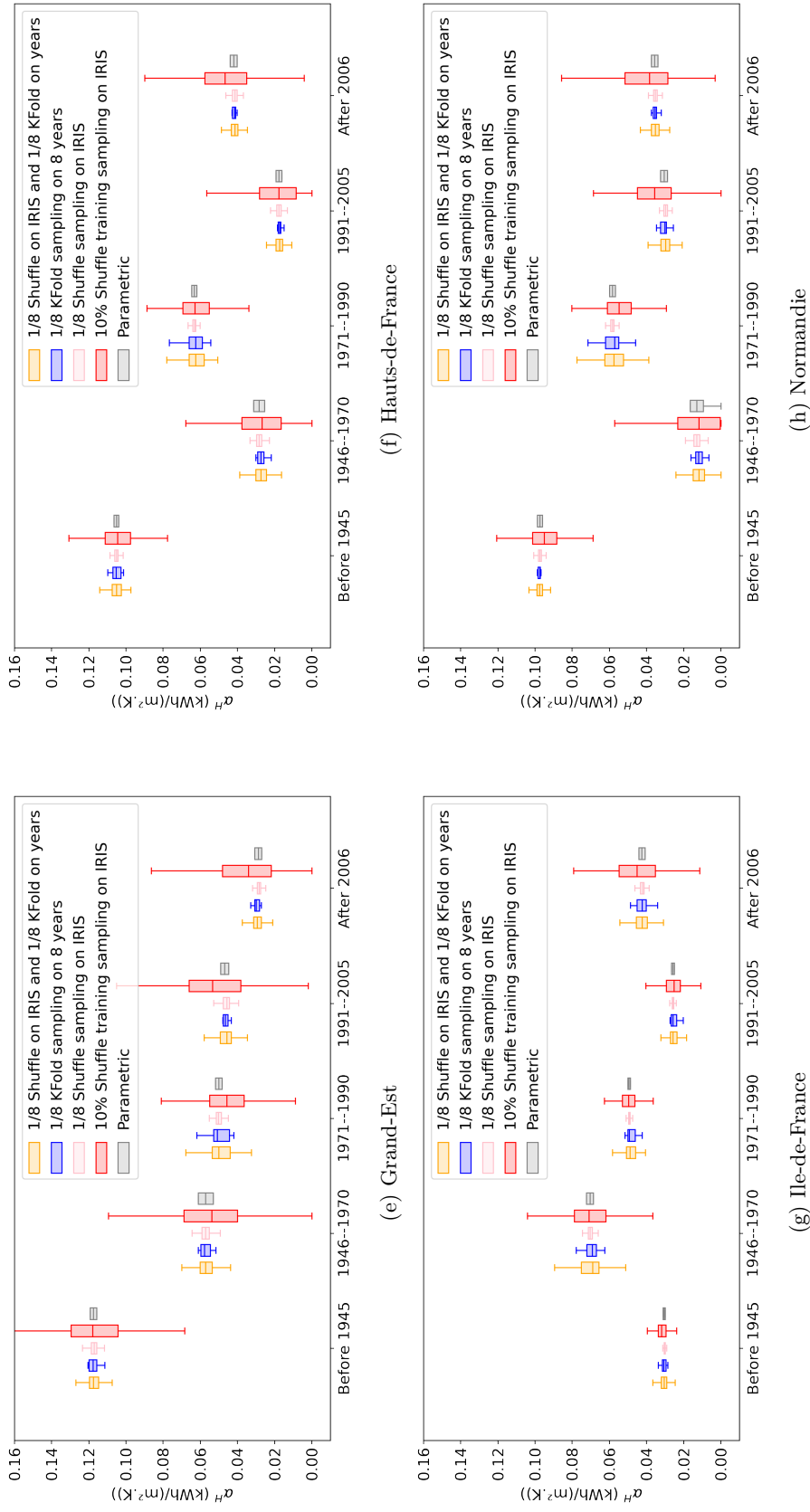
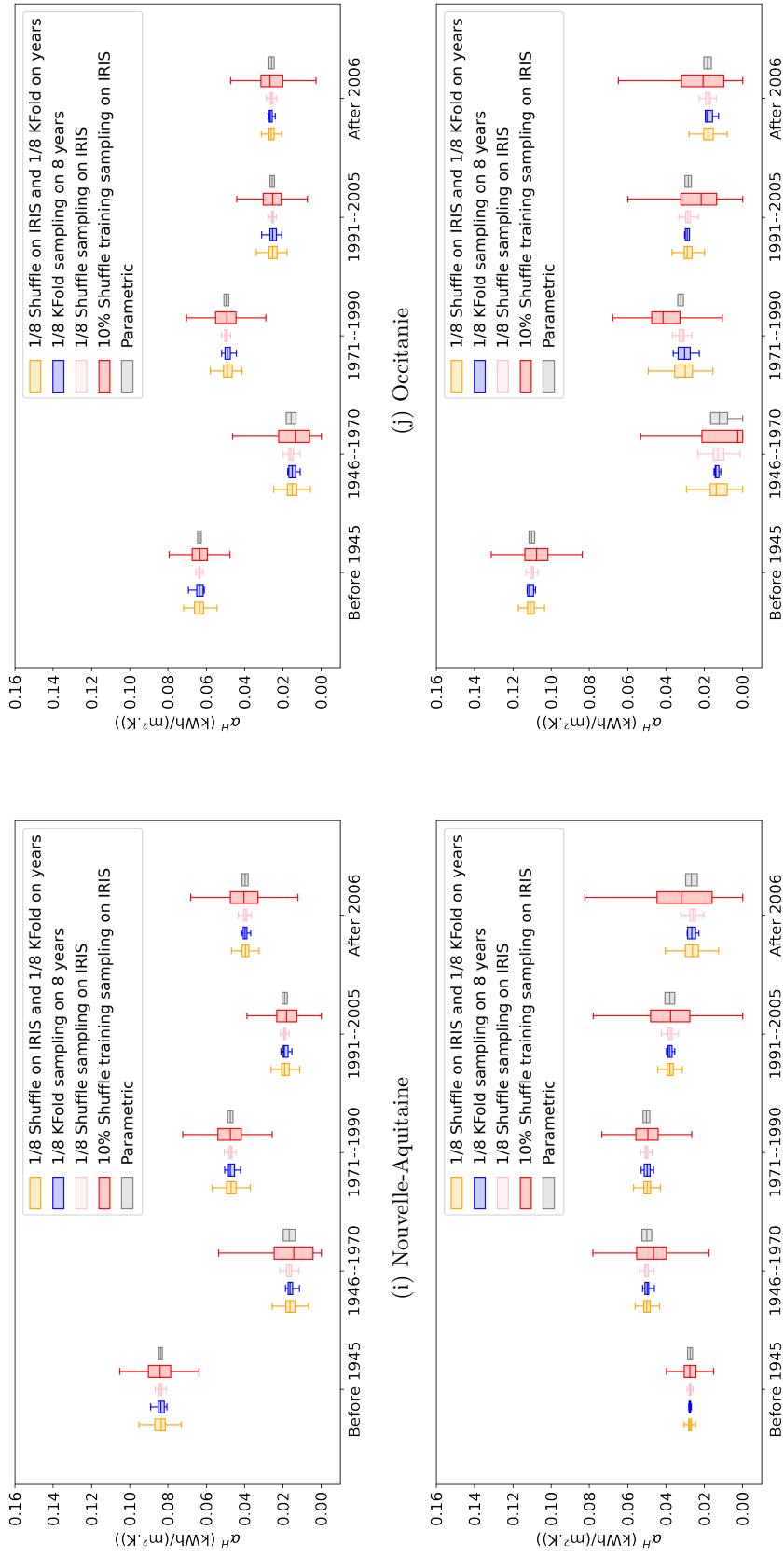


Figure 3.4 25%-75% distribution of estimated temperature sensitivities related to different construction periods α_a^H of different administrative regions using different test sampling scenarios. (cont.)



(i) Nouvelle-Aquitaine

(j) Occitanie

(k) PACA

(l) Pays-de-la-Loire.png

Figure 3.4 25%-75% distribution of estimated temperature sensitivities related to different construction periods α_H of different administrative regions using different test sampling scenarios. (cont.)

temperature. This means that heating consumption is higher for households living in buildings constructed between 1946 and 1970. However, for other areas (except PACA), the temperature sensitivity coefficients for this period are smaller than for adjacent periods. Otherwise, the temperature sensitivity coefficients for the construction before 1945 always have larger values (except for Ile-de-France and PACA). We were expecting a larger heating consumption for the construction period of 1946 to 1970 while a smaller value for the one before 1945 as the result of neighboring countries (Brito, 2016; Cozza et al., 2020b). However, in the study, the sampling test shows the robustness of coefficient estimation. Thus, one explanation might come from the renovation works that have not been considered during the coefficient calibrations. If we compare only the median values, the improvements between 1991-2005 and 1971-1990 are consistent for all administrative regions. All households living in buildings constructed between 1991 and 2005 consume less heating energy than in the previous period. Otherwise, the significance of the difference is questionable for ARA, Grand-Est, and Pays de la Loire. The improvement seems robust after the implementation of thermal regulation in 1988. However, the most surprising result for more than half of the administrative regions (i.e. ARA, BFC, Bretagne, Centre-Val de Loire, Hauts-de-France, Ile-de-France, Normandie, and Nouvelle-Aquitaine) is the importance of the coefficient values for the latest period. Implementing RT2005 did not reduce heating consumption as expected in these regions.

Once the temperature sensitivity coefficient is estimated for each family of dwellings, it is used to calculate the consumption estimation at the buildings' level and compare it to the theoretical heating consumption with the datasets of ADEME. However, the dataset of ADEME is not fully representative compared to Enedis and only represents less than 15% of the total housings. A direct comparison between the model outputs and the ADEME's EPC poses a problem of inconsistent samples, which can introduce sampling bias in the energy performance gap. Therefore, we apply the model coefficients to the ADEME building datasets to compare the estimated thermosensitive consumption for these buildings. However, this raises the issue of model uncertainties, as the model may not be as robust due to building sub-sampling (i.e. larger coefficient uncertainties). IRIS sampling can be considered a similar approach to building sampling, allowing for testing the model's robustness in construction periods and electrification rates without relying on other factors. The red boxplots shown in Fig. 3.2 represent the distribution of the possible coefficients using 10% of the input as training sets due to the IRIS sampling. These distributions are then used to compute the temperature-sensitive final energy consumption for each building given with EPC estimation of heating needs using Eq. (3.2). These estimations of final energy consumption using our model are then compared to the EPC given by ADEME, which gives us the EPG. Another advantage of using IRIS sampling with the size of the ADEME sample is that its uncertainty is larger than that of temporal sampling and much larger than global error. Hence, normally, we have maximized the potential uncertainty in our estimation of temperature-sensitive consumption.

3.3.1.1 Regional coefficients uncertainty comparison

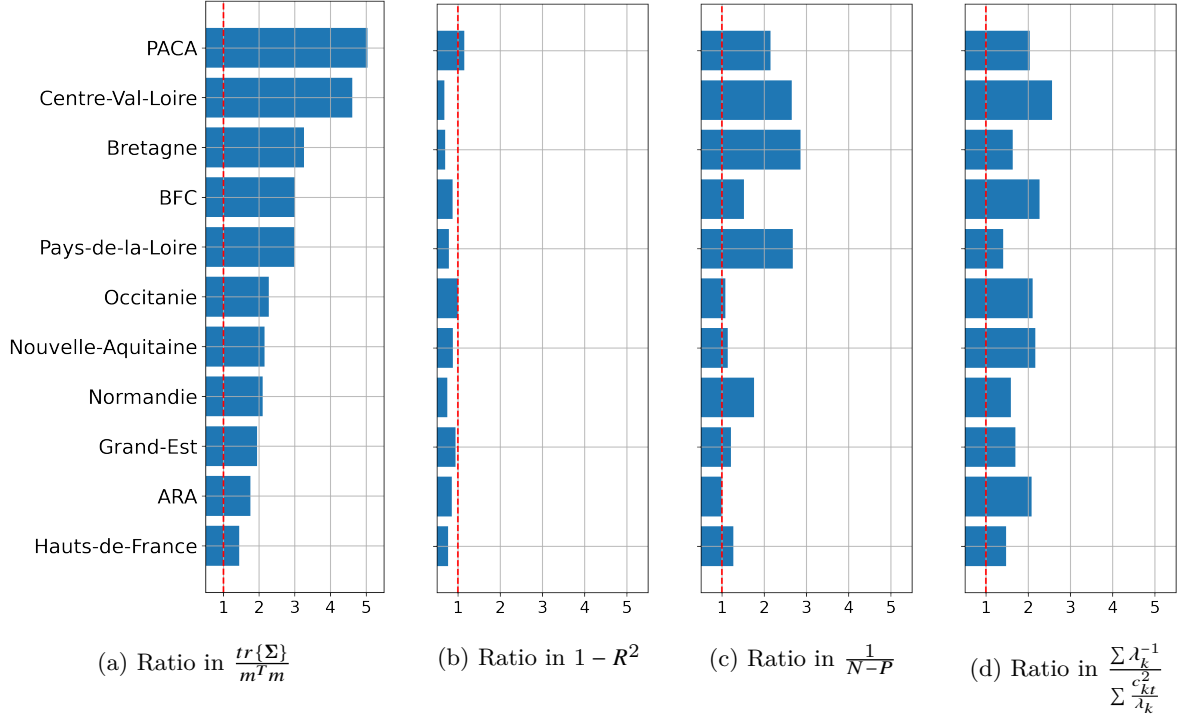


Figure 3.5 Comparison of the relative coefficients uncertainty with the explicit sources as described in Eq. (3.8) between other administrative regions and Ile-de-France as ratios (Ile-de-France has the smallest relative coefficients uncertainty and is used as the reference for the comparison).

The relative coefficient uncertainty for each administrative region is calculated with Eq. (3.8). Ile-de-France has the lowest relative coefficient uncertainty and is the reference for comparing regions. To understand the sources of regional difference in coefficient errors, Fig. 3.5 compares the relative coefficient uncertainty with the explicit sources between other administrative regions and Ile-de-France under the form of ratios. The main sources, as described in Eq. (3.8), are the model training performance ($1-R^2$), the sample size N , and the unknown effect of the distributions of the eigenvalues and the correlations between the principal components and the response variable. All the comparison inter-regions of the sources are presented in ratios as shown in Fig. 3.5b, Fig. 3.5c, and Fig. 3.5d.

From the second sub-figure, we can see that Ile-de-France has the penultimate smallest R^2 (only PACA has a larger $1-R^2$ compared to it), so its training performance is not as good as others. However, the total relative error of all coefficients of Ile-de-France remains the smallest. Hence, even though a better model training performance (i.e., large R^2) is expected to have a smaller relative error, the model training performance has the least impact on the relative errors of the coefficients.

However, since the number of IRIS in Ile-de-France is the second largest (just after ARA),

and especially since the region has a small value of $\frac{\sum \lambda_k^{-1}}{\sum \frac{c_{kt}^2}{\lambda_k}}$, the relative coefficient error for this region becomes the smallest. On the other hand, the effects of the other two factors complement each other, and the significance of the effects seems similar.

In summary, in our case study, the correlation between variable inputs and consumption outputs (represented with $\frac{\sum \lambda_k^{-1}}{\sum \frac{c_{kt}^2}{\lambda_k}}$) and the total sample size (represented with the number of IRIS N) have the greatest impact on the relative coefficient errors. It is desirable to have as many samples as possible to train the model and to have as much correlation as possible between the input variables and the consumption output.

3.3.1.2 Total prediction uncertainty sources analysis

The total prediction uncertainty mainly comes from the assumptions made during the model construction process.

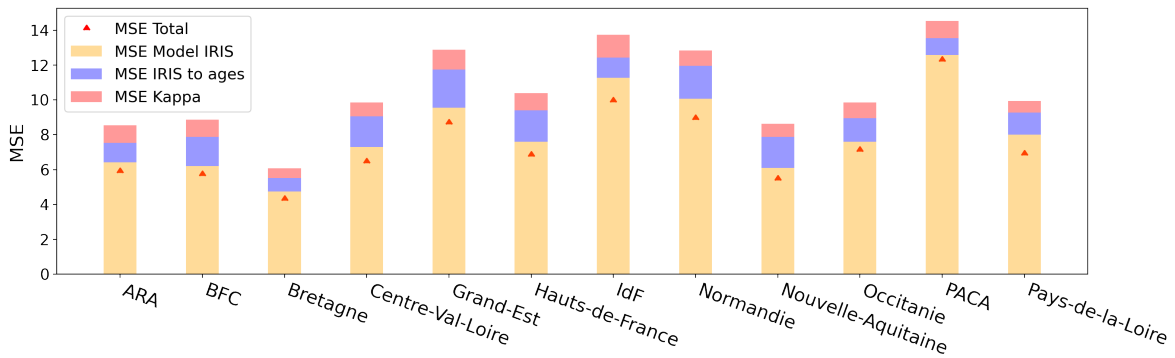


Figure 3.6 Stacked bar chart of uncertainty sources represented by Mean-Squared-Error (MSE) for all 12 administrative regions in France.

Figure 3.6 shows the quantification of the different sources of uncertainty due to the assumptions made during model construction as presented in Section 3.2.3.2. We can see that the first source due to the assumption of linearity between electricity consumption and temperature at the IRIS level (IRIS model) dominates the others. However, this part of the uncertainty was tested in the previous chapter, and the results proved robust. The other sources have less influence on the total uncertainty, with the assumption that $\eta_{i,a}^{El} = \kappa_a \eta_i^{El}$ introducing less uncertainty than the model construction. The total uncertainty is even smaller than that of the IRIS model because the sum of the two model modification assumptions is compensated by the covariance between the errors, demonstrating the robustness of the assumptions. We conclude that the estimates of temperature sensitivity coefficients for all administrative regions are reliable and can be used to estimate heating consumption.

3.3.2 Energy performance gap (EPG)

Once the temperature sensitivity coefficients are determined, they are applied to each building using Eq. (3.2) to get the estimated actual heating consumption. Then, the energy performance gap (EPG) can be evaluated based on Eq. (1.1).

Figure 3.7 shows the distribution of EPG for different building ages in France with ADEME's 1.46 million housings as the sample. The median EPG for all buildings except those constructed after 2006 is always negative. 56% of housings constructed before 1945, 83% of housings constructed between 1946 and 1970, 57% of housings constructed between 1971 and 1990, and 69% of housings constructed between 1991 and 2005 consume less heating energy than expected under standard calculation. For the construction period of 1946 and 1970, globally, more than 60% of households consume less than half of the theoretically predicted heating demand (i.e. EPG less than -50%). This means that the theoretical heating demand is much higher for buildings constructed during that period than the actual consumption. On the other hand, the variation in EPG is the largest for the newest buildings, where thermal performance is expected to improve. For the newest buildings constructed after 2006, only 6% of the EPCs are worse than E, while more than 74% of the EPGs are positive. Unlike the older buildings, these new buildings consume much more electricity than expected. (Cozza et al., 2020a) found similar results in his study for Switzerland. The newer or better thermal performance buildings (categories A or B) usually have positive EPG. In contrast, old or poor thermal performance buildings (categories F or G) usually have negative EPG. A negative EPG means the actual heating consumption is lower than the theoretical estimation under standard user behaviors. Previous studies show that the more socially disadvantaged the resident, the more underheated the home tends to be (Coyne and Denny, 2021; Sunikka-Blank and Galvin, 2012).

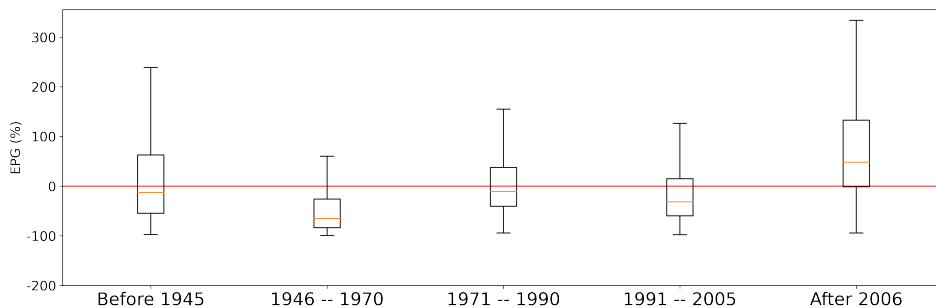


Figure 3.7 Energy Performance Gap (EPG) distribution, which compares the heating consumption between 3CL calculation and model estimation based on actual consumption of France with 1.46 million housing observations.

A large EPG is related to the user behavior side of the economic impact and the quality of the EPC. The quality of the EPC is questionable because the manipulation can be easily done to change the EPC category, for example, by modifying the living area using the 3CL method. Studies observe in the ADEME EPC reference data an overrepresentation of primary

energy consumption near the upper limits of the energy class, accompanied by a symmetrical underrepresentation near the lower limits, which is the easiest error to detect due to manipulation (Jeanne et al., 2024; Robin and Yassine, 2022). Although we considered the EPC from ADEME a reliable reference in our study, the quality of the datasets remains a major source of uncertainty that has not been documented.

Figure 3.8 shows the maps of negative EPG percentages for the 12 French administrative regions for different groups of construction periods. We observe that, although there is a large spatial variability, the construction period between 1946 and 1970 displays the most negative EPG, while most of the newest buildings constructed after 2006 consume more heating energy than they should. However, Ile-de-France and PACA are not in the same situation as other regions. Their oldest buildings have a more negative EPG compared to the adjacent period. At the same time, a boundary line that separates eastern France from western France for all buildings constructed after 1946 seems to mean that fewer buildings in the eastern part of France underheat their house as expected.

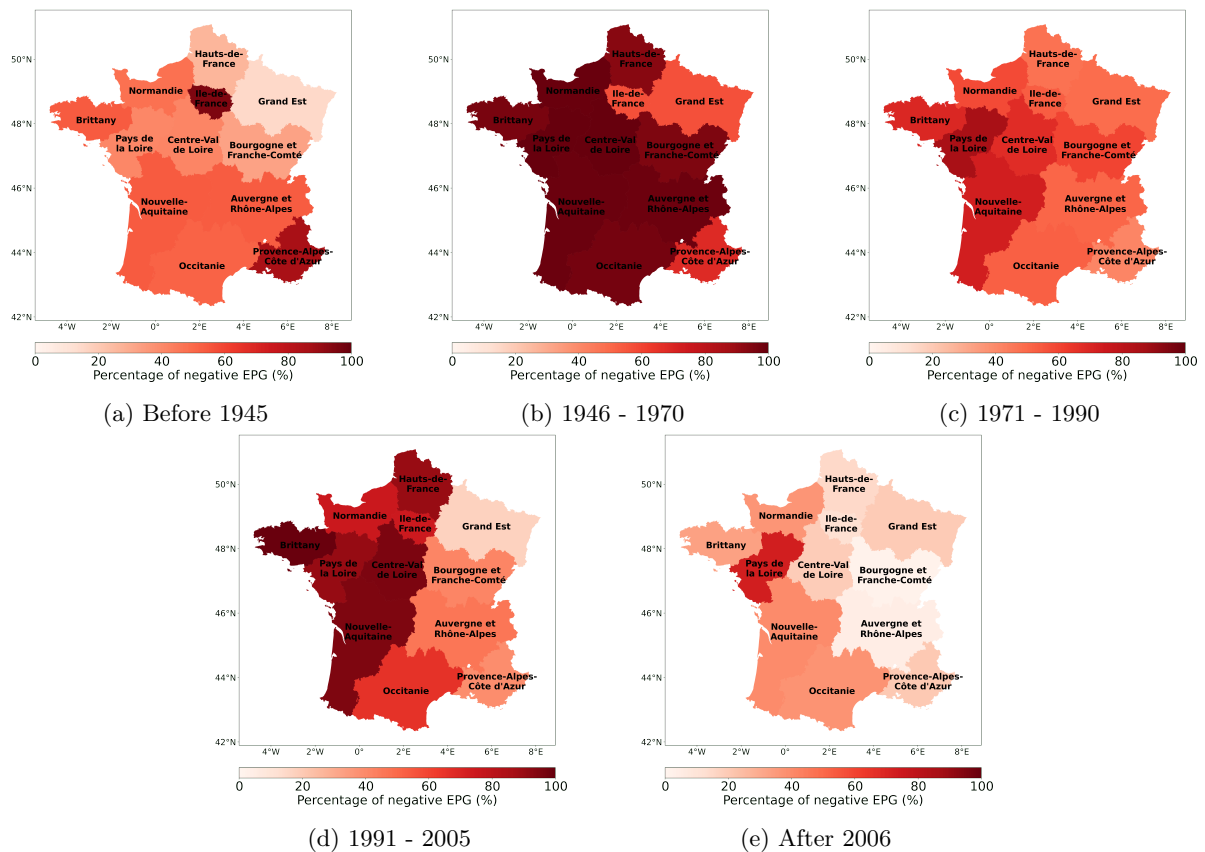


Figure 3.8 Map of percentage of negative EPG for French 12 administrative regions for different groups of construction periods (negative EPG indicates lower actual heating consumption compared to expected heating consumption).

3.3.3 Retrofitting projection

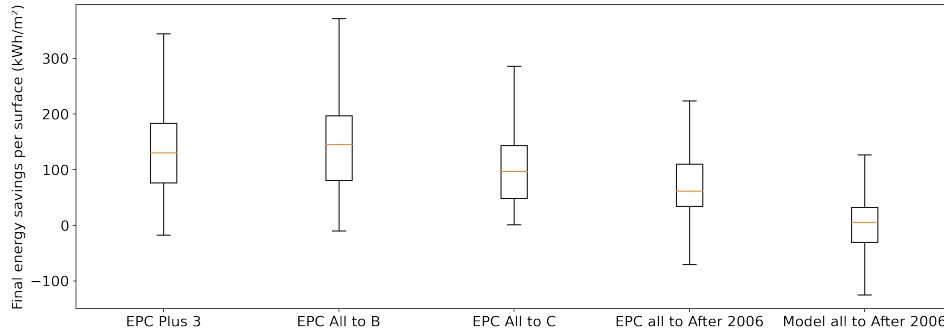


Figure 3.9 Comparison of the distribution of potential savings under four different scenarios using EPCs and one scenario using the estimation of our model for the case of France.

Projections of potential heating energy savings under the different retrofit scenarios are shown in Fig. 3.9. We recall that the first three scenarios (the first three box plots) use the EPC label as a pre-and post-retrofit group differentiation for the paired distribution quantification approach. We assume that buildings with poorer energy labels perform the same as buildings with better-expected labels after their renovation. The last two box plots consider the same case of retrofitting buildings based on building age: all households living in buildings built before 2005 have the same thermal performance and consumption behavior as buildings built after 2005 after their renovation. The first four box plots use EPC’s estimates of heating demand, while the last box plot uses our model’s estimates. Since the last two box plots use the same scenario but with different inputs, we can directly compare the retrofit gain of EPC estimates to our model.

The results show that the potential energy savings estimated using the first three EPC scenarios are positive in all cases. The difference only comes from the current buildings’ EPC different distributions. If we compare the results between the scenarios just using EPC, the last retrofitting scenario, considering all households living in retrofitted buildings built before 2005 have the same thermal performance and consumption behavior as buildings built after 2005, have a much lower expectation in energy gains and even gets 4% of negative values. This is mainly due to the positive EPG for this construction period compared to others, as shown in the previous section. However, in the case of estimation using our model based on actual energy consumption, there is a 47% chance that the energy savings are lower than expected. Although the uncertainty in the coefficients is large and the estimates may be biased, it still suggests a shortfall in energy savings from energy efficiency retrofits. Such lower-than-expected energy savings are more or less common across the country, as illustrated in Fig. 3.10. Retrofitting projections also show spatial variability. Figure 3.10a shows a plot of the median expected benefits of energy efficiency retrofits based on EPC estimates, Fig. 3.10a shows a plot of the median expected benefits of energy efficiency retrofits based on our model estimates, and

Fig. 3.10c shows the percentage likelihood that energy savings are lower than expected. We can see that retrofitting is always profitable in areas such as Grand Est and PACA, however, the benefits of retrofitting expected by our model suggest that areas such as ARA and BFC need attention.

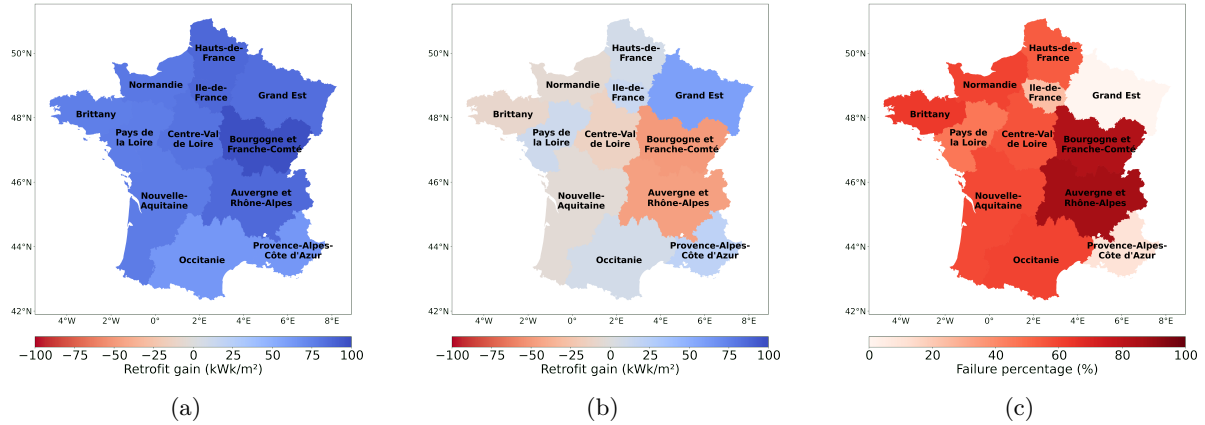


Figure 3.10 Map of 12 French administrative regions with (a) the median expected retrofit gains (in kWh/m²) based on EPC estimates; (b) the median expected retrofit gains (in kWh/m²) based on our model estimates, and (c) the percentage likelihood that energy savings are lower than expected.

It is important to understand that in the standard EPC calculations, the impact of human behavior is limited by the standard; for example, heating time and temperature are uniform for homes in the same location. Therefore, the difference in energy consumption only reflects the thermal performance of the building. However, in our model, the actual electricity consumption is used as the calculation source, and all factors that influence the actual electricity consumption are included. Therefore, both physical (thermal) performance and human behavior impact energy consumption. We also use the term "retrofit" rather than "renovation" because not only does the thermal performance of a building change, but so does human behavior. In this study, we could not model the distinction between socio-economic effects and the physical characteristics of buildings. After retrofitting, consumer behavior changes, impacting energy consumption that can offset energy efficiency improvements. This has been emphasized in many studies of pre- or rebound effects (Cali et al., 2016; Cayre et al., 2011; Coyne and Denny, 2021; Cozza et al., 2020b; Sunikka-Blank and Galvin, 2012; Wiedenhofer et al., 2013) and should always be well considered in future energy savings projections.

3.3.4 Impact of socio-economic factors

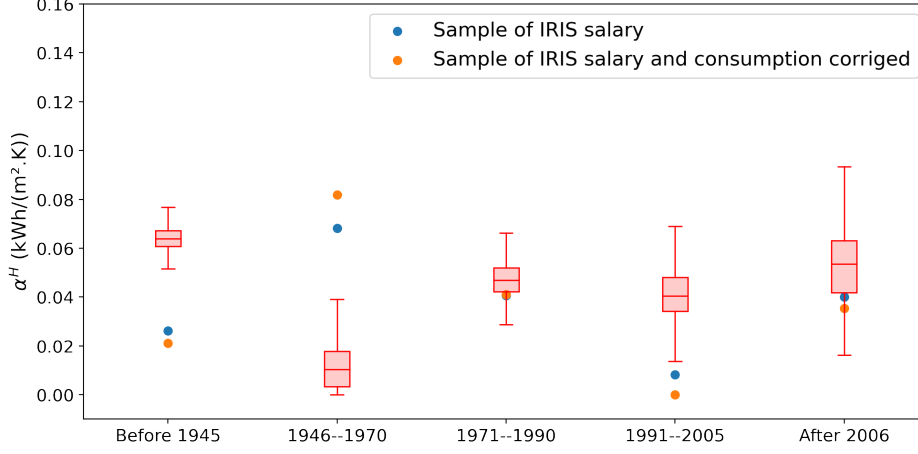


Figure 3.11 Distribution of estimated temperature sensitivities related to different construction periods α_a^H of the region Auvergne-Rhône-Alpes using test sampling size as the income input, blue dots represent estimated coefficients for the sample of income as input and orange dots represent the estimated coefficients with input corrected.

Although socio-economic impacts are not identified in the model in Eq. (3.1), we investigate the confounding of inputs by socio-economic factors (income) that impact heating consumptions, hence on temperature sensitivities. Figure 3.11 shows, with the example of Auvergne-Rhône-Alpes, the distribution of the temperature sensitivity coefficients with the same sample size as the income dataset, along with coefficient estimates from a model that uses the exact IRIS of the income dataset as the sample (the blue dots) and a model that corrects the electricity consumption by income using Eq. (3.14) (the orange dots):

$$E_i^* = \frac{E_i}{W_i} \bar{W} \quad (3.14)$$

with E^* the corrected consumption, W the socio-economic factor which is the median income of the cell i and \bar{W} the average median income of all cells in the same administrative region. The distribution of coefficients compared to the results with income corrections for other administrative regions are given in Appendix Section 3.B.

The results show that income impacts the estimation of temperature sensitivity coefficients for all administrative regions. The differences appear to be larger in the with/without income case for some construction periods, e.g., for Ile-de-France, the difference between the blue and orange points (i.e., with/without income) is significant for the 1946-1970 construction period. We also can see that with the corrected income, the buildings of this construction period tend to be more sensitive to temperature for most administrative regions, which may be related to the pre-bound effect (i.e., if people living in poorer buildings are poorer, they tend to consume

less).

However, it is worth noting that the confounding factors are questioned because the sample is not representative. For most cases, the sampling effect is larger than the correction by income. Indeed, let us compare the coefficients of the income sample with the initial model that does not consider income (i.e. the blue dots compared to the distributions), and we find that they are systematically biased. In most administrative regions, the coefficient results obtained using the income sample IRIS fall within the outliers of the distribution of coefficients obtained by IRIS sampling (the blue points are not in the extreme range). Especially for the eldest construction period (before 1945), the income sample estimates smaller temperature coefficients while for the second period (1946 – 1970) the sample estimates a larger temperature coefficient. This suggests that, except for Ile-de-France and PACA, which have the most representative income dataset, the IRIS samples of the income dataset for most of the administrative regions are overly specific.

3.4 Conclusion

This study assesses the potential future energy gains from retrofitting in France. EPC-like indicators based on actual electricity consumption are statistically modeled using aggregated data to achieve broad geographic coverage. We compare EPC-like indicators based on actual electricity consumption with existing EPCs based on theoretical calculations to explore differences in energy performance (EPG) across household groups. We point out the problems that may be encountered in future retrofits and the key areas that need attention.

A linear temperature sensitivity model based on the previous study was modified for the study's aims. The linear model uses IRIS-level aggregated actual consumption data and extends the buildings' physical characteristics (the age of the building) to estimate temperature-sensitive consumption for each administrative area, grouped by the age of the building. These estimates of temperature-sensitive consumption for each group of buildings based on actual consumption are dominated by heating and are considered heating consumption, which can be compared with theoretical heating consumption estimated through Energy Performance Certificate (EPC) standard calculations. Subsequently, using the temperature sensitivities for each group of buildings, we estimated the retrofit benefits and compared them to the EPC-based benefits.

First, our findings indicate that implementing the RT1974 and RT2005 thermal norms did not improve energy consumption reduction rates as expected in most administrative areas. The original goals of implementing these norms were to reduce energy consumption by 25% and 15%, respectively, compared to previous buildings. Temperature sensitivity coefficients indicate that the expected goals have not been achieved. We also examined model uncertainty in geographic and temporal sampling to ensure that the results of energy performance differences and future retrofit benefit projections are robust. A clear difference can be seen in the comparison, and this difference between actual and conventional consumption is also referred to as the Energy

Performance Gap (EPG). The EPG is positively larger for newer buildings than for older buildings in all regions. This positive EPG suggests that the newest buildings are supposed to have lower energy consumption, but the actual energy consumption is higher than expected. This result is consistent with findings from other neighboring countries. However, the trend of increasing energy performance differences with age is inconsistent, and the relationship between ages varies across administrative regions. According to traditional calculations, if all buildings had the same thermal performance as new buildings built after 2006, the expected gain from retrofitting would be about 60%, i.e., a 60% reduction in heating consumption. If, as a rough guide, heating accounts for 33% of the energy consumption of the whole house, then the total energy consumption of the whole house would be reduced by 20%. However, according to our calculations, 47% of the building will consume more energy than before the retrofitting, which is problematic in terms of achieving the net-zero energy target. Our findings also suggest that temperature sensitivity coefficients can be affected by socio-economic factors. Correlation tests show that the age distribution of housing is related to revenue. Thus, rebound effects may differ across building age groups.

This study aims to map the departure between actual and EPC-based conventional energy consumption at the finest possible scale based on a temperature-sensitive consumption model. These results allow us to assess the expected improvement of the energy performance gap and project building retrofit. The expected savings from the model-based approach show an apparent overestimation of the benefits expected from the EPC approach, consistent with results published in neighboring countries. Indeed, it is important to accelerate the renovation work to improve the physical and thermal characteristics and reduce the heating needs of all housing, especially those low-income households living in buildings with poor thermal performance. Consumers should also be more informed of the difference between energy bills that highly depend on behaviors and energy performance labels.

However, sampling tests show that our model results are highly sensitive to IRIS samplings, especially when the sampling sizes are small. Such a model could be improved if more quality data on other explanatory factors, such as wages, were available. Other factors related to the physical characteristics of buildings are also important and should be included in the model. For example, differences between aggregated dwellings and individual buildings can lead to differences in thermal performance due to interactions between dwellings. It is also important to note that the study does not include data on current renovations in France. The effect of renovation could help to explain the reason for the difference between different construction periods. But it would not affect the estimation of the temperature sensitivity coefficients and would not affect our further studies on EPG and future projections because the aggregated actual electricity consumption data has already taken into account all the dwellings, regardless of the building renovation state. On the other hand, to the best of our knowledge, publicly available data do not allow for further improvements. This study, therefore, calls for an effort to make more data publicly available.

Appendix 3.A Bayesian Ridge analysis

Bayesian inference is another tool for analyzing coefficient errors due to model training sets. This method offers the advantage of estimating uncertainty directly from the input data without relying on regression techniques. Additionally, it provides insights into the sources of uncertainty by modeling and quantifying the inherent uncertainty in the data and model parameters. Another reason that we present Bayesian inference here is that it links to the case using the Ridge method for linear regression. Even though OLS is more suitable for our case, the Ridge regression is still more common and can be applied to other case studies. The definitions of estimated coefficients m as well as the estimates of coefficients error Σ under the Bayesian inference are given as (Bishop, 2006):

$$\begin{cases} \Sigma = (\alpha \mathbf{I} + \beta \mathbf{X}^T \mathbf{X})^{-1} \\ m = \beta \Sigma \mathbf{X}^T y. \end{cases} \quad (3.15)$$

Here α and β are Bayesian Ridge hyperparameters used to regularize the model, and they are not linked to our temperature sensitivity coefficients, although they use the same letters. Following Bishop (2006) and maximizing the evidence function gives us the best values of α as:

$$\alpha = \frac{\gamma}{m^T m} \quad \text{with} \quad \gamma = \sum_k \frac{\beta N \lambda_k}{\alpha + \beta N \lambda_k}, \quad (3.16)$$

where $\{\lambda_k\}_{1 \leq k \leq P}$ are the eigenvalues of covariance matrix $\frac{\mathbf{X}^T \mathbf{X}}{N}$. Since we have $\gamma = \sum_k \frac{\beta N \lambda_k}{\alpha + \beta N \lambda_k} = P - \alpha \sum_k \frac{1}{\alpha + \beta N \lambda_k} = P - \alpha \text{tr}\{\Sigma\}$, so that the total relative errors of coefficients is:

$$\frac{\text{tr}\{\Sigma\}}{m^T m} = \frac{P}{\gamma} - 1. \quad (3.17)$$

To compare the total relative error of coefficients estimation between regions, we just need to compare the value of γ . However, γ is the solution of Eq. (3.16) for which we do not have an explicit solution.

In the case of orthogonal inputs, the results could be equivalent to those of PCAs. However, the regularization is on the principal components (PCs), each separately, not on the original inputs, so there is no longer equivalent regularization between inputs and PCs. In this case, we have for each PC:

$$\alpha_k = \frac{\gamma_k}{m_k^2} \quad \text{with} \quad \gamma_k = \frac{\beta N \lambda_k}{\alpha_k + \beta N \lambda_k}, \quad (3.18)$$

and the error for each coefficient can be expressed as:

$$\Sigma_{kk} = \frac{1}{\alpha_k + \beta N \lambda_k}. \quad (3.19)$$

So that

$$\begin{aligned}\gamma_k &= 1 - \alpha_k \frac{\Sigma_{kk}}{m_k^2} = 1 - \frac{\gamma_k \Sigma_{kk}}{m_k^2} \\ \frac{\Sigma_{kk}}{m_k^2} &= \frac{1}{\gamma_k} - 1.\end{aligned}\quad (3.20)$$

From this relationship, we can see that γ_k determines the relative error of m_k . At the same time, in the PCA space we have:

$$m_k = \frac{c_{kt} \sigma_t}{\sqrt{\lambda_k}}, \quad (3.21)$$

so that an explicit solution can be determined with

$$\begin{aligned}\gamma_k &= \frac{\beta N \lambda_k}{\alpha_k + \beta N \lambda_k} \\ &= \frac{1}{1 + \frac{\gamma_k}{\beta N \lambda_k m_k^2}} \\ &= \frac{1}{1 + \frac{\gamma_k}{\beta N \lambda_k \frac{c_{kt}^2 \sigma_t^2}{\lambda_k}}} \\ &= \frac{1}{1 + \frac{\gamma_k}{\beta \sigma_t^2 N c_{kt}^2}}\end{aligned}\quad (3.22)$$

so that

$$\gamma_k = 1 - \frac{1}{\beta \sigma_t^2 N c_{kt}^2}. \quad (3.23)$$

The above explicit equation is for the orthogonal inputs case. However, we are in the non-orthogonal case. The anisotropy on the priors of the coefficients of the original inputs does not help because the hyperparameter in the original space no longer equals the one in the PCA space $\alpha_i \neq \alpha_k$. We consider that the α is already fixed, and any other feedback on α is not considered. From the second equation in Eq. (3.22) we can see that the larger λ_k , the larger γ_k and so the larger γ . Moreover, from the general case of the total relative error equation:

$$\frac{tr\{\Sigma\}}{m^T m} = \frac{\sum_k \frac{1}{\alpha + \beta N \lambda_k}}{\sum_k \gamma_k^2 (m_k^{OLS,PCA})^2} \quad \text{with} \quad m_k^{OLS,PCA} = \frac{c_{kt} \sigma_t}{\sqrt{\lambda_k}}, \quad (3.24)$$

we can see that the numerator function is concave with positive values of λ_k , so having a low spread of $\{\lambda_k\}_{1 \leq k \leq P}$ is better. But at the same time, we can see that the effect of the distribution of c_{kt}^2 is not trivial since the spread of $\{\frac{c_{kt}^2 \gamma_k^2}{\lambda_k}\}_{1 \leq k \leq P}$ around the mean decreases α and so increases γ . Overall, the effect of the distribution of λ_k and c_{kt}^2 are opposite. Hence, to conclude from the Bayesian analysis, if we want the total relative errors of coefficient estimation to be small, we need the following:

- The number of samples N as large as possible;
- The overall model quality $\beta \sigma_i^2$ as large as possible;
- Check the ensemble effect of both distributions of λ_k and c_{kt}^2 .

We can see a similarity between the Bayesian and parametric frequentist analyses. This coincidence under the uninformative prior case is also explained in [Murphy \(2013\)](#).

Appendix 3.B Impact of income results

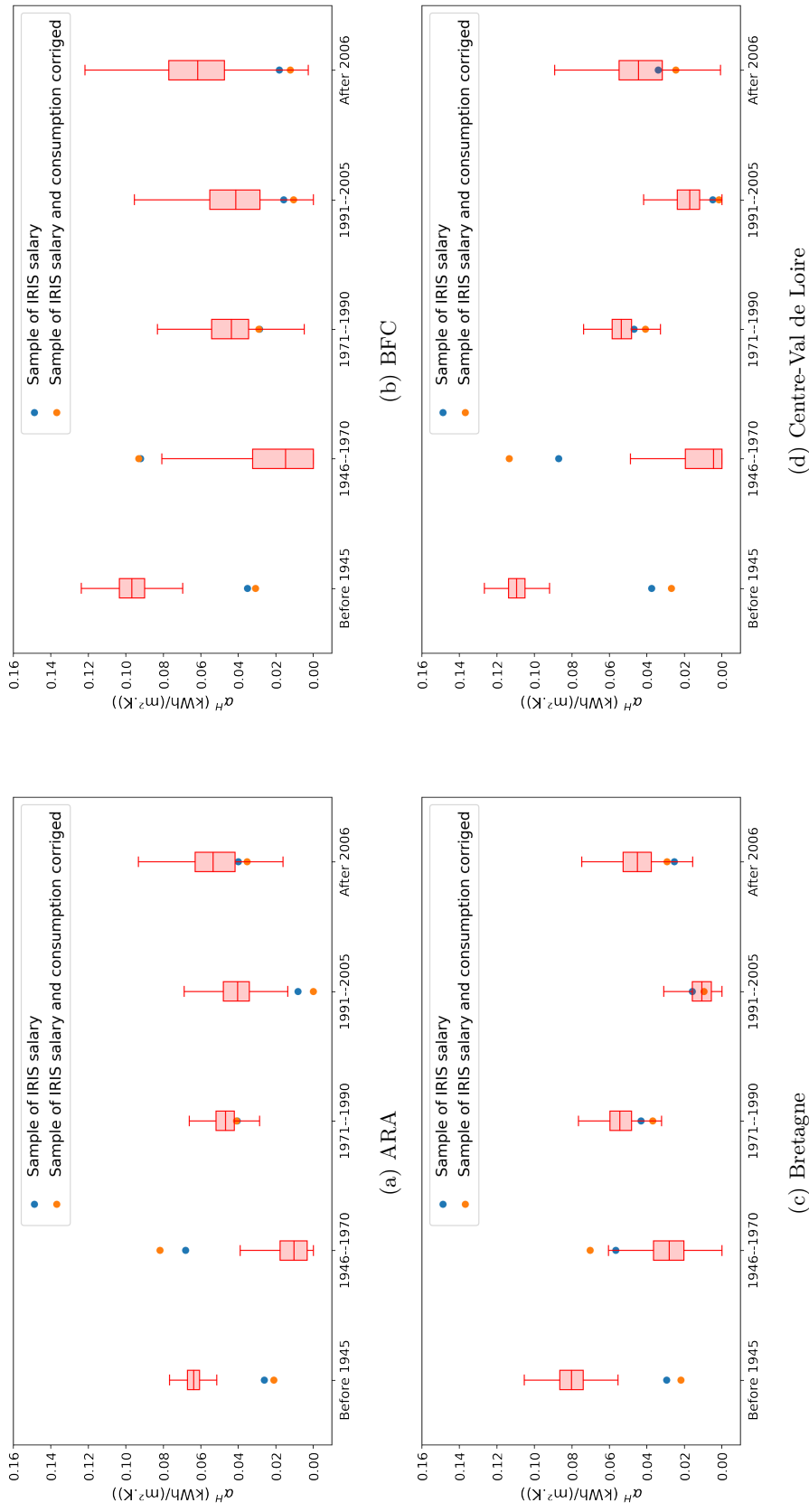


Figure 3.12 Distribution of estimated temperature sensitivities related to different construction periods α_a^H using test sampling size as the income input, blue dots represent estimated coefficients for the income sample as input, and orange dots represent the estimated coefficients with input corrected.

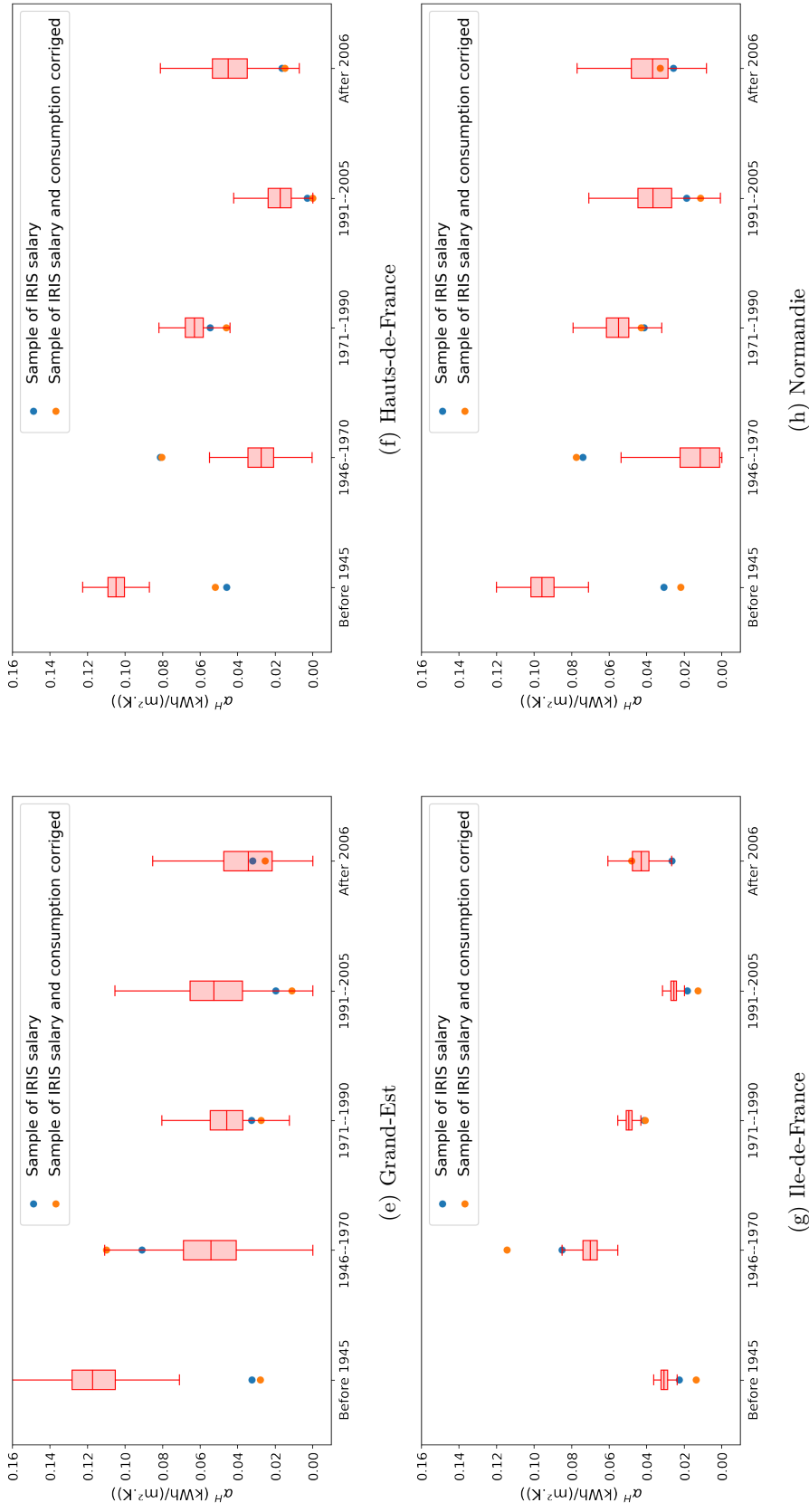


Figure 3.12 Distribution of estimated temperature sensitivities related to different construction periods α_a^H using test sampling size as the income input, blue dots represent estimated coefficients for the income sample as input, and orange dots represent the estimated coefficients with input corrected. (cont.)

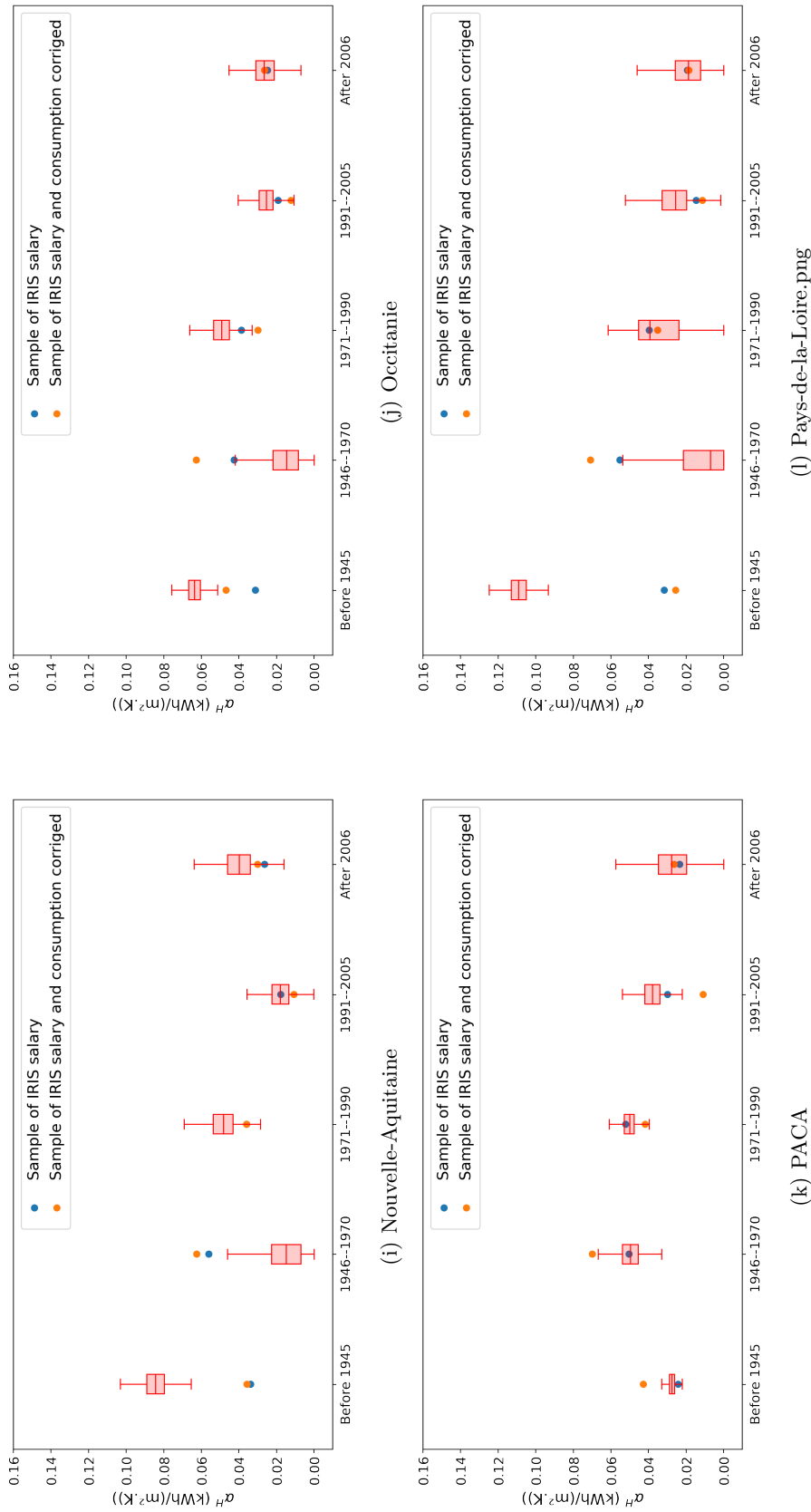


Figure 3.12 Distribution of estimated temperature sensitivities related to different construction periods α_a^H using test sampling size as the income input, blue dots represent estimated coefficients for the income sample as input, and orange dots represent the estimated coefficients with input corrected. (cont.)

Chapter 4

Decarbonizing the residential sector by implementing self-consumption with rooftop photovoltaic (PV)

This chapter is the subject of an article under review submitted to the journal *Sustainable Cities and Society* (Tao et al., 2024b). It focuses on decarbonizing the residential sector by integrating distributed rooftop PV. Temperature sensitivity results from the previous chapters allow for the downscaling of regional hourly electricity consumption at the IRIS level. The hourly consumption profiles are obtained not only for the residential sector but also for the commercial sector to investigate the energy supply-demand balance between sectors with local PV productions. The case study is in the Grand Paris metropolis with a focus on the complementarity of users with different perimeters or region areas, emphasizing technical aspects such as self-consumption rate (SCR) and self-sufficiency rate (SSR).

Contents

4.1	Introduction	84
4.2	Methodology and materials	87
4.2.1	Energy balance indicators	87
4.2.2	Economic evaluation	89
4.2.3	Hourly electricity consumption model	89
4.2.4	Grand Paris metropolis case study data	92
4.3	Results	96
4.3.1	Supply-demand balance analysis	96
4.3.2	Economic impacts	101
4.4	Conclusion	103

4.1 Introduction

Cities are geographic units that impact climate change and have a huge potential for climate mitigation actions (Davi et al., 2022). Urban sustainability will be one of the main challenges of this century (Cuesta-Fernández et al., 2023; Droege, 2018; Mi et al., 2019; Pincetl, 2017). The ongoing urbanization process will generate resource availability and sustainability issues at local and global levels, which must be addressed effectively. Led by several initiatives such as the Covenant of Mayors or the Global Urban Platform C40, hundreds of cities worldwide have committed to decarbonizing or becoming carbon neutral as soon as possible (Hoffmann, 2011; van der Heijden, 2016). Given the spatial density of the population and energy consumption, decarbonizing dense large cities is a key focus for achieving the EU's net-zero carbon target (Cramer et al., 2018; Cuesta-Fernández et al., 2023).

One of the largest cities in Europe, Paris and its suburbs (also known as the Grand Paris metropolis) cover only 0.15% of France's metropolitan territory, with an area of 814 square kilometers, but are home to more than 7 million people, or 10% of the country's population. The region consumes 67% of its energy from fossil fuels, and only 10% of its energy supply is produced locally (7.4% from renewable energy and energy recovery) (Philippe et al., 2022). Responsible for 10% of the country's greenhouse gas emissions, the Grand Paris metropolis must address energy issues in the face of major constraints such as high population density, energy dependency, and vulnerability to climate change.

The French government has set ambitious targets to increase the share of renewable energy in the national energy mix, aiming to achieve a 40% share of renewable energy by 2030. Rooftop photovoltaics (PV) could play an important role in achieving this goal. For example, the French Electricity Transmission System Operator (known as RTE) has proposed several future energy scenarios, of which Scenario M1 emphasizes distributed PV (i.e. rooftop PV) and predicts that 35 GW of residential rooftop PV will be installed in France by 2050 (about half of all individual houses) (RTE, 2021). According to International Energy Agency (2023), solar power will dominate future electricity generation technologies. By 2050, solar power will account for 30% of global electricity generation, among which distributed rooftop PV power generation is strongly promoted by subsidies in many countries (Avril et al., 2012; Nousedilis et al., 2018; The European Commission, 2016).

The benefits of distributed PV generation are various. It helps diversify energy sources, improves grid efficiency by reducing transmission losses (Begovic and Kim, 2011; Hoff and Shugar, 1995), and enables local consumption, reducing extraction from the grid (Amabile et al., 2021; Nousedilis et al., 2018). In addition, distributed PV contributes to electrification goals (Torres-Rivas et al., 2022). It promotes the environmental sustainability of urban areas, especially in the context of the European requirement for near-zero energy buildings (European Parliament and Council, 2021). This shift towards local consumption and decentralized generation, accelerated by economic factors such as lower electricity tariffs and reduced investment costs, heralds a

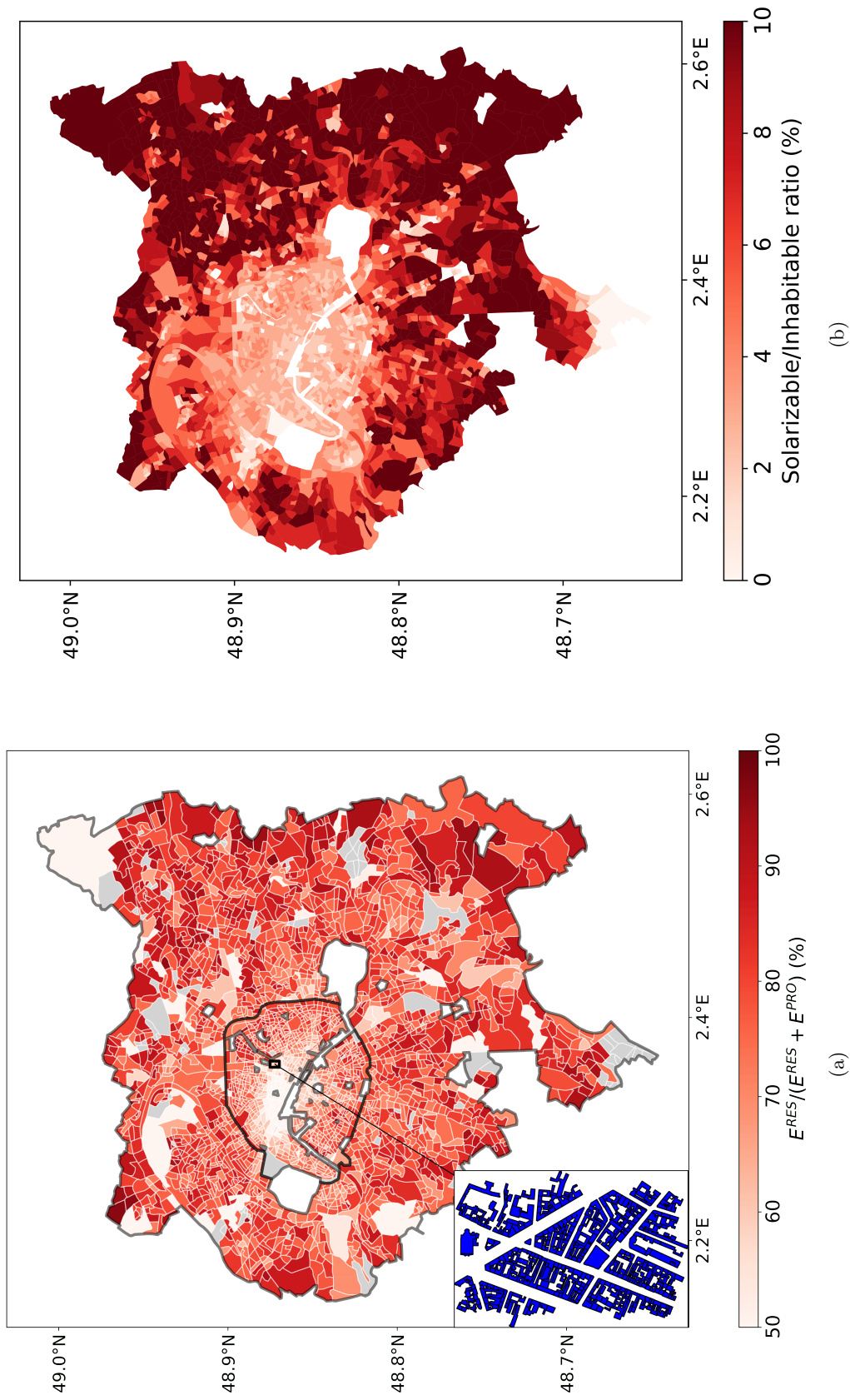


Figure 4.1 (a) Map of the ratios between residential electricity consumption E^{RES} over the sum of residential and commercial electricity consumptions $E^{RES} + E^{PRO}$ for the Grand Paris metropolis with white lines representing more than 2700 IRIS cells. The thick black line outlines Paris, surrounded by its periphery. During the present study, the smaller center is named Paris center, and the periphery is named Paris surroundings. The inset map shows in blue an example of rooftop areas identified by APUR (2019). (b) Ratios between the favorable rooftop surfaces for PV installation (i.e. for which the radiation potential is greater than 1000 kWh/m² per year) and the inhabitable housing surfaces estimated using the APUR data. (Both maps and the subsequent ones are produced for a plate carrée projection.)

change in energy production and consumption patterns. It is also important in helping citizens regain control of their energy supply (Vernay et al., 2023).

In previous studies, the primary focus of energy researchers and urban planners has been to quantify the maximum potential for urban PV power generation. For example, Torres-Rivas et al. (2022) studies the region of Catalonia based on aggregated annual data and finds that rooftop PV could meet between 8% and 30% of the region's residential electricity consumption. Montero et al. (2022) studies 14 public hospitals in southwestern Spain and finds that by dedicating 30-50% of the roof area to PV power generation, PV could meet 25-30% of consumption. Yuan et al. (2016) states that PV can meet about 56% of total electricity consumption in the commercial sector or 34% in the commercial and industrial sectors for Osaka city in Japan. A growing number of studies on the potential of urban PV show the magnitude of the challenge of maximizing PV self-generation within dense, compact urban boundaries (Cuesta-Fernández et al., 2023; Natanian et al., 2019; Vulkan et al., 2018). However, as Cuesta-Fernández et al. (2023) points out, studies quantifying the contribution of metropolitan areas to the PV potential of cities are virtually non-existent, let alone quantifying the complementarity between compact, dense cities and metropolitan areas.

The center of Paris and its suburbs have different characteristics, e.g., Figure 4.1a shows the ratio of residential electricity consumption over both residential and commercial electricity consumption, whereas Figure 4.1b shows the ratio of the useful roof area to the residential area. The smaller roof surfaces with respect to inhabitable housing surfaces in the central area indicate that the buildings there are taller and denser. In contrast, the peripheral area has a higher ratio of residential electricity consumption.

Due to the variable nature of renewable energy sources (especially distributed PV), their integration introduces complexity into grid management. A generation that does not match demand will be injected into the grid, potentially leading to reverse power flows and voltage fluctuations, destabilizing grid operations. These issues require careful energy balancing to maintain grid reliability and quality. Indeed, the increasing amount of distributed rooftop PV implies an increasingly complex energy balance. Severe imbalances imply (1) the need for additional generation capacity in other interconnected areas in the face of growing electricity consumption, (2) possible upward adjustments in the transmission capacity of distribution and transmission networks if congestion issues occur, and (3) additional line losses. Moreover, matching the electricity production of rooftop PV installations with the current consumption at these scales (i.e., without considering electrification) depends not only on the installed capacity of rooftop PV but also on the complementarity between different consumption scenarios, especially between residents and professionals and between dense urban and suburban areas. Meanwhile, the economic interests of consumers indirectly impact rooftop PV promotion and affect the difficulty of implementing new energy policies on a large scale.

With Paris's and its surroundings' different characteristics, our main research question is to what extent rooftop PV installations contribute to the balance/imbalance between electricity

supply and demand at different scales in the Grand Paris metropolis. To this end, we study the supply-demand balance from a scale of districts of about 2000 people to a metropolis scale of about 12 billion people, using PV data and useful rooftop area data, and analyze the electricity consumption of all residential and small commercial properties, with a focus on the Grand Paris metropolis. The analysis also includes simplified economic fusers. To measure the contribution of rooftop PV to the electricity balance, we use two metrics: the self-consumption rate, defined as the share of consumption covered by PV relative to total production, and the self-sufficiency rate, defined as the share of consumption covered by PV relative to total consumption. From the grid perspective, increasing the self-consumption and self-sufficiency rates can reduce grid instability. From the consumer's point of view, expanding the self-consumption and self-sufficiency rates can reduce energy costs and increase profits. Therefore, in this study, we investigate the impact of infrastructure on the supply-demand balance by examining these two rates. Unlike most previous studies, this study uses these two indicators to assess the energy balance rather than the level of PV generation.

Real-time electricity consumption profiles and solar power generation are important for accurately assessing the performance of self-consumption and self-sufficiency rates. However, hourly data was only available at a regional level during our study. Therefore, we used a temperature sensitivity model to estimate the hourly evolution of electricity consumption per consumer for the residential and commercial sectors to downscale electricity consumption geographically. The paper is organized into four sections. Section 4.2 describes the methodology of energy balance evaluation, the consumption model, and the data used for the Grand Paris metropolis case study. Section 4.3 presents and discusses the results. Finally, Section 4.4 draws conclusions and the perspectives of future studies.

4.2 Methodology and materials

This section presents the indicators used to evaluate the energy balance with the integration of distributed rooftop PV, as well as the simplified economic metrics used. It explains how the residential and commercial sectors' hourly electricity consumption per consumer is estimated when only aggregated data are available to assess self-consumption and self-sufficiency rates. We also present the data for the application to the Grand Paris metropolis. This study's total period of historical data is less than 30 years, so the results and conclusions drawn apply only to the current climate.

4.2.1 Energy balance indicators

The degree of mismatch between PV generation and electricity consumption is measured using the following two indicators. First, we define quantities $P_i^{C,x}(t)$ and $P_i^{PV,x}(t)$ respectively as the electricity consumption power and the PV electricity generation power for the sector x

(RES for residential or PRO for commercial or can be the sum) in the cell i at time step t with a time step of one hour generally. The $E_i^{C,x}$ and $E_i^{PV,x}$ are thus defined as the energy transferred during the total time period T with $E_i^{C,x} = \sum_{t=0}^T P_i^{C,x}(t)$ and $E_i^{PV,x} = \sum_{t=0}^T P_i^{PV,x}(t)$. Then, the Self-Sufficiency Rate (SSR) that measures the share of consumption $E_i^{SC,x}$ covered by PV relative to total consumption $E_i^{C,x}$ for the sector x in the given cell i is defined as:

$$\begin{aligned} \text{SSR}_i^x [\%] &= \frac{E_i^{\text{SC},x}}{E_i^{\text{C},x}} \times 100\% \\ &= \frac{\sum_{t=0}^T \min(P_i^{\text{C},x}(t), P_i^{\text{PV},x}(t))}{\sum_{t=0}^T P_i^{\text{C},x}(t)} \times 100\%. \end{aligned} \quad (4.1)$$

And the Self-Consumption Rate (SCR) that measures the share of consumption $E_i^{SC,x}$ covered by PV relative to total production $E_i^{PV,x}$ for the sector x in a given cell i is defined as:

$$\begin{aligned} \text{SCR}_i^x [\%] &= \frac{E_i^{\text{SC},x}}{E_i^{\text{PV},x}} \times 100\% \\ &= \frac{\sum_{t=0}^T \min(P_i^{\text{C},x}(t), P_i^{\text{PV},x}(t))}{\sum_{t=0}^T P_i^{\text{PV},x}(t)} \times 100\%. \end{aligned} \quad (4.2)$$

The indicators per domain or subdomain that are larger than the cell when considering energy exchange between the cells inside are defined in the same way, replacing the cell consumption and production with the aggregated consumption and production of the domain of the subdomain. Let A be the set of cells (i.e., $A=P$ for all cells in the Paris center and $A=S$ for all cells in the Paris surroundings, and $A=GP$ for Grand-Paris with $GP=P \cup S$), and the SSR and SCR are defined as:

$$\begin{aligned} [\text{SSR}]_A^x [\%] &= \frac{E_A^{\text{SC},x}}{E_A^{\text{C},x}} \times 100\% \\ &= \frac{\sum_{t=0}^T \min(\sum_{i \in A} P_i^{\text{C},x}(t), \sum_{i \in A} P_i^{\text{PV},x}(t))}{\sum_{t=0}^T \sum_{i \in A} P_i^{\text{C},x}(t)} \times 100\%, \end{aligned} \quad (4.3)$$

and

$$\begin{aligned} [\text{SCR}]_A^x [\%] &= \frac{E_A^{\text{SC},x}}{E_A^{\text{PV},x}} \times 100\% \\ &= \frac{\sum_{t=0}^T \min(\sum_{i \in A} P_i^{\text{C},x}(t), \sum_{i \in A} P_i^{\text{PV},x}(t))}{\sum_{t=0}^T \sum_{i \in A} P_i^{\text{PV},x}(t)} \times 100\%. \end{aligned} \quad (4.4)$$

Then, we define the average SSR and SCR at the IRIS level by:

$$\langle \text{SSR} \rangle_A^x [\%] = \frac{\sum_{i \in A} E_i^{\text{SC},x}}{\sum_{i \in A} E_i^{\text{C},x}} = \frac{\sum_{i \in A} \text{SSR}_i E_i^{\text{C},x}}{\sum_{i \in A} E_i^{\text{C},x}}, \quad (4.5)$$

and

$$\langle \text{SCR} \rangle_A^x [\%] = \frac{\sum_{i \in A} E_i^{\text{SC},x}}{\sum_{i \in A} E_i^{\text{PV},x}} = \frac{\sum_{i \in A} \text{SCR}_i E_i^{\text{PV},x}}{\sum_{i \in A} E_i^{\text{PV},x}}. \quad (4.6)$$

A weighted average is needed to evaluate the average SSR and SCR performance without considering the energy sharing between the cells. This is because the cells inside a domain or a subdomain do not have the same PV generation or electricity consumption. With the above definitions, for all the domains or subdomains, we have $[\text{SSR}]_A^x \geq \langle \text{SSR} \rangle_A^x$.

However, if $C=A \cup B$ where A and B are two disjoint sets of cells, it may be that $[\text{SSR}]_C^x < \langle \text{SSR} \rangle_A^x$. To reach an SSR of 100%, we need both for the total production to be larger or equal to the total consumption and for the production to occur at the time to satisfy the consumption at each time step. When the first condition is satisfied, the SSR can not be larger than $\frac{E^{\text{PV}}}{E^{\text{C}}}$.

4.2.2 Economic evaluation

Although we prioritize the aspects of energy balance, the economic perspective is still very important when studying the potential of distributed PV power generation, as it can affect practical feasibility. We ignore the investment part in the study to simplify the problem. Since the diffusion of rooftop PV is considered maximum (PV panels will be installed on all suitable rooftops), the investment can be considered a constant that does not vary with the contracted perimeter. Thus, the normalized cost per kilowatt purchased can be expressed as follows:

$$\text{Price} = \frac{\text{Cost}}{E^{\text{C}}} = \frac{E^{\text{C}} \pi_a - E^{\text{SC}} \pi_v}{E^{\text{C}}} = \pi_a - \text{SSR} \pi_v \quad (4.7)$$

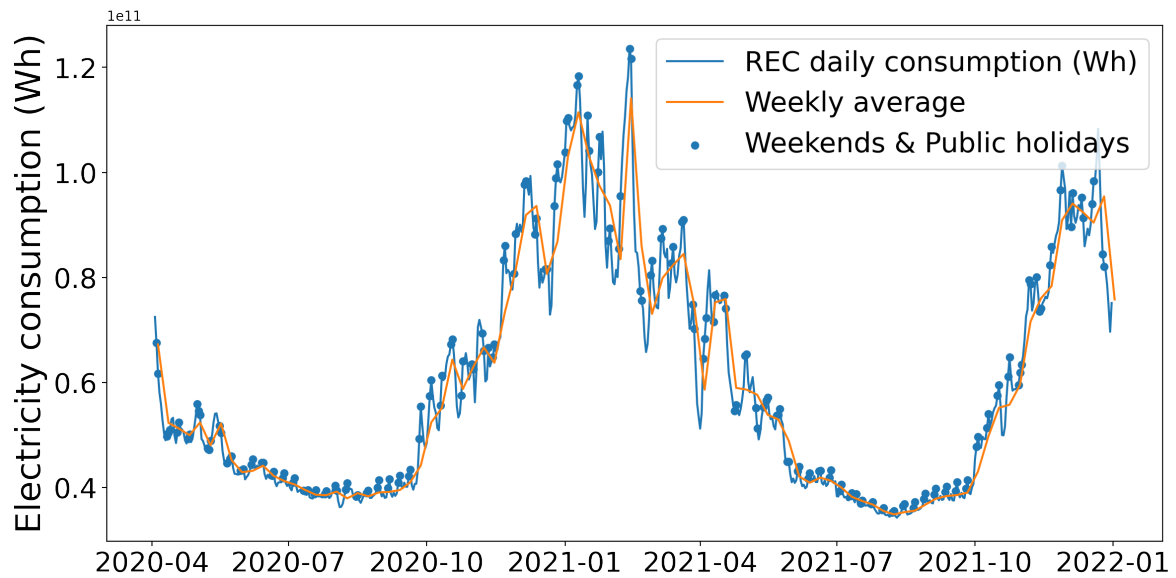
where π_a is the initial purchase price for each kilowatt of electricity consumed and π_v is the FIT (feed-in tariff). With this definition, we have that:

$$\text{Price}_A > \text{Price}_B \equiv \text{SSR}_A < \text{SSR}_B \quad (4.8)$$

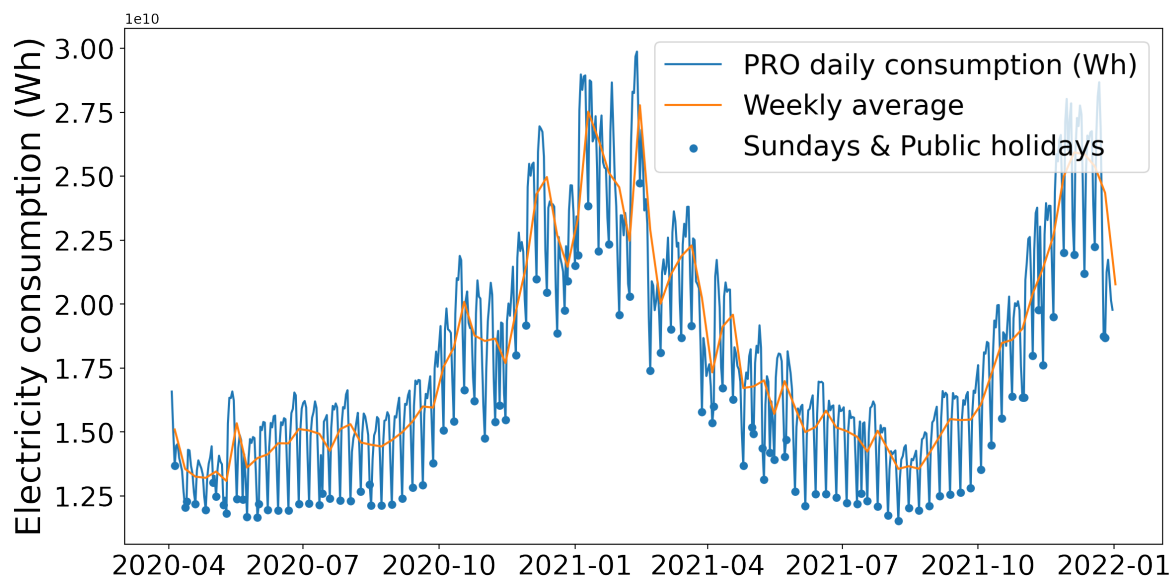
4.2.3 Hourly electricity consumption model

In energy balance studies, the evolution of the electricity consumption of buildings over time (especially hours, also known as building demand curves) is important because demand curves have a strong impact on the grid (Linszen et al., 2017; Montero et al., 2022; Roberts et al., 2019). One of our study's objectives is to examine the complementary impacts of different sectors and urban areas on the energy balance. Therefore, we must obtain hourly electricity consumption profiles for both Residential (RES) and Small Businesses (PRO) sectors at smaller geographic scales. As needed, we can aggregate these data to any larger area.

Figure 4.2a shows the daily consumption of households (RES), while Figure 4.2b shows the daily consumption of all small businesses (PRO) in the region. We can see that both data have similar seasonality due to temperature sensitivity. Indeed, the outdoor temperature affects



(a)



(b)

Figure 4.2 Daily consumption evolution summed over the Grand Paris metropolis with $P \leq 36$ kVA during the 2020/04/02–2022/01/01 period. The blue line (resp. the orange line) represents daily (resp. weekly) running averages. (a) Residential electricity consumption (RES) and the blue dots represent daily consumption on weekends and public holidays. (b) Small businesses' electricity consumption (PRO) and the blue dots represent daily consumption on Sundays and public holidays.

electricity consumption, especially outside a certain comfort range. Total consumption can generally be divided into different components: a regular part not influenced by temperature plus a weather-sensitive part. Thus for each given area i , hourly consumption profile $E_i^{C,x}(d, h)$ can be split into a temperature-sensitive part $E_i^{\text{th},x}(d, h)$ and a base part $E_i^{\text{b},x}(d, h)$ as:

$$E_i^{C,x}(d, h) = E_i^{\text{th},x}(d, h) + E_i^{\text{b},x}(d, h). \quad (4.9)$$

The daily temperature-sensitive consumption $E_i^{\text{th},x}(d)$ for each sector x for each area i can be estimated using the degree-days (HDD_i and CDD_i) and temperature sensitivity coefficients β_i^{H} and β_i^{C} for each sector following the previous chapters [Tao et al. \(2024a\)](#) :

$$E_i^{\text{th},x}(d) = (\text{HDD}_i(d) \beta_i^{\text{H}} + \text{CDD}_i(d) \beta_i^{\text{C}}) \text{NC}_i. \quad (4.10)$$

In addition, since temperature-sensitive electricity use is related to daily variations in outdoor temperatures, the hourly variations in the electricity use curves are mainly due to basic, non-temperature-dependent electricity use such as lighting and cooking. However, the number of occupants per hour in residential buildings and small commercial businesses' equipment and lighting habits are difficult to control, and detailed and accurate data are difficult to obtain. These variables may vary simultaneously between weekdays and holidays. Therefore, our estimated hourly electricity consumption is the average electricity consumption per household or per business and will vary on weekdays and holidays. With two main assumptions, we can finally downscale the regional electricity consumption into sub-regional areas:

- The daily temperature-sensitive consumption $E_i^{\text{th},x}(d)$ is assumed to be evenly distributed during the 24 hours.
- The hourly consumption profile $E_i^{\text{b},x}(d, h)$ is assumed to be the same for all households or all business sites in the same region but has different profiles depending on the month and type of day, as consumer habits may change.

So that Eq. (4.9) can be replaced by the following equation based on the assumptions:

$$E_i^{C,x}(d, h) = \frac{1}{24} E_i^{\text{th},x}(d) + \text{NC}_i E_i^{\text{b},x}(d, h), \quad (4.11)$$

where NC_i is the number of households or commercial sites inside the area i , and NC is the regional number of households or commercial sites with $\text{NC} = \sum_{i \in A} \text{NC}_i$. The regional hourly electricity consumption $E^{\text{C}}(d, h)$ is the sum of all sub-regional hourly consumptions $E_i^{C,x}(d, h)$,

hence at the regional level, we have:

$$\begin{aligned}
E^C(d, h) &= \sum_{i \in A} E_i^{C,x}(d, h) \\
&= \frac{1}{24} \sum_{i \in A} E_i^{\text{th},x}(d) + \sum_{i \in A} \text{NC}_i E^{\text{b},x}(d, h) \\
&= \frac{1}{24} \sum_{i \in A} E_i^{\text{th},x}(d) + \text{NC} E^{\text{b},x}(d, h).
\end{aligned} \tag{4.12}$$

We can finally determine the consumption profiles for each sector $E^{\text{b},x}(d, h)$ using the inputs NC, $E^C(d, h)$ and the previously determined temperature-sensitive consumptions $E_i^{\text{th},x}(d)$. After that, the hourly electricity consumption of each area $E_i^{C,x}(d, h)$, whether residential or commercial, is estimated using Equation (4.11). To include as much data as possible, hourly consumption is estimated for the whole period when HDD and CDD are available, from 2011 to 2020. When examining the energy balance performance, all ten years of data are used for the average to eliminate the multi-year effect.

4.2.4 Grand Paris metropolis case study data

4.2.4.1 Electricity consumption data

The study used data from Enedis, the French public company managing France's electricity distribution network. We analyzed data on all contracts for electricity consumption up to 36 kVA by households and small commercial users in the Grand Paris metropolis from April 2020 to December 2021. Two main datasets are available: the first provides electricity consumption data recorded half-hourly, 24 hours a day, 365 days a year, at the administrative regional level for several different groups of consumption profiles (Enedis, 2020); the other dataset provides aggregated annual electricity consumption data for different sectors at the IRIS level from 2011 to 2018 (included). The IRIS is the basic (and smallest) administrative unit for which official statistical data is published in France. It consists of a division of the territory into "districts" with a population of about 2,000 inhabitants (IGN, 2009).

Although both sets of data (annual consumption and hourly profile consumption) come from the same source, Enedis, the total number of sites for the Grand Paris metropolis region is inconsistent. The first step is to convert the number of sites per IRIS corresponding to the hourly consumption dataset using population weighting for the two sectors studied (residential and commercial):

$$\text{NC}_i = \left(\frac{\text{NCI}_i(y)}{\sum_{i \in A} \text{NCI}_i(y)} \right) \text{NC} \tag{4.13}$$

where $\text{NCI}_i(y)$ is the annual dataset's number of households or commercial users per IRIS.

After correction, the total consumption per sector is given as:

For the economic evaluation, the initial electricity price π_a was considered to be the same

Table 4.1 Annual electricity consumption and PV production (all in TWh) for the Grand Paris metropolis and its two subdomains (center and surroundings) for different sectors.

Perimeter	Residential (RES)		Small Businesses (PRO)		RES+PRO	
	E^C	E^{PV}	E^C	E^{PV}	E^C	E^{PV}
Paris center	5.0	0.7	2.1	0.1	7.1	0.8
Paris surroundings	7.9	2.9	2.2	0.3	10.1	3.2
Grand Paris	12.9	3.6	4.3	0.4	17.2	4.0

for both the residential and commercial sectors and was given as 20 euro cents per kilowatt, while π_v was also set the same for both sectors and was given as 13.39 euro cents per kilowatt as the value of the year 2020. (Eurostat, 2023)

4.2.4.2 Photovoltaic data

The Atelier Parisien d’Urbanisme (APUR) makes available to the public a dataset containing information on the solar potential (in kWh/m²/year) of each building in the Grand Paris metropolis, indicating its average annual solar radiation, calculated by simulating the average annual solar radiation and taking into account the shading effects of buildings (APUR, 2019). APUR also provides a combination of the building layers corresponding to the footprint with the assignment of typological and morphological information (APUR, 2020). This data layer contains more than 1 million buildings in vector form. Information such as floor area, construction period, and height are available. With this data, we no longer need hypothetical PV simulation data for potential PV studies. In addition, since this paper focuses on maximizing the available solar energy to investigate the impact of distributed PV integration on the energy balance, we used all potential rooftop PV areas that meet certain criteria rather than optimizing the size of the PV system. Indeed, the optimal PV sizing for rooftop PV may have been overly optimistic and overestimated actual PV availability (Narjabadifam et al., 2022; Yeligi et al., 2023). Figure 4.1b shows the ratio between the favorable rooftop areas (i.e., areas where the annual potential is ≥ 1000 kWh/m²) and the residential areas at the IRIS level.

On the other hand, PVGIS (2022) provides an estimate of the hourly PV production for a given site with the chosen PV installation technology and PV panel size and orientation. Roof areas were extracted from the APUR dataset and combined with PVGIS to obtain the PV potential production for each IRIS. Several hypotheses were made when estimating the PV potential at the IRIS level:

- Residential rooftop surface is considered “favorable” for PV installation if the radiation potential is greater than 1000 kWh/m² per year, and only this part of the rooftop surface is taken into account.
- Radiation is the same inside a given IRIS (no difference between buildings inside an IRIS).

- The inclination and azimuth are set to be automatically optimal values provided by PVGIS.
- The panel technology chosen for now is crystalline silicon.

However, we can not distinguish the rooftop of the RES sector from that of the PRO sector with APUR data. To do so, we consider that the roof area is equally distributed according to the number of users, which means that the PV generation should be proportional to the number of users by sector. Therefore, for each IRIS we have:

$$\frac{E_i^{\text{PV,PRO}}}{E_i^{\text{PV,RES}}} = \frac{NC_i^{\text{PRO}}}{NC_i^{\text{RES}}} \quad (4.14)$$

4.2.4.3 Calibrated base demand profiles

Using the methodology described in Section 4.2.3, we have calculated the average residential and commercial electricity consumption curves for the Grand Paris metropolis for holidays and weekdays in different months. Using these demand curves, we can then estimate each cell's total electricity consumption with a known number of consumers per sector. Based on the total electricity consumption curves, the mismatch between supply and demand can be analyzed by comparing demand with PV generation. Figure 4.3a and Figure 4.3b show the average daily electricity consumption pattern of the typical four seasons for residential consumers, and Figure 4.3c and Figure 4.3d for the commercial sector. Profiles of 12 months are used for further energy balance analysis but are not shown here. The seasonal features are typical enough to represent the monthly differences. We also recall that these electricity consumption curves do not include temperature-related electricity consumption.

During working days, the RES profiles show that the highest daily consumption is mostly in the evening, around 19:00, except in summer. Meanwhile, local maximums also occur on workdays before people leave home for work around 7:00 - 8:00 and at lunchtime around 12:00. The difference between the evening peak and the midday peak is particularly large in winter but not evident for other seasons. During weekends, opposite to working days, the highest RES daily consumption is mostly at midday except in winter. Meanwhile, the local maximum in the morning disappears since people no longer prepare to leave for work. No matter the season or the type of day, the local minimum always arrives during nighttime when people sleep and during the afternoon around 14:00 and 16:00 when people are at work. The differences between seasons may be related to seasonal changes in people's behavior. For example, in the summer, many people go on longer vacations and engage in more outdoor activities, while in the winter, they spend more time indoors.

For the PRO profiles, electricity consumption is generally higher on weekdays than on holidays. During the weekdays, the local maximums of PRO consumption occur around 10:00 –

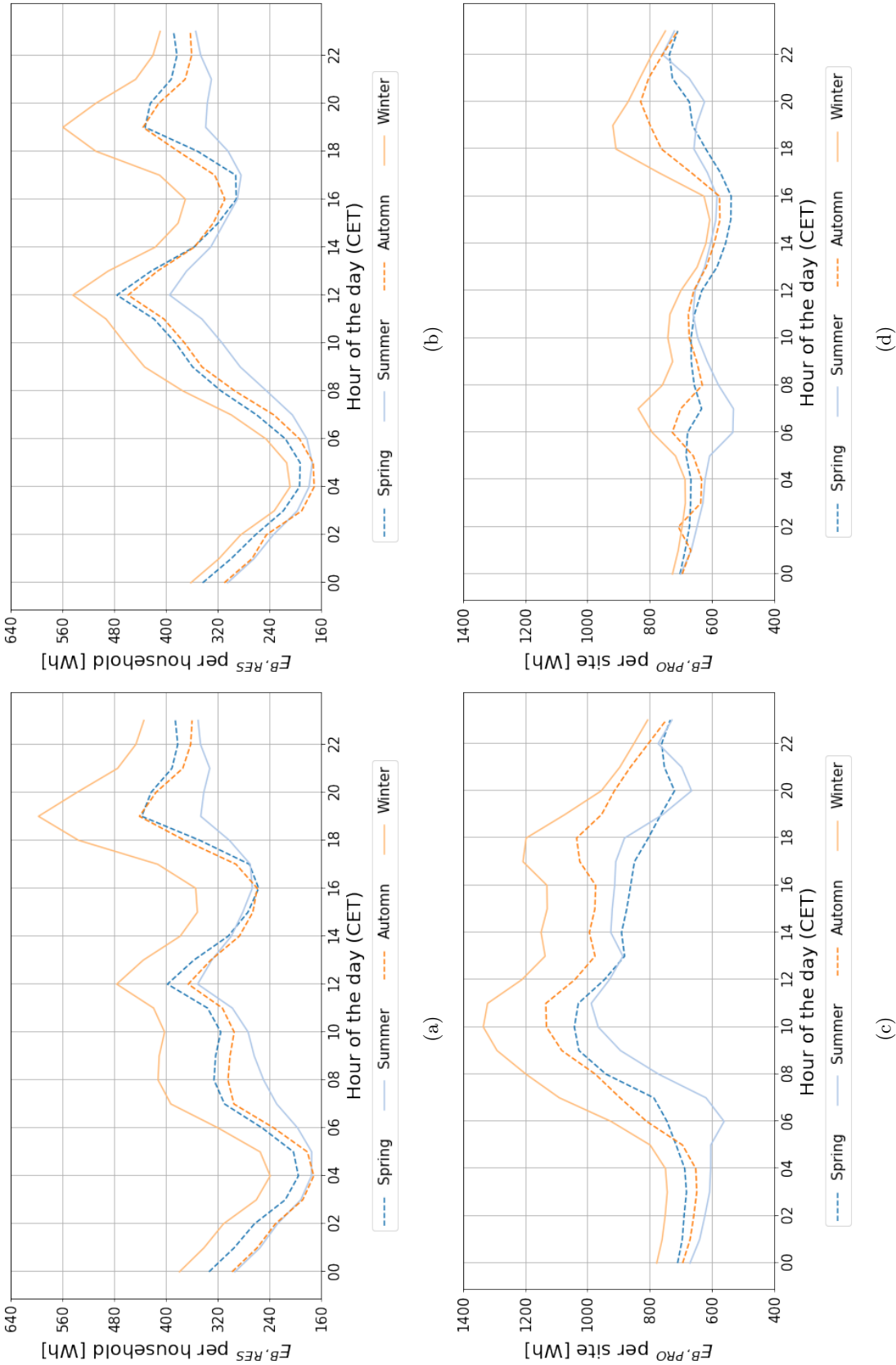


Figure 4.3 Average of the base electricity consumption for each hour of the day and for each season over the period between April 2020 and January 2022. Separate profiles are given for RES (top) and PRO (bottom) and for the weekdays (left) and for the weekends and holidays (right). The Central European Time (CET) standard is used.

11:00 and around 17:00 – 18:00. During the daytime on working days, the PRO consumption remains at a relatively high level, and the period of large PRO consumption from 7:00 to 19:00 correlated to a large extent with the period of PV generation. On public holidays, however, the PRO daily consumption curve remains relatively flat except for the small local maxima in the morning and evening for the winter and autumn months. Our consumption profile results align with other European studies regarding the average demand curve for households (Aberilla et al., 2020; Mavroyeoryos et al., 2017; Møller Andersen et al., 2013). Therefore, we verify that our model can reproduce the qualitative features we expect from the demand.

4.3 Results

4.3.1 Supply-demand balance analysis

Maps of self-consumption rate (SCR) and self-sufficiency rate (SSR) for residential sector RES and commercial PRO alone, as well as the case with complementary sectors, are shown in Figure 4.4. Without allowing any exchange between different sectors or IRIS, we have an average SCR for all IRIS in Grand Paris of around 74.4% for RES alone and 96.4% for PRO. For the SSR, the value is, on average, around 20.5% for RES alone and 9.9% for PRO. These results are also shown in the third rows and first four columns of Table 4.2. Table 4.2 shows all the average and aggregated SSR and SCR for the different perimeters. It is worth noting that the SSR is higher in the peripheral areas of Paris than in the center of Paris, regardless of the sector RES or PRO. It suggests that local PV production in the peripheral areas can offset a greater proportion of consumption. This is possibly due to the lower density of buildings and potentially greater PV installations in the peripheral areas compared to the dense city center. This difference in building density can also be seen on the map in Figure 4.1b. The solarizable rooftop relative to the inhabitable housing surface ratio is lower in cities with higher building densities than in the suburbs, which correlates with the SSR maps. On the other hand, the 100% SCR in the Paris center indicates that all PV is used locally, but this is not the case for the Paris surroundings. From Table 4.1, we can see that the total PV production is low for both subdomains. However, due to the mismatch, some PV production in the Paris surroundings, especially from the RES sector, becomes surplus, and the SCR is lower for these peripheral areas of Paris surroundings. This PV surplus can be injected for the Paris center to improve both performances for the peripheral by reducing loss and for the center to improve the share of PV-covered consumption. The impact of perimeter extension is then studied by combining different users from different IRIS or sectors or subdomains together since the perimeter of users and areas involved may significantly impact the energy balance.

We first examine the case of energy sharing between distinct IRIS within a given subdomain. The results are presented in the fourth and fifth rows of Table 4.2. Comparing these results under this perimeter expansion to the IRIS-weighted average values presented in the first two

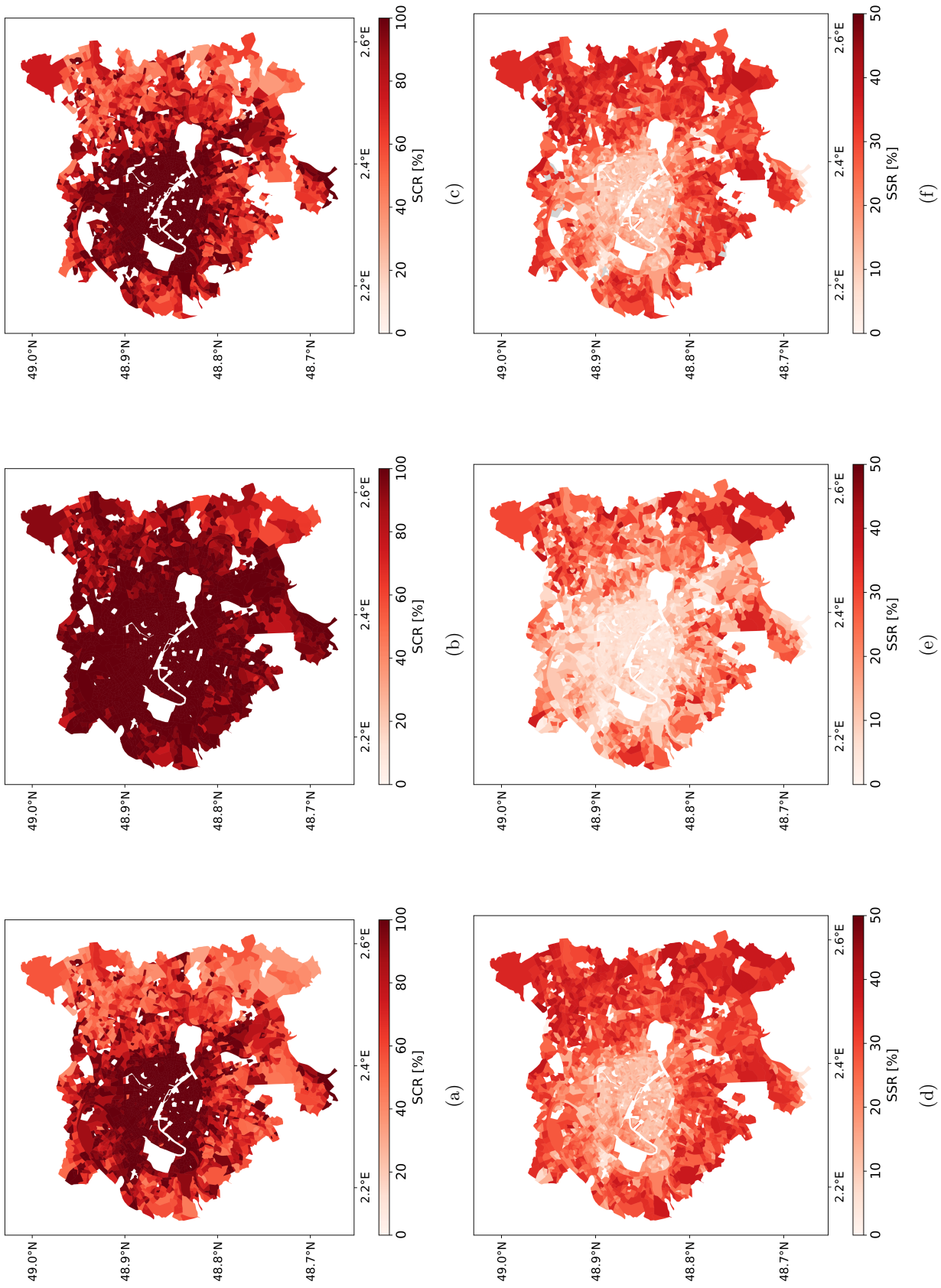


Figure 4.4 Map at the IRIS level, the first row (a, b, c) is of self-consumption rate (SCR) and the second row (d, e, f) is of self-sufficiency rate (SSR). The first column (a, d) is for residential consumption only, the middle column (b, e) is for small businesses only, and the right column (c, f) is for the sum of both sectors.

Table 4.2 Annual self-sufficiency rate (SSR) and self-consumption rate (SCR) for the Grand Paris metropolis and its two subdomains (center and surroundings) compared to the weighted average of IRIS values for different sectors.

Perimeter	Residential (RES)		Commercial (PRO)		RES + PRO weighted-average		RES+PRO	
	SSR (%)	SCR (%)	SSR (%)	SCR (%)	SSR (%)	SCR (%)	SSR (%)	SCR (%)
Paris center IRIS weighted-average	13.1	99.2	6.0	100.0	-	-	11.0	99.3
Paris surroundings IRIS weighted-average	25.1	68.7	13.7	94.9	-	-	22.6	71.3
Grand Paris IRIS weighted-average	20.5	74.4	9.9	96.4	-	-	17.8	76.8
Paris center	13.2	100.0	6.0	100.0	11.1	100	11.1	100
Paris surroundings	28.4	77.8	14.4	100.0	25.4	80.0	27.0	85.0
Grand Paris weighted-average	22.5	81.9	10.3	100.0	-	-	20.4	88.0
Grand Paris	24.6	89.5	10.3	100.0	21.0	90.7	22.4	96.4
								23.2

$\frac{E^{PV}}{F_C}$ (%)

Table 4.3 Self-sufficiency rate (SSR) and self-consumption rate (SCR) for the region Grand Paris and its two subdomains (center and surroundings) compared to the weighted average of IRIS values under different seasons for the sum of RES and PRO sectors.

Perimeter	SSR (%)			SCR (%)				
	Spring	Summer	Autumn	Winter	Spring	Summer	Autumn	Winter
IRIS weighted-average Paris center	14.1	21.0	10.0	4.5	99.7	99.6	99.8	100.0
IRIS weighted-average Paris surroundings	30.1	39.1	22.3	11.8	74.1	62.5	76.6	96.5
IRIS weighted-average Grand Paris	23.5	31.5	17.2	8.8	79.1	69.8	81.2	97.2
Paris center	14.2	21.1	10.0	4.5	100.0	100.0	100.0	100.0
Paris surroundings	35.8	46.4	25.8	12.2	88.2	74.1	88.6	100.0
Grand Paris	29.2	41.8	20.6	9.0	98.3	92.5	97.3	100.0

rows (where each IRIS is a closed cell without energy exchange between IRIS), we observe that all SCR and SSR values increase, regardless of the sector. This improvement is mathematically proven and described in Section 4.2.1. For RES alone, both SSR and SCR improve by 0.8% for the Paris center and by 13% for the Paris surroundings. For PRO alone, both SSR and SCR improve by 5% for the Paris surroundings while remaining the same values for the Paris center. When both sectors interact (i.e., the case of RES+PRO), the SCR and SSR demonstrate improvements of 0.8% in the Paris center and 19% in the Paris surroundings, respectively, in comparison to the weighted average of the subdomains. And in the case of the Grand Paris region, which considers all IRIS within the sum of subdomains, both SCR and SSR improve by 26% compared to the weighted average of all IRIS in Grand Paris. Thanks to the complementarity between IRIS, extending the perimeter for both subdomains can improve both SSR and SCR and allow for greater consumption coverage, with a subsequent reduction in surplus energy injection into the grid. When viewed from an energy balance perspective, this improvement is more pronounced in the Paris surroundings than in the Paris center, irrespective of the sector in question.

We then examine the case of energy sharing between different sectors of RES and PRO, considering IRIS extension simultaneously. The results are presented in the last four rows and last three columns in Table 4.2 with the name of ‘RES+PRO’ and should be compared to each individual sector. With regard to RES alone, the SCR remains 100% in the Paris center, while it improves by 9% (from 77.8% to 85%) in the Paris surroundings. This improvement is a consequence of the complementarity between the two sectors. With regard to PRO, the improvement is more pronounced on the SSR side, with values of 85% (from 6% to 11.1%) and 87.5% (from 14.4% to 27%) for the two subdomains of the Paris center and the Paris surroundings, respectively. In the case of Grand Paris, the SCR improves by 8% compared to RES (from 89.5% to 96.4%), while the SSR improves by 117% compared to PRO (from 10.3% to 22.4%). However, the simultaneous improvement of the SSR and SCR is not observed. In contrast to the improvements, the total SCR decreases compared to PRO alone, while the SSR decreases compared to RES alone. Although the SSR and SCR losses for each sector appear significant, it is necessary to analyze the global performance in order to ascertain whether complementary effects improve the overall energy balance. In order to do this, the results must be compared to the weighted average values of the sectors presented in the columns named ‘RES + PRO weighted-average’ calculated with Eq. (4.6) and Eq. (4.5). For the Paris center, it can be demonstrated that all PV production will be consumed in place when both sectors are consuming the energy, regardless of whether or not sharing the surplus between them. This leads to the SSR’s maximal value of 11.1%, as described in Section 4.2.1. Nevertheless, the improvement resulting from the energy sharing between sectors is significant for the Paris surroundings. In this case, both SSR and SCR improve by 6% (25.4% to 27% and 80% to 85%, respectively). Similarly, in the case of Grand Paris, both SSR and SCR improve by 6.5% (21% to 22.4% and 90.7% to 96.4%, respectively). Consequently, the enhancement in PV offset

and the diminution in PV loss exemplify the advantages of complementarity between sectors with respect to the PV energy balance. This improvement is once more evident in the Paris surroundings.

Finally, we examine the case combining the two subdomains together. Comparing our result of the Grand Paris for RES mixed with PRO to its two subdomains, an improvement in SSR of 102% (11.1% to 22.4%) is found for the Paris center, and SCR improves by 13% (85% to 96.4%) compared to Paris surroundings. However, similar to the results of the previous analysis of impacts by sector, improvements in SSR and SCR are heterogeneous across the two subdomains (e.g. SSR for Paris surroundings and SCR for Paris center are larger than the Grand Paris aggregated value). Again, we need to analyze the global performance by comparing the aggregated values to the weighted averages. The results prove that the loss of energy balance performance in some cells due to the peripheral expansion of the users involved is insignificant compared to the potential gains. Both SSR and SCR improve by 10% (20.4% to 22.4% and 88% to 96.4%) thanks to the complementarity between the subdomains. Thus, our result proves again the significant impact of peripheral expansion on improving energy balance. The supply-demand energy balance is optimal when considering the entire Grand Paris metropolis as a single renewable energy community that allows electricity sharing between all inhabitants and the commercial inside.

Table 4.3 shows SCRs and SSRs with different energy balance perimeters for different seasons. Seasonal variations in the energy balance are evident. France is a heating-dominated country (Martinopoulos et al., 2018), and demand is more concentrated in the winter months when solar radiation is lower and less PV power is generated. Consequently, less PV generation is available in winter than in summer, and less consumption can be covered, resulting in a lower SSR. On the other hand, the SCR describes the remaining PV electricity supply. This ratio is more important in winter than in summer for the same reasons of seasonal variation of electricity consumption and, therefore, puts more pressure on the grid in winter. Due to the complementarity between the different sectors and the number of users, the perimeter improvement also applies to all seasons, but with seasonal variations: for both SSR and SCR, the progress is more significant in summer.

To conclude, our analysis from the pure energy balance perspective shows that a larger perimeter is always better, thanks to the complementarity of more users. The improvement is more significant for rural areas with higher PV production. However, the impact of perimeter extension should also be examined economically.

4.3.2 Economic impacts

Figure 4.5 shows the map of simplified normalized costs calculated based on Equation (4.7). The average savings per kilowatt are 6 cents for the Paris surroundings and 2 cents for the Paris center compared to the initial electricity price of 20 cents in 2020 (Eurostat, 2023). From an

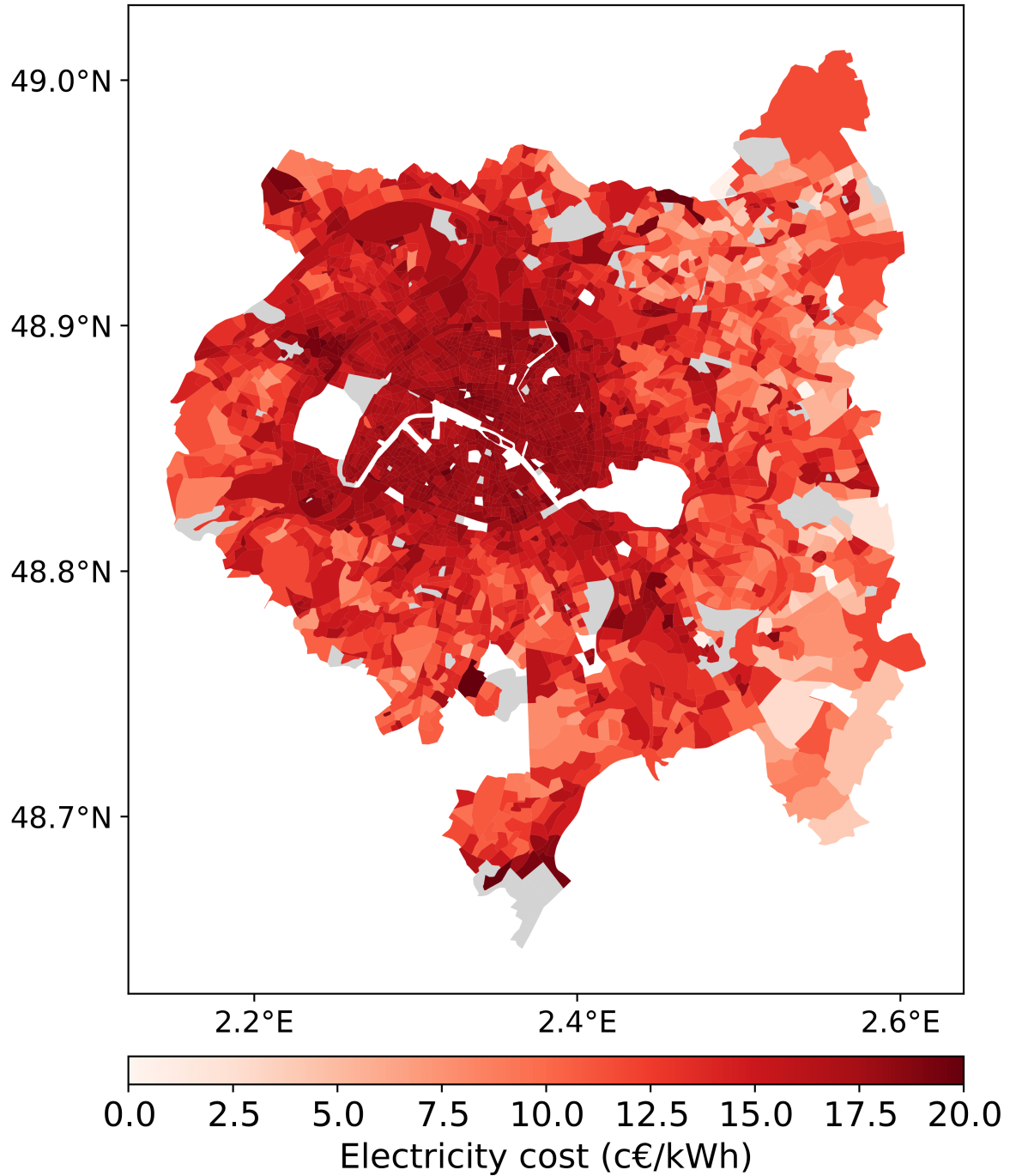


Figure 4.5 IRIS map of average electricity cost (Euro cents per kWh c€/kWh) at the IRIS level after energy sharing between the residential and the commercial sectors with each IRIS as a microgrid.

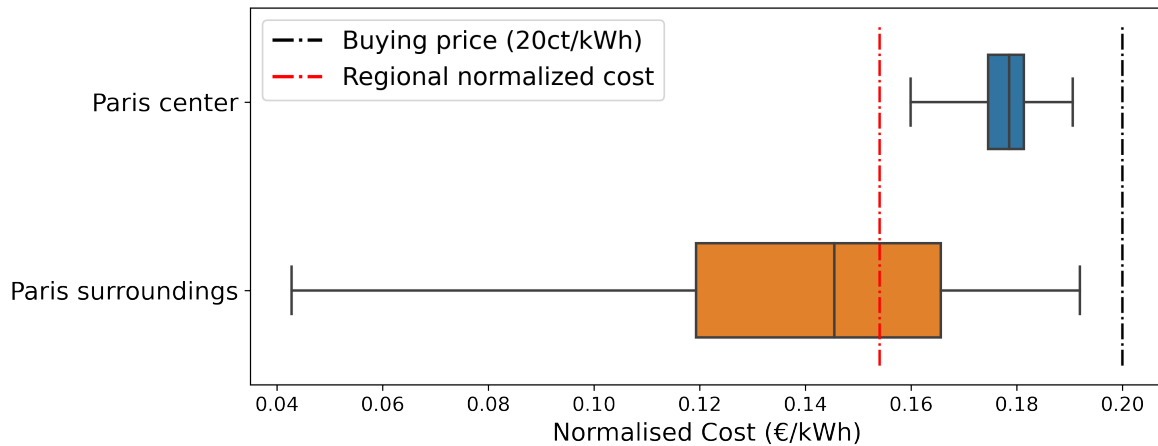


Figure 4.6 Distribution of IRIS normalized cost compared to the regional value of 15.4 c€/kWh with energy sharing in the Grand Paris metropolis between all residential and commercial users (dashed red line) and the initial electricity buying price of 20 c€/kWh (dashed black line).

economic point of view, it is clear that rooftop PV installation is more profitable for residents and businesses in the surrounding areas. This difference between the two subdomains can be explained with Eq. (4.8).

Figure 4.6 shows the distributions of normalized costs for all IRIS in the Paris center and the Paris surroundings separately, as well as the value of the initial purchase price and the price after regional energy sharing, which is considered as the optimal case from the energy balance perspective. Regarding regional energy sharing, the average electricity cost is 0.154 euros per kWh. Comparing the final price with the IRIS distributions, we can see that all the consumers in the Paris center would benefit more thanks to the perimeter extension compared to the initial case of only local consumption. In contrast, 57% of consumers in the peripheral areas of Paris would benefit less compared to the case of microgrids at the IRIS level. However, as mentioned in the previous section, the overall electricity surplus would be significantly reduced, as would the potential cost of feeding the surplus into the grid. Power sharing between the city and the periphery is a win-win project, both from the technical point of view of energy balancing and from the point of view of consumers.

The overarching conclusion from these results is that increasing the perimeter of energy sharing in urban environments improves the performance of SSR and SCR indicators. This suggests the potential for regional energy strategies to optimize the use of PV production, thereby contributing to more sustainable and resilient urban energy systems.

4.4 Conclusion

This paper explores the integration of distributed photovoltaic (PV) generation in the Grand Paris metropolis, using the energy supply-demand balance with a focus on the self-consumption

rate (SCR) and self-sufficiency rate (SSR). Our analysis reveals that the complementary nature of different residential and commercial sectors enables a significant improvement in the total offset energy and reduces the loss of PV surplus across all locations. This complementarity is crucial in the Paris surroundings, markedly enhancing energy efficiency.

From the supply-demand perspective, lower building density and larger roof areas in the Paris outskirts allow a higher SSR (27%). In contrast, central Paris, characterized by high building density, predominates local PV consumption with minimal surplus, resulting in only an 11% coverage of energy consumption and leaving a surplus due to imperfect simultaneity between residential consumption and PV production. Introducing energy sharing between different sectors and different subdomains can mitigate these losses and reduce grid pressure, a benefit that amplifies with geographical expansion. While the perimeter extension is particularly more beneficial for the Paris surroundings from the energy balance perspective, it is important to notice that it is also more advantageous for the more urban area of the Paris center from a simplified economic perspective, considering only electricity prices. Moreover, considering the entire Grand Paris metropolis as a unified renewable energy community that permits electricity sharing among all inhabitants and businesses emerges as the most optimal scenario. This arrangement covers 22.4% of consumption with rooftop PV, achieving 96.4% of the potential in perfect production-consumption simultaneity.

While this study provides valuable insights, it's important to acknowledge that it simplifies economic considerations. Future work should delve deeper into the economic impacts, particularly the investment and distribution costs that are crucial for large-scale PV integration. Although the results show that a larger perimeter is always better, the effect on the grid within the perimeter is unclear. The costs of improving the distribution and cable operation could offset the potential benefits. On the other hand, as discussed in previous studies, the overall profitability of energy communities is highly dependent on government policies. However, in reality, this feed-in tariff could vary with the type of consumer and depends on the price, which also depends on the contracted power. This emphasis on economic factors is essential for a comprehensive understanding of the challenges and opportunities in this field.

Finally, the electricity consumption in the current study is based on historical data and is assumed not to change. However, citizens' adoption of distributed PV systems marks a shift in how energy is produced and consumed. By producing electricity at the point of use, individuals can reduce their dependence on the grid and have the opportunity to tailor energy consumption and production to their interests and needs, potentially accelerating electrification efforts. This decentralization of energy production increases the flexibility of the electricity system, as consumers can adjust their energy use according to availability and potentially participate in demand response programs. This evolution of consumption patterns should be considered, especially in projections of future energy balances.

Chapter 5

Conclusion and Perspectives

Contents

5.1 Conclusion	105
5.1.1 Main results and messages	105
5.1.2 Reflexion around limits of the thesis	107
5.2 Perspectives	108

5.1 Conclusion

5.1.1 Main results and messages

The decarbonization of buildings is an interdisciplinary study involving different aspects of technology, economic impacts, and policy implications. My research aims to understand how current conditions and climate change can contribute to the decarbonization of the residential sector. Specifically, I focus on the existing residential stock and ways to reduce their energy consumption in France. The French government has set ambitious decarbonization targets for buildings: a 50% reduction in final energy consumption by 2050 and a 20% reduction by 2030, based on 2012 levels. Our research initially aimed to assess the feasibility of these targets and explore the factors that could help achieve them.

In this thesis, we first investigated the impact of climate change on residential electricity consumption. For this purpose, a linear temperature sensitivity model fitted with annual observed electricity consumption data and historical temperature was applied intra-regionally to project future French Residential Electricity Consumption (REC). The model accounted for climate change, increased air conditioning (AC) use, and spatial variability. We found that in countries with moderate climates, such as France, increasing temperatures lead to an overall decrease in REC. For the French case, the most carbon-intense scenario RCP8.5, might lead to a decrease in REC of 8TWh by 2040 and to 20TWh by 2100, with significant spatial variability

that had never been quantified and mapped before due to the lack of appropriate methodology and limited available data at the finest scale. However, the results also showed that the potential increase in AC use is not negligible, especially in the long term. AC promotion could increase RECs by 2% by 2040 and as much as 32% by 2100.

Next, decarbonization was considered from two perspectives: energy efficiency improvements through retrofitting and introducing renewable energy through rooftop photovoltaics (PV). For the retrofitting analysis, the temperature sensitivity model was then modified to include building age as a variable to assess the heating consumption of buildings by groups of building ages. The model allowed us to estimate the heating consumption for each household with its given area, construction period, and location, which can be compared with the theoretical heating consumption estimated through Energy Performance Certificate (EPC) standard calculations. The results showed that implementing the RT1974 and RT2005 thermal codes did not improve the energy consumption reduction rates as expected in most administrative regions. According to traditional calculations, if all retrofitted buildings had the same thermal performance as new buildings built after 2006, the expected gain from renovation would be about 60%, i.e. a 60% reduction in heating consumption. However, according to our projections, based on current actual consumption, 47% of the buildings would consume more energy than before the retrofit. The expected energy savings from the retrofit would be minimal, especially when climate-related reductions in energy demand are considered.

Finally, an alternative way to decarbonize the residential sector by increasing renewable energy sources was also studied by introducing rooftop photovoltaics (PV). We focused on the Grand Paris metropolis as a case study because it must address energy issues facing major constraints such as high population density, energy dependence, and vulnerability to climate change. We also believed that the case of Grand Paris could be replicated by other major cities worldwide to address urban sustainability issues. The previous results of the temperature sensitivity model were used to downscale the regional hourly electricity consumption profiles to IRIS levels. The hourly consumption of both the residential and commercial sectors was then examined by comparing rooftop PV generation. The results showed that allowing energy sharing between sectors significantly reduces excess PV losses and improves grid stability. In the center of Paris, 11% of consumption could be offset by PV, while for the periphery, PV could offset 27% of consumption. We have also shown that different levels of complementarity affect the balance between energy supply and demand. Thanks to the energy exchange between the center of Paris and the periphery, the energy balance would be more stable than for each sub-region. In economic terms, rooftop PV installations would offer greater savings for residents and businesses in the periphery than in central Paris. However, exchanges between the sub-regions would benefit users in central Paris. The study concluded that extending the energy exchange perimeter in urban areas would optimize PV production and contribute to more sustainable and resilient urban energy systems.

However, despite technological advances and increasing awareness of reducing carbon

emissions, the sector is far from reaching its set targets. Previous studies focusing on the impact of policies are also pessimistic, with results showing that emissions reduction targets will not be met and fuel poverty will only be partially alleviated [Charlier et al. \(2018\)](#); [Giraudet et al. \(2021\)](#); [Vivier and Giraudet \(2024\)](#). The unpredictability of household energy consumption patterns complicates efforts and makes it difficult to implement one-size-fits-all solutions.

The results of the thesis could provide insights into future policymaking. General takeaway messages for policy implications are the following:

- Large spatial variability in current REC and its future trend shows that policymaking should be steered to the local specificities (building-scale or community-scale).
- The potential REC rise due to AC usage could be canceled by increasing the cooling setpoint to 26-27°C.
- The potential retrofit gain based on EPCs is overoptimal. Whether to introduce more accurate energy assessment tools or provide users with easier-to-understand information needs to be considered. We also call for efforts to make more data publicly available.
- Expanding the perimeter of self-consumption should be considered to allow the exchange between areas with different morphologies (residential and commercial areas or urban and rural areas) to maximize self-consumption and reduce PV surplus.

5.1.2 Reflexion around limits of the thesis

Several limitations of the conclusions drawn from the thesis should be noted.

I have developed and worked with a top-down model to analyze downscaled characteristics using aggregated statistics as input during the whole thesis. Even though the IRIS are relatively small, they are still "big" since there are about 2000 inhabitants in each cell. However, such a top-down model lacks more flexibility beyond current practice ([Hourcade et al., 2006](#)). Since the model's main features are calibrated from historical data, there is no guarantee that the values of these parameters will remain valid. Some evolution in the calibrated elasticities has been accounted for in the future projection process (e.g., the introduction of air conditioning in Chapter 3). However, there are still some unaccounted effects that have not been addressed. For example, the current study does not consider population and economic growth. However, both growth rates influence energy consumption ([Mazur, 1994](#); [Sadorsky, 2014](#); [York, 2007](#)). The growth in energy demand due to population and economic growth should be considered when making more accurate quantitative forecasts, especially in the long term.

Other limitations also occur due to the simplification of the model by assumptions. The model's first main assumption is the simple linearity between electricity consumption and Degree-Days (DD). Several previous studies ([Pagliarini et al., 2019](#); [Sailor and Muñoz, 1997](#)) prove the linearity, while others try to predict consumption using a more complex model

(Beccali et al., 2008; Bessec and Fouquau, 2008; Eskeland and Mideksa, 2010; Moral-Carcedo and Vicéns-Otero, 2005; Silva et al., 2020). However, no consensus exists on the best approach to such a model. The model's accuracy and complexity (e.g., regularization) highly depend on the studied area's data, and the model's accuracy level depends on the study's needs. For example, my thesis studied the projection's trend compared to the current consumption state. Thus, comparing the model over two periods should partially compensate for the effect of the model's simplification. However, similar to the previous point about the growth rate, if the study needs more proper quantitative future prediction results, the simple linearity of the model should be dealt with carefully.

The next section will discuss other improvable limitations of the current study and future work perspectives.

5.2 Perspectives

In the current work, some assumptions have been made to simplify the model due to a lack of information or available data, such as the type of residence (e.g. collective or individual), or due to the over-complexity of the factors included (e.g. economic factors). In the thesis, consumption models are aggregated either at the IRIS level or collectively for a given age group due to the aggregation of available variables. Some possible improvements to the consumption model should be considered in future work. If conditions allow, more human factor variables can be included in the model to make it more accurate. For example, Lévy and Belaïd (2018) studied the French National Housing Survey and categorized the types of consumption patterns. Indeed, studies also show a positive correlation between EPC labeling and house prices (Cespedes-Lopez et al., 2019; Eichholtz et al., 2010, 2013; Fuerst et al., 2015; Wiley et al., 2008). Socio-economic factors influence the behavior of users, and such differences should be used as inputs in our model to explain the spatial variability of energy consumption. It is important to know the different consumption patterns by user type, as they can be further applied to study flexibility under the renewable energy scenario in the future. They are also useful for studying future consumption, especially during heat waves.

From a PV perspective, the most important economic factor not considered is the economics, which should include system costs. Due to a lack of information and time, system costs were not considered in this study. (In fact, all economic perspectives such as investment and electricity prices were not considered). All these factors affect the diffusion of PV projects and should be fully considered. As the number of users participating in PV sharing increases, distribution losses will increase, so the perimeter expansion is not infinite. At some point, the system cost will be more important than the losses and will no longer be cost-effective.

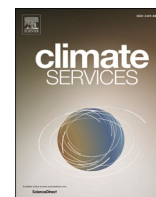
On the other hand, by combining renovation projections and collective self-consumption with PV generation, it is possible to analyze the global decarbonization of the residential sector. This is the work of Torres-Rivas et al. (2022) and Canova et al. (2022), who used EPCs to

predict future renovation gains and combined them with PV self-consumption to study overall decarbonization potentials. The advantage of our work over these papers is that both future electricity consumption and retrofit gains are based on actual electricity consumption, allowing climate change impacts to be incorporated into decarbonization projections.

For this part, we should also consider the building stock part, where renovation statistics should be considered and updated in the model. Although we have not taken into account the renovations that have been carried out, almost 2.1 million renovations were carried out in France in 2020 ([ONRE](#)). Even if most of them were so-called light renovations, only one measure was carried out to improve the thermal performance of the building. The total number is not negligible, and the real gain before and after the renovation could be studied directly if energy bill data were available.

Let us suppose that the future works will be completed in several steps. In this case, they should be carried out as follows:

- First, we need to identify the main socio-economic factors influencing residential energy consumption.
- Then, different consumption patterns, whether spatially variable or socio-economically related, should be studied for different groups of users.
- The evolution of patterns and future PV production under climate change should then be investigated.
- The system costs at different scales should be evaluated, possibly providing an optimal perimeter for self-consumption projects in urban and rural areas.



Sub-regional variability of residential electricity consumption under climate change and air-conditioning scenarios in France

Qiqi Tao^{a,*}, Marie Naveau^a, Alexis Tantet^a, Jordi Badosa^a, Philippe Drobinski^a

^a Laboratoire de Météorologie Dynamique – Institut Pierre-Simon Laplace, Ecole Polytechnique – Institut Polytechnique de Paris, Ecole Normale Supérieure – PSL Université, Sorbonne Université, CNRS, Palaiseau 91128, France

ARTICLE INFO

Keywords:

Residential electricity consumption
Cooling demand
Climate change impacts

ABSTRACT

The residential sector is important for the energy transition to combat global warming. Due to the geographical variability of socio-economic factors, the highly dependent residential electricity consumption (REC) should be studied locally. This study aims to project future French REC considering climate change and air-conditioning (AC) scenarios and to quantify its spatial variability. For this purpose, a linear temperature sensitivity model fitted by annual observed electricity consumption data and historical temperature is applied at an intra-regional scale. Future temperature-sensitive REC is computed by applying the model to temperature projections under the climate change pathway RCP8.5. Three AC scenarios are considered: (1) A 100% AC rate scenario assuming that any region partially equipped with AC systems nowadays will have all its households equipped with AC, but local temperature sensitivity will no longer progress; (2) A gradual spreading scenario mimicking “do like my neighbor” behavior; (3) A combination of the two scenarios. Increasing temperatures lead to an overall REC decrease (−8 TWh by 2040 and down to −20 TWh by 2100) with significant spatial variability, which had never been quantified and mapped due to a lack of suited methodology and limited available data at the finest scale. The evolution of REC is modulated by the evolution of cooling needs and the deployment of AC systems to meet those needs. In the first 2 AC scenarios, the decrease of REC due to climate change could be totally offset in the South of France, which would then display an increase in REC. When the 2 AC scenarios are combined, an increase in REC could be seen over the whole country. The most extreme AC scenario shows a potential REC rise due to AC usage by 2% by 2040 and even 32% by 2100, which could be canceled by increasing the cooling setpoint up to 26–27 °C.

Practical implications

The residential sector is the leading electricity consumer in France, representing more than one-third of the final electricity uses. This sector has therefore to implement a pathway to reduce energy demand and greenhouse gas emissions. The relevance of related policies depends on the expected change in residential electricity consumption (REC) for various climate change scenarios and user behavior. REC change in climate change scenarios has already been studied at the country scale, but important physical (e.g. local weather conditions) and socio-economic (revenue, air-conditioning use, etc.) determinants of REC display a large spatial variability which implies REC should be studied locally.

The REC model is computed using a linear temperature sensitivity

model fitted by annual observed electricity consumption data and daily temperatures applied at the smallest French geographic census unit named Ilots Regroupés pour l'Information Statistique (IRIS), which divides the territory into meshes of about 2000 inhabitants per unit cell. Once the current electricity sensitivity is fitted for each IRIS, the REC change is computed by applying the model to temperature projections under climate change scenario RCP8.5 at intermediate (2025–2055) and far (2070–2100) time horizons based on 5 climate simulations performed in the frame of the international CORDEX program. In addition, two cooling scenarios based on the air-conditioning adoption rate and the cooling temperature sensitivity are also investigated.

When only climate change is considered, REC is projected to decrease with decreasing heating needs in most IRIS cells. However, because of already deployed cooling equipment, REC is expected to

* Corresponding author.

E-mail address: qiqi.tao@hotmail.com (Q. Tao).

<https://doi.org/10.1016/j.cliser.2023.100426>

increase in 3–7% of the territory, totally offsetting the effect of reduced heating needs. A larger variability is found within administrative regions, including a few hundred to thousands of IRIS, than between administrative regions. Including AC scenarios offset in part the REC negative trend, with REC projected to increase in the South-East in the most conservative scenario to nearly the entire territory when large spreading and rate of AC use are assumed. Large AC use may lead to REC change ranging from 2% by 2040 to 32% by 2100, contributing to enhanced greenhouse gas emission and the urban heat island effect.

Such results call for targeted and local information actions where the risk of spreading is high to limit the spreading and rate of use or mitigate their effect with more energy-efficient AC systems. As our projected future climate in Southern France is similar to the present climate of countries more to the South, which has not seen a large deployment of AC equipment, analyzing the socio-economic drivers, the energy policies of these countries and drawing inspiration from them to deploy locally adapted actions should be considered. Also, adapting the cooling setpoint could help elaborate energy policies to lower the cooling temperature-sensitive REC. Based on our model, shifting the cooling setpoint from 21 °C at present to 23–24 °C by 2040 and 26–27 °C by 2085 would prevent any cooling REC rise in our worst-case scenarios. These values are consistent with existing recommendations (e.g. US DoE). Finally, low-tech alternative solutions, such as cool white roof coating widely implemented in subtropical regions, can be implemented in France to improve the thermal comfort of buildings and reduce the use of AC equipment and their impact on the environment.

1. Introduction

France is committed, with the energy transition law for green growth of 2015, to reducing its greenhouse gas emissions by 40% by 2030 and divided by four by 2050. It also plans to reduce its consumption of fossil fuels by 30% by 2030 and to halve its final energy consumption in 2050 compared to 2012 (regulations passed under the *Law for the ecological transition and green growth*¹). This regulation contributes to the *Paris climate agreement*² to keep temperature increases well below 2 °C and to pursue efforts for 1.5 °C. The French residential sector represents 20% of the CO₂ emission of the country and 30% of the final energy uses. Hence, this sector could be a significant opportunity and challenge for policies to combat global warming. Indeed, the law text emphasizes improving building energy efficiency, thermal renovation of buildings, and constructing buildings with high energy performance.

Limiting electricity consumption in the residential sector through actions aimed at improving the energy performance of buildings is therefore a major environmental challenge for communities. However, residential electricity consumption (REC) is highly dependent on household income, the thermal quality of occupied dwellings, and the cost of energy with regard to the purchasing power of the households (Giraudet et al., 2012; Branger et al., 2015; Frederiks et al., 2015) and therefore displays a very large spatial variability, especially in urban areas which are characterized by the heterogeneity of their demographic, socio-economic, environmental and cultural characteristics (Li and Kwan, 2018; Pickett et al., 2017) underlying urban resource demands (Rosales and Worrell, 2018; Voskamp et al., 2020). The case of France has been investigated specifically and supports studies conducted in other countries (Lévy and Belaid, 2018).

Electricity demand also depends on the outdoor temperature. Demand for cooling rises once the temperature exceeds a cooling setpoint, while electricity demand for heating grows once the temperature drops below a heating setpoint (Petrick et al., 2010; Auffhammer and Mansur, 2014; Damm et al., 2017; Wenz et al., 2017; Kozarcenin et al., 2019). As a result, a theoretical U-shaped link exists between electricity demand

and temperature. Choices made by individuals to utilize heating and cooling systems to maintain a comfortable temperature in their residences directly impact electricity demand (Emodi et al., 2018; Emekekwe and Emodi, 2022). Substantiated correlations between consumption and climate and weather conditions (Meng et al., 2020), demographic and economic factors (Bettignies et al., 2019) and urban and architectural morphological characteristics (Chen et al., 2020; You and Kim, 2018) cause the large spatial variability in residential energy demand. Climate, socio-economic and morphological characteristics have proven explanatory variables for energy demand and its spatial pattern (Chen et al., 2020; Kennedy et al., 2015; Wiedenhofer et al., 2013).

The link between temperature and electricity demand has been studied using various models [e.g. (Narayan et al., 2007; Emodi et al., 2018)]. One approach is to model this nonlinear relationship by a smooth but nonlinear function of the temperature. For instance, Moral-Carcedo and Vicéns-Otero (2005) and Damm et al. (2017) used a Logistic Smooth Transition (LSTR) function to model the electricity demand response to temperature variations in European countries. The advantage of such a model is that it adequately captures the rather smooth response of electricity demand summed over a large domain to temperature variations. On the other hand, it is less straightforward to interpret the physical meaning of the parameters of such a model. Another approach is to model the electricity demand as a linear combination of nonlinear functions of the temperature (making it a generalized linear model). For instance, Sailor and Muñoz (1997) studied the monthly electricity and gas consumption for states in the US using a linear model with degree-day (DD) inputs in addition to wind speed and relative humidity.

In France, outdoor temperature increase could reach up to 3.8 °C by 2100 with regards to 1900–1930 if no policy is in place to reduce greenhouse gas emissions (Ribes et al., 2022). Pili-Sihvola et al. (2010) have investigated the impact of climate change using the DD approach on building energy demand for heating and cooling and the associated energy cost using climate simulations of the 3rd Coupled Model Inter-comparison Project (CMIP3). More recently, Larsen et al. (2020) find in downscaled CMIP5-climate simulations that when temperature evolution is considered as the only factor of change, needs for cooling increase by 33% to 204% between 2050 and 2010 and needs for heating decrease by –31% to –6% while Damm et al. (2017) predict the impact of a +2 °C global temperature change on European electricity demand, with for France, an estimated decrease in total electricity consumption between -10TWh and -16TWh. The optimistic reduction in electricity projection is due to France's current heating-dominated state. All households in the country utilize specific heating systems such as gas, oil, wood, or district heating, among which 37% employ electric heating. In contrast, the national adoption of air-conditioning (AC) remains relatively low, standing at only approximately 22% when considering all types and sizes of air conditioners, including mobile and heat pump units.

Rising temperatures and temperature extremes, in particular, imply increased use of air conditioners, both in hot and humid emerging economies where incomes are rising and in industrialized economies where consumer expectations in terms of thermal comfort are constantly growing (van Ruijven et al., 2019). Previous studies (van Ruijven et al., 2019; ?; ?) suggest that climatic conditions will encourage more households to adopt AC systems, therefore affecting electricity expenditures. On a global scale, the final energy consumption for AC in residential and commercial buildings has more than tripled between 1990 and 2016. The share of cooling in REC increased from around 2.5% to 6% during the same period. The use of AC equipment is expected to increase dramatically, becoming one of the main drivers of global electricity demand (International Energy Agency, 2018).

In France, as heat waves are more and more frequent and long, many households and businesses are equipped with AC for more comfort (Lemonsu et al., 2015). In 2020, for the first time, the number of equipment sold exceeded 800,000 units, whereas it had stabilized at

¹ <https://www.legifrance.gouv.fr/loda/id/JORFTEXT000031044385>

² https://unfccc.int/sites/default/files/english_paris_agreement.pdf

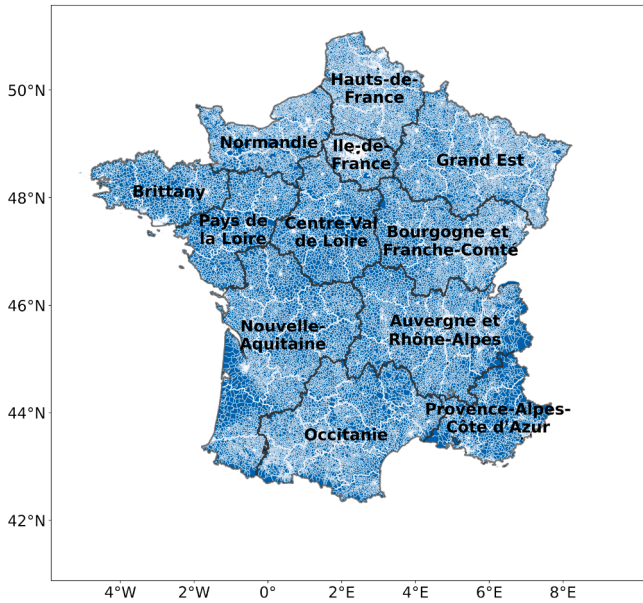


Fig. 1. Map of 12 administrative regions of metropolitan France, with thicker white lines representing 94 departments and thinner white lines representing more than 48000 IRIS cells. (Plate carrée projection, same projection used in the presented study).

around 350,000 per year previously. In 2020, 25% of individuals are equipped compared to 14% in 2016, with disparities linked to the type of dwelling (31% of owners of individual houses compared to 20% of households living in collective housing), socio-professional category (37% of liberal professions, executives and higher intellectual professions against only 19% of households whose reference person is unemployed or inactive) and place of residence (e.g. 47% of inhabitants of the South-East and Corsica against only 11% in Brittany) (ADEME, CODA STRATEGIES, 2021).

However, most previous studies of future consumption projection only focus on continental and national scales while not considering the sub-national disparity of temperature changes and non-climatic factors listed above. We aim to fill this gap by examining whether the national results proposed by these earlier studies remain consistent at smaller scales, given that changes in consumption and geographical variations in adaptation can lead to inequalities. We provide valuable information on the local impacts of climate change and building cooling strategies on residential energy demand, which can aid local climate and energy planning and decision-making. Specifically, we focus on the sub-regional variability of changes in residential AC requirements for cooling needs in the context of climate change. To this end, we use a

modified temperature sensitivity model to project future REC at a fine scale. The smallest geographic scale used in this study is the so-called Ilots Regroupés pour l'Information Statistique (IRIS), here referred to as cells, which divides the French territory into a collection of about 2000 inhabitants per cell. These cells are defined by respecting geographic and demographic criteria and have recognizable contours without ambiguity and stability over time. France has a total of 50,800 cells (IGN, 2009). In metropolitan France, these cells are distributed among 12 administrative regions represented in Fig. 1. This model is designed to distinguish between different aspects of electricity use using data from all residential buildings, irrespective of their heating or cooling equipment. The projection of future residential electricity consumption is based on climate change pathway RCP8.5, using down-scaled CMIP5 climate simulations carried out as part of EURO-CORDEX (Jacob et al., 2014) and MEC-CORDEX (Ruti et al., 2016), while considering different scenarios of AC use for cooling - full generalization or saturation.

After the introduction in Section 1, the details of the model can be found in Section 2, with information about the temperature and REC data that are applied to fit the model as inputs for the case of France and the future temperature projection and AC use scenarios. REC projection results and discussion are presented in Section 3, and the conclusion and policy implications are given in Section 4. The global flow chart of the total work is shown in Fig. 2.

2. Methodology and data

In this section, we explain how the REC is projected at the sub-communal scale by applying a temperature sensitivity model trained on historical data to climate projections. We also present the data for the application to France and define the scenarios used as projections of AC use with widespread adoption or saturation cases.

2.1. Temperature sensitivity statistical model

The relationship between the surface air temperature and the energy consumption over a domain is what we call the temperature sensitivity of the consumption. It has been modeled in various ways as presented in the previous section. The advantages of the DD approach are that it is simple to implement as a linear regression model with standard machine learning software and that it is straightforward to interpret the coefficients of the models as temperature sensitivities. For these reasons, we follow the DD approach in this study. The heating degree-days (HDD) (resp. the cooling degree-days (CDD)) for a domain is a positive quantity computed from data for the (weighted-) average temperature of the domain. It is given by the sum over a period of the degrees below (resp. above) a certain setpoint temperature per timestep. Here, the timestep d is a day and the period y a year between 2011 and 2018 (included),

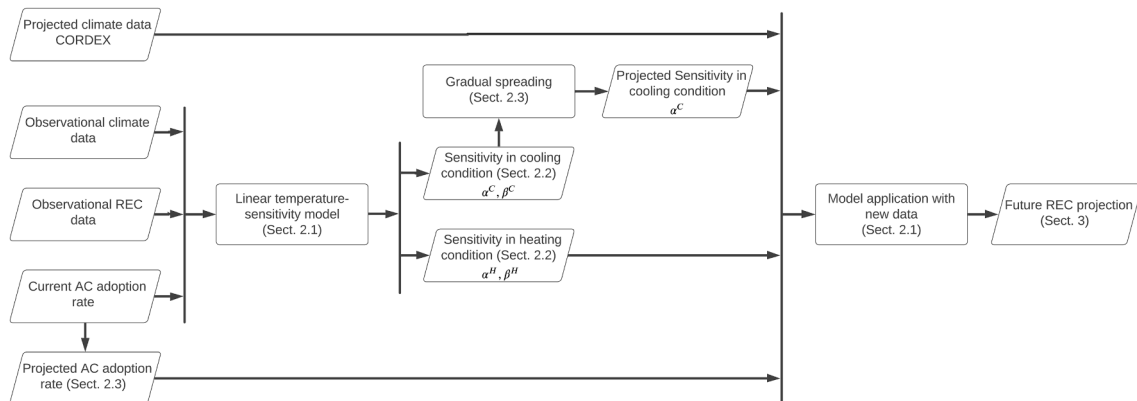


Fig. 2. Flow chart of the present study.

Table 1
Summary of variables and their physical meanings presented in Eq. 2.

Variable	Meaning
$E_i(y)$	Annual REC normalized by surface for cell i and year y (kWh/ m ²)
B_i	The basic daily REC for cell i (kWh/ m ²)
N_y	The number of days in a year y (365 or 366)
α_i^H	Heating temperature sensitivity for cell i (kWh/ (DD m ²))
α_i^C	Cooling temperature sensitivity for cell i and year y (kWh/ (DD m ²))
$\eta_i^{El}(y)$	Rate of electric heating for cell i and year y (%)
$\eta_i^{AC}(y)$	Rate of AC adoption for cell i and year y (%)
$\beta_i^H(y)$	Coefficient measuring increase in yearly REC per HDD and unit of area for cell i and year y (kWh/ (DD m ²))
$\beta_i^C(y)$	Coefficient measuring increase in yearly REC per CDD and unit of area for cell i and year y (kWh/ (DD m ²))

while different domains, or cells, i are considered, each corresponding to a different IRIS. The HDD and CDD are thus defined here as (Moral-Carcedo and Vicéns-Otero, 2005),

$$\begin{aligned} \text{HDD}_i(y) &:= \sum_{d=1}^{N_y} \max(0; T_i^H - T_i(y, d)) \\ \text{CDD}_i(y) &:= \sum_{d=1}^{N_y} \max(0; T_i(y, d) - T_i^C), \end{aligned} \quad (1)$$

where $T_i(y, d)$ is the daily-mean surface air temperature for a day d of year y averaged over cell i , T_i^H and T_i^C with $T_i^C \geq T_i^H$ are respectively the heating and cooling setpoints for cell i , and N_y (365 or 366) is the number of days in year y . The heating and cooling setpoints T_i^H and T_i^C are parameters to be estimated.

The REC scales with the living area in each cell. To leave out this factor, we divide the REC by the living area, giving the normalized annual REC $E_i(y)$ for cell i and year y in kWh/ m². For a given scenario (see Section 2.3), the general temperature sensitivity model is then expressed as,

$$\begin{aligned} E_i(y) &= \beta_i^H(y) \text{HDD}_i(y) + B_i N_y + \beta_i^C(y) \text{CDD}_i(y) \\ &= \alpha_i^H \eta_i^{El}(y) \text{HDD}_i(y) + B_i N_y + \alpha_i^C \eta_i^{AC}(y) \text{CDD}_i(y). \end{aligned} \quad (2)$$

The first equation in (2) relates $E_i(y)$ to a heating, a basic, and a cooling REC (from left to right). The basic daily REC B_i (kWh/ m²) is part of the REC that does not depend on temperature. It determines the REC fully when $T_i^H \leq T_i(y, d) \leq T_i^C$. In this study, we focus on the effect of climate change and the rate of air-conditioning (AC) adoption on the REC. Factors affecting the basic REC are thus assumed to remain fixed so that B_i does not depend on time. The temperature-sensitive RECs for a given year are proportional to DD. The coefficients of proportionality $\beta_i^H(y)$ and $\beta_i^C(y)$ (kWh/ (DD m²)) measure the increase in yearly REC per DD and unit of area in cell i . Each cell includes residential buildings with and without electric appliances. Thus, other things remain the same, lowering the fraction η_i^{El} of residential buildings in cell i with electric heating lowers β_i^H . To estimate the temperature-sensitive electric consumption restricted to residential buildings with electric heating, β_i^H is developed as the product of η_i^{El} with the heating temperature sensitivity α_i^H (kWh/ (DD m²)) of cell i . Factors affecting the heating temperature sensitivity (consumer behavior, thermal efficiency of residential buildings, etc.) are also assumed to remain fixed so that α_i^H is independent of time.

However, the rate of electric heating η_i^{El} may vary in time. Yet, the data used in this study only provides estimates of η_i^{El} for the year 2018 (Section 2.2.1). We therefore assume that this rate is fixed to that of 2018, $\eta_i^{El}(y) = \eta_i^{El}(2018) := \eta_i^{El}$, and so $\beta_i^H(y) = \beta_i^H(2018)$, for all years and all cells. This implies that an Ordinary Least-Squares (OLS) regression with β_i^H as coefficient and $\text{HDD}_i(y)$ as input is equivalent to an OLS

regression with α_i^H as coefficient and $\eta_i^{El} \text{HDD}_i(y)$ as input. Similarly, β_i^C is developed as the product of the fraction η_i^{AC} of residential buildings in cell i equipped with AC with the cooling temperature sensitivity α_i^C (kWh/ (DD m²)) of cell i . Note, however, that while all residential buildings include some form of heating so that η_i^{El} reflects the choice of heating system, all AC systems are electric, and η_i^{AC} gives the adoption rate of AC equipment. Regarding η_i^{AC} , as presented in the previous section, the AC adoption rate has increased during the past several years and hence depends on the year during the training (Section 2.2.4). For future projection, both α_i^C and η_i^{AC} vary with the choice of AC use scenario, but they are assumed constant during a given period (Section 2.3.2).

In summary, all the parameters with their physical meanings are given in Table 1. For all pairs (i, y) of cells i and years y , the model inputs are.

- $\eta_i^{El}(y) \text{HDD}_i(y)$ and
- $\eta_i^{AC}(y) \text{CDD}_i(y)$,

where $\text{HDD}_i(y)$ and $\text{CDD}_i(y)$ depend on the daily-mean temperatures $T_i(y, d)$ for all days d in y . The model coefficients are the temperature sensitivities α_i^H and α_i^C and the hyperparameters are T_i^H and T_i^C . The total number of cells is assumed to remain fixed. In the following sections, we present how this model is trained and applied to climate and AC projections to project the REC.

2.2. Training the temperature sensitivity model for the French REC

To apply the temperature sensitivity model to the case of France at the finest spatial scales, one needs (i) pairs of input and target historical data to train and validate the model and (ii) input data from 21st century temperature projections on which to apply the trained model to project the REC. We present the training and validation data set in this subsection while the presentation of the 21st century temperature projections is left for Section 2.3.

We thus need data for the inputs of the model: the yearly DD, electric-heating rates, and AC adoption rates. The former is computed from daily surface air temperatures and heating and cooling setpoints. The target $E_i(y)$ is computed from the cell's REC and living surface. Several of these variables used to compute both the inputs and the targets are taken from a dataset provided by the French distribution system operator, Enedis. We first present this dataset and then describe how it is crossed with additional data sources to produce the input and the target training data. The longest training period that the following datasets permit ranges from 2011 to 2018 (included), which is the training period we use.

2.2.1. Energy and building characteristics per cell

The Enedis dataset is accessed via their website (Enedis, 2020) and includes the following variables that are relevant to this study:

- longitude and latitude coordinates of the cell centroids used to assign meteorological stations to cells in Section 2.2.2;
- yearly REC data per cell from 2011 to 2018 (included) used as the target in Section 2.2.5;
- electric-heating rates η_i^{El} for 2018;
- fraction of cell buildings with surfaces in different intervals used to compute the target in Section 2.2.5;
- Enedis estimates of β_i^H using a linear model based on DD akin to the model (2) (see below);
- yearly HDDs used in this Enedis model since 2018, but only at the department level, thus not satisfying our needs;
- heating setpoints used to estimate the HDDs used here as described Section 2.2.3;

Table 2
Heating setpoints T_r^H for all regions of metropolitan France computed according to Section 2.2.3.

Region name	T_r^H [°C]
Auvergne-Rhône-Alpes	16.0
Bourgogne-Franche-Comté	16.3
Brittany	14.8
Centre-Val-Loire	15.0
Grand-Est	16.6
Hauts-de-France	16.0
Ile-de-France	15.8
Normandie	15.0
Nouvelle-Aquitaine	15.3
Occitanie	16.4
Provance-Alpes-Côte d'Azur (PACA)	17.4
Pays-de-la-Loire	15.0

Table 3
AC adoption rates (%) for 2011 and 2018.

Region name	η_{2011}^{AC}	η_{2018}^{AC}
Auvergne-Rhône-Alpes	4.3	17.4
Bourgogne-Franche-Comté	3.4	13.9
Brittany	2.5	10.5
Centre-Val-Loire	4.0	16.5
Grand-Est	3.4	13.9
Hauts-de-France	2.5	10.5
Ile-de-France	4.5	18.3
Normandie	2.7	11.3
Nouvelle-Aquitaine	4.3	17.4
Occitanie	5.6	22.6
PACA	10.5	41.7
Pays-de-la-Loire	2.9	12.2

The Enedis estimates of β^H rely on consumption data at higher temporal resolutions (semi-annual, monthly, or daily) than the publicly available data. They thus can fit their temperature sensitivity model at the highest temporal resolution and average over each cell the estimated β^H for the different delivery points in the cell. However, the β^H of a cell is provided only if the estimate is considered sufficiently precise, i.e. if a minimum of 500 delivery points is available in the cell. As a result, around 50% of the cells are missing, whereas the model (2) can be applied to the annual consumption data to provide estimates of the temperature sensitivities for all cells in France.

2.2.2. Surface temperatures for training

To train the model (2), we use E-OBS version 20.0 (ECA&D, 2020) of the European Climate Assessment & Data (Klok and Klein Tank, 2009; Cornes et al., 2018) (ECA&D for continental gridded surface air temperature (Haylock et al., 2008)). This gridded dataset is available at daily timesteps and a spatial resolution of 0.1 ° over Europe and the Mediterranean and spans from 1950 to the present. Among the available daily statistics, only the daily mean is retained here. Data observations are aggregated from several weather stations and gridded using an interpolation procedure combining spline interpolation and kriging. This dataset is a reference dataset for regional climate studies [e.g. (Haylock and Goodess, 2004; Santos et al., 2007; Stefanon et al., 2012; Raymond et al., 2016; Raymond et al., 2018)] and the evaluation of regional climate models [e.g. (Frei et al., 2003; Räisänen et al., 2004; Kjellström et al., 2010; Flaounas et al., 2013; Stéfanon et al., 2014; Ayar et al., 2016; Drobinski et al., 2018; Raymond et al., 2018)]. E-OBS includes some errors and uncertainties (changes in station locations or can induce those interpolation uncertainties, for example). Flaounas et al. (2013) assessed the E-OBS gridded dataset with temperatures displaying relatively small biases.

The temperature sensitivity model (2) requires temperatures for each cell to compute the HDD and CDD, but the cells (i.e. the IRIS in the case of France) do not correspond to the E-OBS grid points. We thus need to

adjust E-OBS gridded temperatures to the cells over the French domain. This is done here using a nearest-neighbor interpolation using the Euclidean distance between temperature grid points and the cell centroids from Enedis (Section 2.2.1) in a plate carrée projected coordinate system. In order to match the target REC data from Enedis (Section 2.2.1), only the E-OBS data is kept from 2011 to 2018 (included) is kept as training input.

2.2.3. Heating and cooling setpoints estimates

A couple of temperature setpoints T_i^H and T_i^C are required for each cell i in order to compute the HDDs and the CDDs in the temperature sensitivity model (2). The estimation of the temperature setpoints is based on those available in the Enedis dataset (Section 2.2.1) and which Enedis uses to compute the HDDs in their own temperature sensitivity model. In our case, the model is simplified by identifying T_i^H for each cell i in the given administrative region r of France with the average T_r^H of all the values of T^H provided by Enedis for locations in r . The heating setpoint is thus constant over each region, i.e. $T_i^H = T_r^H$ for all cells i in r , where r runs over all the administrative regions of France. The resulting T_r^H estimates are shown in Table 2.

On the other hand, no cooling setpoints are provided by Enedis. Instead, we fix T_i^C for all the cells in France to the value of 21 °C used by EUROSTAT (YYYY) and International Energy Agency (2020).

Another approach to choose T_i^H and T_i^C could be to assume that these temperature setpoints are constant inside each region and to fit them as hyperparameters via a grid search. Doing so, it is found that the prediction error estimated via cross-validation is only marginally improved and that the main conclusions of this study remain unchanged (not shown here). Considering the higher complexity of this approach, the methodology presented in the previous paragraphs of this subsection is preferred here.

2.2.4. AC adoption rates for training

In addition to surface temperatures, the model (2) requires as input AC adoption rates η_i^{AC} for each cell in France. However, this information is not available at such a small geographical scale. Based on the evolution of the national AC adoption rate (ADEME, CODA STRATEGIES, 2021) and the regional distribution data in 2019 (Daguenet et al., 2021), we estimated the regional AC adoption rates at the regional level between 2011 and 2020 and assumed that all cells inside one administration region share the same adoption rate, i.e. $\eta_i^{AC}(y) = \eta_r^{AC}(y)$. This progression in AC adoption rate during the training period is assumed to be geometric. We calculated the average ratio between different years, which indicates a growth of 20% between two consecutive years. This AC adoption rate progression ratio is assumed constant during training, i.e. $\frac{\eta_i^{AC}(y+1)}{\eta_i^{AC}(y)} = \text{constant} = 120\%$. The population-weighted national average is then compared to the reference used in ADEME, CODA STRATEGIES (2021) and is consistent for 2016–2020. The estimated rate for the years 2011 and 2018 are shown in Table 3 with in between a geometric evolution. More details about the initial data used for the estimation can be found in Section C. Errors due to this factor are not studied but should be kept in mind as a limit due to the accessibility of data.

2.2.5. Living area to standardize REC

The model (2) is trained using as targets the yearly REC data from the Enedis dataset (Section 2.2.1). See in Section A for the details of the REC dataset. However, we are interested in the consumption per unit of area. Moreover, the number of buildings per cell — also provided by Enedis — varies from one year to the next. We thus need to normalize the REC of each cell by the corresponding total living surface. Unfortunately, Enedis does not provide the total living surface but the fraction τ_i^k of buildings in cell i for which the living surface belongs to an interval I_k in $\{(0, 30), (30, 40), (40, 60), (60, 80), (80, 100), (100, +\infty)\}$ (m²). Owing

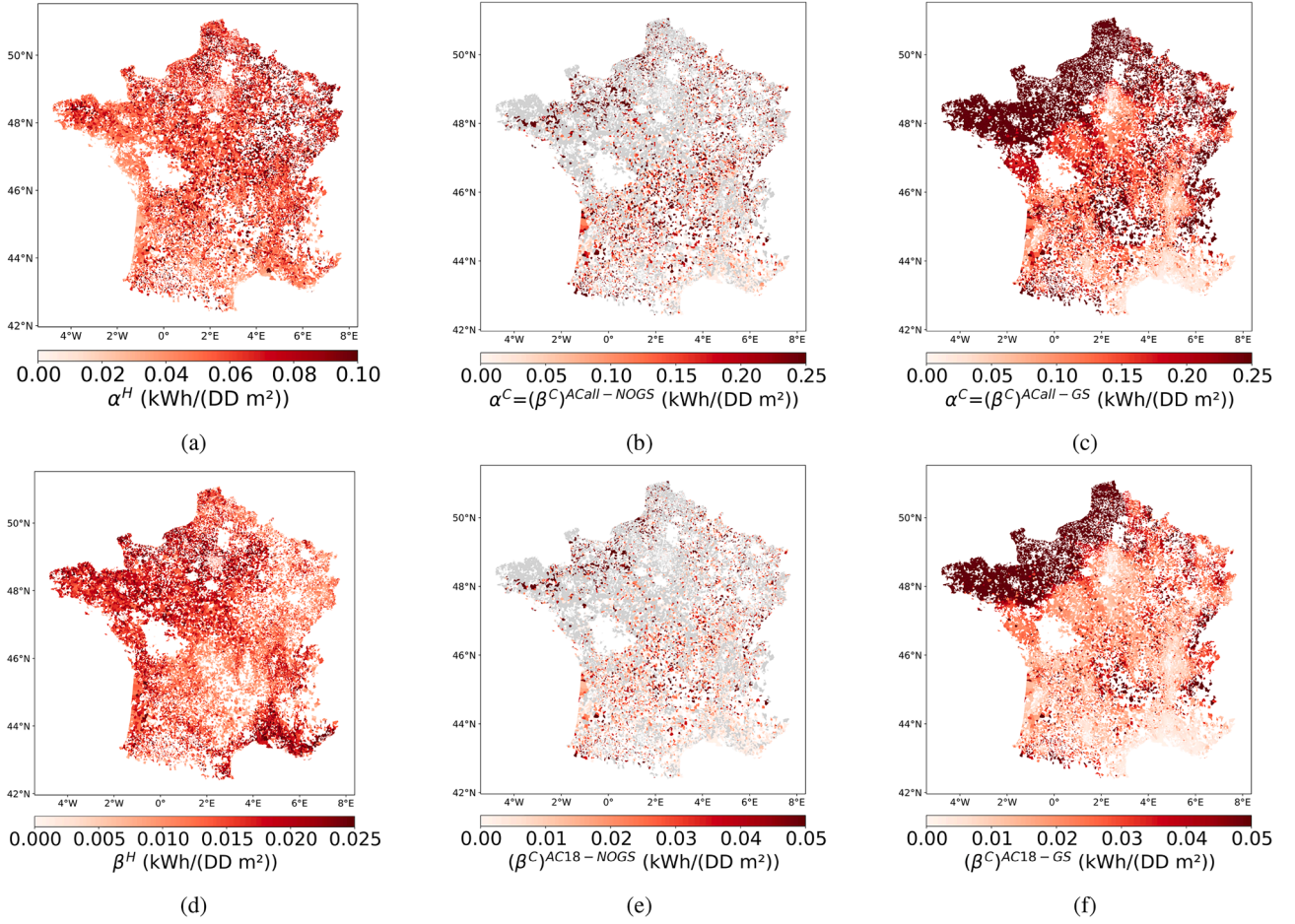


Fig. 3. Top: Estimates of α^H (left) and α^C (middle) obtained by training the model (2) on the observational data (Section 2.2). Projections of α^C (right) by gradual spreading (Section 2.3.2). Bottom: Corresponding values of β^H (left) and β^C (middle), and projections of β^C (right) for the AC2018 scenario (Section 2.3.2).

to the data constraints, we cannot get more specific information at the building level and can only present the distribution of intervals at the IRIS level. Thus, for each interval, we approximate the living surface of buildings with a surface in I_k by the center C_k (m^2) of the interval, except for the first and last intervals. We take the end value of $30 m^2$ for the first interval rather than the median value due to the legal limitations on small living surfaces. For the last interval, we take the finite end of the interval $100 m^2$, primarily because we lack further information on the distribution within the interval and also to counterbalance any potential overestimation for the first interval. It's important to note that these assumptions were made out of necessity due to the data limitations, and the accuracy of these estimates could potentially be improved with data availability at the building level. Then, the average living surface is estimated from the t_i^k provided by Enedis with the following formula:

$$\bar{S}_i = \sum_k t_i^k C_k \left(m^2 \right). \quad (3)$$

2.2.6. Trained temperature sensitivities

As an intermediate methodological result, the maps of the estimated α^H and α^C and corresponding β^H and β^C for cells with statistically significant coefficients at the 5% significance level (60% of all cells) are shown in the left and middle panels of Fig. 3. The OLS regression was used with a constraint on coefficients to be positive. Regression methods with regularization (Lasso and Ridge) were also tested, but this led to an increase in the test R^2 score of less than 10% (not shown here), so the OLS was preferred to limit the number of parameters of the model. All the test scores are estimated using k-fold cross-validation with one fold

per year of data (8 folds in total). The test R^2 score averaged over all cells is about 0.68 with a 25% quartile of 0.56 and a 75% quartile of 0.79. More details about the test R^2 score are given in Section B as well as the validation of the model with comparison to Enedis datasets in Section A.

2.3. Projection data and scenarios definitions

As mentioned in Section 2.1, the basic consumption, represented by B in (2), is assumed to be stationary all the time. As far as the heating REC is concerned, we assume that α^H , T^H and η^{El} are also stationary so that only the HDDs change in response to temperature changes. Regarding the cooling REC, we follow a similar approach as for the heating REC, but η^{AC} and α^C also change in some AC scenarios (T^C is always stationary). We thus need to associate each cell with a temperature projection for a given climate change pathway, as well as with projections of η^{AC} and of α^C .

2.3.1. Temperature projection data under a climate change pathway

In this study, the most severe climate change pathway, the Representative Concentration Pathways (RCP) 8.5, is selected. The corresponding bias-corrected daily-mean temperature change is obtained from multiple regional climate models from the CORDEX program. In this study, these projections are completed with the corresponding historical experiments that serve as a reference to measure the effect of climate change. Due to modeling uncertainty, the projected statistics of the atmosphere may vary significantly with the choice of Regional Climate Model (RCM) and of driving Global Climate Model (GCM). Hence, multi-model ensembles are commonly used in climate studies to

Table 4
Institute, GCM name and RCP name for the 5 climate change simulations used in this study.

No.	Institute	Driving GCM model	RCM model
1	CNRM	CERFACS-CM5	ARPEGE51
2	CNRM	CERFACS-CM5	RCA4
3	IPSL	CM5A-MR	RCA4
4	IPSL	CM5A-MR	WRF331F
5	ICHEC	EC-EARTH	RACM022E

provide a partial estimation of the modeling error. This is why the five model combinations listed in Table 4 are used in this study. These simulations are accessed via the Copernicus Climate Change Service database (<https://climate.copernicus.eu/>).

To associate a cell to a climate-model simulation, the same methodology as for the temperature observations used for training is followed (Section 2.2.2). Three climate-simulation periods of 30 years are considered, which are distinct from the training period defined in Section 2.2: a historical period from 1975 to 2005 (excluded) — used as reference — and two projection periods, one from 2025 to 2055 and one from 2070 to 2100. Results associated with the latter are respectively referred to as CC2040 and CC2085 (based on the central year of the period).

As intermediate methodological results, mean historical HDD and CDDs, as well as the corresponding projected changes, are represented in Fig. 4. One can see that the temperature increase projected over France

leads to a general decrease in the HDDs (top panels) and to a general increase in the CDDs. These changes are however not homogeneous since the decrease in the HDDs is strongest in the southern and eastern parts of France, while the increase in the CDDs is largest in the southern part of France.

2.3.2. AC use scenarios

In the present framework, two factors are sensitive to the evolution of AC use during the 21st century: the AC adoption rate η_i^{AC} , and the switch of a cell from an α_i^C of zero to a positive α_i^C , for each cell i . While the former reflects the evolution of AC use within a cell, the latter corresponds to a conversion of a cell from having no AC user at all to having some AC users. Here, we do not attempt to make plausible projections of these factors based on current signals. Instead, as summarized in Table 5

Table 5
Definition of the four AC scenarios in terms of AC adoption rate and α^C spreading strategy. XXXX is either 2040 or 2085, corresponding to the central year of the climate change projection window considered.

Name	Definition	
	η^{AC}	Gradual Spreading of α^C
CCXXXX-AC18-NOGS	Same as in 2018	No
CCXXXX-AC18-GS	Same as in 2018	Yes
CCXXXX-ACall-NOGS	100%	No
CCXXXX-ACall-GS	100%	Yes

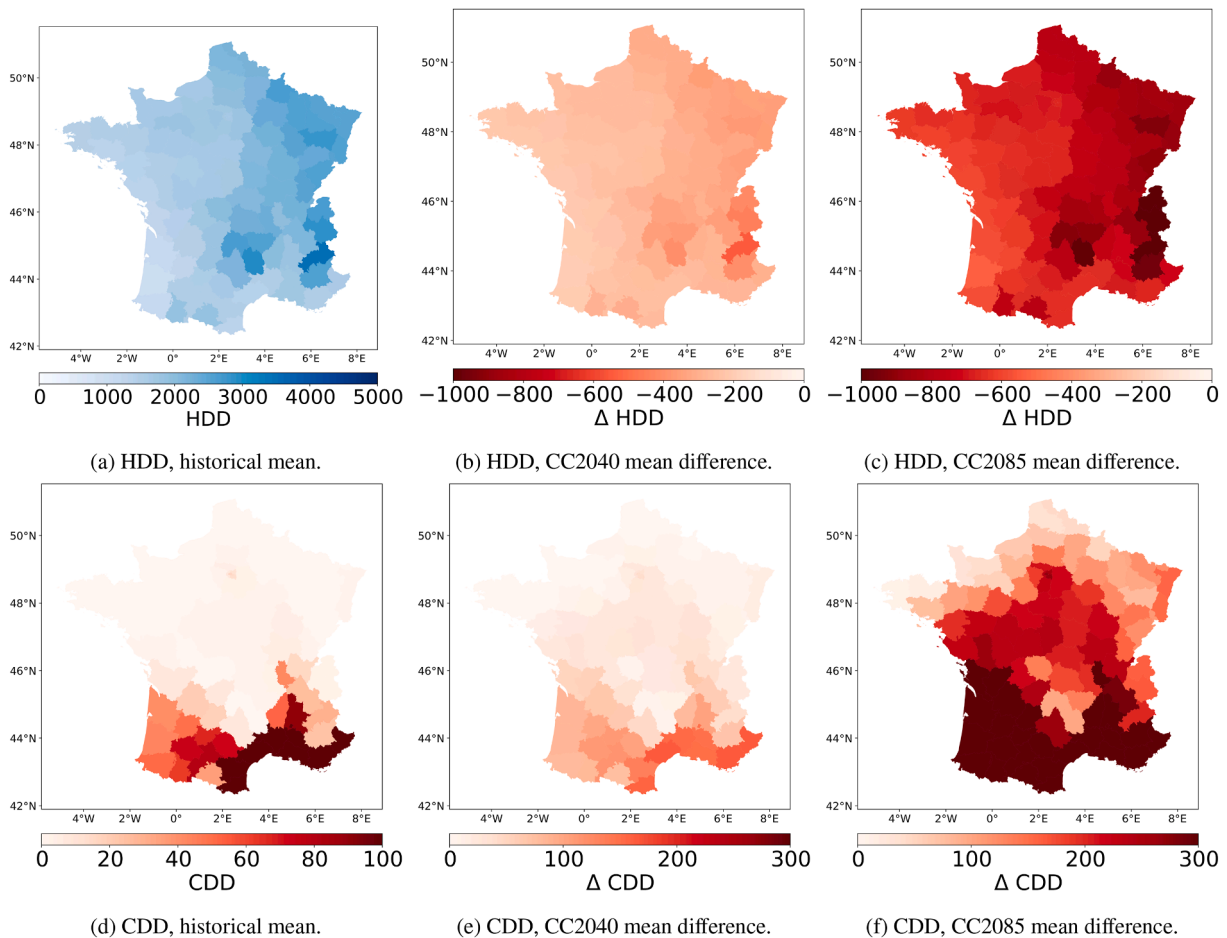


Fig. 4. Mean over 1975–2005, mean change over 2025–2055 wrt. 1975–2005 (CC2040), and mean change over 2070–2100 wrt. 1975–2005 (CC2085) for the HDDs (top) and CDDs (bottom) computed according to Eq. 1. The temperature data for 1975–2005 is from the historical CORDEX simulations, while that for 2025–2055 and 2070–2100 is from the RCP8.5 CORDEX simulations. The results are spatially averaged over the departments and averaged over the climate-model simulations listed in Table 4. Warm colors represent situations associated with warm temperatures (i.e. to a decrease in heating REC and to an increase in cooling REC).

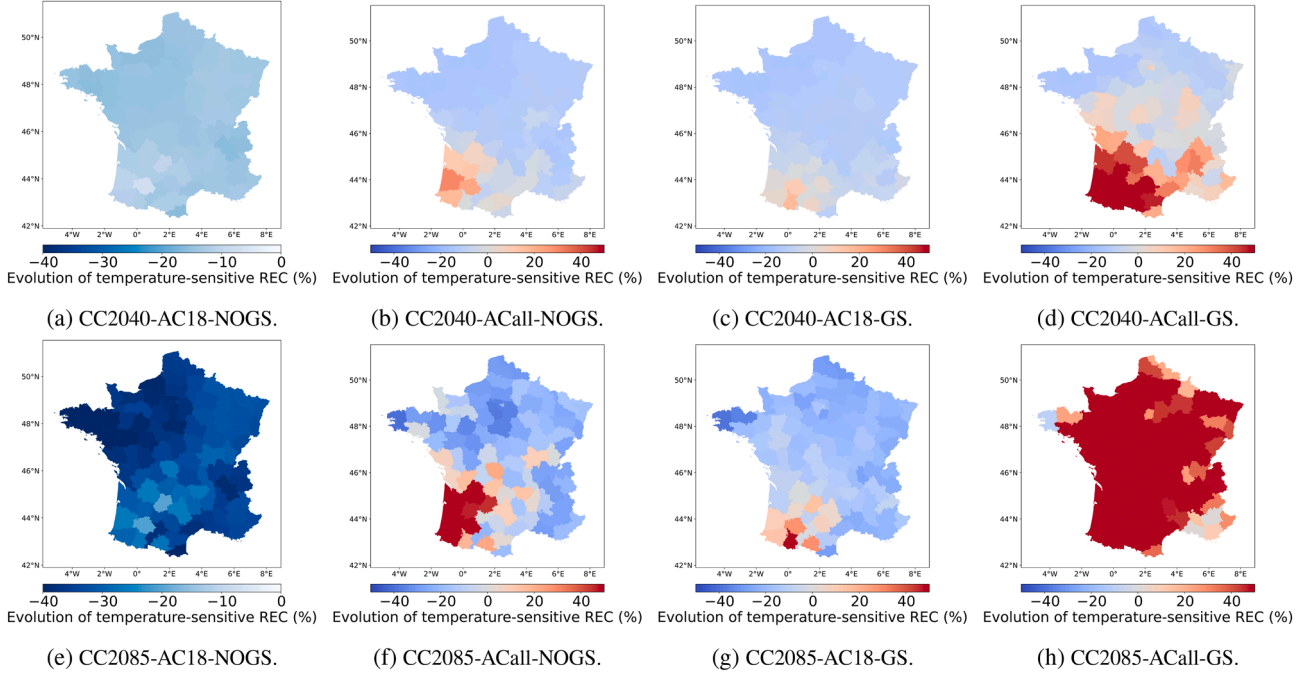


Fig. 5. Relative change (%) in REC wrt. to the historical period (1975–2005) for CC2040 (top) and CC2085 (bottom) and for different AC scenarios: AC18-NOGS (left column), ACall-NOGS (second column), AC18-GS (third column) and ACall-GS (right column).

and explained below, two extreme cases are considered for both factors and indifferently for the 2025–2055 and the 2070–2100 periods.

Regarding η^{AC} , the minimal scenario is that η^{AC} remains fixed to its 2018 cell values (Section 2.2.4), corresponding to a situation in which AC installation no longer progresses. The maximal scenario is that η^{AC} has reached 100% in every cell before the beginning of the projection period and remains fixed over the period, corresponding to a situation in which all households are equipped with AC (regardless of the technology).

Regarding α^{C} , the minimal scenario is that cells with no cooling temperature sensitivity remain so. The maximal scenario is that all cells become cooling-sensitive. In this case, further assumptions are needed to determine α^{C} for these cells that were not cooling-sensitive historically. Here, we assume that α^{C} for these cells is the result of interpolation from the α^{C} values of the surrounding cells with a positive α^{C} . A nearest-neighbor interpolation is performed for a given number of neighbors and for the Euclidean distance in the plate carrée projection. The number of neighbors is optimized based on the methodology described in Section D, giving an optimal number of 25 cells. We refer to this scenario as the gradual spreading of α^{C} and the resulting α^{C} estimates are shown in Fig. 3c. The gradual spreading scenario mimics a “do like my neighbor” behavior.

2.4. Quantifying the uncertainty in the projected REC change

For a given cell i , a model m (Table 4) and a scenario s (Table 5), we define the absolute change in REC, $\Delta \bar{E}_i^{m,s}$, as the difference (Δ) at i between the REC averaged ($\bar{\cdot}$) over the CORDEX historical period and the REC averaged over one of the two CORDEX projection periods, estimated with the model m simulations for the scenario s . In addition, the relative REC change is defined as the absolute REC change divided by the REC averaged over the CORDEX historical period. Given the stationarity assumptions (Section 2.3), the absolute REC change is given by

$$\Delta \bar{E}_i^{m,s} = \alpha_i^{\text{H}} \eta_i^{\text{El}} \Delta [\overline{\text{HDD}}_i^{m,s}] + \Delta [(\alpha_i^{\text{C}} \eta_i^{\text{AC}})^s \overline{\text{CDD}}_i^{m,s}]. \quad (4)$$

In the AC18-NOGS scenario, α^{C} and η^{AC} are also stationary, so that

$$\Delta \bar{E}_i^{m,s} = \alpha_i^{\text{H}} \eta_i^{\text{El}} \Delta [\overline{\text{HDD}}_i^{m,s}] + (\alpha_i^{\text{C}} \eta_i^{\text{AC}})^{\text{AC18-NOGS}} \Delta [\overline{\text{CDD}}_i^{m,s}], \quad (5)$$

in this case.

The corresponding multi-model average is

$$\left\langle \Delta \bar{E}_i^s \right\rangle := \frac{1}{M} \sum_{m=0}^{M-1} \Delta \bar{E}_i^{m,s}. \quad (6)$$

An essential part of this study is quantifying the uncertainty of our estimates of temperature-sensitive REC change ($\Delta \bar{E}_i^s$). From (6), we can see that errors may come from.

- the temperature sensitivity model design,
- the stationarity assumptions on the model coefficients and on electric appliances adoption rate η_i^{El} and η_i^{AC} during scenarios studies,
- the regression of the coefficients from a particular training dataset,
- the historical estimates of η_i^{El} and η_i^{AC} ,
- the climate models (Jacob et al., 2014; Ruti et al., 2016),
- the choice of climate change pathway and AC use scenario.

Here, only the worst-case climate change pathway is considered (i.e. RCP8.5, Section 2.3.1), so that uncertainty in the climate-model pathway is not assessed. On the other hand, a partial estimate of climate-model errors is provided in the results Section 3 from the variations of the projected REC change with the choice of the climate model. To estimate the sensitivity of temperature-sensitive REC change to AC adoption rate projections, extreme scenarios are considered (Section 2.3), while measurements of the electric-heating rate are assumed to be reliable and representative of other years than the year it is provided for. The assumption of the stationary temperature sensitivity model coefficients restricts the scope of the results of this study. It is not tested in-depth in this work, but a simple analysis is conducted in Section 3.2 and further discussed in terms of policy implications in Section 4. Finally, the errors from the model design and the regression are estimated using cross-validation (Section 3.4).

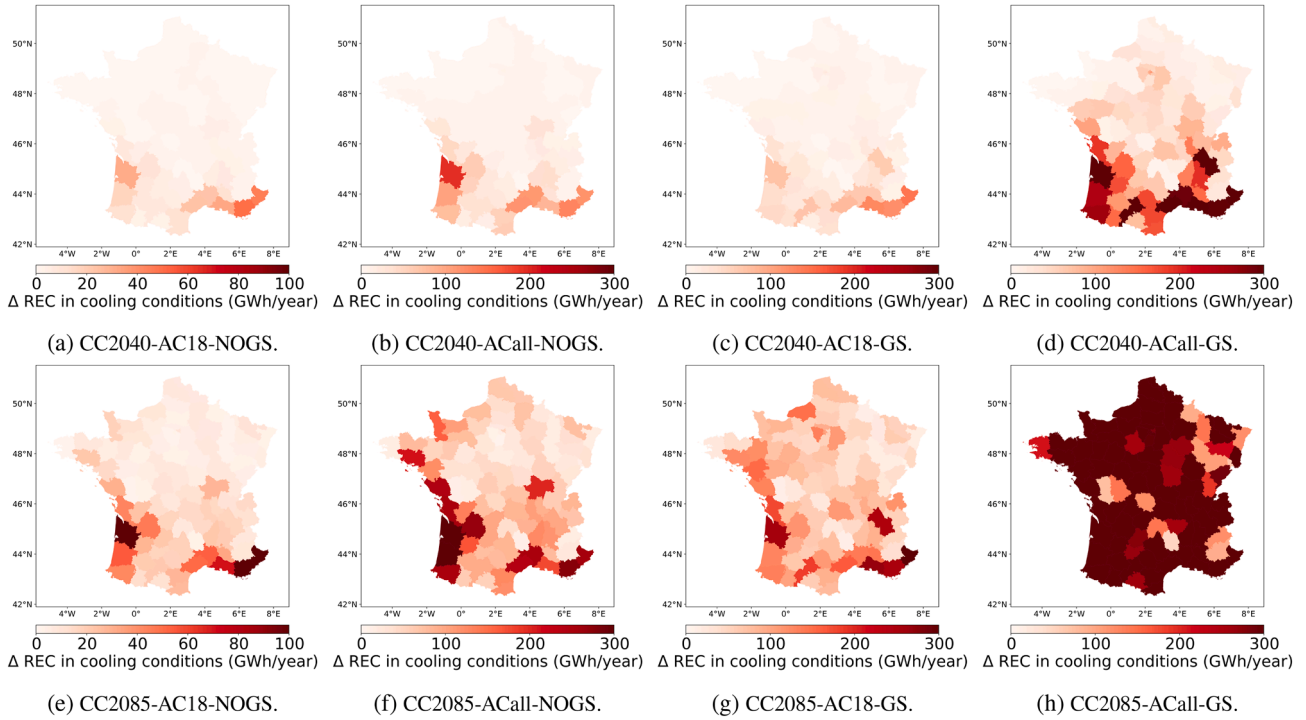


Fig. 7. Same as Fig. 5 but for the cooling REC.

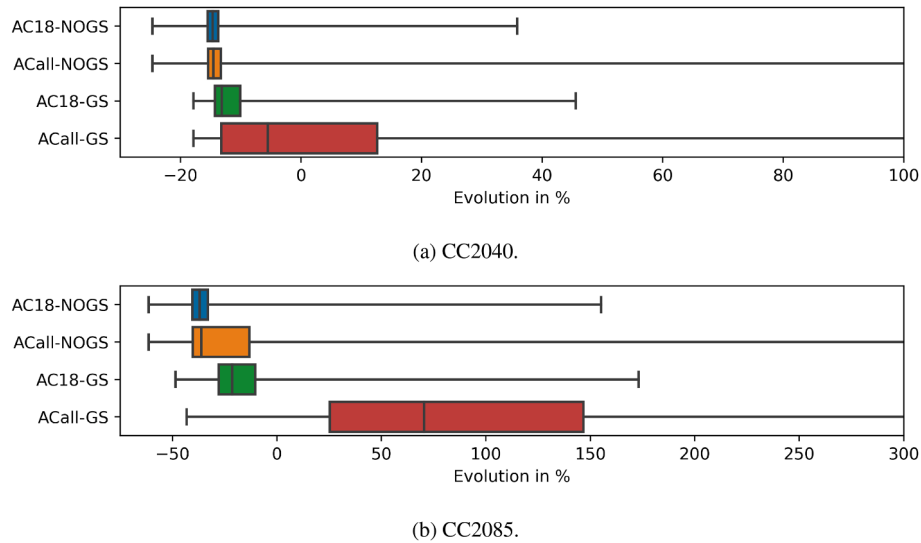


Fig. 6. Boxplots over the cells of the relative change in temperature-sensitive REC corresponding to Fig. 5. The whiskers here show the minimum on the left and the 99% quantile on the right.

Table 6

Decomposition of variability into different geographical scales for different studied variables in terms of proportion (%).

Variable y_i	$\frac{\sigma^2(y_i - \langle y_i \rangle_d)}{\sigma^2(y_i)}$	$\frac{\sigma^2(\langle y_i \rangle_d - \langle y_i \rangle_r)}{\sigma^2(y_i)}$	$\frac{\sigma^2(\langle y_i \rangle_r - \langle y_i \rangle_n)}{\sigma^2(y_i)}$
β_i^H	75%	13%	12%
α_i^C	77%	4%	19%
$\langle \Delta HDD_i \rangle^{CC2040}$	24%	20%	56%
$\langle \Delta HDD_i \rangle^{CC2085}$	29%	23%	48%
$\langle \Delta CDD_i \rangle^{CC2040}$	13%	15%	72%
$\langle \Delta CDD_i \rangle^{CC2085}$	14%	13%	73%
$\langle \Delta \bar{E}_i \rangle^{AC18-NOGS}$	82%	7%	11%

3. Results and discussion

We now analyze the projected changes in the REC, first for the scenarios where the AC uses remain fixed, then for scenarios with AC uses changes. The discussion of the uncertainty in the results is left for the next Section 4, the main conclusions from these results being robust.

3.1. Projected REC change without change in AC use

The projections of temperature-sensitive REC changes for fixed AC use (AC18-NOGS) are shown in Fig. 5a and Fig. 5e. In general, the REC decreases between 7% and 16% in all departments for CC2040, down to 20% to 42% for CC2085. Aggregated at the country scale, the REC

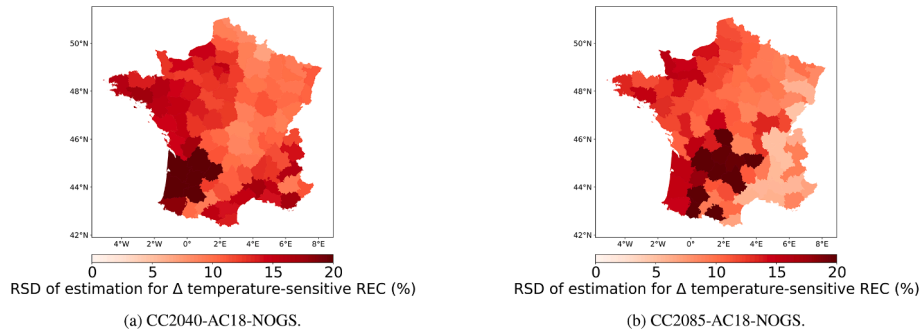


Fig. 8. The global uncertainty of estimation of evolution in temperature-sensitive REC by combining all possible estimated coefficients with the leave-one-out cross-validation method and the 5 CORDEX simulations, represented by the Relative Standard Deviation (RSD) for the CC2040-AC18-NOGS (left) and the CC2085-AC18-NOGS (right) scenarios.

Table 7

Average values with uncertainty for all possible combinations, the uncertainty is converted to the same magnitude by averaging over the number of cells. A t-test shows that mean values of REC change under all scenarios are significant.

Time	Scenario name	Mean (GWh/cell)	Std (GWh/cell)		
			Cell	Department	Country
2040	CC-AC18-NOGS	-0.22	0.037	0.029	0.024
	CC-AC18-GS	-0.16	0.053	0.038	0.031
	CC-ACall-NOGS	-0.16	0.066	0.042	0.032
	CC-ACall-GS	0.08	0.191	0.146	0.125
2085	CC-AC18-NOGS	-0.53	0.085	0.057	0.047
	CC-AC18-GS	-0.28	0.185	0.150	0.136
	CC-ACall-NOGS	-0.26	0.236	0.159	0.138
	CC-ACall-GS	1.26	1.019	0.867	0.790

Table 8

Comparison of uncertainty due to model or CORDEX for scenario AC18-NOGS in the form of standard deviation (GWh/cell).

Time	Cell		Commune		Country	
	Model	CORDEX	Model	CORDEX	Model	CORDEX
2040	0.020	0.034	0.012	0.029	0.010	0.022
2085	0.056	0.066	0.031	0.052	0.026	0.040

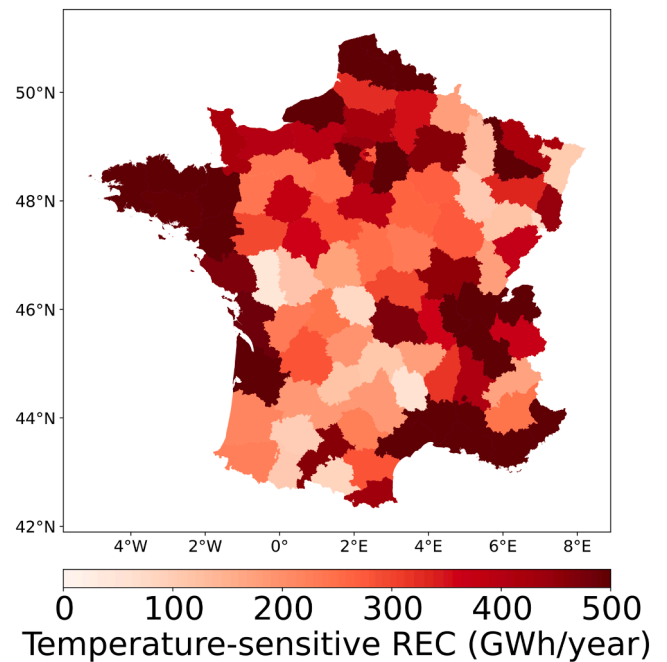


Fig. 10. Total temperature-sensitive REC reference aggregated at the department level, estimated with our model using the temperature of 1975–2005 from CORDEX simulations on all valid cells (60% of the cells).

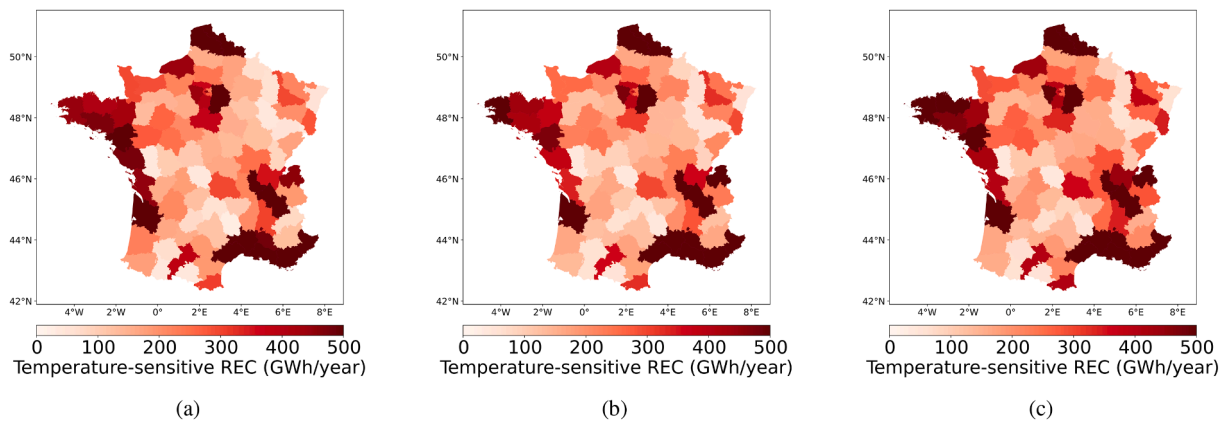


Fig. 9. Temperature-sensitive REC per year averaged over departments estimated from (a) the Enedis β^H estimates for 2018 (for 50% of the cells only, Section 2.2.1), (b) the model (2) applied to the E-OBS temperatures for 2018 and (c) the model (2) applied to the CORDEX historical temperatures over the 1975–2005 period and averaged over the period and over the climate-model simulations (Section 2.3.1).

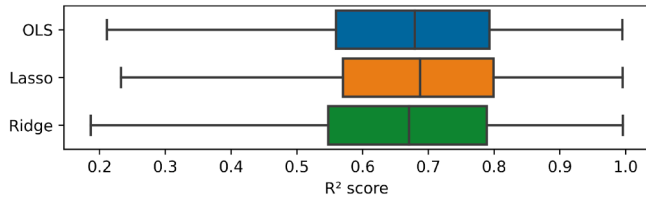


Fig. 11. Comparison between linear regression methods of R^2 score distribution for all valid IRIS.

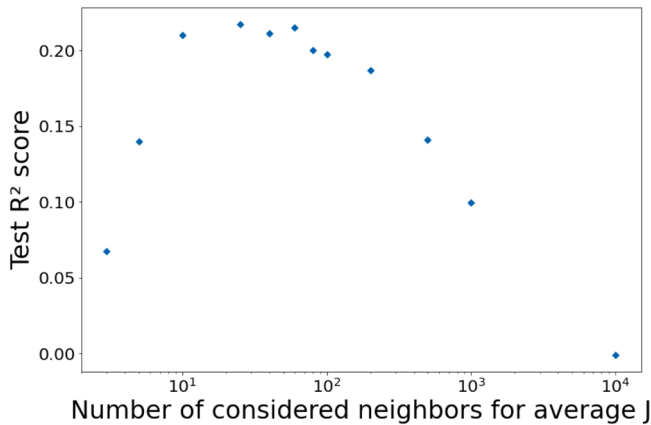


Fig. 12. Test R^2 score between estimated α^c with Gradual Spreading method and regression model estimation as a function of the chosen number of neighbors J taken into account for the calculation of average (Gradual Spreading).

decreases by about 8TWh and 20TWh, respectively. This is consistent with the results of Damm et al. (2017); Spinoni et al., 2018, but significant variations are observed between departments.

For this scenario and for a given cell, according to (5), the projected heating and cooling REC changes are proportional to the HDD and CDD changes, respectively, represented in Fig. 4. However, the coefficients of proportionality, $\alpha_i^H \eta_i^{El}$ and $(\alpha_i^C \eta_i^{AC})^{AC18-NOGS}$, represented in Fig. 3, depend on the cell. From this can be deduced that the REC changes for this scenario are dominated by the large decrease in the HDDs (Fig. 4b and Fig. 4c) modulated by variations in β^H with the cells (Fig. 3d). This effect can for instance be seen in the weaker reduction of the REC in the North-East and the South-West of France.

In addition, the REC decrease is reduced in the south of France due to the significant increase in the cooling REC with the increase in the CDDs (Fig. 4e and Fig. 4f) in conjunction with the positive β^C there (Fig. 3e). This is more obvious from the plots of the cooling REC for the AC18-NOGS scenario in Fig. 7a and Fig. 7e. One can see that, according to this scenario, the cooling REC increases everywhere, but this is particularly evident along the Atlantic coast and South of $46^\circ N$ latitude, between the Massif Central and the Alps, especially for the CC2085 period. At these locations, HDDs indeed tend to increase significantly, but the correlation is not perfect, since, for this scenario, the translation of this change in a cooling REC change depends on AC being already in use there (Fig. 3e). A substantial increase in the cooling REC is also observed in the Northwest part of France for CC2085 (Fig. 7f), even though the increase in CDDs is relatively weak there (Fig. 4f). This is explained by the fact that a significant number of cells there have a large β^C (Fig. 3e).

The distribution of the temperature-sensitive REC change at the cell level is shown in Fig. 6 in the form of box plots. The distribution for scenario CC2040 without AC use changes (AC18-NOGS) is right-skewed, meaning the temperature-sensitive REC is expected to decrease around 15% in most regions. In the longer term, the disparity between IRIS increases with decreasing averaged temperature-sensitive REC. Indeed,

some IRIS may display a positive temperature-sensitive REC change (i.e. an increase in temperature-sensitive REC) over 3% of the French territory in the near future and up to 7% by the end of the 21st century.

3.2. Projected REC change with change in AC use

The projections of temperature-sensitive REC change with different AC scenarios are shown in 5b-5d and 5f-5h. Contrary to the results including temperature change only, some regions display an increase of temperature-sensitive REC whose pace and spatial extent depend on the AC scenario.

Results also show that the different factors have diverse effects. In the case where the AC rate is changed without spreading geographically, the temperature-sensitive REC is expected to increase in the South-West of France and in the South along the Mediterranean Sea (Fig. 5b and Fig. 5f). Indeed, in this region, α^H is relatively low with respect to other regions, and AC systems are already deployed so that α^C is different from zero. But α^C in these regions has a relatively low value, so if the temperature change is only accounted for, increased CDD makes the decline in temperature-sensitive REC less rapid. However, in the considered scenario, the change in AC rate directly multiplies the current cooling demand by four to five times. The electricity savings from heating in the South-West are thus expected to be fully offset by cooling in the near future (Fig. 7b). In the far future, this trend should be exacerbated in the South-West and in the South and spread significantly along the Atlantic coast and South of $46^\circ N$ (Fig. 7f). As there is no spatial spreading of AC usage, the geographical patterns of temperature-sensitive REC change are similar between Fig. 7a and Fig. 7e, and Fig. 7b and Fig. 7f.

With regards to the AC rate scenario, the gradual spreading of the present AC rate lowers the change of REC for cooling needs, but REC for cooling needs becoming positive spreads geographically (Fig. 5c and Fig. 5g). Gradual spreading does not change the values instantly in regions where most IRIS cells are already given with non-null estimation for α^C . However, it helps to smooth the map of coefficients as shown in Fig. 3b and Fig. 3c. Based on observational data, many cells in Ile-de-France, Auvergne-Rhône-Alpes, and along the Atlantic coast have been given null estimates for α^C . However, some nearby cells still received significant values for α^C with high regression scores. Assigned with proximity averages, these areas mixed with sporadic large values are most affected. Fig. 6 shows that a 100% AC rate in already equipped cells (ACall-NOGS) modifies the shape of the distribution, with an increased number of cells with positive evolution. More positive values correspond to the cells currently equipped with AC at which the AC rate is increased from its current value to 100% and where the change of REC for cooling needs exceeds that for heating needs. No change is expected for the cells currently without AC hence the minimal, the first quartile even the median values remain the same as for AC18-NOGS. In the gradual spreading scenario (AC18-GS), the shape of the distribution displays an even larger positive skewness than in the 100% AC rate scenario. Less negative values correspond to the larger number of cells equipped with AC and bring an increase to all cells.

In a scenario combining gradual spreading and 100% AC rate, almost half of the territory, except the North of France, sees the REC increasing in the near-term future, amounting to a global change of +2%. At the end of the 21st century, this fraction of positive trend increases up to 90%, leading to a global change of +32%.

The results of these scenarios motivate actions allowing at least to prevent AC from inducing an increase in cooling REC. A simple approach, applicable to the whole country, consists at least in the region of South of France with the greatest AC impact to modify in the future climate scenarios only the cooling setpoint in such a way as to maintain the cooling REC unchanged with respect to the present situation. Such an approach leads to the most constraining action as it sets for the whole country the highest cooling setpoint, but it ensures at least unchanged cooling REC in the South of France and in most regions of France a

negative cooling REC trend. The cooling setpoint preventing any cooling REC increase over the whole country varies with the time horizon, which is about 23–24 °C by 2040 and 26–27 °C by 2085.

3.3. Spatial heterogeneity

The maps shown in Fig. 3 and Fig. 5 show an apparent geographical disparity of temperature sensitivities and temperature-sensitive REC changes. To compare the intra-department variability with the one of inter-department, each studied variable y_i (sensitivity coefficients α_i^H, α_i^C , DD evolution $\langle \Delta \overline{HDD}_i^s \rangle, \langle \Delta \overline{CDD}_i^s \rangle$) and the REC evolution $\langle \Delta \overline{E}_i^s \rangle$) can be decomposed as:

$$y_i = (y_i - \langle y_i \rangle_d) + (\langle y_i \rangle_d - \langle y_i \rangle_r) + (\langle y_i \rangle_r - \langle y_i \rangle_n) + \langle y_i \rangle_n. \quad (7)$$

with $\langle y_i \rangle_d$ the average value of cells inside a given department, $\langle y_i \rangle_r$ the average value of cells inside a given administrative region, and $\langle y_i \rangle_n$ the average value of all cells in France. Hence with the above equation, the variability of all cells can be decomposed into disparities at several stages:

$$\sigma^2(y_i) = \sigma^2(y_i - \langle y_i \rangle_d) + \sigma^2(\langle y_i \rangle_d - \langle y_i \rangle_r) + \sigma^2(\langle y_i \rangle_r - \langle y_i \rangle_n). \quad (8)$$

where $\sigma^2(y_i - \langle y_i \rangle_d)$ represents the variability of cells inside the department while $\sigma^2(\langle y_i \rangle_d - \langle y_i \rangle_r)$ represents the variability of departments inside a given administration region and $\sigma^2(\langle y_i \rangle_r - \langle y_i \rangle_n)$ the variability between different administrative regions. Table 6 shows the proportion of variability at each geographical scale over the whole variability.

The regional variability is more important than the local difference for the DD changes. However, the variability of temperature sensitivities between cells within the same department dominates. At the same time, because of the large spatial variability of β^H and α^C within the administrative regions, a larger disparity of temperature-sensitive REC changes is found between cells than between administrative regions. For both temperature sensitivities, β^H and α^C and temperature-sensitive REC changes, it shows that the variability between the cells is more significant than the difference between regions, which justifies our choice of study at a small geographical scale.

3.4. REC change error estimates

In this study, public data are used to train the temperature sensitivity model with only eight annual samples applied for the regression. Compared to models with a larger dataset, our model can be easily influenced by outliers and may have coefficients over-fitted.

We did not choose regularized regression because the performance did not improve much, but this method may be more attractive if a more extensive input is available. Nonetheless, the possibility of applying the leave-one-out cross-validation over the training gives us eight possible models and, thus, a range of eight different results of the temperature sensitivities with uncertainty.

At the same time, CORDEX simulations from different models may produce different future temperature projections. Combining the five different simulations and all possible estimated coefficients with the leave-one-out cross-validation method, the global uncertainty of our results, quantified by the Relative Standard Deviation (RSD), is shown in Fig. 8. The relative error is large in the South-West, where $\alpha^C > 0$, due to the biased model regressions as the observed temperatures do not largely and frequently exceed the 21 °C cooling setpoint.

The global uncertainty for all the scenarios is presented in Table 7. The standard deviation is identified after aggregating REC at different levels. For the results to have the same order of magnitude and to be comparable, the REC change is normalized by the average number of IRIS in the desired geographical scale. The method using a REC linear model together with the CORDEX simulations derives robust estimates of future REC with an error of less than 18.4% without assumptions on

AC uses. The uncertainty of scenario ACall-GS is the largest among all other scenarios because the results may become less precise with all the assumptions together. We can see clearly that with spatial aggregation, the error decreases because there can be compensation between IRIS within the large scales, and the variation becomes smaller. For the average values of all possible combinations, a t-test shows that the mean values of REC change under all scenarios are significant.

The global error of future REC mainly comes from the multi-model ensemble spread of the projected temperatures and the training bias and variance of the REC linear model. To find the standard deviation due to different sources, we use the average values of the cross-validated coefficients estimated by the model or the average of the five simulations of CORDEX, respectively. The uncertainty due to the simulations of CORDEX and to the model regression can be found in the following Table 8. With the previous tables, we can see clearly that the uncertainty due to the various simulations of CORDEX leads to a more significant error than the one from the regression. This 10% error due to the model is reassuring the basis of a temperature sensitivity model: the temperature sensitivity is quasi-constant under a stable climate. Nevertheless, this error can still be improved if more annual consumption data are available or daily consumption data can be accessible.

4. Conclusions and policy implications

A number of key messages can be drawn from the results of this study. First, REC varies significantly at very fine spatial scales, from the IRIS size (region of 2,000 inhabitants) to the administrative departments (96 departments on the European continent and 5 overseas) and regions (13 on the European continent and 5 overseas). Such variability had never been quantified and mapped due to a lack of suited methodology and limited available data at the finest scale (IRIS). Such variability which is the largest at the finest spatial scale calls for solutions and policies steered to the local specificities.

With increasing temperatures due to climate change, the heating needs decrease especially in the North-East which displays a continental climate with very hot summers and very cold winters (Köppen, 1936) and thus a strong sensitivity to any heating need reduction. Conversely, the South and Western regions along the Mediterranean Sea and the Atlantic Ocean, respectively, display a smaller trend in heating needs as they display a Mediterranean climate (hot, dry summers and cool, wet winters) and a maritime climate (cool summers and mild winters) (Köppen, 1936), respectively with warmer winters with regards to the North-East of France. At the end of the 21st century, in the worst-case climate scenario (RCP8.5), the spatial variability of the trend decreases as many regions are expected to experience temperatures much more rarely below their heating setpoint. There is a strong link between the heating needs and its evolution with that of REC.

However, the evolution of REC is modulated by the evolution of cooling needs and the deployment of AC systems to meet those needs. Our worst-case scenarios suppose either a 100% AC adoption rate in the IRIS already equipped at present, or a gradual spreading of AC systems, which mimics a "do like my neighbor" behavior. We also consider a combination of the two. In any scenario, the decrease in REC due to climate change could be totally offset in the South of France, which would then display an increase in REC. When the 2 AC scenarios are combined, an increase in REC could be seen over the whole country.

One key message deals with the overall uncertainty of our modeling setup. The uncertainty of our REC trends, including climate change impact and AC system deployment, is dominated by the spread between the climate simulations of our ensemble. The regression-based REC model does not add up much to the overall uncertainty. Such a result was not straightforward as the data available at the IRIS scale was at best limited in time, at worst available on an annual basis only, and sparse in some regions. The level of overall uncertainty therefore allows for drawing some recommendations in terms of practical applications and energy policies.

Takeaways for policy implications can be formulated from these results. In our scenario, AC gradual spreading mimics a “do like my neighbor” behavior. Our results show that such behavior has a major and detrimental impact on REC (more than 100% AC rate scenario). Such results call for targeted and local information actions where the risk of spreading is high (i.e. in areas where households are already equipped with AC systems) to limit the spreading or mitigate its effect with at least the most energy-efficient AC systems. A more straightforward result is that the South of France is where the REC trend is expected to occur first with possible impacts on the energy system. Therefore there is a need to target actions to prevent any further deployment of AC systems. Especially, the climate of the South of France is expected to become similar to the present climate of countries more to the South, such as Italy or Morocco (Hallegatte et al., 2007). In Morocco, there is no visible impact on REC of AC use (Bouramdane et al., 2021). In Italy, the signal on REC of the use of AC is very limited (Tantet et al., 2019) but locally the evolution of cooling needs can have a significant impact on REC (De Felice et al., 2013; Scapin et al., 2016). Therefore, analyzing the socio-economic drivers, and the energy policies of these countries and drawing inspiration from them to deploy actions adapted to the local specificities of some French regions should be considered. Our worst-case results clearly show the detrimental impact of the increase in AC rate and spreading. Increasing the cooling setpoint T^C (e.g. recommended temperature of 26 °C by the US Department of Energy) or maintaining an optimal difference with outdoor air temperature to about 7–8 °C to maximize the energy efficiency of the AC equipment, could lower the cooling REC. Based on our model, shifting the cooling setpoint from 21 °C at present to 23–24 °C by 2040 and 26–27 °C by 2085 would prevent any cooling REC increase in our worst-case scenarios. These values are consistent with existing recommendations. Low-tech alternative solutions also exist which are widely implemented in subtropical regions, and can be implemented in France to improve the thermal comfort of buildings and reduce the use of AC equipment and their impact on the environment, such as the reflective white coating on the buildings or roofs (Viguié et al., 2020; Rawat et al., 2022).

There are still several limits to this study. The temperature sensitivity results from a regression between REC and temperature, and the model implicitly integrates “human behaviors” related to other factors such as electricity costs and household revenue (Frederiks et al., 2015; Gertler et al., 1366). However, at this stage, no approach to segment the consumption data along multiple socio-economic dimensions (e.g. price, revenue) has been successful with the available data (e.g. time sampling and spatial granularity too coarse and aggregated) which would have been valuable to reduce global uncertainty. It could have been relevant to perform a sensitivity analysis on the temperature sensitivity through η^{el} to account for the further electrification of heating (e.g. fuel oil or gas to heat pumps) or through α^C to account for improved efficiency of AC systems. Regarding α^C , regions of the North-West along the Atlantic

coast where the AC rate is on average 14% (versus 22% at the national level in 2019) can display surprisingly large positive α^C values. The causes should be further explored, whether due to statistical processing or behavioral in origin (e.g. residents may be less adapted to extreme heat events and more likely to install AC equipment for use during such extreme events (He et al., 2022)). Finally, the study from Pagliarini et al. (2019) shows that in a warmer climate, the electricity increases faster than linearly because of the efficiency drop of air-cooled chillers at high temperatures. Such a phenomenon should also be considered in the future.

CRediT authorship contribution statement

Qiqi Tao: Conceptualization, Data curation, Formal analysis, Investigation, Methodology, Visualization, Writing - original draft, Writing - review & editing. **Marie Naveau:** Conceptualization, Data curation, Formal analysis, Investigation, Methodology. **Alexis Tantet:** Conceptualization, Supervision, Validation, Writing - review & editing. **Jordi Badosa:** Conceptualization, Data curation, Formal analysis, Validation, Writing - review & editing. **Philippe Drobinski:** Conceptualization, Formal analysis, Supervision, Validation, Writing - review & editing.

Data availability

Input data are all publicly available, produced data will be made available by request.

Declaration of Competing Interest

The authors declare that they have no known competing financial interests or personal relationships that could have appeared to influence the work reported in this paper.

Data availability

Data will be made available on request.

Acknowledgments

This work was carried out at the Energy4Climate Interdisciplinary Center (E4C) of IP Paris and Ecole des Ponts, supported by 3rd Programme d'Investissements d'Avenir [ANR-18-EUR-0006-02]. It was funded by nam'R company through a collaboration grant. The authors thank L.G. Giraudet and V. Viguié for fruitful discussions and comments. We acknowledge the E-OBS dataset from the EU-FP6 project UERRA (<http://www.uerra.eu>) and the data providers in the ECA&D project (<https://www.ecad.eu>)

Appendix A. Reference REC and verification of climate data on REC

Fig. 9 shows the temperature-sensitive REC aggregating over the 12 administrative regions the values at the IRIS where such estimate by Enedis exists from Enedis processing (a), by applying the model (2) to temperatures from E-OBS dataset (b) and historical CORDEX simulations (c). Visually, the three show a very similar pattern. Fig. 9a and Fig. 9b illustrate the quality of the model prediction and quantitatively a R^2 score of 0.77 is found between the common cells. Fig. 9c shows how historical climate simulations can satisfactorily reproduce the temperature-sensitive REC for climate projection studies which rely on the climate projections produced in a consistent way with the historical climate simulations. However, in Section 3, the temperature-sensitive REC based on the CORDEX regional climate simulations is estimated over a larger number of IRIS than those of the Enedis subset. At the IRIS kept in the dataset, the estimates of α^{H} and α^C passed a significance test. The reference REC for the period 1975–2005 used to calculate the change of temperature-sensitive REC is shown in Fig. 10.

Appendix B. Cross-validation method for trained temperature sensitivities

During the present study, for each cell we have 8 years of annual REC as inputs to train the model described in Equation 2. The Leave-One-Out cross-validation method has been used to fit the model and to validate the model's performance. Each time we extract one year out as test and

train the model with the other 7 years' data and get the prediction using the one test data. And this procedure repeats 8 times. After that, the 8 predicted values with the test data are compared to their initial values, which gives us a test R^2 score. Such test is done for all the cells and a significance test is also performed to get the valid cells. A comparison of different linear regression models has been made with this test method and the distribution of related test R^2 scores are shown in Fig. 11.

Appendix C. AC adoption rate initial data

CODA STRATEGIES uses data from UNICLIMA (the professional union bringing together manufacturers and marketers of AC equipment in France) to estimate the national AC adoption rate from 2004 until 2020, including all types of AC equipment (mobile, heat pump). The national AC rates estimated by CODA STRATEGIES are published by ADEME (the French Agency for Ecological Transition) and are consistent with INSEE (for 2017) and EDF (for 2016 and 2019) data (ADEME, CODA STRATEGIES, 2021). At a finer scale, a study from Ecole des Ponts (Daguenet et al., 2021) calculated the regional AC adoption rate for 2019 based on data from Likibu (a house rental search engine) for over 800 households. The national population-weighted AC rate is found to be 22% for 2019, which is consistent with the EDF study and CODA STRATEGIES dataset.

These studies show that the cooling equipment market increase is not constant and has accelerated in recent years (ADEME, CODA STRATEGIES, 2021), resulting in a more geometric overall progression of about 20% per year at the country scale. From these studies, we have regional rates for 2019 only and national rates from 2016 to 2020 from which regional rates from 2011 to 2018 are deduced assuming a spatially homogeneous progression rate. Once estimated, the national rate "population-weighted national average" is deduced from the estimate of the regional rate for the different years and compared to the reference from ADEME (EDF and INSEE). This reconstruction is consistent for 2016–2020.

Appendix D. AC gradual spreading method and optimal number of neighbors

With the historical REC data, around 60% of the cells are estimated with zero current cooling temperature sensitivity (i.e. $\alpha_i^c = 0$). As described in Section 2.3.2, so-called Gradual Spreading is our way of estimating future α^c based on an interpolation assumption of actual values, especially for cells without current α^c . For cells with positive non-null cooling temperature sensitivity, the future cooling temperature sensitivity is assumed to be consistent with the current value (i.e. $(\alpha_i^c)^{GS} = \alpha_i^c > 0$), while for other cells without current α^c , a nearest-neighbor interpolation is performed with the following formula:

$$(\alpha_i^c)^{GS} = \frac{1}{J} \sum_{j=0}^{J-1} \alpha_j^c.$$

For a studied cell i , all the cells with current non-null sensitivity $\alpha_j^c > 0$ are ordered by the Euclidean distance with the given cell in the plate carrée projection, and J is the number of nearest cells taken into account for the calculation of the average.

This assumption has been tested with the group of cells where α^c are estimated non-null in the first place. During the test, 60% of these cells are selected randomly to become zero, conforming to the actual situation, and are given an estimation with the Gradual Spreading method. Then the estimated values with Gradual Spreading are compared with the model's initial estimation α^c . This process repeats 30 times for each J , and the average test R^2 score as a function of the number of neighbors J is given in Fig. 12. It can be seen clearly that there exists a local similarity: the test R^2 score is larger when $J \in [10, 60]$. In our study, the optimal value for J is 25. Despite selecting the optimal number of cells per cluster based on evidence of local similarity through a pre-test, the resulting prediction R^2 score remains low (below 0.23). This uncertainty in the future assumption of the coefficient α^c remains a limitation of the scenario study with the Gradual Spreading approach.

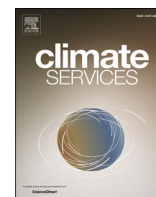
References

- ADEME, CODA STRATEGIES, 2021. La climatisation de confort dans les bâtiments résidentiels et tertiaires. Technical Report. ADEME. 110 pages, URL:https://librairie.ademe.fr.
- Auffhammer, M., Mansur, E.T., 2014. Measuring climatic impacts on energy consumption: A review of the empirical literature. *Energy Econ.* 46, 522–530.
- Bettignies, Y., Meirelles, J., Fernandez, G., Meinherz, F., Hoekman, P., Bouillard, P., Athanassiadis, A., 2019. The Scale-Dependent Behaviour of Cities: A Cross-Cities Multiscale Driver Analysis of Urban Energy Use. *Sustainability* 11, 3246. Number: 12 Publisher: Multidisciplinary Digital Publishing Institute.
- Bouramdane, A., Tantet, A., Drobinski, P., 2021. Utility-scale pv-battery versus csp-thermal storage in morocco: Storage and cost effect under penetration scenarios. *Energies* 14.
- Branger, F., Giraudet, L.G., Guivarch, C., Quirion, P., 2015. Global sensitivity analysis of an energy-economy model of the residential building sector. *Environ. Modelling Softw.* 70, 45–54.
- Chen, H.C., Han, Q., De Vries, B., 2020. Modeling the spatial relation between urban morphology, land surface temperature and urban energy demand. *Sustainable Cities Soc.* 60, 102246.
- Chen, H.C., Han, Q., de Vries, B., 2020. Urban morphology indicator analyzes for urban energy modeling. *Sustainable Cities Soc.* 52, 101863.
- Cornes, R.C., van der Schrier, G., van den Besselaar, E.J.M., Jones, P.D., 2018. An Ensemble Version of the E-OBS Temperature and Precipitation Data Sets. *J. Geophys. Res.: At.* 123, 9391–9409. eprint: https://onlinelibrary.wiley.com/doi/pdf/10.1029/2017JD028200.
- Daguenet, C., Gredigui, P., Teixeira Costa, F., Maugenest, M., Pedro Saint Martin, D., Sena Fracaroli, N., 2021. évolution des besoins en chaud et en froid dans le secteur résidentiel.
- Damm, A., Köberl, J., Pretenthaler, F., Rogler, N., Töglhofer, C., 2017. Impacts of +2 C global warming on electricity demand in Europe. *Climate Services* 7, 12–30.
- De Felice, M., Alessandri, A., Ruti, P.M., 2013. Electricity demand forecasting over Italy: Potential benefits using numerical weather prediction models. *Electric Power Systems Research* 104, 71–79.
- Drobinski, P., Silva, N.D., Panthou, G., Bastin, S., Muller, C., Ahrens, B., Borga, M., Conte, D., Fossier, G., Giorgi, F., Güttler, I., Kotroni, V., Li, L., Morin, E., Onol, B., Quintana-Segui, P., Romera, R., Torma, C.Z., 2018. Scaling precipitation extremes with temperature in the Mediterranean: past climate assessment and projection in anthropogenic scenarios. *Clim. Dyn.* 51, 1237–1257.
- ECA&D, 2020. E-OBS data access. URL:https://knmi-ecad-assets-prd.s3.amazonaws.com/ensembles/data/Grid_0.1deg_reg_ensemble/tg_ens_mean_0.1deg_reg_v20.0e.nc. Last visited 2021-06-13.
- Emenekwe, C.C., Emodi, N.V., 2022. Temperature and Residential Electricity Demand for Heating and Cooling in G7 Economies: A Method of Moments Panel Quantile Regression Approach. *Climate* 10, 142. Number: 10 Publisher: Multidisciplinary Digital Publishing Institute.
- Emodi, N.V., Chaiechi, T., Alam Beg, A.R., 2018. The impact of climate change on electricity demand in Australia. *Energy Environ.* 29, 1263–1297.
- Enedis, 2020. Consommation et thermosensibilité électriques par secteur d'activité à la maille IRIS. URL:https://data.enedis.fr/explore/dataset/consommation-electrique-par-secteur-dactivite-iris/. Last visited 2020-09-30.
- EUROSTAT, Heating and cooling degree days - statistics.
- Flaounas, E., Drobinski, P., Bastin, S., 2013. Dynamical downscaling of IPSL-CM5 CMIP5 historical simulations over the Mediterranean: benefits on the representation of regional surface winds and cyclogenesis. *Clim. Dyn.* 40, 2497–2513.
- Flaounas, E., Drobinski, P., Bastin, S., Lebeaupin Brossier, C., Borga, M., Vrac, M., Calvet, J.C., Stéfanon, M., 2013. Precipitation and temperature space-time variability and extremes in the mediterranean region: Evaluation of dynamical and statistical downscaling methods. *Clim. Dyn.* 40.
- Frederiks, E., Stenner, K., Hobman, E., 2015. The Socio-Demographic and Psychological Predictors of Residential Energy Consumption: A Comprehensive Review. *Energies* 8, 573–609.

- Frei, C., Christensen, J.H., Déqué, M., Jacob, D., Jones, R.G., Vidale, P.L., 2003. Daily precipitation statistics in regional climate models: Evaluation and intercomparison for the European Alps. *J. Geophys. Res.*: At. 108. [eprint: https://onlinelibrary.wiley.com/doi/pdf/10.1029/2002JD002287](https://onlinelibrary.wiley.com/doi/pdf/10.1029/2002JD002287).
- Gertler, P.J., Shelef, O., Wolfram, C.D., Fuchs, A., The demand for energy-using assets among the world's rising middle classes. *American Economic Review* 106, 1366–1401.
- Giraudet, L.G., Guivarch, C., Quirion, P., 2012. Exploring the potential for energy conservation in French households through hybrid modeling. *Energy Economics* 34, 426–445.
- Hallegatte, S., Hourcade, J., Ambrosi, P., 2007. Using climate analogues for assessing climate change economic impacts in urban areas. *Climatic Change* 82, 47–60.
- Haylock, M.R., Goodess, C.M., 2004. Interannual variability of European extreme winter rainfall and links with mean large-scale circulation. *Int. J. Climatol.* 24, 759–776.
- Haylock, M.R., Hofstra, N., Klein Tank, A.M.G., Klok, E.J., Jones, P.D., New, M., 2008. A European daily high-resolution gridded data set of surface temperature and precipitation for 1950–2006. *J. Geophys. Res.*: At. 113. [eprint: https://onlinelibrary.wiley.com/doi/pdf/10.1029/2008JD010201](https://onlinelibrary.wiley.com/doi/pdf/10.1029/2008JD010201).
- He, P., Liu, P., Qiu, Y.L., Liu, L., 2009. The weather affects air conditioner purchases to fill the energy efficiency gap. *Nature Communications* 13, 5772. Number: 1 Publisher: Nature Publishing Group.
- IGN, 2009. Contours...Iris - Descriptif de contenu et de livraison. Technical Report. Institut Géographique National. URL:https://geoservices.ign.fr/sites/default/files/2022-03/DC_DL_Contours_Iris_09.pdf.
- International Energy Agency, Cooling degree days in France, 2000–2020 - Charts - Data & Statistics.
- International Energy Agency, 2018. The Future of Cooling.
- Jacob, D., Petersen, J., Eggert, B., Alias, A., Christensen, O.B., Bouwer, L.M., Braun, A., Colette, A., Déqué, M., Georgievski, G., Georgopoulou, E., Gobiet, A., Menut, L., Nikulin, G., Haensler, A., Hempelmann, N., Jones, C., Keuler, K., Kovats, S., Kröner, N., Kotlarski, S., Kriegsmann, A., Martin, E., van Meijgaard, E., Moseley, C., Pfeifer, S., Preuschmann, S., Radermacher, C., Radtke, K., Rechid, D., Rounsevell, M., Samuelsson, P., Somot, S., Soussana, J.F., Teichmann, C., Valentini, R., Vautard, R., Weber, B., Yiou, P., 2014. EURO-CORDEX: new high-resolution climate change projections for European impact research. *Reg. Environ. Change* 14, 563–578.
- Kennedy, C.A., Stewart, I., Facchini, A., Cersosimo, I., Mele, R., Chen, B., Uda, M., Kansal, A., Chiu, A., Kim, K.g., Dubeux, C., Rovere, E.L.L., Cunha, B., Pincetl, S., Keirstead, J., Barles, S., Pusaka, S., Gunawan, J., Adegbile, M., Nazariha, M., Hoque, S., Marcotullio, P.J., Otharàn, F.G., Genena, T., Ibrahim, N., Farooqui, R., Cervantes, G., Sahin, A.D., 2015. Energy and material flows of megacities. *Proceedings of the National Academy of Sciences* 112, 5985.
- Kjellström, E., Boberg, F., Castro, M., Christensen, J., Nikulin, G., Sanchez, E., 2010. Daily and monthly temperature and precipitation statistics as performance indicators for regional climate models. *Climate Res.* 44, 135–150.
- Klok, E.J., Klein Tank, A.M.G., 2009. Updated and extended European dataset of daily climate observations. *Int. J. Climatol.* 29, 1182–1191.
- Köppen, W., 1936. *Das geographische system der klimate*, 46 pp.
- Kozarcanin, S., Andresen, G.B., Staffell, I., 2019. Estimating country-specific space heating threshold temperatures from national gas and electricity consumption data. *Energy and Buildings* 199, 368–380.
- Larsen, M., Petrovic, S., Radoszynski, A., McKenna, R., Balyk, O., 2020. Climate change impacts on trends and extremes in future heating and cooling demands over Europe. *Energy and Buildings* 226, 110397.
- Lemonsu, A., Vigiúé, V., Daniel, M., Masson, V., 2015. Vulnerability to heat waves: Impact of urban expansion scenarios on urban heat island and heat stress in Paris (France). *Urban Climate* 14, 586–605.
- Li, H., Kwan, M.P., 2018. Advancing analytical methods for urban metabolism studies. *Resour. Conserv. Recycl.* 132, 239–245.
- Lévy, J.P., Belaïd, F., 2018. The determinants of domestic energy consumption in France: Energy modes, habitat, households and life cycles. *Renew. Sustain. Energy Rev.* 81, 2104–2114.
- Meng, Q., Xiong, C., Mourshed, M., Wu, M., Ren, X., Wang, W., Li, Y., Song, H., 2020. Change-point multivariable quantile regression to explore effect of weather variables on building energy consumption and estimate base temperature range. *Sustainable Cities Soc.* 53, 101900.
- Moral-Carcedo, J., Vicéns-Otero, J., 2005. Modelling the non-linear response of Spanish electricity demand to temperature variations. *Energy Economics* 27, 477–494.
- Narayan, P.K., Smyth, R., Prasad, A., 2007. Electricity consumption in G7 countries: A panel cointegration analysis of residential demand elasticities. *Energy Policy* 35, 4485–4494.
- Pagliarini, G., Bonfiglio, C., Vocale, P., 2019. Outdoor temperature sensitivity of electricity consumption for space heating and cooling: An application to the city of Milan. *North of Italy. Energy and Buildings* 204, 109512.
- Petrick, S., Rehdanz, K., Tol, R., 2010. *The Impact of Temperature Changes on Residential Energy Consumption*. Kiel Institute for the World Economy, Kiel Working Papers.
- Pickett, S.T.A., Cadenasso, M.L., Rosi-Marshall, E.J., Belt, K.T., Groffman, P.M., Grove, J.M., Irwin, E.G., Kaushal, S.S., LaDeau, S.L., Nilon, C.H., Swan, C.M., Warren, P.S., 2017. Dynamic heterogeneity: a framework to promote ecological integration and hypothesis generation in urban systems. *Urban Ecosyst.* 20, 1–14.
- Pilli-Sihvola, K., Remes, P., Ollikainen, M., Tuomenvirta, H., 2010. Climate change and electricity consumption—witnessing increasing or decreasing use and costs? *Energy Policy* 38, 2409–2419.
- Rawat, M., Singh, R.N., 2022. A study on the comparative review of cool roof thermal performance in various regions. *Energy and Built Environment* 3, 327–347.
- Raymond, F., Ullmann, A., Camberlin, P., Drobinski, P., Smith, C.C., 2016. Extreme dry spell detection and climatology over the Mediterranean Basin during the wet season. *Geophys. Res. Lett.* 43, 7196–7204. [eprint: https://onlinelibrary.wiley.com/doi/pdf/10.1002/2016GL069758](https://onlinelibrary.wiley.com/doi/pdf/10.1002/2016GL069758).
- Raymond, F., Ullmann, A., Camberlin, P., Oueslati, B., Drobinski, P., 2018. Atmospheric conditions and weather regimes associated with extreme winter dry spells over the Mediterranean basin. *Clim. Dyn.* 50, 4437–4453.
- Ribes, A., Boé, J., Qasmi, S., Dubuisson, B., Douville, H., Terray, L., 2022. An updated assessment of past and future warming over France based on a regional observational constraint. *Earth Syst. Dyn.* 13, 1397–1415.
- Rosales Carreón, J., Worrell, E., 2018. Urban energy systems within the transition to sustainable development. A research agenda for urban metabolism. *Resour. Conserv. Recycl.* 132, 258–266.
- van Ruijven, B.J., De Cian, E., Sue Wing, I., 2019. Amplification of future energy demand growth due to climate change. *Nat Commun* 10, 2762. Number: 1 Publisher: Nature Publishing Group.
- Ruti, P.M., Somot, S., Giorgi, F., Dubois, C., Flaouas, E., Obermann, A., Dell'Aquila, A., Pisacane, G., Harzallah, A., Lombardi, E., Ahrens, B., Akhtar, N., Alias, A., Arsouze, T., Aznar, R., Bastin, S., Bartholy, J., Béranger, K., Beuvier, J., Bouffies-Cloché, S., Brauch, J., Cabos, W., Calmanti, S., Calvet, J.C., Carillo, A., Conte, D., Coppola, E., Djurdjevic, V., Drobinski, P., Elizalde-Arellano, A., Gaertner, M., Galán, P., Gallardo, C., Gualdi, S., Goncalves, M., Joba, O., Jordà, G., L'Heveder, B., Lebeaupin-Brossier, C., Li, L., Liguori, G., Lionello, P., Maciàs, D., Nabat, P., Önol, B., Raikovic, B., Ramage, K., Sevault, F., Sannino, G., Struglia, M.V., Sanna, A., Torma, C., Vervatis, V., 2016. Med-CORDEX Initiative for Mediterranean Climate Studies. *Bulletin of the American Meteorological Society* 97, 1187–1208. Publisher: American Meteorological Society Section: Bulletin of the American Meteorological Society.
- Räisänen, J., Hansson, U., Ullerstig, A., Döscher, R., Graham, L.P., Jones, C., Meier, H.E.M., Samuelsson, P., Willén, U., 2004. European climate in the late twenty-first century: regional simulations with two driving global models and two forcing scenarios. *Clim. Dyn.* 22, 13–31.
- Sailor, D.J., Muñoz, J.R., 1997. Sensitivity of electricity and natural gas consumption to climate in the U.S.A.—Methodology and results for eight states. *Energy* 22, 987–998.
- Santos, J.A., Corte-Real, J., Ulbrich, U., Palutikof, J., 2007. European winter precipitation extremes and large-scale circulation: a coupled model and its scenarios. *Theor. Appl. Climatol.* 87, 85–102.
- Scapin, S., Apadula, F., Brunetti, M., Maugeri, M., 2016. High-resolution temperature fields to evaluate the response of Italian electricity demand to meteorological variables: an example of climate service for the energy sector. *Theor. Appl. Climatol.* 125, 729–742.
- Spinoni, J., Vogt, J.V., Barbosa, P., Dosio, A., McCormick, N., Bigano, A., Füssel, H.M., 2018. Changes of heating and cooling degree-days in Europe from 1981 to 2100. *Int. J. Climatol.* 38, e191–e208. [eprint: https://onlinelibrary.wiley.com/doi/pdf/10.1002/joc.5362](https://onlinelibrary.wiley.com/doi/pdf/10.1002/joc.5362).
- Stefanon, M., D'Andrea, F., Drobinski, P., 2012. Heatwave classification over Europe and the Mediterranean region. *Environ. Res. Lett.* 7, 014023. Publisher: IOP Publishing.
- Stéfanon, M., Drobinski, P., D'Andrea, F., Lebeaupin-Brossier, C., Bastin, S., 2014. Soil moisture-temperature feedbacks at meso-scale during summer heat waves over Western Europe. *Clim Dyn* 42, 1309–1324.
- Tantet, A., Stéfanon, M., Drobinski, P., Badosa, J., Concettini, S., Cretí, A., D'Ambrosio, C., Thomopoulos, D., Tankov, P., 2019. e4clim 1.0: The Energy for a Climate Integrated Model: Description and Application to Italy. *Energies* 12, 4299.
- Vaithinada Ayar, P., Vrac, M., Bastin, S., Carreau, J., Déqué, M., Gallardo, C., 2016. Intercomparison of statistical and dynamical downscaling models under the EURO- and MED-CORDEX initiative framework: present climate evaluations. *Clim Dyn* 46, 1301–1329.
- Vigiúé, V., Lemonsu, A., Hallegatte, S., Beaulant, A.L., Marchadier, C., Masson, V., Pigeon, G., Salagnac, J.L., 2020. Early adaptation to heat waves and future reduction of air-conditioning energy use in Paris. *Environ. Res. Lett.* 15, 075006. Publisher: IOP Publishing.
- Voskamp, I.M., Sutton, N.B., Stremke, S., Rijnaarts, H.H.M., 2020. A systematic review of factors influencing spatiotemporal variability in urban water and energy consumption. *J. Cleaner Prod.* 256, 120310.
- Wenz, L., Levermann, A., Auffhammer, M., 2017. North-south polarization of European electricity consumption under future warming. *Proceedings of the National Academy of Sciences* 114, 201704339.
- Wiedenhofer, D., Lenzen, M., Steinberger, J.K., 2013. Energy requirements of consumption: Urban form, climatic and socio-economic factors, rebounds and their policy implications. *Energy Policy* 63, 696–707.
- You, Y., Kim, S., 2018. Revealing the mechanism of urban morphology affecting residential energy efficiency in Seoul, Korea. *Sustainable Cities Soc.* 43, 176–190.

Appendix A

Article published in *Climate
Services*



Sub-regional variability of residential electricity consumption under climate change and air-conditioning scenarios in France

Qiqi Tao^{a,*}, Marie Naveau^a, Alexis Tantet^a, Jordi Badosa^a, Philippe Drobinski^a

^a Laboratoire de Météorologie Dynamique – Institut Pierre-Simon Laplace, Ecole Polytechnique – Institut Polytechnique de Paris, Ecole Normale Supérieure – PSL Université, Sorbonne Université, CNRS, Palaiseau 91128, France

ARTICLE INFO

Keywords:

Residential electricity consumption
Cooling demand
Climate change impacts

ABSTRACT

The residential sector is important for the energy transition to combat global warming. Due to the geographical variability of socio-economic factors, the highly dependent residential electricity consumption (REC) should be studied locally. This study aims to project future French REC considering climate change and air-conditioning (AC) scenarios and to quantify its spatial variability. For this purpose, a linear temperature sensitivity model fitted by annual observed electricity consumption data and historical temperature is applied at an intra-regional scale. Future temperature-sensitive REC is computed by applying the model to temperature projections under the climate change pathway RCP8.5. Three AC scenarios are considered: (1) A 100% AC rate scenario assuming that any region partially equipped with AC systems nowadays will have all its households equipped with AC, but local temperature sensitivity will no longer progress; (2) A gradual spreading scenario mimicking “do like my neighbor” behavior; (3) A combination of the two scenarios. Increasing temperatures lead to an overall REC decrease (−8 TWh by 2040 and down to −20 TWh by 2100) with significant spatial variability, which had never been quantified and mapped due to a lack of suited methodology and limited available data at the finest scale. The evolution of REC is modulated by the evolution of cooling needs and the deployment of AC systems to meet those needs. In the first 2 AC scenarios, the decrease of REC due to climate change could be totally offset in the South of France, which would then display an increase in REC. When the 2 AC scenarios are combined, an increase in REC could be seen over the whole country. The most extreme AC scenario shows a potential REC rise due to AC usage by 2% by 2040 and even 32% by 2100, which could be canceled by increasing the cooling setpoint up to 26–27 °C.

Practical implications

The residential sector is the leading electricity consumer in France, representing more than one-third of the final electricity uses. This sector has therefore to implement a pathway to reduce energy demand and greenhouse gas emissions. The relevance of related policies depends on the expected change in residential electricity consumption (REC) for various climate change scenarios and user behavior. REC change in climate change scenarios has already been studied at the country scale, but important physical (e.g. local weather conditions) and socio-economic (revenue, air-conditioning use, etc.) determinants of REC display a large spatial variability which implies REC should be studied locally.

The REC model is computed using a linear temperature sensitivity

model fitted by annual observed electricity consumption data and daily temperatures applied at the smallest French geographic census unit named Ilots Regroupés pour l'Information Statistique (IRIS), which divides the territory into meshes of about 2000 inhabitants per unit cell. Once the current electricity sensitivity is fitted for each IRIS, the REC change is computed by applying the model to temperature projections under climate change scenario RCP8.5 at intermediate (2025–2055) and far (2070–2100) time horizons based on 5 climate simulations performed in the frame of the international CORDEX program. In addition, two cooling scenarios based on the air-conditioning adoption rate and the cooling temperature sensitivity are also investigated.

When only climate change is considered, REC is projected to decrease with decreasing heating needs in most IRIS cells. However, because of already deployed cooling equipment, REC is expected to

* Corresponding author.

E-mail address: qiqi.tao@hotmail.com (Q. Tao).

<https://doi.org/10.1016/j.cliser.2023.100426>

increase in 3–7% of the territory, totally offsetting the effect of reduced heating needs. A larger variability is found within administrative regions, including a few hundred to thousands of IRIS, than between administrative regions. Including AC scenarios offset in part the REC negative trend, with REC projected to increase in the South-East in the most conservative scenario to nearly the entire territory when large spreading and rate of AC use are assumed. Large AC use may lead to REC change ranging from 2% by 2040 to 32% by 2100, contributing to enhanced greenhouse gas emission and the urban heat island effect.

Such results call for targeted and local information actions where the risk of spreading is high to limit the spreading and rate of use or mitigate their effect with more energy-efficient AC systems. As our projected future climate in Southern France is similar to the present climate of countries more to the South, which has not seen a large deployment of AC equipment, analyzing the socio-economic drivers, the energy policies of these countries and drawing inspiration from them to deploy locally adapted actions should be considered. Also, adapting the cooling setpoint could help elaborate energy policies to lower the cooling temperature-sensitive REC. Based on our model, shifting the cooling setpoint from 21 °C at present to 23–24 °C by 2040 and 26–27 °C by 2085 would prevent any cooling REC rise in our worst-case scenarios. These values are consistent with existing recommendations (e.g. US DoE). Finally, low-tech alternative solutions, such as cool white roof coating widely implemented in subtropical regions, can be implemented in France to improve the thermal comfort of buildings and reduce the use of AC equipment and their impact on the environment.

1. Introduction

France is committed, with the energy transition law for green growth of 2015, to reducing its greenhouse gas emissions by 40% by 2030 and divided by four by 2050. It also plans to reduce its consumption of fossil fuels by 30% by 2030 and to halve its final energy consumption in 2050 compared to 2012 (regulations passed under the *Law for the ecological transition and green growth*¹). This regulation contributes to the *Paris climate agreement*² to keep temperature increases well below 2 °C and to pursue efforts for 1.5 °C. The French residential sector represents 20% of the CO₂ emission of the country and 30% of the final energy uses. Hence, this sector could be a significant opportunity and challenge for policies to combat global warming. Indeed, the law text emphasizes improving building energy efficiency, thermal renovation of buildings, and constructing buildings with high energy performance.

Limiting electricity consumption in the residential sector through actions aimed at improving the energy performance of buildings is therefore a major environmental challenge for communities. However, residential electricity consumption (REC) is highly dependent on household income, the thermal quality of occupied dwellings, and the cost of energy with regard to the purchasing power of the households (Giraudet et al., 2012; Branger et al., 2015; Frederiks et al., 2015) and therefore displays a very large spatial variability, especially in urban areas which are characterized by the heterogeneity of their demographic, socio-economic, environmental and cultural characteristics (Li and Kwan, 2018; Pickett et al., 2017) underlying urban resource demands (Rosales and Worrell, 2018; Voskamp et al., 2020). The case of France has been investigated specifically and supports studies conducted in other countries (Lévy and Belaid, 2018).

Electricity demand also depends on the outdoor temperature. Demand for cooling rises once the temperature exceeds a cooling setpoint, while electricity demand for heating grows once the temperature drops below a heating setpoint (Petrick et al., 2010; Auffhammer and Mansur, 2014; Damm et al., 2017; Wenz et al., 2017; Kozarcenin et al., 2019). As a result, a theoretical U-shaped link exists between electricity demand

and temperature. Choices made by individuals to utilize heating and cooling systems to maintain a comfortable temperature in their residences directly impact electricity demand (Emodi et al., 2018; Emekekwe and Emodi, 2022). Substantiated correlations between consumption and climate and weather conditions (Meng et al., 2020), demographic and economic factors (Bettignies et al., 2019) and urban and architectural morphological characteristics (Chen et al., 2020; You and Kim, 2018) cause the large spatial variability in residential energy demand. Climate, socio-economic and morphological characteristics have proven explanatory variables for energy demand and its spatial pattern (Chen et al., 2020; Kennedy et al., 2015; Wiedenhofer et al., 2013).

The link between temperature and electricity demand has been studied using various models [e.g. (Narayan et al., 2007; Emodi et al., 2018)]. One approach is to model this nonlinear relationship by a smooth but nonlinear function of the temperature. For instance, Moral-Carcedo and Vicéns-Otero (2005) and Damm et al. (2017) used a Logistic Smooth Transition (LSTR) function to model the electricity demand response to temperature variations in European countries. The advantage of such a model is that it adequately captures the rather smooth response of electricity demand summed over a large domain to temperature variations. On the other hand, it is less straightforward to interpret the physical meaning of the parameters of such a model. Another approach is to model the electricity demand as a linear combination of nonlinear functions of the temperature (making it a generalized linear model). For instance, Sailor and Muñoz (1997) studied the monthly electricity and gas consumption for states in the US using a linear model with degree-day (DD) inputs in addition to wind speed and relative humidity.

In France, outdoor temperature increase could reach up to 3.8 °C by 2100 with regards to 1900–1930 if no policy is in place to reduce greenhouse gas emissions (Ribes et al., 2022). Pili-Sihvola et al. (2010) have investigated the impact of climate change using the DD approach on building energy demand for heating and cooling and the associated energy cost using climate simulations of the 3rd Coupled Model Inter-comparison Project (CMIP3). More recently, Larsen et al. (2020) find in downscaled CMIP5-climate simulations that when temperature evolution is considered as the only factor of change, needs for cooling increase by 33% to 204% between 2050 and 2010 and needs for heating decrease by –31% to –6% while Damm et al. (2017) predict the impact of a +2 °C global temperature change on European electricity demand, with for France, an estimated decrease in total electricity consumption between -10TWh and -16TWh. The optimistic reduction in electricity projection is due to France's current heating-dominated state. All households in the country utilize specific heating systems such as gas, oil, wood, or district heating, among which 37% employ electric heating. In contrast, the national adoption of air-conditioning (AC) remains relatively low, standing at only approximately 22% when considering all types and sizes of air conditioners, including mobile and heat pump units.

Rising temperatures and temperature extremes, in particular, imply increased use of air conditioners, both in hot and humid emerging economies where incomes are rising and in industrialized economies where consumer expectations in terms of thermal comfort are constantly growing (van Ruijven et al., 2019). Previous studies (van Ruijven et al., 2019; ?; ?) suggest that climatic conditions will encourage more households to adopt AC systems, therefore affecting electricity expenditures. On a global scale, the final energy consumption for AC in residential and commercial buildings has more than tripled between 1990 and 2016. The share of cooling in REC increased from around 2.5% to 6% during the same period. The use of AC equipment is expected to increase dramatically, becoming one of the main drivers of global electricity demand (International Energy Agency, 2018).

In France, as heat waves are more and more frequent and long, many households and businesses are equipped with AC for more comfort (Lemonsu et al., 2015). In 2020, for the first time, the number of equipment sold exceeded 800,000 units, whereas it had stabilized at

¹ <https://www.legifrance.gouv.fr/loda/id/JORFTEXT000031044385>

² https://unfccc.int/sites/default/files/english_paris_agreement.pdf

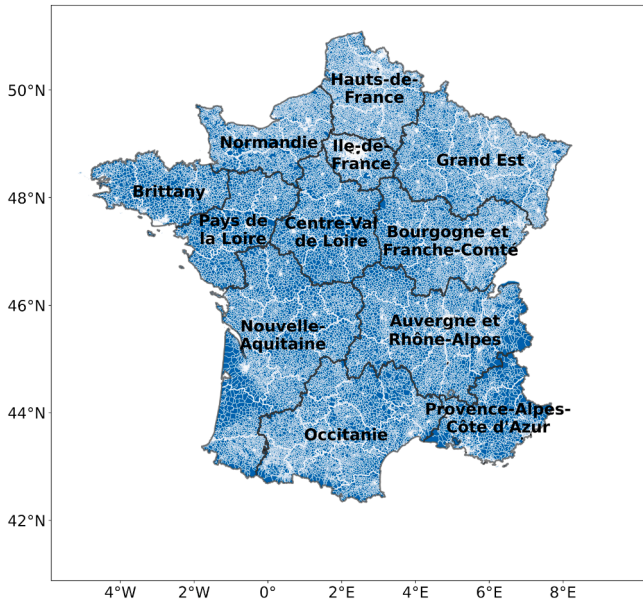


Fig. 1. Map of 12 administrative regions of metropolitan France, with thicker white lines representing 94 departments and thinner white lines representing more than 48000 IRIS cells. (Plate carrée projection, same projection used in the presented study).

around 350,000 per year previously. In 2020, 25% of individuals are equipped compared to 14% in 2016, with disparities linked to the type of dwelling (31% of owners of individual houses compared to 20% of households living in collective housing), socio-professional category (37% of liberal professions, executives and higher intellectual professions against only 19% of households whose reference person is unemployed or inactive) and place of residence (e.g. 47% of inhabitants of the South-East and Corsica against only 11% in Brittany) (ADEME, CODA STRATEGIES, 2021).

However, most previous studies of future consumption projection only focus on continental and national scales while not considering the sub-national disparity of temperature changes and non-climatic factors listed above. We aim to fill this gap by examining whether the national results proposed by these earlier studies remain consistent at smaller scales, given that changes in consumption and geographical variations in adaptation can lead to inequalities. We provide valuable information on the local impacts of climate change and building cooling strategies on residential energy demand, which can aid local climate and energy planning and decision-making. Specifically, we focus on the sub-regional variability of changes in residential AC requirements for cooling needs in the context of climate change. To this end, we use a

modified temperature sensitivity model to project future REC at a fine scale. The smallest geographic scale used in this study is the so-called Ilots Regroupés pour l'Information Statistique (IRIS), here referred to as cells, which divides the French territory into a collection of about 2000 inhabitants per cell. These cells are defined by respecting geographic and demographic criteria and have recognizable contours without ambiguity and stability over time. France has a total of 50,800 cells (IGN, 2009). In metropolitan France, these cells are distributed among 12 administrative regions represented in Fig. 1. This model is designed to distinguish between different aspects of electricity use using data from all residential buildings, irrespective of their heating or cooling equipment. The projection of future residential electricity consumption is based on climate change pathway RCP8.5, using down-scaled CMIP5 climate simulations carried out as part of EURO-CORDEX (Jacob et al., 2014) and MEC-CORDEX (Ruti et al., 2016), while considering different scenarios of AC use for cooling - full generalization or saturation.

After the introduction in Section 1, the details of the model can be found in Section 2, with information about the temperature and REC data that are applied to fit the model as inputs for the case of France and the future temperature projection and AC use scenarios. REC projection results and discussion are presented in Section 3, and the conclusion and policy implications are given in Section 4. The global flow chart of the total work is shown in Fig. 2.

2. Methodology and data

In this section, we explain how the REC is projected at the sub-communal scale by applying a temperature sensitivity model trained on historical data to climate projections. We also present the data for the application to France and define the scenarios used as projections of AC use with widespread adoption or saturation cases.

2.1. Temperature sensitivity statistical model

The relationship between the surface air temperature and the energy consumption over a domain is what we call the temperature sensitivity of the consumption. It has been modeled in various ways as presented in the previous section. The advantages of the DD approach are that it is simple to implement as a linear regression model with standard machine learning software and that it is straightforward to interpret the coefficients of the models as temperature sensitivities. For these reasons, we follow the DD approach in this study. The heating degree-days (HDD) (resp. the cooling degree-days (CDD)) for a domain is a positive quantity computed from data for the (weighted-) average temperature of the domain. It is given by the sum over a period of the degrees below (resp. above) a certain setpoint temperature per timestep. Here, the timestep d is a day and the period y a year between 2011 and 2018 (included),

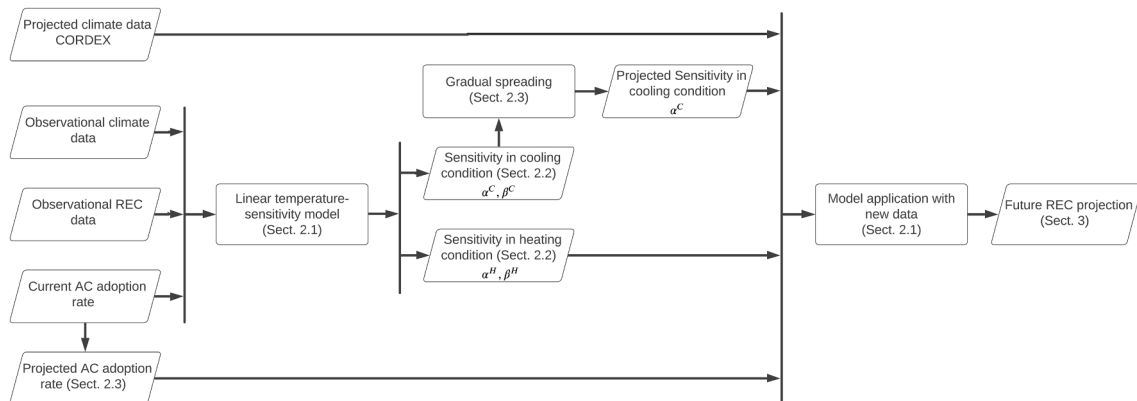


Fig. 2. Flow chart of the present study.

Table 1
Summary of variables and their physical meanings presented in Eq. 2.

Variable	Meaning
$E_i(y)$	Annual REC normalized by surface for cell i and year y (kWh/ m ²)
B_i	The basic daily REC for cell i (kWh/ m ²)
N_y	The number of days in a year y (365 or 366)
α_i^H	Heating temperature sensitivity for cell i (kWh/ (DD m ²))
α_i^C	Cooling temperature sensitivity for cell i and year y (kWh/ (DD m ²))
$\eta_i^{El}(y)$	Rate of electric heating for cell i and year y (%)
$\eta_i^{AC}(y)$	Rate of AC adoption for cell i and year y (%)
$\beta_i^H(y)$	Coefficient measuring increase in yearly REC per HDD and unit of area for cell i and year y (kWh/ (DD m ²))
$\beta_i^C(y)$	Coefficient measuring increase in yearly REC per CDD and unit of area for cell i and year y (kWh/ (DD m ²))

while different domains, or cells, i are considered, each corresponding to a different IRIS. The HDD and CDD are thus defined here as (Moral-Carcedo and Vicéns-Otero, 2005),

$$\begin{aligned} \text{HDD}_i(y) &:= \sum_{d=1}^{N_y} \max(0; T_i^H - T_i(y, d)) \\ \text{CDD}_i(y) &:= \sum_{d=1}^{N_y} \max(0; T_i(y, d) - T_i^C), \end{aligned} \quad (1)$$

where $T_i(y, d)$ is the daily-mean surface air temperature for a day d of year y averaged over cell i , T_i^H and T_i^C with $T_i^C \geq T_i^H$ are respectively the heating and cooling setpoints for cell i , and N_y (365 or 366) is the number of days in year y . The heating and cooling setpoints T_i^H and T_i^C are parameters to be estimated.

The REC scales with the living area in each cell. To leave out this factor, we divide the REC by the living area, giving the normalized annual REC $E_i(y)$ for cell i and year y in kWh/ m². For a given scenario (see Section 2.3), the general temperature sensitivity model is then expressed as,

$$\begin{aligned} E_i(y) &= \beta_i^H(y) \text{HDD}_i(y) + B_i N_y + \beta_i^C(y) \text{CDD}_i(y) \\ &= \alpha_i^H \eta_i^{El}(y) \text{HDD}_i(y) + B_i N_y + \alpha_i^C \eta_i^{AC}(y) \text{CDD}_i(y). \end{aligned} \quad (2)$$

The first equation in (2) relates $E_i(y)$ to a heating, a basic, and a cooling REC (from left to right). The basic daily REC B_i (kWh/ m²) is part of the REC that does not depend on temperature. It determines the REC fully when $T_i^H \leq T_i(y, d) \leq T_i^C$. In this study, we focus on the effect of climate change and the rate of air-conditioning (AC) adoption on the REC. Factors affecting the basic REC are thus assumed to remain fixed so that B_i does not depend on time. The temperature-sensitive RECs for a given year are proportional to DD. The coefficients of proportionality $\beta_i^H(y)$ and $\beta_i^C(y)$ (kWh/ (DD m²)) measure the increase in yearly REC per DD and unit of area in cell i . Each cell includes residential buildings with and without electric appliances. Thus, other things remain the same, lowering the fraction η_i^{El} of residential buildings in cell i with electric heating lowers β_i^H . To estimate the temperature-sensitive electric consumption restricted to residential buildings with electric heating, β_i^H is developed as the product of η_i^{El} with the heating temperature sensitivity α_i^H (kWh/ (DD m²)) of cell i . Factors affecting the heating temperature sensitivity (consumer behavior, thermal efficiency of residential buildings, etc.) are also assumed to remain fixed so that α_i^H is independent of time.

However, the rate of electric heating η_i^{El} may vary in time. Yet, the data used in this study only provides estimates of η_i^{El} for the year 2018 (Section 2.2.1). We therefore assume that this rate is fixed to that of 2018, $\eta_i^{El}(y) = \eta_i^{El}(2018) := \eta_i^{El}$, and so $\beta_i^H(y) = \beta_i^H(2018)$, for all years and all cells. This implies that an Ordinary Least-Squares (OLS) regression with β_i^H as coefficient and $\text{HDD}_i(y)$ as input is equivalent to an OLS

regression with α_i^H as coefficient and $\eta_i^{El} \text{HDD}_i(y)$ as input. Similarly, β_i^C is developed as the product of the fraction η_i^{AC} of residential buildings in cell i equipped with AC with the cooling temperature sensitivity α_i^C (kWh/ (DD m²)) of cell i . Note, however, that while all residential buildings include some form of heating so that η_i^{El} reflects the choice of heating system, all AC systems are electric, and η_i^{AC} gives the adoption rate of AC equipment. Regarding η_i^{AC} , as presented in the previous section, the AC adoption rate has increased during the past several years and hence depends on the year during the training (Section 2.2.4). For future projection, both α_i^C and η_i^{AC} vary with the choice of AC use scenario, but they are assumed constant during a given period (Section 2.3.2).

In summary, all the parameters with their physical meanings are given in Table 1. For all pairs (i, y) of cells i and years y , the model inputs are.

- $\eta_i^{El}(y) \text{HDD}_i(y)$ and
- $\eta_i^{AC}(y) \text{CDD}_i(y)$,

where $\text{HDD}_i(y)$ and $\text{CDD}_i(y)$ depend on the daily-mean temperatures $T_i(y, d)$ for all days d in y . The model coefficients are the temperature sensitivities α_i^H and α_i^C and the hyperparameters are T_i^H and T_i^C . The total number of cells is assumed to remain fixed. In the following sections, we present how this model is trained and applied to climate and AC projections to project the REC.

2.2. Training the temperature sensitivity model for the French REC

To apply the temperature sensitivity model to the case of France at the finest spatial scales, one needs (i) pairs of input and target historical data to train and validate the model and (ii) input data from 21st century temperature projections on which to apply the trained model to project the REC. We present the training and validation data set in this subsection while the presentation of the 21st century temperature projections is left for Section 2.3.

We thus need data for the inputs of the model: the yearly DD, electric-heating rates, and AC adoption rates. The former is computed from daily surface air temperatures and heating and cooling setpoints. The target $E_i(y)$ is computed from the cell's REC and living surface. Several of these variables used to compute both the inputs and the targets are taken from a dataset provided by the French distribution system operator, Enedis. We first present this dataset and then describe how it is crossed with additional data sources to produce the input and the target training data. The longest training period that the following datasets permit ranges from 2011 to 2018 (included), which is the training period we use.

2.2.1. Energy and building characteristics per cell

The Enedis dataset is accessed via their website (Enedis, 2020) and includes the following variables that are relevant to this study:

- longitude and latitude coordinates of the cell centroids used to assign meteorological stations to cells in Section 2.2.2;
- yearly REC data per cell from 2011 to 2018 (included) used as the target in Section 2.2.5;
- electric-heating rates η_i^{El} for 2018;
- fraction of cell buildings with surfaces in different intervals used to compute the target in Section 2.2.5;
- Enedis estimates of β^H using a linear model based on DD akin to the model (2) (see below);
- yearly HDDs used in this Enedis model since 2018, but only at the department level, thus not satisfying our needs;
- heating setpoints used to estimate the HDDs used here as described Section 2.2.3;

Table 2
Heating setpoints T_r^H for all regions of metropolitan France computed according to Section 2.2.3.

Region name	T_r^H [°C]
Auvergne-Rhône-Alpes	16.0
Bourgogne-Franche-Comté	16.3
Brittany	14.8
Centre-Val-Loire	15.0
Grand-Est	16.6
Hauts-de-France	16.0
Ile-de-France	15.8
Normandie	15.0
Nouvelle-Aquitaine	15.3
Occitanie	16.4
Provance-Alpes-Côte d'Azur (PACA)	17.4
Pays-de-la-Loire	15.0

Table 3
AC adoption rates (%) for 2011 and 2018.

Region name	η_{2011}^{AC}	η_{2018}^{AC}
Auvergne-Rhône-Alpes	4.3	17.4
Bourgogne-Franche-Comté	3.4	13.9
Brittany	2.5	10.5
Centre-Val-Loire	4.0	16.5
Grand-Est	3.4	13.9
Hauts-de-France	2.5	10.5
Ile-de-France	4.5	18.3
Normandie	2.7	11.3
Nouvelle-Aquitaine	4.3	17.4
Occitanie	5.6	22.6
PACA	10.5	41.7
Pays-de-la-Loire	2.9	12.2

The Enedis estimates of β^H rely on consumption data at higher temporal resolutions (semi-annual, monthly, or daily) than the publicly available data. They thus can fit their temperature sensitivity model at the highest temporal resolution and average over each cell the estimated β^H for the different delivery points in the cell. However, the β^H of a cell is provided only if the estimate is considered sufficiently precise, i.e. if a minimum of 500 delivery points is available in the cell. As a result, around 50% of the cells are missing, whereas the model (2) can be applied to the annual consumption data to provide estimates of the temperature sensitivities for all cells in France.

2.2.2. Surface temperatures for training

To train the model (2), we use E-OBS version 20.0 (ECA&D, 2020) of the European Climate Assessment & Data (Klok and Klein Tank, 2009; Cornes et al., 2018) (ECA&D for continental gridded surface air temperature (Haylock et al., 2008)). This gridded dataset is available at daily timesteps and a spatial resolution of 0.1 ° over Europe and the Mediterranean and spans from 1950 to the present. Among the available daily statistics, only the daily mean is retained here. Data observations are aggregated from several weather stations and gridded using an interpolation procedure combining spline interpolation and kriging. This dataset is a reference dataset for regional climate studies [e.g. (Haylock and Goodess, 2004; Santos et al., 2007; Stefanon et al., 2012; Raymond et al., 2016; Raymond et al., 2018)] and the evaluation of regional climate models [e.g. (Frei et al., 2003; Räisänen et al., 2004; Kjellström et al., 2010; Flaounas et al., 2013; Stéfanon et al., 2014; Ayar et al., 2016; Drobinski et al., 2018; Raymond et al., 2018)]. E-OBS includes some errors and uncertainties (changes in station locations or can induce those interpolation uncertainties, for example). Flaounas et al. (2013) assessed the E-OBS gridded dataset with temperatures displaying relatively small biases.

The temperature sensitivity model (2) requires temperatures for each cell to compute the HDD and CDD, but the cells (i.e. the IRIS in the case of France) do not correspond to the E-OBS grid points. We thus need to

adjust E-OBS gridded temperatures to the cells over the French domain. This is done here using a nearest-neighbor interpolation using the Euclidean distance between temperature grid points and the cell centroids from Enedis (Section 2.2.1) in a plate carrée projected coordinate system. In order to match the target REC data from Enedis (Section 2.2.1), only the E-OBS data is kept from 2011 to 2018 (included) is kept as training input.

2.2.3. Heating and cooling setpoints estimates

A couple of temperature setpoints T_i^H and T_i^C are required for each cell i in order to compute the HDDs and the CDDs in the temperature sensitivity model (2). The estimation of the temperature setpoints is based on those available in the Enedis dataset (Section 2.2.1) and which Enedis uses to compute the HDDs in their own temperature sensitivity model. In our case, the model is simplified by identifying T_i^H for each cell i in the given administrative region r of France with the average T_r^H of all the values of T^H provided by Enedis for locations in r . The heating setpoint is thus constant over each region, i.e. $T_i^H = T_r^H$ for all cells i in r , where r runs over all the administrative regions of France. The resulting T_r^H estimates are shown in Table 2.

On the other hand, no cooling setpoints are provided by Enedis. Instead, we fix T_i^C for all the cells in France to the value of 21 °C used by EUROSTAT (YYYY) and International Energy Agency (2020).

Another approach to choose T_i^H and T_i^C could be to assume that these temperature setpoints are constant inside each region and to fit them as hyperparameters via a grid search. Doing so, it is found that the prediction error estimated via cross-validation is only marginally improved and that the main conclusions of this study remain unchanged (not shown here). Considering the higher complexity of this approach, the methodology presented in the previous paragraphs of this subsection is preferred here.

2.2.4. AC adoption rates for training

In addition to surface temperatures, the model (2) requires as input AC adoption rates η_i^{AC} for each cell in France. However, this information is not available at such a small geographical scale. Based on the evolution of the national AC adoption rate (ADEME, CODA STRATEGIES, 2021) and the regional distribution data in 2019 (Daguenet et al., 2021), we estimated the regional AC adoption rates at the regional level between 2011 and 2020 and assumed that all cells inside one administration region share the same adoption rate, i.e. $\eta_i^{AC}(y) = \eta_r^{AC}(y)$. This progression in AC adoption rate during the training period is assumed to be geometric. We calculated the average ratio between different years, which indicates a growth of 20% between two consecutive years. This AC adoption rate progression ratio is assumed constant during training, i.e. $\frac{\eta_i^{AC}(y+1)}{\eta_i^{AC}(y)} = \text{constant} = 120\%$. The population-weighted national average is then compared to the reference used in ADEME, CODA STRATEGIES (2021) and is consistent for 2016–2020. The estimated rate for the years 2011 and 2018 are shown in Table 3 with in between a geometric evolution. More details about the initial data used for the estimation can be found in Section C. Errors due to this factor are not studied but should be kept in mind as a limit due to the accessibility of data.

2.2.5. Living area to standardize REC

The model (2) is trained using as targets the yearly REC data from the Enedis dataset (Section 2.2.1). See in Section A for the details of the REC dataset. However, we are interested in the consumption per unit of area. Moreover, the number of buildings per cell — also provided by Enedis — varies from one year to the next. We thus need to normalize the REC of each cell by the corresponding total living surface. Unfortunately, Enedis does not provide the total living surface but the fraction τ_i^k of buildings in cell i for which the living surface belongs to an interval I_k in $\{(0, 30), (30, 40), (40, 60), (60, 80), (80, 100), (100, +\infty)\}$ (m²). Owing

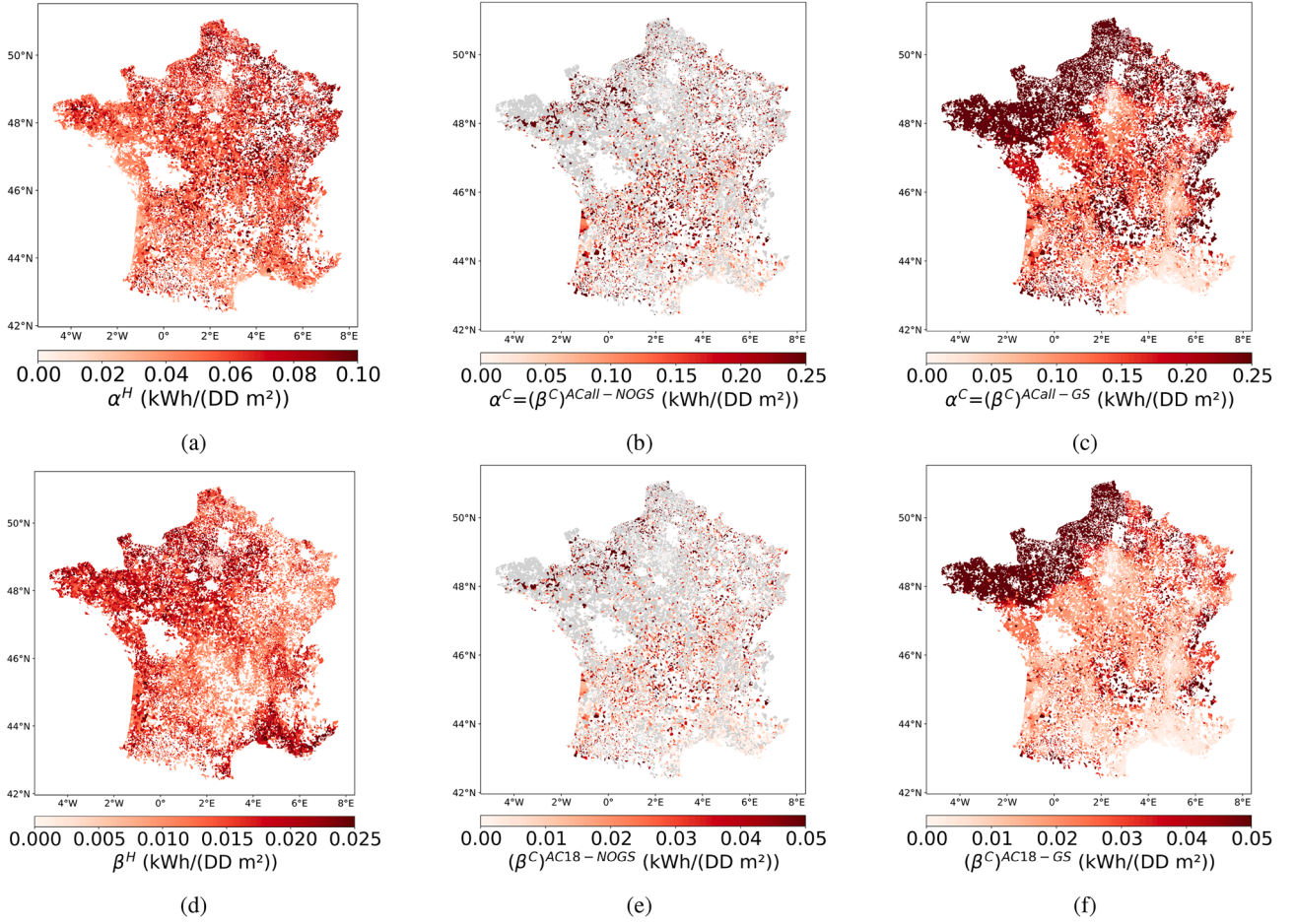


Fig. 3. Top: Estimates of α^H (left) and α^C (middle) obtained by training the model (2) on the observational data (Section 2.2). Projections of α^C (right) by gradual spreading (Section 2.3.2). Bottom: Corresponding values of β^H (left) and β^C (middle), and projections of β^C (right) for the AC2018 scenario (Section 2.3.2).

to the data constraints, we cannot get more specific information at the building level and can only present the distribution of intervals at the IRIS level. Thus, for each interval, we approximate the living surface of buildings with a surface in I_k by the center C_k (m^2) of the interval, except for the first and last intervals. We take the end value of $30 m^2$ for the first interval rather than the median value due to the legal limitations on small living surfaces. For the last interval, we take the finite end of the interval $100 m^2$, primarily because we lack further information on the distribution within the interval and also to counterbalance any potential overestimation for the first interval. It's important to note that these assumptions were made out of necessity due to the data limitations, and the accuracy of these estimates could potentially be improved with data availability at the building level. Then, the average living surface is estimated from the t_i^k provided by Enedis with the following formula:

$$\bar{S}_i = \sum_k t_i^k C_k \left(m^2 \right). \quad (3)$$

2.2.6. Trained temperature sensitivities

As an intermediate methodological result, the maps of the estimated α^H and α^C and corresponding β^H and β^C for cells with statistically significant coefficients at the 5% significance level (60% of all cells) are shown in the left and middle panels of Fig. 3. The OLS regression was used with a constraint on coefficients to be positive. Regression methods with regularization (Lasso and Ridge) were also tested, but this led to an increase in the test R^2 score of less than 10% (not shown here), so the OLS was preferred to limit the number of parameters of the model. All the test scores are estimated using k-fold cross-validation with one fold

per year of data (8 folds in total). The test R^2 score averaged over all cells is about 0.68 with a 25% quartile of 0.56 and a 75% quartile of 0.79. More details about the test R^2 score are given in Section B as well as the validation of the model with comparison to Enedis datasets in Section A.

2.3. Projection data and scenarios definitions

As mentioned in Section 2.1, the basic consumption, represented by B in (2), is assumed to be stationary all the time. As far as the heating REC is concerned, we assume that α^H , T^H and η^{El} are also stationary so that only the HDDs change in response to temperature changes. Regarding the cooling REC, we follow a similar approach as for the heating REC, but η^{AC} and α^C also change in some AC scenarios (T^C is always stationary). We thus need to associate each cell with a temperature projection for a given climate change pathway, as well as with projections of η^{AC} and of α^C .

2.3.1. Temperature projection data under a climate change pathway

In this study, the most severe climate change pathway, the Representative Concentration Pathways (RCP) 8.5, is selected. The corresponding bias-corrected daily-mean temperature change is obtained from multiple regional climate models from the CORDEX program. In this study, these projections are completed with the corresponding historical experiments that serve as a reference to measure the effect of climate change. Due to modeling uncertainty, the projected statistics of the atmosphere may vary significantly with the choice of Regional Climate Model (RCM) and of driving Global Climate Model (GCM). Hence, multi-model ensembles are commonly used in climate studies to

Table 4
Institute, GCM name and RCP name for the 5 climate change simulations used in this study.

No.	Institute	Driving GCM model	RCM model
1	CNRM	CERFACS-CM5	ARPEGE51
2	CNRM	CERFACS-CM5	RCA4
3	IPSL	CM5A-MR	RCA4
4	IPSL	CM5A-MR	WRF331F
5	ICHEC	EC-EARTH	RACM022E

provide a partial estimation of the modeling error. This is why the five model combinations listed in Table 4 are used in this study. These simulations are accessed via the Copernicus Climate Change Service database (<https://climate.copernicus.eu/>).

To associate a cell to a climate-model simulation, the same methodology as for the temperature observations used for training is followed (Section 2.2.2). Three climate-simulation periods of 30 years are considered, which are distinct from the training period defined in Section 2.2: a historical period from 1975 to 2005 (excluded) — used as reference — and two projection periods, one from 2025 to 2055 and one from 2070 to 2100. Results associated with the latter are respectively referred to as CC2040 and CC2085 (based on the central year of the period).

As intermediate methodological results, mean historical HDD and CDDs, as well as the corresponding projected changes, are represented in Fig. 4. One can see that the temperature increase projected over France

leads to a general decrease in the HDDs (top panels) and to a general increase in the CDDs. These changes are however not homogeneous since the decrease in the HDDs is strongest in the southern and eastern parts of France, while the increase in the CDDs is largest in the southern part of France.

2.3.2. AC use scenarios

In the present framework, two factors are sensitive to the evolution of AC use during the 21st century: the AC adoption rate η_i^{AC} , and the switch of a cell from an α_i^C of zero to a positive α_i^C , for each cell i . While the former reflects the evolution of AC use within a cell, the latter corresponds to a conversion of a cell from having no AC user at all to having some AC users. Here, we do not attempt to make plausible projections of these factors based on current signals. Instead, as summarized in Table 5

Table 5
Definition of the four AC scenarios in terms of AC adoption rate and α^C spreading strategy. XXXX is either 2040 or 2085, corresponding to the central year of the climate change projection window considered.

Name	Definition	
	η^{AC}	Gradual Spreading of α^C
CCXXXX-AC18-NOGS	Same as in 2018	No
CCXXXX-AC18-GS	Same as in 2018	Yes
CCXXXX-ACall-NOGS	100%	No
CCXXXX-ACall-GS	100%	Yes

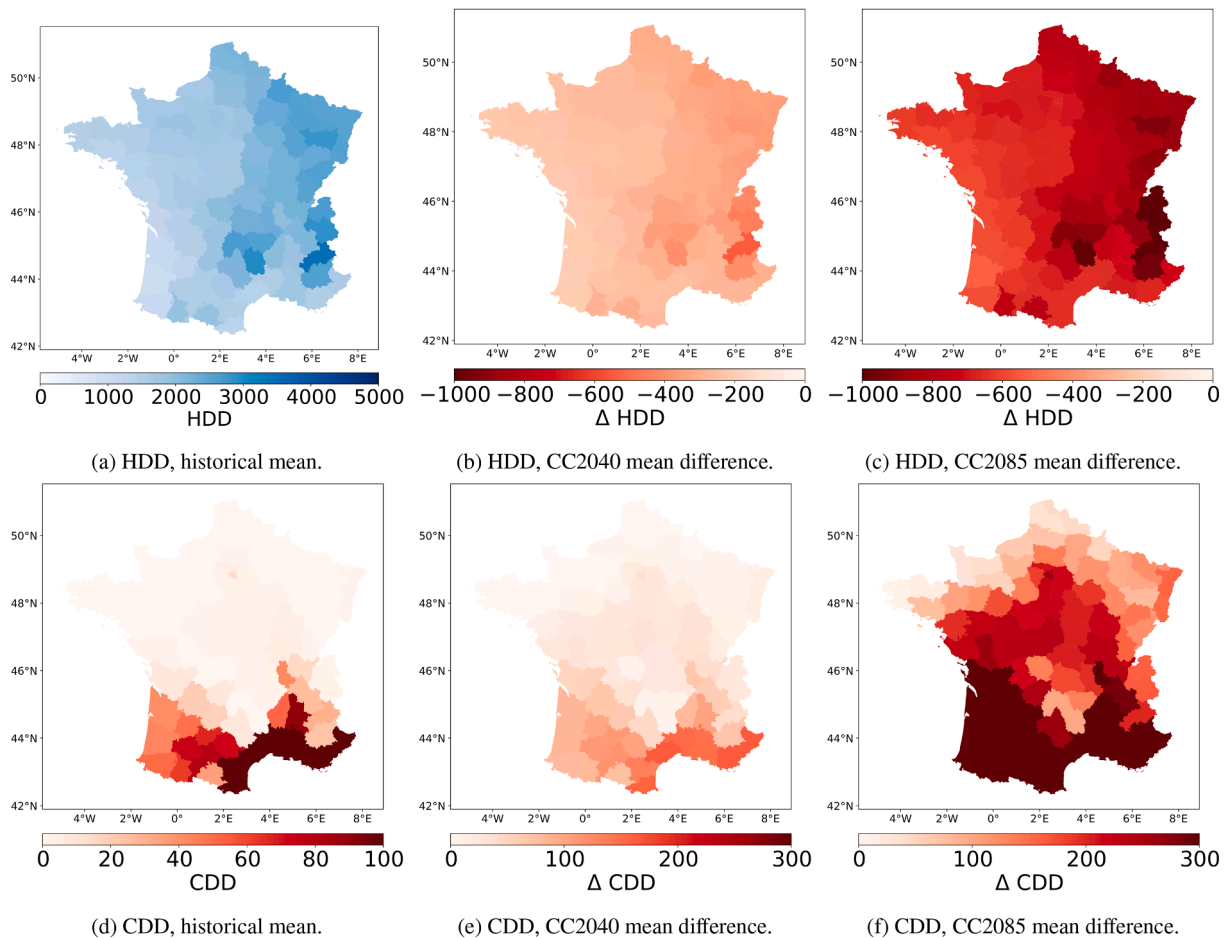


Fig. 4. Mean over 1975–2005, mean change over 2025–2055 wrt. 1975–2005 (CC2040), and mean change over 2070–2100 wrt. 1975–2005 (CC2085) for the HDDs (top) and CDDs (bottom) computed according to Eq. 1. The temperature data for 1975–2005 is from the historical CORDEX simulations, while that for 2025–2055 and 2070–2100 is from the RCP8.5 CORDEX simulations. The results are spatially averaged over the departments and averaged over the climate-model simulations listed in Table 4. Warm colors represent situations associated with warm temperatures (i.e. to a decrease in heating REC and to an increase in cooling REC).

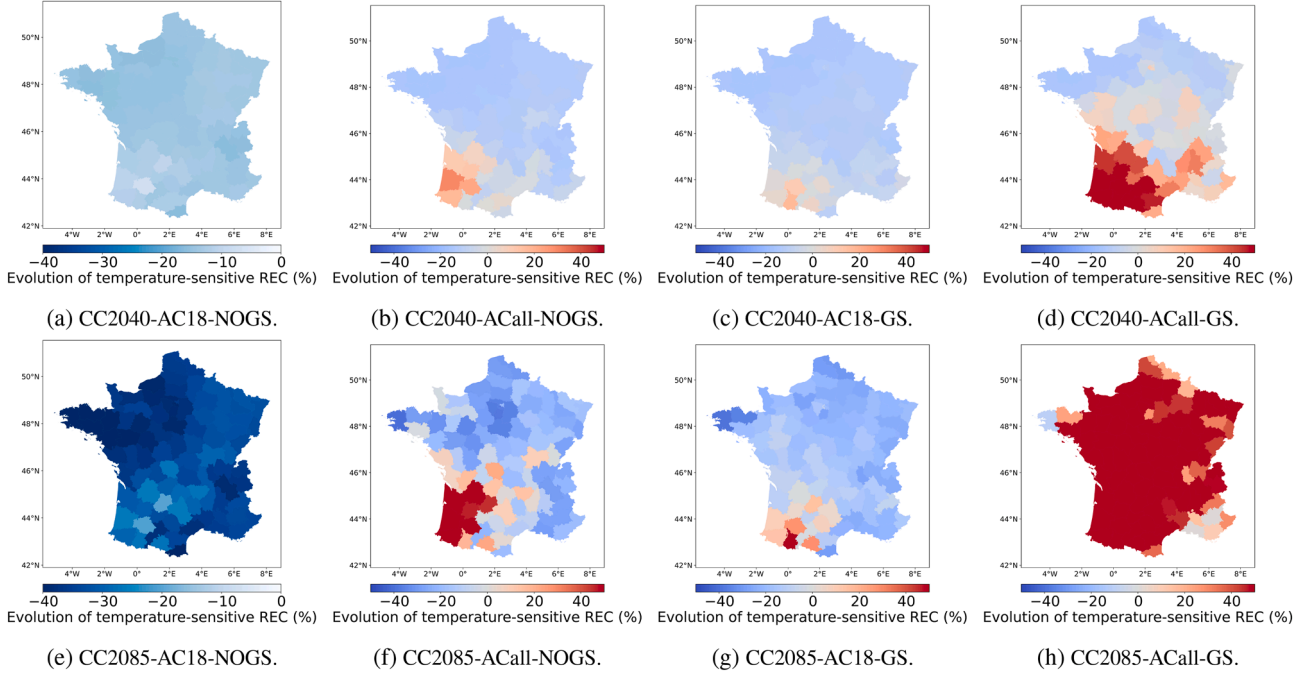


Fig. 5. Relative change (%) in REC wrt. to the historical period (1975–2005) for CC2040 (top) and CC2085 (bottom) and for different AC scenarios: AC18-NOGS (left column), ACall-NOGS (second column), AC18-GS (third column) and ACall-GS (right column).

and explained below, two extreme cases are considered for both factors and indifferently for the 2025–2055 and the 2070–2100 periods.

Regarding η^{AC} , the minimal scenario is that η^{AC} remains fixed to its 2018 cell values (Section 2.2.4), corresponding to a situation in which AC installation no longer progresses. The maximal scenario is that η^{AC} has reached 100% in every cell before the beginning of the projection period and remains fixed over the period, corresponding to a situation in which all households are equipped with AC (regardless of the technology).

Regarding α^{C} , the minimal scenario is that cells with no cooling temperature sensitivity remain so. The maximal scenario is that all cells become cooling-sensitive. In this case, further assumptions are needed to determine α^{C} for these cells that were not cooling-sensitive historically. Here, we assume that α^{C} for these cells is the result of interpolation from the α^{C} values of the surrounding cells with a positive α^{C} . A nearest-neighbor interpolation is performed for a given number of neighbors and for the Euclidean distance in the plate carrée projection. The number of neighbors is optimized based on the methodology described in Section D, giving an optimal number of 25 cells. We refer to this scenario as the gradual spreading of α^{C} and the resulting α^{C} estimates are shown in Fig. 3c. The gradual spreading scenario mimics a “do like my neighbor” behavior.

2.4. Quantifying the uncertainty in the projected REC change

For a given cell i , a model m (Table 4) and a scenario s (Table 5), we define the absolute change in REC, $\Delta \bar{E}_i^{m,s}$, as the difference (Δ) at i between the REC averaged ($\bar{\cdot}$) over the CORDEX historical period and the REC averaged over one of the two CORDEX projection periods, estimated with the model m simulations for the scenario s . In addition, the relative REC change is defined as the absolute REC change divided by the REC averaged over the CORDEX historical period. Given the stationarity assumptions (Section 2.3), the absolute REC change is given by

$$\Delta \bar{E}_i^{m,s} = \alpha_i^{\text{H}} \eta_i^{\text{El}} \Delta [\overline{\text{HDD}}_i^{m,s}] + \Delta [(\alpha_i^{\text{C}} \eta_i^{\text{AC}})^s \overline{\text{CDD}}_i^{m,s}]. \quad (4)$$

In the AC18-NOGS scenario, α^{C} and η^{AC} are also stationary, so that

$$\Delta \bar{E}_i^{m,s} = \alpha_i^{\text{H}} \eta_i^{\text{El}} \Delta [\overline{\text{HDD}}_i^{m,s}] + (\alpha_i^{\text{C}} \eta_i^{\text{AC}})^{\text{AC18-NOGS}} \Delta [\overline{\text{CDD}}_i^{m,s}], \quad (5)$$

in this case.

The corresponding multi-model average is

$$\left\langle \Delta \bar{E}_i^s \right\rangle := \frac{1}{M} \sum_{m=0}^{M-1} \Delta \bar{E}_i^{m,s}. \quad (6)$$

An essential part of this study is quantifying the uncertainty of our estimates of temperature-sensitive REC change ($\Delta \bar{E}_i^s$). From (6), we can see that errors may come from.

- the temperature sensitivity model design,
- the stationarity assumptions on the model coefficients and on electric appliances adoption rate η_i^{El} and η_i^{AC} during scenarios studies,
- the regression of the coefficients from a particular training dataset,
- the historical estimates of η_i^{El} and η_i^{AC} ,
- the climate models (Jacob et al., 2014; Ruti et al., 2016),
- the choice of climate change pathway and AC use scenario.

Here, only the worst-case climate change pathway is considered (i.e. RCP8.5, Section 2.3.1), so that uncertainty in the climate-model pathway is not assessed. On the other hand, a partial estimate of climate-model errors is provided in the results Section 3 from the variations of the projected REC change with the choice of the climate model. To estimate the sensitivity of temperature-sensitive REC change to AC adoption rate projections, extreme scenarios are considered (Section 2.3), while measurements of the electric-heating rate are assumed to be reliable and representative of other years than the year it is provided for. The assumption of the stationary temperature sensitivity model coefficients restricts the scope of the results of this study. It is not tested in-depth in this work, but a simple analysis is conducted in Section 3.2 and further discussed in terms of policy implications in Section 4. Finally, the errors from the model design and the regression are estimated using cross-validation (Section 3.4).

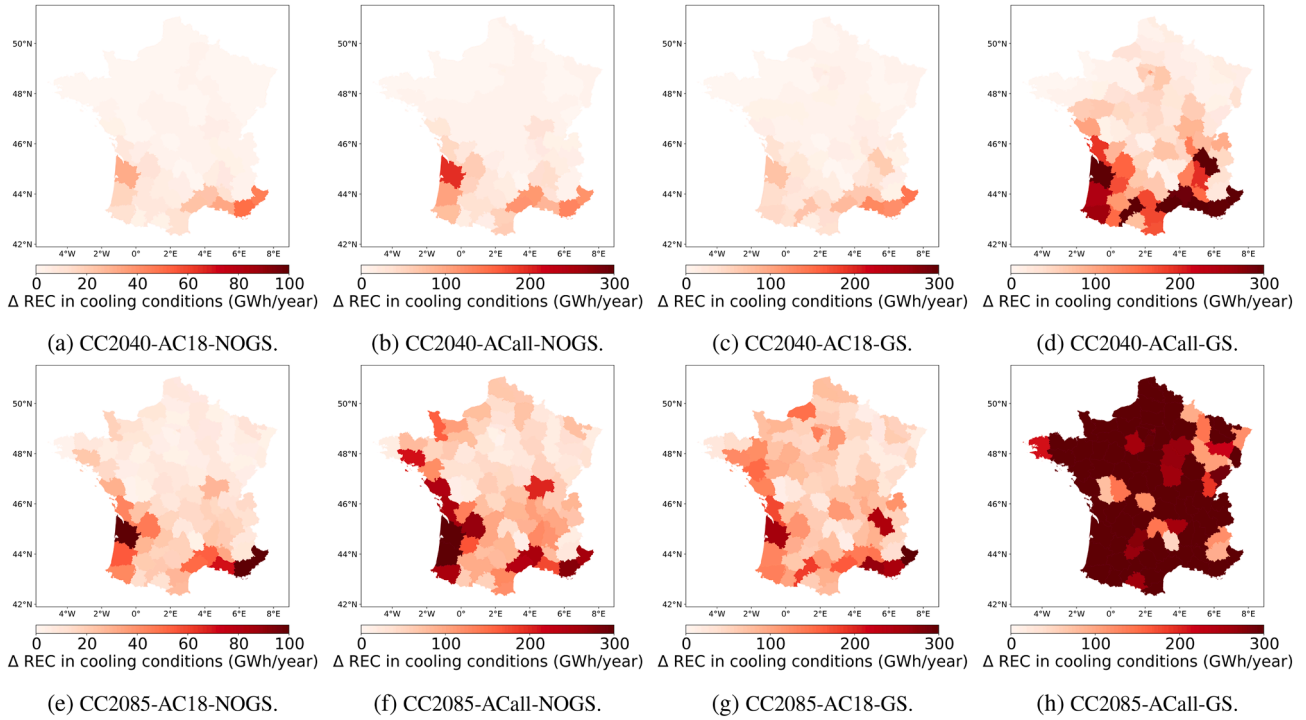


Fig. 7. Same as Fig. 5 but for the cooling REC.

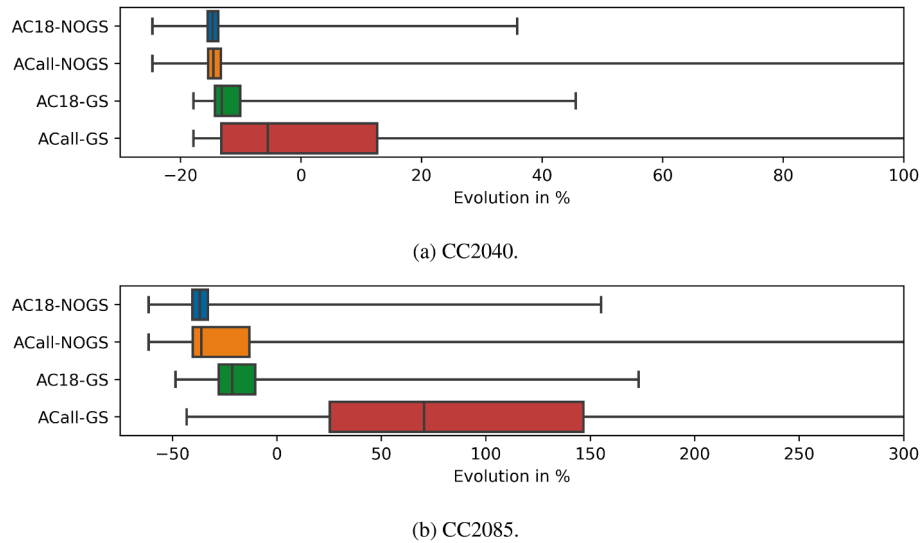


Fig. 6. Boxplots over the cells of the relative change in temperature-sensitive REC corresponding to Fig. 5. The whiskers here show the minimum on the left and the 99% quantile on the right.

Table 6

Decomposition of variability into different geographical scales for different studied variables in terms of proportion (%).

Variable y_i	$\frac{\sigma^2(y_i - \langle y_i \rangle_d)}{\sigma^2(y_i)}$	$\frac{\sigma^2(\langle y_i \rangle_d - \langle y_i \rangle_r)}{\sigma^2(y_i)}$	$\frac{\sigma^2(\langle y_i \rangle_r - \langle y_i \rangle_n)}{\sigma^2(y_i)}$
β_i^H	75%	13%	12%
α_i^C	77%	4%	19%
$\langle \Delta HDD_i \rangle^{CC2040}$	24%	20%	56%
$\langle \Delta HDD_i \rangle^{CC2085}$	29%	23%	48%
$\langle \Delta CDD_i \rangle^{CC2040}$	13%	15%	72%
$\langle \Delta CDD_i \rangle^{CC2085}$	14%	13%	73%
$\langle \Delta \bar{E}_i \rangle^{AC18-NOGS}$	82%	7%	11%

3. Results and discussion

We now analyze the projected changes in the REC, first for the scenarios where the AC uses remain fixed, then for scenarios with AC uses changes. The discussion of the uncertainty in the results is left for the next Section 4, the main conclusions from these results being robust.

3.1. Projected REC change without change in AC use

The projections of temperature-sensitive REC changes for fixed AC use (AC18-NOGS) are shown in Fig. 5a and Fig. 5e. In general, the REC decreases between 7% and 16% in all departments for CC2040, down to 20% to 42% for CC2085. Aggregated at the country scale, the REC

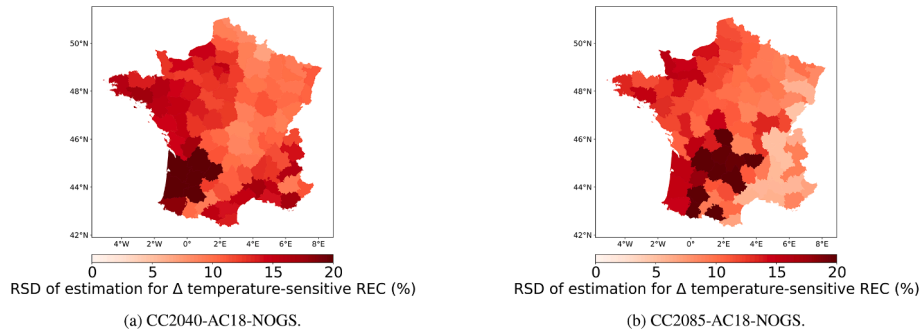


Fig. 8. The global uncertainty of estimation of evolution in temperature-sensitive REC by combining all possible estimated coefficients with the leave-one-out cross-validation method and the 5 CORDEX simulations, represented by the Relative Standard Deviation (RSD) for the CC2040-AC18-NOGS (left) and the CC2085-AC18-NOGS (right) scenarios.

Table 7

Average values with uncertainty for all possible combinations, the uncertainty is converted to the same magnitude by averaging over the number of cells. A t-test shows that mean values of REC change under all scenarios are significant.

Time	Scenario name	Mean (GWh/cell)	Std (GWh/cell)		
			Cell	Department	Country
2040	CC-AC18-NOGS	-0.22	0.037	0.029	0.024
	CC-AC18-GS	-0.16	0.053	0.038	0.031
	CC-ACall-NOGS	-0.16	0.066	0.042	0.032
	CC-ACall-GS	0.08	0.191	0.146	0.125
2085	CC-AC18-NOGS	-0.53	0.085	0.057	0.047
	CC-AC18-GS	-0.28	0.185	0.150	0.136
	CC-ACall-NOGS	-0.26	0.236	0.159	0.138
	CC-ACall-GS	1.26	1.019	0.867	0.790

Table 8

Comparison of uncertainty due to model or CORDEX for scenario AC18-NOGS in the form of standard deviation (GWh/cell).

Time	Cell		Commune		Country	
	Model	CORDEX	Model	CORDEX	Model	CORDEX
2040	0.020	0.034	0.012	0.029	0.010	0.022
2085	0.056	0.066	0.031	0.052	0.026	0.040

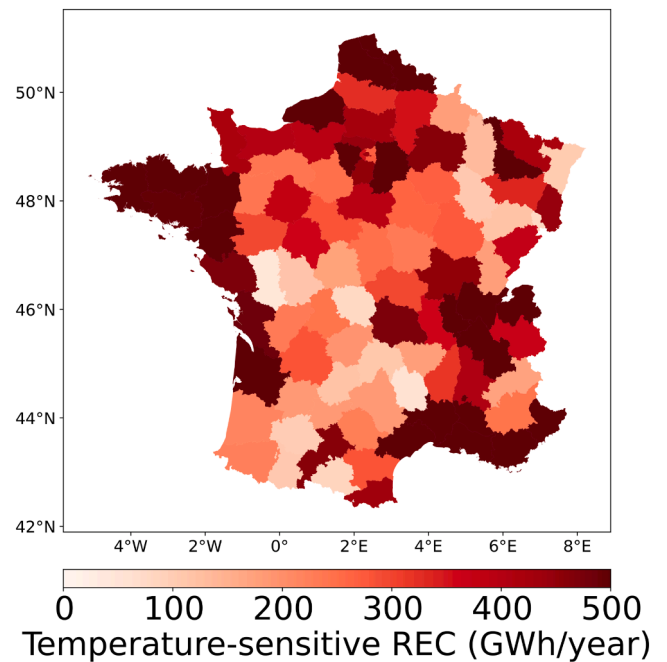


Fig. 10. Total temperature-sensitive REC reference aggregated at the department level, estimated with our model using the temperature of 1975–2005 from CORDEX simulations on all valid cells (60% of the cells).

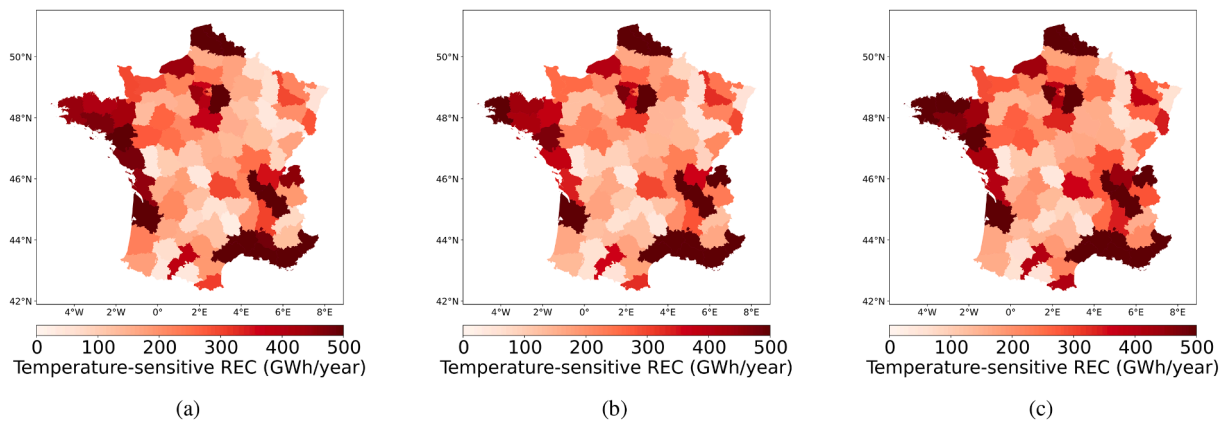


Fig. 9. Temperature-sensitive REC per year averaged over departments estimated from (a) the Enedis β^H estimates for 2018 (for 50% of the cells only, Section 2.2.1), (b) the model (2) applied to the E-OBS temperatures for 2018 and (c) the model (2) applied to the CORDEX historical temperatures over the 1975–2005 period and averaged over the period and over the climate-model simulations (Section 2.3.1).

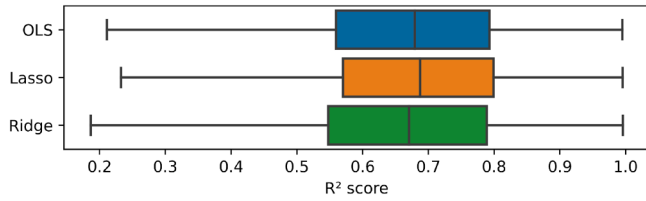


Fig. 11. Comparison between linear regression methods of R^2 score distribution for all valid IRIS.

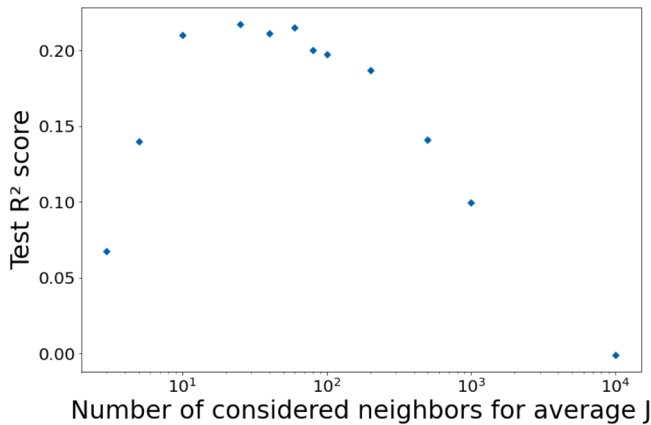


Fig. 12. Test R^2 score between estimated α^c with Gradual Spreading method and regression model estimation as a function of the chosen number of neighbors J taken into account for the calculation of average (Gradual Spreading).

decreases by about 8TWh and 20TWh, respectively. This is consistent with the results of Damm et al. (2017); Spinoni et al., 2018, but significant variations are observed between departments.

For this scenario and for a given cell, according to (5), the projected heating and cooling REC changes are proportional to the HDD and CDD changes, respectively, represented in Fig. 4. However, the coefficients of proportionality, $\alpha_i^H \eta_i^{El}$ and $(\alpha_i^C \eta_i^{AC})^{AC18-NOGS}$, represented in Fig. 3, depend on the cell. From this can be deduced that the REC changes for this scenario are dominated by the large decrease in the HDDs (Fig. 4b and Fig. 4c) modulated by variations in β^H with the cells (Fig. 3d). This effect can for instance be seen in the weaker reduction of the REC in the North-East and the South-West of France.

In addition, the REC decrease is reduced in the south of France due to the significant increase in the cooling REC with the increase in the CDDs (Fig. 4e and Fig. 4f) in conjunction with the positive β^C there (Fig. 3e). This is more obvious from the plots of the cooling REC for the AC18-NOGS scenario in Fig. 7a and Fig. 7e. One can see that, according to this scenario, the cooling REC increases everywhere, but this is particularly evident along the Atlantic coast and South of $46^\circ N$ latitude, between the Massif Central and the Alps, especially for the CC2085 period. At these locations, HDDs indeed tend to increase significantly, but the correlation is not perfect, since, for this scenario, the translation of this change in a cooling REC change depends on AC being already in use there (Fig. 3e). A substantial increase in the cooling REC is also observed in the Northwest part of France for CC2085 (Fig. 7f), even though the increase in CDDs is relatively weak there (Fig. 4f). This is explained by the fact that a significant number of cells there have a large β^C (Fig. 3e).

The distribution of the temperature-sensitive REC change at the cell level is shown in Fig. 6 in the form of box plots. The distribution for scenario CC2040 without AC use changes (AC18-NOGS) is right-skewed, meaning the temperature-sensitive REC is expected to decrease around 15% in most regions. In the longer term, the disparity between IRIS increases with decreasing averaged temperature-sensitive REC. Indeed,

some IRIS may display a positive temperature-sensitive REC change (i.e. an increase in temperature-sensitive REC) over 3% of the French territory in the near future and up to 7% by the end of the 21st century.

3.2. Projected REC change with change in AC use

The projections of temperature-sensitive REC change with different AC scenarios are shown in 5b-5d and 5f-5h. Contrary to the results including temperature change only, some regions display an increase of temperature-sensitive REC whose pace and spatial extent depend on the AC scenario.

Results also show that the different factors have diverse effects. In the case where the AC rate is changed without spreading geographically, the temperature-sensitive REC is expected to increase in the South-West of France and in the South along the Mediterranean Sea (Fig. 5b and Fig. 5f). Indeed, in this region, α^H is relatively low with respect to other regions, and AC systems are already deployed so that α^C is different from zero. But α^C in these regions has a relatively low value, so if the temperature change is only accounted for, increased CDD makes the decline in temperature-sensitive REC less rapid. However, in the considered scenario, the change in AC rate directly multiplies the current cooling demand by four to five times. The electricity savings from heating in the South-West are thus expected to be fully offset by cooling in the near future (Fig. 7b). In the far future, this trend should be exacerbated in the South-West and in the South and spread significantly along the Atlantic coast and South of $46^\circ N$ (Fig. 7f). As there is no spatial spreading of AC usage, the geographical patterns of temperature-sensitive REC change are similar between Fig. 7a and Fig. 7e, and Fig. 7b and Fig. 7f.

With regards to the AC rate scenario, the gradual spreading of the present AC rate lowers the change of REC for cooling needs, but REC for cooling needs becoming positive spreads geographically (Fig. 5c and Fig. 5g). Gradual spreading does not change the values instantly in regions where most IRIS cells are already given with non-null estimation for α^C . However, it helps to smooth the map of coefficients as shown in Fig. 3b and Fig. 3c. Based on observational data, many cells in Ile-de-France, Auvergne-Rhône-Alpes, and along the Atlantic coast have been given null estimates for α^C . However, some nearby cells still received significant values for α^C with high regression scores. Assigned with proximity averages, these areas mixed with sporadic large values are most affected. Fig. 6 shows that a 100% AC rate in already equipped cells (ACall-NOGS) modifies the shape of the distribution, with an increased number of cells with positive evolution. More positive values correspond to the cells currently equipped with AC at which the AC rate is increased from its current value to 100% and where the change of REC for cooling needs exceeds that for heating needs. No change is expected for the cells currently without AC hence the minimal, the first quartile even the median values remain the same as for AC18-NOGS. In the gradual spreading scenario (AC18-GS), the shape of the distribution displays an even larger positive skewness than in the 100% AC rate scenario. Less negative values correspond to the larger number of cells equipped with AC and bring an increase to all cells.

In a scenario combining gradual spreading and 100% AC rate, almost half of the territory, except the North of France, sees the REC increasing in the near-term future, amounting to a global change of +2%. At the end of the 21st century, this fraction of positive trend increases up to 90%, leading to a global change of +32%.

The results of these scenarios motivate actions allowing at least to prevent AC from inducing an increase in cooling REC. A simple approach, applicable to the whole country, consists at least in the region of South of France with the greatest AC impact to modify in the future climate scenarios only the cooling setpoint in such a way as to maintain the cooling REC unchanged with respect to the present situation. Such an approach leads to the most constraining action as it sets for the whole country the highest cooling setpoint, but it ensures at least unchanged cooling REC in the South of France and in most regions of France a

negative cooling REC trend. The cooling setpoint preventing any cooling REC increase over the whole country varies with the time horizon, which is about 23–24 °C by 2040 and 26–27 °C by 2085.

3.3. Spatial heterogeneity

The maps shown in Fig. 3 and Fig. 5 show an apparent geographical disparity of temperature sensitivities and temperature-sensitive REC changes. To compare the intra-department variability with the one of inter-department, each studied variable y_i (sensitivity coefficients α_i^H, α_i^C , DD evolution $\langle \Delta \overline{HDD}_i^s \rangle, \langle \Delta \overline{CDD}_i^s \rangle$) and the REC evolution $\langle \Delta \overline{E}_i^s \rangle$) can be decomposed as:

$$y_i = (y_i - \langle y_i \rangle_d) + (\langle y_i \rangle_d - \langle y_i \rangle_r) + (\langle y_i \rangle_r - \langle y_i \rangle_n) + \langle y_i \rangle_n. \quad (7)$$

with $\langle y_i \rangle_d$ the average value of cells inside a given department, $\langle y_i \rangle_r$ the average value of cells inside a given administrative region, and $\langle y_i \rangle_n$ the average value of all cells in France. Hence with the above equation, the variability of all cells can be decomposed into disparities at several stages:

$$\sigma^2(y_i) = \sigma^2(y_i - \langle y_i \rangle_d) + \sigma^2(\langle y_i \rangle_d - \langle y_i \rangle_r) + \sigma^2(\langle y_i \rangle_r - \langle y_i \rangle_n). \quad (8)$$

where $\sigma^2(y_i - \langle y_i \rangle_d)$ represents the variability of cells inside the department while $\sigma^2(\langle y_i \rangle_d - \langle y_i \rangle_r)$ represents the variability of departments inside a given administration region and $\sigma^2(\langle y_i \rangle_r - \langle y_i \rangle_n)$ the variability between different administrative regions. Table 6 shows the proportion of variability at each geographical scale over the whole variability.

The regional variability is more important than the local difference for the DD changes. However, the variability of temperature sensitivities between cells within the same department dominates. At the same time, because of the large spatial variability of β^H and α^C within the administrative regions, a larger disparity of temperature-sensitive REC changes is found between cells than between administrative regions. For both temperature sensitivities, β^H and α^C and temperature-sensitive REC changes, it shows that the variability between the cells is more significant than the difference between regions, which justifies our choice of study at a small geographical scale.

3.4. REC change error estimates

In this study, public data are used to train the temperature sensitivity model with only eight annual samples applied for the regression. Compared to models with a larger dataset, our model can be easily influenced by outliers and may have coefficients over-fitted.

We did not choose regularized regression because the performance did not improve much, but this method may be more attractive if a more extensive input is available. Nonetheless, the possibility of applying the leave-one-out cross-validation over the training gives us eight possible models and, thus, a range of eight different results of the temperature sensitivities with uncertainty.

At the same time, CORDEX simulations from different models may produce different future temperature projections. Combining the five different simulations and all possible estimated coefficients with the leave-one-out cross-validation method, the global uncertainty of our results, quantified by the Relative Standard Deviation (RSD), is shown in Fig. 8. The relative error is large in the South-West, where $\alpha^C > 0$, due to the biased model regressions as the observed temperatures do not largely and frequently exceed the 21 °C cooling setpoint.

The global uncertainty for all the scenarios is presented in Table 7. The standard deviation is identified after aggregating REC at different levels. For the results to have the same order of magnitude and to be comparable, the REC change is normalized by the average number of IRIS in the desired geographical scale. The method using a REC linear model together with the CORDEX simulations derives robust estimates of future REC with an error of less than 18.4% without assumptions on

AC uses. The uncertainty of scenario ACall-GS is the largest among all other scenarios because the results may become less precise with all the assumptions together. We can see clearly that with spatial aggregation, the error decreases because there can be compensation between IRIS within the large scales, and the variation becomes smaller. For the average values of all possible combinations, a t-test shows that the mean values of REC change under all scenarios are significant.

The global error of future REC mainly comes from the multi-model ensemble spread of the projected temperatures and the training bias and variance of the REC linear model. To find the standard deviation due to different sources, we use the average values of the cross-validated coefficients estimated by the model or the average of the five simulations of CORDEX, respectively. The uncertainty due to the simulations of CORDEX and to the model regression can be found in the following Table 8. With the previous tables, we can see clearly that the uncertainty due to the various simulations of CORDEX leads to a more significant error than the one from the regression. This 10% error due to the model is reassuring the basis of a temperature sensitivity model: the temperature sensitivity is quasi-constant under a stable climate. Nevertheless, this error can still be improved if more annual consumption data are available or daily consumption data can be accessible.

4. Conclusions and policy implications

A number of key messages can be drawn from the results of this study. First, REC varies significantly at very fine spatial scales, from the IRIS size (region of 2,000 inhabitants) to the administrative departments (96 departments on the European continent and 5 overseas) and regions (13 on the European continent and 5 overseas). Such variability had never been quantified and mapped due to a lack of suited methodology and limited available data at the finest scale (IRIS). Such variability which is the largest at the finest spatial scale calls for solutions and policies steered to the local specificities.

With increasing temperatures due to climate change, the heating needs decrease especially in the North-East which displays a continental climate with very hot summers and very cold winters (Köppen, 1936) and thus a strong sensitivity to any heating need reduction. Conversely, the South and Western regions along the Mediterranean Sea and the Atlantic Ocean, respectively, display a smaller trend in heating needs as they display a Mediterranean climate (hot, dry summers and cool, wet winters) and a maritime climate (cool summers and mild winters) (Köppen, 1936), respectively with warmer winters with regards to the North-East of France. At the end of the 21st century, in the worst-case climate scenario (RCP8.5), the spatial variability of the trend decreases as many regions are expected to experience temperatures much more rarely below their heating setpoint. There is a strong link between the heating needs and its evolution with that of REC.

However, the evolution of REC is modulated by the evolution of cooling needs and the deployment of AC systems to meet those needs. Our worst-case scenarios suppose either a 100% AC adoption rate in the IRIS already equipped at present, or a gradual spreading of AC systems, which mimics a "do like my neighbor" behavior. We also consider a combination of the two. In any scenario, the decrease in REC due to climate change could be totally offset in the South of France, which would then display an increase in REC. When the 2 AC scenarios are combined, an increase in REC could be seen over the whole country.

One key message deals with the overall uncertainty of our modeling setup. The uncertainty of our REC trends, including climate change impact and AC system deployment, is dominated by the spread between the climate simulations of our ensemble. The regression-based REC model does not add up much to the overall uncertainty. Such a result was not straightforward as the data available at the IRIS scale was at best limited in time, at worst available on an annual basis only, and sparse in some regions. The level of overall uncertainty therefore allows for drawing some recommendations in terms of practical applications and energy policies.

Takeaways for policy implications can be formulated from these results. In our scenario, AC gradual spreading mimics a “do like my neighbor” behavior. Our results show that such behavior has a major and detrimental impact on REC (more than 100% AC rate scenario). Such results call for targeted and local information actions where the risk of spreading is high (i.e. in areas where households are already equipped with AC systems) to limit the spreading or mitigate its effect with at least the most energy-efficient AC systems. A more straightforward result is that the South of France is where the REC trend is expected to occur first with possible impacts on the energy system. Therefore there is a need to target actions to prevent any further deployment of AC systems. Especially, the climate of the South of France is expected to become similar to the present climate of countries more to the South, such as Italy or Morocco (Hallegatte et al., 2007). In Morocco, there is no visible impact on REC of AC use (Bouramdane et al., 2021). In Italy, the signal on REC of the use of AC is very limited (Tantet et al., 2019) but locally the evolution of cooling needs can have a significant impact on REC (De Felice et al., 2013; Scapin et al., 2016). Therefore, analyzing the socio-economic drivers, and the energy policies of these countries and drawing inspiration from them to deploy actions adapted to the local specificities of some French regions should be considered. Our worst-case results clearly show the detrimental impact of the increase in AC rate and spreading. Increasing the cooling setpoint T^C (e.g. recommended temperature of 26 °C by the US Department of Energy) or maintaining an optimal difference with outdoor air temperature to about 7–8 °C to maximize the energy efficiency of the AC equipment, could lower the cooling REC. Based on our model, shifting the cooling setpoint from 21 °C at present to 23–24 °C by 2040 and 26–27 °C by 2085 would prevent any cooling REC increase in our worst-case scenarios. These values are consistent with existing recommendations. Low-tech alternative solutions also exist which are widely implemented in subtropical regions, and can be implemented in France to improve the thermal comfort of buildings and reduce the use of AC equipment and their impact on the environment, such as the reflective white coating on the buildings or roofs (Viguié et al., 2020; Rawat et al., 2022).

There are still several limits to this study. The temperature sensitivity results from a regression between REC and temperature, and the model implicitly integrates “human behaviors” related to other factors such as electricity costs and household revenue (Frederiks et al., 2015; Gertler et al., 1366). However, at this stage, no approach to segment the consumption data along multiple socio-economic dimensions (e.g. price, revenue) has been successful with the available data (e.g. time sampling and spatial granularity too coarse and aggregated) which would have been valuable to reduce global uncertainty. It could have been relevant to perform a sensitivity analysis on the temperature sensitivity through η^{el} to account for the further electrification of heating (e.g. fuel oil or gas to heat pumps) or through α^C to account for improved efficiency of AC systems. Regarding α^C , regions of the North-West along the Atlantic

coast where the AC rate is on average 14% (versus 22% at the national level in 2019) can display surprisingly large positive α^C values. The causes should be further explored, whether due to statistical processing or behavioral in origin (e.g. residents may be less adapted to extreme heat events and more likely to install AC equipment for use during such extreme events (He et al., 2022)). Finally, the study from Pagliarini et al. (2019) shows that in a warmer climate, the electricity increases faster than linearly because of the efficiency drop of air-cooled chillers at high temperatures. Such a phenomenon should also be considered in the future.

CRediT authorship contribution statement

Qiqi Tao: Conceptualization, Data curation, Formal analysis, Investigation, Methodology, Visualization, Writing - original draft, Writing - review & editing. **Marie Naveau:** Conceptualization, Data curation, Formal analysis, Investigation, Methodology. **Alexis Tantet:** Conceptualization, Supervision, Validation, Writing - review & editing. **Jordi Badosa:** Conceptualization, Data curation, Formal analysis, Validation, Writing - review & editing. **Philippe Drobinski:** Conceptualization, Formal analysis, Supervision, Validation, Writing - review & editing.

Data availability

Input data are all publicly available, produced data will be made available by request.

Declaration of Competing Interest

The authors declare that they have no known competing financial interests or personal relationships that could have appeared to influence the work reported in this paper.

Data availability

Data will be made available on request.

Acknowledgments

This work was carried out at the Energy4Climate Interdisciplinary Center (E4C) of IP Paris and Ecole des Ponts, supported by 3rd Programme d'Investissements d'Avenir [ANR-18-EUR-0006-02]. It was funded by nam'R company through a collaboration grant. The authors thank L.G. Giraudet and V. Viguié for fruitful discussions and comments. We acknowledge the E-OBS dataset from the EU-FP6 project UERRA (<http://www.uerra.eu>) and the data providers in the ECA&D project (<https://www.ecad.eu>)

Appendix A. Reference REC and verification of climate data on REC

Fig. 9 shows the temperature-sensitive REC aggregating over the 12 administrative regions the values at the IRIS where such estimate by Enedis exists from Enedis processing (a), by applying the model (2) to temperatures from E-OBS dataset (b) and historical CORDEX simulations (c). Visually, the three show a very similar pattern. Fig. 9a and Fig. 9b illustrate the quality of the model prediction and quantitatively a R^2 score of 0.77 is found between the common cells. Fig. 9c shows how historical climate simulations can satisfactorily reproduce the temperature-sensitive REC for climate projection studies which rely on the climate projections produced in a consistent way with the historical climate simulations. However, in Section 3, the temperature-sensitive REC based on the CORDEX regional climate simulations is estimated over a larger number of IRIS than those of the Enedis subset. At the IRIS kept in the dataset, the estimates of α^{H} and α^C passed a significance test. The reference REC for the period 1975–2005 used to calculate the change of temperature-sensitive REC is shown in Fig. 10.

Appendix B. Cross-validation method for trained temperature sensitivities

During the present study, for each cell we have 8 years of annual REC as inputs to train the model described in Equation 2. The Leave-One-Out cross-validation method has been used to fit the model and to validate the model's performance. Each time we extract one year out as test and

train the model with the other 7 years' data and get the prediction using the one test data. And this procedure repeats 8 times. After that, the 8 predicted values with the test data are compared to their initial values, which gives us a test R^2 score. Such test is done for all the cells and a significance test is also performed to get the valid cells. A comparison of different linear regression models has been made with this test method and the distribution of related test R^2 scores are shown in Fig. 11.

Appendix C. AC adoption rate initial data

CODA STRATEGIES uses data from UNICLIMA (the professional union bringing together manufacturers and marketers of AC equipment in France) to estimate the national AC adoption rate from 2004 until 2020, including all types of AC equipment (mobile, heat pump). The national AC rates estimated by CODA STRATEGIES are published by ADEME (the French Agency for Ecological Transition) and are consistent with INSEE (for 2017) and EDF (for 2016 and 2019) data (ADEME, CODA STRATEGIES, 2021). At a finer scale, a study from Ecole des Ponts (Daguenet et al., 2021) calculated the regional AC adoption rate for 2019 based on data from Likibu (a house rental search engine) for over 800 households. The national population-weighted AC rate is found to be 22% for 2019, which is consistent with the EDF study and CODA STRATEGIES dataset.

These studies show that the cooling equipment market increase is not constant and has accelerated in recent years (ADEME, CODA STRATEGIES, 2021), resulting in a more geometric overall progression of about 20% per year at the country scale. From these studies, we have regional rates for 2019 only and national rates from 2016 to 2020 from which regional rates from 2011 to 2018 are deduced assuming a spatially homogeneous progression rate. Once estimated, the national rate "population-weighted national average" is deduced from the estimate of the regional rate for the different years and compared to the reference from ADEME (EDF and INSEE). This reconstruction is consistent for 2016–2020.

Appendix D. AC gradual spreading method and optimal number of neighbors

With the historical REC data, around 60% of the cells are estimated with zero current cooling temperature sensitivity (i.e. $\alpha_i^c = 0$). As described in Section 2.3.2, so-called Gradual Spreading is our way of estimating future α^c based on an interpolation assumption of actual values, especially for cells without current α^c . For cells with positive non-null cooling temperature sensitivity, the future cooling temperature sensitivity is assumed to be consistent with the current value (i.e. $(\alpha_i^c)^{GS} = \alpha_i^c > 0$), while for other cells without current α^c , a nearest-neighbor interpolation is performed with the following formula:

$$(\alpha_i^c)^{GS} = \frac{1}{J} \sum_{j=0}^{J-1} \alpha_j^c.$$

For a studied cell i , all the cells with current non-null sensitivity $\alpha_j^c > 0$ are ordered by the Euclidean distance with the given cell in the plate carrée projection, and J is the number of nearest cells taken into account for the calculation of the average.

This assumption has been tested with the group of cells where α^c are estimated non-null in the first place. During the test, 60% of these cells are selected randomly to become zero, conforming to the actual situation, and are given an estimation with the Gradual Spreading method. Then the estimated values with Gradual Spreading are compared with the model's initial estimation α^c . This process repeats 30 times for each J , and the average test R^2 score as a function of the number of neighbors J is given in Fig. 12. It can be seen clearly that there exists a local similarity: the test R^2 score is larger when $J \in [10, 60]$. In our study, the optimal value for J is 25. Despite selecting the optimal number of cells per cluster based on evidence of local similarity through a pre-test, the resulting prediction R^2 score remains low (below 0.23). This uncertainty in the future assumption of the coefficient α^c remains a limitation of the scenario study with the Gradual Spreading approach.

References

- ADEME, CODA STRATEGIES, 2021. La climatisation de confort dans les bâtiments résidentiels et tertiaires. Technical Report. ADEME. 110 pages, URL: <https://librairie.ademe.fr>.
- Auffhammer, M., Mansur, E.T., 2014. Measuring climatic impacts on energy consumption: A review of the empirical literature. *Energy Econ.* 46, 522–530.
- Bettignies, Y., Meirelles, J., Fernandez, G., Meinherz, F., Hoekman, P., Bouillard, P., Athanassiadis, A., 2019. The Scale-Dependent Behaviour of Cities: A Cross-Cities Multiscale Driver Analysis of Urban Energy Use. *Sustainability* 11, 3246. Number: 12 Publisher: Multidisciplinary Digital Publishing Institute.
- Bouramdane, A., Tantet, A., Drobinski, P., 2021. Utility-scale pv-battery versus csp-thermal storage in morocco: Storage and cost effect under penetration scenarios. *Energies* 14.
- Branger, F., Giraudet, L.G., Guivarch, C., Quirion, P., 2015. Global sensitivity analysis of an energy-economy model of the residential building sector. *Environ. Modelling Softw.* 70, 45–54.
- Chen, H.C., Han, Q., De Vries, B., 2020. Modeling the spatial relation between urban morphology, land surface temperature and urban energy demand. *Sustainable Cities Soc.* 60, 102246.
- Chen, H.C., Han, Q., de Vries, B., 2020. Urban morphology indicator analyzes for urban energy modeling. *Sustainable Cities Soc.* 52, 101863.
- Cornes, R.C., van der Schrier, G., van den Besselaar, E.J.M., Jones, P.D., 2018. An Ensemble Version of the E-OBS Temperature and Precipitation Data Sets. *J. Geophys. Res.: At.* 123, 9391–9409. eprint: <https://onlinelibrary.wiley.com/doi/pdf/10.1029/2017JD028200>.
- Daguenet, C., Gredigui, P., Teixeira Costa, F., Maugenest, M., Pedro Saint Martin, D., Sena Fracaroli, N., 2021. évolution des besoins en chaud et en froid dans le secteur résidentiel.
- Damm, A., Köberl, J., Pretenthaler, F., Rogler, N., Töglhofer, C., 2017. Impacts of +2 C global warming on electricity demand in Europe. *Climate Services* 7, 12–30.
- De Felice, M., Alessandri, A., Ruti, P.M., 2013. Electricity demand forecasting over Italy: Potential benefits using numerical weather prediction models. *Electric Power Systems Research* 104, 71–79.
- Drobinski, P., Silva, N.D., Panthou, G., Bastin, S., Muller, C., Ahrens, B., Borga, M., Conte, D., Fossier, G., Giorgi, F., Güttler, I., Kotroni, V., Li, L., Morin, E., Onol, B., Quintana-Segui, P., Romera, R., Torma, C.Z., 2018. Scaling precipitation extremes with temperature in the Mediterranean: past climate assessment and projection in anthropogenic scenarios. *Clim. Dyn.* 51, 1237–1257.
- ECA&D, 2020. E-OBS data access. URL: https://knmi-ecad-assets-prd.s3.amazonaws.com/ensembles/data/Grid_0.1deg_reg_ensemble/tg_ens_mean_0.1deg_reg_v20.0e.nc. Last visited 2021-06-13.
- Emenekwe, C.C., Emodi, N.V., 2022. Temperature and Residential Electricity Demand for Heating and Cooling in G7 Economies: A Method of Moments Panel Quantile Regression Approach. *Climate* 10, 142. Number: 10 Publisher: Multidisciplinary Digital Publishing Institute.
- Emodi, N.V., Chaiechi, T., Alam Beg, A.R., 2018. The impact of climate change on electricity demand in Australia. *Energy Environ.* 29, 1263–1297.
- Enedis, 2020. Consommation et thermosensibilité électriques par secteur d'activité à la maille IRIS. URL: <https://data.enedis.fr/explore/dataset/consommation-electrique-par-secteur-dactivite-iris/>. Last visited 2020-09-30.
- EUROSTAT, Heating and cooling degree days - statistics.
- Flaounas, E., Drobinski, P., Bastin, S., 2013. Dynamical downscaling of IPSL-CM5 CMIP5 historical simulations over the Mediterranean: benefits on the representation of regional surface winds and cyclogenesis. *Clim. Dyn.* 40, 2497–2513.
- Flaounas, E., Drobinski, P., Bastin, S., Lebeaupin Brossier, C., Borga, M., Vrac, M., Calvet, J.C., Stéfanon, M., 2013. Precipitation and temperature space-time variability and extremes in the mediterranean region: Evaluation of dynamical and statistical downscaling methods. *Clim. Dyn.* 40.
- Frederiks, E., Stenner, K., Hobman, E., 2015. The Socio-Demographic and Psychological Predictors of Residential Energy Consumption: A Comprehensive Review. *Energies* 8, 573–609.

- Frei, C., Christensen, J.H., Déqué, M., Jacob, D., Jones, R.G., Vidale, P.L., 2003. Daily precipitation statistics in regional climate models: Evaluation and intercomparison for the European Alps. *J. Geophys. Res.*: At. 108. [eprint: https://onlinelibrary.wiley.com/doi/pdf/10.1029/2002JD002287](https://onlinelibrary.wiley.com/doi/pdf/10.1029/2002JD002287).
- Gertler, P.J., Shelef, O., Wolfram, C.D., Fuchs, A., The demand for energy-using assets among the world's rising middle classes. *American Economic Review* 106, 1366–1401.
- Giraudet, L.G., Guivarch, C., Quirion, P., 2012. Exploring the potential for energy conservation in French households through hybrid modeling. *Energy Economics* 34, 426–445.
- Hallegatte, S., Hourcade, J., Ambrosi, P., 2007. Using climate analogues for assessing climate change economic impacts in urban areas. *Climatic Change* 82, 47–60.
- Haylock, M.R., Goodess, C.M., 2004. Interannual variability of European extreme winter rainfall and links with mean large-scale circulation. *Int. J. Climatol.* 24, 759–776.
- Haylock, M.R., Hofstra, N., Klein Tank, A.M.G., Klok, E.J., Jones, P.D., New, M., 2008. A European daily high-resolution gridded data set of surface temperature and precipitation for 1950–2006. *J. Geophys. Res.*: At. 113. [eprint: https://onlinelibrary.wiley.com/doi/pdf/10.1029/2008JD010201](https://onlinelibrary.wiley.com/doi/pdf/10.1029/2008JD010201).
- He, P., Liu, P., Qiu, Y.L., Liu, L., 2009. The weather affects air conditioner purchases to fill the energy efficiency gap. *Nature Communications* 13, 5772. Number: 1 Publisher: Nature Publishing Group.
- IGN, 2009. Contours...Iris - Descriptif de contenu et de livraison. Technical Report. Institut Géographique National. URL:https://geoservices.ign.fr/sites/default/files/2022-03/DC_DL_Contours_Iris_09.pdf.
- International Energy Agency, Cooling degree days in France, 2000–2020 - Charts - Data & Statistics.
- International Energy Agency, 2018. The Future of Cooling.
- Jacob, D., Petersen, J., Eggert, B., Alias, A., Christensen, O.B., Bouwer, L.M., Braun, A., Colette, A., Déqué, M., Georgievski, G., Georgopoulou, E., Gobiet, A., Menut, L., Nikulin, G., Haensler, A., Hempelmann, N., Jones, C., Keuler, K., Kovats, S., Kröner, N., Kotlarski, S., Kriegsmann, A., Martin, E., van Meijgaard, E., Moseley, C., Pfeifer, S., Preuschmann, S., Radermacher, C., Radtke, K., Rechid, D., Rounsevell, M., Samuelsson, P., Somot, S., Soussana, J.F., Teichmann, C., Valentini, R., Vautard, R., Weber, B., Yiou, P., 2014. EURO-CORDEX: new high-resolution climate change projections for European impact research. *Reg. Environ. Change* 14, 563–578.
- Kennedy, C.A., Stewart, I., Facchini, A., Cersosimo, I., Mele, R., Chen, B., Uda, M., Kansal, A., Chiu, A., Kim, K.g., Dubeux, C., Rovere, E.L.L., Cunha, B., Pincetl, S., Keirstead, J., Barles, S., Pusaka, S., Gunawan, J., Adegbile, M., Nazariha, M., Hoque, S., Marcotullio, P.J., Otharàn, F.G., Genena, T., Ibrahim, N., Farooqui, R., Cervantes, G., Sahin, A.D., 2015. Energy and material flows of megacities. *Proceedings of the National Academy of Sciences* 112, 5985.
- Kjellström, E., Boberg, F., Castro, M., Christensen, J., Nikulin, G., Sanchez, E., 2010. Daily and monthly temperature and precipitation statistics as performance indicators for regional climate models. *Climate Res.* 44, 135–150.
- Klok, E.J., Klein Tank, A.M.G., 2009. Updated and extended European dataset of daily climate observations. *Int. J. Climatol.* 29, 1182–1191.
- Köppen, W., 1936. *Das geographische system der klimate*, 46 pp.
- Kozarcanin, S., Andresen, G.B., Staffell, I., 2019. Estimating country-specific space heating threshold temperatures from national gas and electricity consumption data. *Energy and Buildings* 199, 368–380.
- Larsen, M., Petrovic, S., Radoszynski, A., McKenna, R., Balyk, O., 2020. Climate change impacts on trends and extremes in future heating and cooling demands over Europe. *Energy and Buildings* 226, 110397.
- Lemonsu, A., Vigiúé, V., Daniel, M., Masson, V., 2015. Vulnerability to heat waves: Impact of urban expansion scenarios on urban heat island and heat stress in Paris (France). *Urban Climate* 14, 586–605.
- Li, H., Kwan, M.P., 2018. Advancing analytical methods for urban metabolism studies. *Resour. Conserv. Recycl.* 132, 239–245.
- Lévy, J.P., Belaïd, F., 2018. The determinants of domestic energy consumption in France: Energy modes, habitat, households and life cycles. *Renew. Sustain. Energy Rev.* 81, 2104–2114.
- Meng, Q., Xiong, C., Mourshed, M., Wu, M., Ren, X., Wang, W., Li, Y., Song, H., 2020. Change-point multivariable quantile regression to explore effect of weather variables on building energy consumption and estimate base temperature range. *Sustainable Cities Soc.* 53, 101900.
- Moral-Carcedo, J., Vicéns-Otero, J., 2005. Modelling the non-linear response of Spanish electricity demand to temperature variations. *Energy Economics* 27, 477–494.
- Narayan, P.K., Smyth, R., Prasad, A., 2007. Electricity consumption in G7 countries: A panel cointegration analysis of residential demand elasticities. *Energy Policy* 35, 4485–4494.
- Pagliarini, G., Bonfiglio, C., Vocale, P., 2019. Outdoor temperature sensitivity of electricity consumption for space heating and cooling: An application to the city of Milan. *North of Italy. Energy and Buildings* 204, 109512.
- Petrick, S., Rehdanz, K., Tol, R., 2010. *The Impact of Temperature Changes on Residential Energy Consumption*. Kiel Institute for the World Economy, Kiel Working Papers.
- Pickett, S.T.A., Cadenasso, M.L., Rosi-Marshall, E.J., Belt, K.T., Groffman, P.M., Grove, J.M., Irwin, E.G., Kaushal, S.S., LaDeau, S.L., Nilon, C.H., Swan, C.M., Warren, P.S., 2017. Dynamic heterogeneity: a framework to promote ecological integration and hypothesis generation in urban systems. *Urban Ecosyst.* 20, 1–14.
- Pilli-Sihvola, K., Remes, P., Ollikainen, M., Tuomenvirta, H., 2010. Climate change and electricity consumption—witnessing increasing or decreasing use and costs? *Energy Policy* 38, 2409–2419.
- Rawat, M., Singh, R.N., 2022. A study on the comparative review of cool roof thermal performance in various regions. *Energy and Built Environment* 3, 327–347.
- Raymond, F., Ullmann, A., Camberlin, P., Drobinski, P., Smith, C.C., 2016. Extreme dry spell detection and climatology over the Mediterranean Basin during the wet season. *Geophys. Res. Lett.* 43, 7196–7204. [eprint: https://onlinelibrary.wiley.com/doi/pdf/10.1002/2016GL069758](https://onlinelibrary.wiley.com/doi/pdf/10.1002/2016GL069758).
- Raymond, F., Ullmann, A., Camberlin, P., Oueslati, B., Drobinski, P., 2018. Atmospheric conditions and weather regimes associated with extreme winter dry spells over the Mediterranean basin. *Clim. Dyn.* 50, 4437–4453.
- Ribes, A., Boé, J., Qasmi, S., Dubuisson, B., Douville, H., Terray, L., 2022. An updated assessment of past and future warming over France based on a regional observational constraint. *Earth Syst. Dyn.* 13, 1397–1415.
- Rosales Carreón, J., Worrell, E., 2018. Urban energy systems within the transition to sustainable development. A research agenda for urban metabolism. *Resour. Conserv. Recycl.* 132, 258–266.
- van Ruijven, B.J., De Cian, E., Sue Wing, I., 2019. Amplification of future energy demand growth due to climate change. *Nat Commun* 10, 2762. Number: 1 Publisher: Nature Publishing Group.
- Ruti, P.M., Somot, S., Giorgi, F., Dubois, C., Flaouas, E., Obermann, A., Dell'Aquila, A., Pisacane, G., Harzallah, A., Lombardi, E., Ahrens, B., Akhtar, N., Alias, A., Arsouze, T., Aznar, R., Bastin, S., Bartholy, J., Béranger, K., Beuvier, J., Bouffies-Cloché, S., Brauch, J., Cabos, W., Calmanti, S., Calvet, J.C., Carillo, A., Conte, D., Coppola, E., Djurdjevic, V., Drobinski, P., Elizalde-Arellano, A., Gaertner, M., Galán, P., Gallardo, C., Gualdi, S., Goncalves, M., Joba, O., Jordà, G., L'Heveder, B., Lebeaupin-Brossier, C., Li, L., Liguori, G., Lionello, P., Maciàs, D., Nabat, P., Önol, B., Raikovic, B., Ramage, K., Sevault, F., Sannino, G., Struglia, M.V., Sanna, A., Torma, C., Vervatis, V., 2016. Med-CORDEX Initiative for Mediterranean Climate Studies. *Bulletin of the American Meteorological Society* 97, 1187–1208. Publisher: American Meteorological Society Section: Bulletin of the American Meteorological Society.
- Räisänen, J., Hansson, U., Ullerstig, A., Döscher, R., Graham, L.P., Jones, C., Meier, H.E.M., Samuelsson, P., Willén, U., 2004. European climate in the late twenty-first century: regional simulations with two driving global models and two forcing scenarios. *Clim. Dyn.* 22, 13–31.
- Sailor, D.J., Muñoz, J.R., 1997. Sensitivity of electricity and natural gas consumption to climate in the U.S.A.—Methodology and results for eight states. *Energy* 22, 987–998.
- Santos, J.A., Corte-Real, J., Ulbrich, U., Palutikof, J., 2007. European winter precipitation extremes and large-scale circulation: a coupled model and its scenarios. *Theor. Appl. Climatol.* 87, 85–102.
- Scapin, S., Apadula, F., Brunetti, M., Maugeri, M., 2016. High-resolution temperature fields to evaluate the response of Italian electricity demand to meteorological variables: an example of climate service for the energy sector. *Theor. Appl. Climatol.* 125, 729–742.
- Spinoni, J., Vogt, J.V., Barbosa, P., Dosio, A., McCormick, N., Bigano, A., Füssel, H.M., 2018. Changes of heating and cooling degree-days in Europe from 1981 to 2100. *Int. J. Climatol.* 38, e191–e208. [eprint: https://onlinelibrary.wiley.com/doi/pdf/10.1002/joc.5362](https://onlinelibrary.wiley.com/doi/pdf/10.1002/joc.5362).
- Stefanon, M., D'Andrea, F., Drobinski, P., 2012. Heatwave classification over Europe and the Mediterranean region. *Environ. Res. Lett.* 7, 014023. Publisher: IOP Publishing.
- Stéfanon, M., Drobinski, P., D'Andrea, F., Lebeaupin-Brossier, C., Bastin, S., 2014. Soil moisture-temperature feedbacks at meso-scale during summer heat waves over Western Europe. *Clim Dyn* 42, 1309–1324.
- Tantet, A., Stéfanon, M., Drobinski, P., Badosa, J., Concettini, S., Cretí, A., D'Ambrosio, C., Thomopoulos, D., Tankov, P., 2019. e4clim 1.0: The Energy for a Climate Integrated Model: Description and Application to Italy. *Energies* 12, 4299.
- Vaittinada Ayar, P., Vrac, M., Bastin, S., Carreau, J., Déqué, M., Gallardo, C., 2016. Intercomparison of statistical and dynamical downscaling models under the EURO- and MED-CORDEX initiative framework: present climate evaluations. *Clim Dyn* 46, 1301–1329.
- Vigiúé, V., Lemonsu, A., Hallegatte, S., Beaulant, A.L., Marchadier, C., Masson, V., Pigeon, G., Salagnac, J.L., 2020. Early adaptation to heat waves and future reduction of air-conditioning energy use in Paris. *Environ. Res. Lett.* 15, 075006. Publisher: IOP Publishing.
- Voskamp, I.M., Sutton, N.B., Stremke, S., Rijnaarts, H.H.M., 2020. A systematic review of factors influencing spatiotemporal variability in urban water and energy consumption. *J. Cleaner Prod.* 256, 120310.
- Wenz, L., Levermann, A., Auffhammer, M., 2017. North-south polarization of European electricity consumption under future warming. *Proceedings of the National Academy of Sciences* 114, 201704339.
- Wiedenhofer, D., Lenzen, M., Steinberger, J.K., 2013. Energy requirements of consumption: Urban form, climatic and socio-economic factors, rebounds and their policy implications. *Energy Policy* 63, 696–707.
- You, Y., Kim, S., 2018. Revealing the mechanism of urban morphology affecting residential energy efficiency in Seoul, Korea. *Sustainable Cities Soc.* 43, 176–190.

Bibliography

- Jhud Mikhail Aberilla, Alejandro Gallego-Schmid, Laurence Stamford, and Adisa Azapagic. Design and environmental sustainability assessment of small-scale off-grid energy systems for remote rural communities. *Applied Energy*, 258:114004, 2020. ISSN 03062619. doi: 10.1016/j.apenergy.2019.114004. URL <https://linkinghub.elsevier.com/retrieve/pii/S0306261919316915>.
- ADEME, CODA STRATEGIES. La climatisation de confort dans les bâtiments résidentiels et tertiaires. Technical report, ADEME, 2021. URL https://bibliothèque.ademe.fr/air-et-bruit/4745-la-climatisation-de-confort-dans-les-batiments-residentiels-et-tertiaires.html?search_query=climatisation&results=46. 110 pages, <https://bibliothèque.ademe.fr>.
- Loris Amabile, Delphine Bresch-Pietri, Gilbert El Hajje, Sébastien Labbé, and Nicolas Petit. Optimizing the self-consumption of residential photovoltaic energy and quantification of the impact of production forecast uncertainties. *Advances in Applied Energy*, 2:100020, May 2021. ISSN 2666-7924. doi: 10.1016/j.adapen.2021.100020. URL <https://www.sciencedirect.com/science/article/pii/S2666792421000135>.
- APUR. Vers un cadastre solaire 2.0. 2019. https://www.apur.org/sites/default/files/documents/publication/documents-associes/note_148_cadastre_solaire.pdf?token=Gub3RT44.
- APUR. EMPRISE BATIE PARIS, 2020. URL <https://opendata.apur.org/maps/emprise-batie-paris>.
- Maximilian Auffhammer and Erin T. Mansur. Measuring climatic impacts on energy consumption: A review of the empirical literature. *Energy Economics*, 46:522–530, November 2014. ISSN 0140-9883. doi: 10.1016/j.eneco.2014.04.017. URL <https://www.sciencedirect.com/science/article/pii/S0140988314001017>.
- S. Avril, C. Mansilla, M. Busson, and T. Lemaire. Photovoltaic energy policy: Financial estimation and performance comparison of the public support in five representative countries. *Energy Policy*, 51:244–258, 2012. ISSN 0301-4215. doi: 10.1016/j.enpol.2012.07.050. URL <https://www.sciencedirect.com/science/article/pii/S0301421512006441>.
- K. Rushikesh Babu and C. Vyjayanthi. Implementation of net zero energy building (nzeb) prototype with renewable energy integration. In *2017 IEEE Region 10 Symposium (TENSYMP)*. IEEE, July 2017. doi: 10.1109/tenconspring.2017.8069994. URL <http://dx.doi.org/10.1109/TENCONSPRING.2017.8069994>.
- Salomé Bakaloglou and Dorothée Charlier. The role of individual preferences in explaining the energy performance gap. *Energy Economics*, 104:105611, December 2021. ISSN 0140-9883. doi: 10.1016/j.eneco.2021.105611. URL <https://www.sciencedirect.com/science/article/pii/S0140988321004771>.
- M. Beccali, M. Cellura, V. Lo Brano, and A. Marvuglia. Short-term prediction of household electricity consumption: Assessing weather sensitivity in a Mediterranean area. *Renewable and Sustainable Energy Reviews*, 12(8):2040–2065, October 2008. ISSN 1364-0321. doi: 10.1016/j.rser.2007.04.010. URL <https://www.sciencedirect.com/science/article/pii/S1364032107000664>.
- C. Becchio, S.P. Corgnati, C. Delmastro, V. Fabi, and P. Lombardi. The role of nearly-zero energy buildings in the transition towards post-carbon cities. *Sustainable Cities and Society*, 27:324–337, November 2016. ISSN 2210-6707. doi: 10.1016/j.scs.2016.08.005. URL <http://dx.doi.org/10.1016/J.SCS.2016.08.005>.
- Miroslav M. Begovic and Insu Kim. Distributed renewable PV generation in urban distribution networks. pages 1–3, March 2011. doi: 10.1109/PSCE.2011.5772614. URL <https://ieeexplore.ieee.org/document/5772614>.

- Marie Bessec and Julien Fouquau. The non-linear link between electricity consumption and temperature in Europe: A threshold panel approach. *Energy Economics*, 30(5):2705–2721, September 2008. ISSN 0140-9883. doi: 10.1016/j.eneco.2008.02.003. URL <https://www.sciencedirect.com/science/article/pii/S0140988308000418>.
- Yves Bettignies, Joao Meirelles, Gabriela Fernandez, Franziska Meinherz, Paul Hoekman, Philippe Bouillard, and Aristide Athanassiadis. The Scale-Dependent Behaviour of Cities: A Cross-Cities Multiscale Driver Analysis of Urban Energy Use. *Sustainability*, 11(12):3246, January 2019. ISSN 2071-1050. doi: 10.3390/su11123246. URL <https://www.mdpi.com/2071-1050/11/12/3246>. Number: 12 Publisher: Multidisciplinary Digital Publishing Institute.
- Christopher Bishop. *Pattern Recognition and Machine Learning*. Information Science and Statistics. Springer, New York, NY, 1 edition, aug 2006. ISBN 978-0-387-31073-2.
- A.A. Bouramdane, A. Tantet, and P. Drobinski. Utility-scale pv-battery versus csp-thermal storage in morocco: Storage and cost effect under penetration scenarios. *Energies*, 14(15), 2021. ISSN 1996-1073. doi: 10.3390/en14154675. URL <https://www.mdpi.com/1996-1073/14/15/4675>.
- Frédéric Branger, Louis-Gaëtan Giraudet, Céline Guivarch, and Philippe Quirion. Global sensitivity analysis of an energy–economy model of the residential building sector. *Environmental Modelling & Software*, 70:45–54, August 2015. ISSN 1364-8152. doi: 10.1016/j.envsoft.2015.03.021. URL <https://www.sciencedirect.com/science/article/pii/S1364815215001097>.
- Dean Brian and Dulac John. The global status report. Technical report, GABC, UNEP, 2016.
- NS Brito. Mismatch, exclusion and inclusion: Threats/opportunities for historic buildings in the current energy efficiency paradigm. *EECHB-2016 Energy Efficiency and Comfort of Historic Buildings*, page 18, 2016.
- Dirk Brounen, Nils Kok, and John M. Quigley. Residential energy use and conservation: Economics and demographics. *European Economic Review*, 56(5):931–945, July 2012. ISSN 0014-2921. doi: 10.1016/j.euroecorev.2012.02.007. URL <http://dx.doi.org/10.1016/J.EUROECOREV.2012.02.007>.
- Davide Calì, Tanja Osterhage, Rita Streblov, and Dirk Müller. Energy performance gap in refurbished German dwellings: Lesson learned from a field test. *Energy and Buildings*, 127:1146–1158, September 2016. ISSN 0378-7788. doi: 10.1016/j.enbuild.2016.05.020. URL <https://www.sciencedirect.com/science/article/pii/S0378778816303814>.
- Aldo Canova, Paolo Lazzeroni, Gianmarco Lorenti, Francesco Moraglio, Adamo Porcelli, and Maurizio Repetto. Decarbonizing residential energy consumption under the italian collective self-consumption regulation. *Sustainable Cities and Society*, 87:104196, December 2022. ISSN 2210-6707. doi: 10.1016/j.scs.2022.104196. URL <http://dx.doi.org/10.1016/j.scs.2022.104196>.
- Joan Carreras, Dieter Boer, Gonzalo Guillén-Gosálbez, Luisa F. Cabeza, Marc Medrano, and Laureano Jiménez. Multi-objective optimization of thermal modelled cubicles considering the total cost and life cycle environmental impact. *Energy and Buildings*, 88:335–346, February 2015. ISSN 0378-7788. doi: 10.1016/j.enbuild.2014.12.007. URL <http://dx.doi.org/10.1016/j.enbuild.2014.12.007>.
- E. Cayre, Benoit Allibe, Marie-Helene Laurent, and Dominique Osso. There are people in the house!: How the results of purely technical analysis of residential energy consumption are misleading for energy policies. volume 7, June 2011.
- Cespedes-Lopez, Mora-Garcia, Perez-Sanchez, and Perez-Sanchez. Meta-analysis of price premiums in housing with energy performance certificates (epc). *Sustainability*, 11(22):6303, November 2019. ISSN 2071-1050. doi: 10.3390/su11226303. URL <http://dx.doi.org/10.3390/su11226303>.
- Dorothee Charlier and Anna Risch. Evaluation of the impact of environmental public policy measures on energy consumption and greenhouse gas emissions in the french residential sector. *Energy Policy*, 46:170–184, July 2012. ISSN 0301-4215. doi: 10.1016/j.enpol.2012.03.048. URL <http://dx.doi.org/10.1016/J.ENPOL.2012.03.048>.
- Dorothee Charlier, Anna Risch, and Claire Salmon. Energy burden alleviation and greenhouse gas emissions reduction: Can we reach two objectives with one policy? *Ecological Economics*, 143:294–313, jan 2018. ISSN 0921-8009. doi: 10.1016/j.ecolecon.2017.07.002. URL <http://dx.doi.org/10.1016/j.ecolecon.2017.07.002>.

- Hung-Chu Chen, Qi Han, and Bauke De Vries. Modeling the spatial relation between urban morphology, land surface temperature and urban energy demand. *Sustainable Cities and Society*, 60:102246, September 2020a. ISSN 2210-6707. doi: 10.1016/j.scs.2020.102246. URL <https://www.sciencedirect.com/science/article/pii/S2210670720304674>.
- Hung-Chu Chen, Qi Han, and Bauke de Vries. Urban morphology indicator analyzes for urban energy modeling. *Sustainable Cities and Society*, 52:101863, January 2020b. ISSN 2210-6707. doi: 10.1016/j.scs.2019.101863. URL <https://www.sciencedirect.com/science/article/pii/S2210670719313162>.
- Raymond J. Cole and Laura Fedoruk. Shifting from net-zero to net-positive energy buildings. *Building Research & Information*, 43(1):111–120, October 2014. ISSN 1466-4321. doi: 10.1080/09613218.2014.950452. URL <http://dx.doi.org/10.1080/09613218.2014.950452>.
- Francesco Pietro Colelli, Ian Sue Wing, and Enrica De Cian. Air-conditioning adoption and electricity demand highlight climate change mitigation–adaptation tradeoffs. *Sci Rep*, 13(1):4413, March 2023. ISSN 2045-2322. doi: 10.1038/s41598-023-31469-z. URL <https://www.nature.com/articles/s41598-023-31469-z>.
- Richard C. Cornes, Gerard van der Schrier, Else J. M. van den Besselaar, and Philip D. Jones. An Ensemble Version of the E-OBS Temperature and Precipitation Data Sets. *Journal of Geophysical Research: Atmospheres*, 123(17):9391–9409, 2018. ISSN 2169-8996. doi: 10.1029/2017JD028200. URL <https://onlinelibrary.wiley.com/doi/abs/10.1029/2017JD028200>. _eprint: <https://onlinelibrary.wiley.com/doi/pdf/10.1029/2017JD028200>.
- Council of European Union. Energy performance of buildings directive, 2018. URL https://energy.ec.europa.eu/topics/energy-efficiency/energy-efficient-buildings/energy-performance-buildings-directive_en. Directive (EU) 2018/844.
- Bryan Coyne and Eleanor Denny. Mind the energy performance gap: testing the accuracy of building energy performance certificates in ireland. *Energy Efficiency*, 14(6), July 2021. ISSN 1570-6478. doi: 10.1007/s12053-021-09960-1. URL <http://dx.doi.org/10.1007/s12053-021-09960-1>.
- Stefano Cozza, Jonathan Chambers, Chirag Deb, Jean-Louis Scartezzini, Arno Schlüter, and Martin K. Patel. Do energy performance certificates allow reliable predictions of actual energy consumption and savings? Learning from the Swiss national database. *Energy and Buildings*, 224:110235, October 2020a. ISSN 0378-7788. doi: 10.1016/j.enbuild.2020.110235. URL <https://www.sciencedirect.com/science/article/pii/S0378778820303315>.
- Stefano Cozza, Jonathan Chambers, and Martin K. Patel. Measuring the thermal energy performance gap of labelled residential buildings in switzerland. *Energy Policy*, 137:111085, February 2020b. ISSN 0301-4215. doi: 10.1016/j.enpol.2019.111085. URL <http://dx.doi.org/10.1016/j.enpol.2019.111085>.
- Stefano Cozza, Jonathan Chambers, Arianna Brambilla, and Martin K. Patel. In search of optimal consumption: A review of causes and solutions to the Energy Performance Gap in residential buildings. *Energy and Buildings*, 249:111253, October 2021. ISSN 0378-7788. doi: 10.1016/j.enbuild.2021.111253. URL <https://www.sciencedirect.com/science/article/pii/S0378778821005375>.
- Wolfgang Cramer, Joël Guiot, Marianela Fader, Joaquim Garrabou, Jean-Pierre Gattuso, Ana Iglesias, Manfred A. Lange, Piero Lionello, Maria Carmen Llasat, Shlomit Paz, Josep Peñuelas, Maria Snoussi, Andrea Toret, Michael N. Tsimplis, and Elena Xoplaki. Climate change and interconnected risks to sustainable development in the mediterranean. *Nature Climate Change*, 8(11):972–980, 2018. ISSN 1758-6798. doi: 10.1038/s41558-018-0299-2. URL <https://www.nature.com/articles/s41558-018-0299-2>. Publisher: Nature Publishing Group.
- Alberto Cuchí Burgos and Peter Sweatman. *A National Perspective of Spain's Buildings Sector: A Roadmap for a New Housing Sector*, Green Building Council Espana and Fundacion Conama. 2011.
- Ivan Cuesta-Fernández, Carlos Vargas-Salgado, David Alfonso-Solar, and Tomás Gómez-Navarro. The contribution of metropolitan areas to decarbonize the residential stock in mediterranean cities: A GIS-based assessment of rooftop PV potential in valencia, spain. *Sustainable Cities and Society*, 97:104727, 2023. ISSN 2210-6707. doi: 10.1016/j.scs.2023.104727. URL <https://www.sciencedirect.com/science/article/pii/S2210670723003384>.

- Clement Dagueuet, Paul Gredigui, Fernanda Teixeira Costa, Matthieu Maugenest, Damian Pedro Saint Martin, and Narciso Sena Fracaroli. *Évolution des besoins en chaud et en froid dans le secteur résidentiel*, 2021. URL https://ecoledespoints.fr/sites/ecoledespoints.fr/files/documents/rapport_seminaire_departement_sp_chaud_froid.pdf.
- Andrea Damm, Judith Köberl, Franz Pretenthaler, Nikola Rogler, and Christoph Töglhofer. Impacts of +2 °C global warming on electricity demand in Europe. *Climate Services*, 7:12–30, August 2017. ISSN 24058807. doi: 10.1016/j.cliser.2016.07.001. URL <https://linkinghub.elsevier.com/retrieve/pii/S2405880716300012>.
- Dodman Davi, Hayward Bronwyn, Pelling Mark, Castán Broto Vanesa, Chow Winston, Chu Eric, Dawson Richard, Khirfan Luna, McPhearson Timon, Prakash Anjal, Zheng Yan, and Ziervogel Gina. *Cities, Settlements and Key Infrastructure*. Cambridge University Press, 1 edition, 2022. ISBN 978-1-00-932584-4. doi: 10.1017/9781009325844. URL <https://www.cambridge.org/core/product/identifier/9781009325844/type/book>.
- Enrica De Cian and Ian Sue Wing. Global Energy Demand in a Warming Climate. *SSRN Journal*, 2016. ISSN 1556-5068. doi: 10.2139/ssrn.2744532. URL <http://www.ssrn.com/abstract=2744532>.
- Matteo De Felice, Andrea Alessandri, and Paolo M. Ruti. Electricity demand forecasting over Italy: Potential benefits using numerical weather prediction models. *Electric Power Systems Research*, 104:71–79, November 2013. ISSN 0378-7796. doi: 10.1016/j.epr.2013.06.004. URL <https://www.sciencedirect.com/science/article/pii/S0378779613001545>.
- Carsten F. Dormann, Jane Elith, Sven Bacher, Carsten Buchmann, Gudrun Carl, Gabriel Carré, Jaime R. García Marquéz, Bernd Gruber, Bruno Lafourcade, Pedro J. Leitão, Tamara Münkemüller, Colin McClean, Patrick E. Osborne, Björn Reineking, Boris Schröder, Andrew K. Skidmore, Damaris Zurell, and Sven Lautenbach. Collinearity: a review of methods to deal with it and a simulation study evaluating their performance. *Ecography*, 36(1):27–46, May 2012. ISSN 1600-0587. doi: 10.1111/j.1600-0587.2012.07348.x. URL <http://dx.doi.org/10.1111/j.1600-0587.2012.07348.x>.
- Philippe Drobinski, Nicolas Da Silva, Gérémy Panthou, Sophie Bastin, Caroline Muller, Bodo Ahrens, Marco Borgia, Dario Conte, Giorgia Fosser, Filippo Giorgi, Ivan Güttler, Vassiliki Kotroni, Laurent Li, Efrat Morin, Barış Önoğlu, Pere Quintana-Seguí, Raquel Romera, and Csaba Zsolt Torma. Scaling precipitation extremes with temperature in the Mediterranean: past climate assessment and projection in anthropogenic scenarios. *Clim Dyn*, 51(3):1237–1257, August 2018. ISSN 1432-0894. doi: 10.1007/s00382-016-3083-x. URL <https://doi.org/10.1007/s00382-016-3083-x>.
- Peter Droege. *Urban Energy Transition: Renewable Strategies for Cities and Regions*. Elsevier, 2018. ISBN 978-0-08-102075-3. Google-Books-ID: f7FoDwAAQBAJ.
- A. Druckman and T. Jackson. Household energy consumption in the uk: A highly geographically and socio-economically disaggregated model. *Energy Policy*, 36(8):3177–3192, August 2008. ISSN 0301-4215. doi: 10.1016/j.enpol.2008.03.021. URL <http://dx.doi.org/10.1016/J.ENPOL.2008.03.021>.
- ECA&D. E-OBS data access. https://knmi-ecad-assets-prd.s3.amazonaws.com/ensembles/data/Grid_0.1deg_reg_ensemble/tg_ens_mean_0.1deg_reg_v20.0e.nc, May 2020. Last visited 2021-06-13.
- M. Economidou, V. Todeschi, P. Bertoldi, D. D’Agostino, P. Zangheri, and L. Castellazzi. Review of 50 years of EU energy efficiency policies for buildings. *Energy and Buildings*, 225:110322, October 2020. ISSN 0378-7788. doi: 10.1016/j.enbuild.2020.110322. URL <https://www.sciencedirect.com/science/article/pii/S0378778820317229>.
- Piet Eichholtz, Nils Kok, and John M Quigley. Doing well by doing good? green office buildings. *American Economic Review*, 100(5):2492–2509, December 2010. ISSN 0002-8282. doi: 10.1257/aer.100.5.2492. URL <http://dx.doi.org/10.1257/aer.100.5.2492>.
- Piet Eichholtz, Nils Kok, and John M. Quigley. The economics of green building. *Review of Economics and Statistics*, 95(1):50–63, March 2013. ISSN 1530-9142. doi: 10.1162/rest_a_00291. URL http://dx.doi.org/10.1162/REST_a_00291.

- Chukwuemeka Chinonso Emenekwe and Nnaemeka Vincent Emodi. Temperature and Residential Electricity Demand for Heating and Cooling in G7 Economies: A Method of Moments Panel Quantile Regression Approach. *Climate*, 10(10):142, October 2022. ISSN 2225-1154. doi: 10.3390/cli10100142. URL <https://www.mdpi.com/2225-1154/10/10/142>. Number: 10 Publisher: Multidisciplinary Digital Publishing Institute.
- Nnaemeka Vincent Emodi, Taha Chaiechi, and ABM Rabiul Alam Beg. The impact of climate change on electricity demand in Australia. *Energy & Environment*, 29(7):1263–1297, November 2018. ISSN 0958-305X, 2048-4070. doi: 10.1177/0958305X18776538. URL <http://journals.sagepub.com/doi/10.1177/0958305X18776538>.
- Enedis. Enedis consumption database, 2018. URL <https://data.enedis.fr/explore/dataset/consommation-electrique-par-secteur-dactivite-iris/information/>.
- Enedis. Consommation et thermosensibilité électriques par secteur d’activité à la maille IRIS. <https://data.enedis.fr/explore/dataset/consommation-electrique-par-secteur-dactivite-iris/>, 2020. Last visited 2020-09-30.
- Gunnar S. Eskeland and Torben K. Mideksa. Electricity demand in a changing climate. *Mitig Adapt Strateg Glob Change*, 15(8):877–897, December 2010. ISSN 1573-1596. doi: 10.1007/s11027-010-9246-x. URL <https://doi.org/10.1007/s11027-010-9246-x>.
- European Commission. Renovation and decarbonisation of buildings, 2021. URL https://ec.europa.eu/commission/presscorner/detail/en/IP_21_6683.
- European Parliament and Council. Directive 2010/31/EU of the European Parliament and of the Council of 19 May 2010 on the energy performance of buildings (recast), January 2021. URL <http://data.europa.eu/eli/dir/2010/31/2021-01-01/eng>. Legislative Body: OP_DATPRO.
- EUROSTAT. Heating and cooling degree days - statistics. URL https://ec.europa.eu/eurostat/statistics-explained/index.php?title=Heating_and_cooling_degree_days_-_statistics.
- Eurostat. Electricity prices for household consumers - bi-annual data (from 2007 onwards). https://ec.europa.eu/eurostat/databrowser/view/nrg_pc_204/bookmark/table?lang=en&bookmarkId=60713508-c664-4f2a-a5c7-b8116123291d, 2023. [Accessed 13-03-2024].
- Emmanouil Flaounas, Philippe Drobinski, and Sophie Bastin. Dynamical downscaling of IPSL-CM5 CMIP5 historical simulations over the Mediterranean: benefits on the representation of regional surface winds and cyclogenesis. *Clim Dyn*, 40(9):2497–2513, May 2013a. ISSN 1432-0894. doi: 10.1007/s00382-012-1606-7. URL <https://doi.org/10.1007/s00382-012-1606-7>.
- Emmanouil Flaounas, Philippe Drobinski, Sophie Bastin, Cindy Lebeau-pin Brossier, Marco Borga, Mathieu Vrac, Jean-Christophe Calvet, and Marc Stéfanon. Precipitation and temperature space-time variability and extremes in the mediterranean region: Evaluation of dynamical and statistical downscaling methods. *Climate Dynamics*, 40, 06 2013b. doi: 10.1007/s00382-012-1558-y.
- France. Décret,n° 2017-676 du 28 avril 2017 relatif à l’autoconsommation d’électricité et modifiant les articles d. 314-15 et d. 314-23 à d. 314-25 du code de l’énergie - légifrance, 2017. URL <https://www.legifrance.gouv.fr/jorf/id/JORFTEXT000034517272>.
- Elisha Frederiks, Karen Stenner, and Elizabeth Hobman. The Socio-Demographic and Psychological Predictors of Residential Energy Consumption: A Comprehensive Review. *Energies*, 8(1):573–609, January 2015. ISSN 1996-1073. doi: 10.3390/en8010573. URL <http://www.mdpi.com/1996-1073/8/1/573>.
- Christoph Frei, Jens Hesselbjerg Christensen, Michel Déqué, Daniela Jacob, Richard G. Jones, and Pier Luigi Vidale. Daily precipitation statistics in regional climate models: Evaluation and intercomparison for the European Alps. *Journal of Geophysical Research: Atmospheres*, 108(D3), 2003. ISSN 2156-2202. doi: 10.1029/2002JD002287. URL <https://onlinelibrary.wiley.com/doi/abs/10.1029/2002JD002287>. _eprint: <https://onlinelibrary.wiley.com/doi/pdf/10.1029/2002JD002287>.

- Franz Fuerst, Patrick McAllister, Anupam Nanda, and Peter Wyatt. Does energy efficiency matter to homebuyers? an investigation of epc ratings and transaction prices in england. *Energy Economics*, 48:145–156, March 2015. ISSN 0140-9883. doi: 10.1016/j.eneco.2014.12.012. URL <http://dx.doi.org/10.1016/j.eneco.2014.12.012>.
- Paul J. Gertler, Orié Shelef, Catherine D. Wolfram, and Alan Fuchs. The demand for energy-using assets among the world’s rising middle classes. *American Economic Review*, 106(6):1366–1401, 2016. ISSN 0002-8282. doi: 10.1257/aer.20131455. URL <https://www.aeaweb.org/articles?id=10.1257/aer.20131455>.
- Louis-Gaëtan Giraudet, Céline Guivarch, and Philippe Quirion. Exploring the potential for energy conservation in French households through hybrid modeling. *Energy Economics*, 34(2):426–445, March 2012. ISSN 0140-9883. doi: 10.1016/j.eneco.2011.07.010. URL <https://www.sciencedirect.com/science/article/pii/S014098831100140X>.
- Louis-Gaëtan Giraudet, Cyril Bourgeois, and Philippe Quirion. Policies for low-carbon and affordable home heating: A french outlook. *Energy Policy*, 151:112140, apr 2021. ISSN 0301-4215. doi: 10.1016/j.enpol.2021.112140. URL <http://dx.doi.org/10.1016/j.enpol.2021.112140>.
- S. Hallegatte, J.C. Hourcade, and P. Ambrosi. Using climate analogues for assessing climate change economic impacts in urban areas. *Climatic Change*, 82:47–60, 2007. doi: 10.1007/s10584-006-9161-z. URL <https://doi.org/10.1007/s10584-006-9161-z>.
- Trevor Hastie, Robert Tibshirani, and Jerome Friedman. *The Elements of Statistical Learning*. Springer New York, 2009. ISBN 9780387848587. doi: 10.1007/978-0-387-84858-7. URL <http://dx.doi.org/10.1007/978-0-387-84858-7>.
- M. R. Haylock and C. M. Goodess. Interannual variability of European extreme winter rainfall and links with mean large-scale circulation. *Int. J. Climatol.*, 24(6):759–776, May 2004. ISSN 0899-8418, 1097-0088. doi: 10.1002/joc.1033. URL <https://onlinelibrary.wiley.com/doi/10.1002/joc.1033>.
- M. R. Haylock, N. Hofstra, A. M. G. Klein Tank, E. J. Klok, P. D. Jones, and M. New. A European daily high-resolution gridded data set of surface temperature and precipitation for 1950–2006. *Journal of Geophysical Research: Atmospheres*, 113(D20), 2008. ISSN 2156-2202. doi: 10.1029/2008JD010201. URL <https://onlinelibrary.wiley.com/doi/abs/10.1029/2008JD010201>. _eprint: <https://onlinelibrary.wiley.com/doi/pdf/10.1029/2008JD010201>.
- Pan He, Pengfei Liu, Yueming (Lucy) Qiu, and Lufan Liu. The weather affects air conditioner purchases to fill the energy efficiency gap. *Nature Communications*, 13(1):5772, 2022. ISSN 2041-1723. doi: 10.1038/s41467-022-33531-2. URL <https://www.nature.com/articles/s41467-022-33531-2>. Number: 1 Publisher: Nature Publishing Group.
- T. Hoff and D.S. Shugar. The value of grid-support photovoltaics in reducing distribution system losses. *IEEE Transactions on Energy Conversion*, 10(3):569–576, September 1995. ISSN 1558-0059. doi: 10.1109/60.464884. URL <https://ieeexplore.ieee.org/document/464884>. Conference Name: IEEE Transactions on Energy Conversion.
- Matthew J. Hoffmann. *Climate Governance at the Crossroads: Experimenting with a Global Response after Kyoto*. Oxford University Press, 2011. ISBN 978-0-19-983833-2. Google-Books-ID: 8sOnHfu69GgC.
- Jean-Charles Hourcade, Mark Jaccard, Chris Bataille, and Frédéric Ghersi. Hybrid modeling: New answers to old challenges introduction to the special issue of the energy journal. *The Energy Journal*, 27(2_suppl):1–11, 2006. ISSN 1944-9089. doi: 10.5547/issn0195-6574-ej-volsi2006-nosi2-1. URL <https://journals.sagepub.com/doi/10.5547/ISSN0195-6574-EJ-VolSI2006-NoSI2-1>.
- IEA. World Energy Outlook 2020 – Analysis, 2020. URL <https://www.iea.org/reports/world-energy-outlook-2020>.
- IEA. Approximately 100 million households rely on rooftop solar pv by 2030. <https://www.iea.org/reports/approximately-100-million-households-rely-on-rooftop-solar-pv-by-2030>, 2022. Accessed: 2024-3-28.
- IEA and Dr Fatih Birol. Key World Energy Statistics 2021. 2021.

- IGN. Contours...iris © - descriptif de contenu et de livraison. Technical report, Institut Géographique National, 2009. https://geoservices.ign.fr/sites/default/files/2022-03/DC_DL_Contours_Iris_09.pdf.
- INSEE. Revenus, pauvreté et niveau de vie en 2017 (iris). <https://www.insee.fr/fr/statistiques/6049648>, 2017. URL <https://www.insee.fr/fr/statistiques/6049648>. [Accessed 10-04-2024].
- International Energy Agency. Cooling degree days in France, 2000-2020 – Charts – Data & Statistics. URL <https://www.iea.org/data-and-statistics/charts/cooling-degree-days-in-france-2000-2020>.
- International Energy Agency. *The Future of Cooling*. 2018. doi: <https://doi.org/https://doi.org/10.1787/9789264301993-en>. URL <https://www.oecd-ilibrary.org/content/publication/9789264301993-en>.
- International Energy Agency. *France 2021 Energy Policy Review*. IEA Energy Policy Reviews. OECD, December 2021. ISBN 978-92-64-73411-1. doi: 10.1787/2c889667-en. URL https://www.oecd-ilibrary.org/energy/france-2021-energy-policy-review_2c889667-en.
- International Energy Agency. Renewables 2023 Analysis and forecast to 2028. https://iea.blob.core.windows.net/assets/96d66a8b-d502-476b-ba94-54ffda84cf72/Renewables_2023.pdf, 2023. [Accessed 12-03-2024].
- Daniela Jacob, Juliane Petersen, Bastian Eggert, Antoinette Alias, Ole Bøssing Christensen, Laurens M. Boucher, Alain Braun, Augustin Colette, Michel Déqué, Goran Georgievski, Elena Georgopoulou, Andreas Gobiet, Laurent Menut, Grigory Nikulin, Andreas Haensler, Nils Hempelmann, Colin Jones, Klaus Keuler, Sari Kovats, Nico Kröner, Sven Kotlarski, Arne Kriegsmann, Eric Martin, Erik van Meijgaard, Christopher Moseley, Susanne Pfeifer, Swantje Preuschmann, Christine Radermacher, Kai Radtke, Diana Rechid, Mark Rounsevell, Patrick Samuelsson, Samuel Somot, Jean-Francois Soussana, Claas Teichmann, Riccardo Valentini, Robert Vautard, Björn Weber, and Pascal Yiou. EURO-CORDEX: new high-resolution climate change projections for European impact research. *Reg Environ Change*, 14(2):563–578, April 2014. ISSN 1436-378X. doi: 10.1007/s10113-013-0499-2. URL <https://doi.org/10.1007/s10113-013-0499-2>.
- Astier Jeanne, Salem Ariane, Fack Gabrielle, Fournel Julien, and Maisonneuve Flavie. cae-eco.fr. <https://www.cae-eco.fr/staticfiles/pdf/focus-103-dpe-230110.pdf>, 2024. [Accessed 04-04-2024].
- Christopher A. Kennedy, Iain Stewart, Angelo Facchini, Igor Cersosimo, Renata Mele, Bin Chen, Mariko Uda, Arun Kansal, Anthony Chiu, Kwi-gon Kim, Carolina Dubeux, Emilio Lebre La Rovere, Bruno Cunha, Stephanie Pincetl, James Keirstead, Sabine Barles, Semerdanta Pusaka, Juniati Gunawan, Michael Adegbile, Mehrdad Nazariha, Shamsul Hoque, Peter J. Marcotullio, Florencia González Otharín, Tarek Genena, Nadine Ibrahim, Rizwan Farooqui, Gemma Cervantes, and Ahmet Duran Sahin. Energy and material flows of megacities. *Proceedings of the National Academy of Sciences*, 112(19):5985, 2015. ISSN 0027-8424. URL https://www.academia.edu/28925031/Energy_and_material_flows_of_megacities.
- Aras Khazal and Ole Jakob Sønstebo. Valuation of energy performance certificates in the rental market – Professionals vs. nonprofessionals. *Energy Policy*, 147:111830, December 2020. ISSN 0301-4215. doi: 10.1016/j.enpol.2020.111830. URL <https://www.sciencedirect.com/science/article/pii/S0301421520305474>.
- Charles J. Kibert and Maryam Mirhadi Fard. Differentiating among low-energy, low-carbon and net-zero-energy building strategies for policy formulation. *Building Research & Information*, 40(5):625–637, October 2012. ISSN 1466-4321. doi: 10.1080/09613218.2012.703489. URL <http://dx.doi.org/10.1080/09613218.2012.703489>.
- Erik Kjellström, Fredrik Boberg, Manuel Castro, Jens Christensen, Grigory Nikulin, and Enrique Sanchez. Daily and monthly temperature and precipitation statistics as performance indicators for regional climate models. *Climate Research*, 44:135–150, June 2010. ISSN 0936-577X. doi: 10.3354/cr00932.
- E. J. Klok and A. M. G. Klein Tank. Updated and extended European dataset of daily climate observations. *Int. J. Climatol.*, 29(8):1182–1191, June 2009. ISSN 08998418, 10970088. doi: 10.1002/joc.1779. URL <https://onlinelibrary.wiley.com/doi/10.1002/joc.1779>.
- Joshua Kneifel and David Webb. Predicting energy performance of a net-zero energy building: A statistical approach. *Applied Energy*, 178:468–483, September 2016. ISSN 0306-2619. doi: 10.1016/j.apenergy.2016.06.013. URL <http://dx.doi.org/10.1016/J.APENERGY.2016.06.013>.
- W Köppen. Das geographische system der klimate. page 46 pp., 1936.

- S. Kozarcanin, G. B. Andresen, and I. Staffell. Estimating country-specific space heating threshold temperatures from national gas and electricity consumption data. *Energy and Buildings*, 199:368–380, September 2019. ISSN 0378-7788. doi: 10.1016/j.enbuild.2019.07.013. URL <https://www.sciencedirect.com/science/article/pii/S0378778819303317>.
- Kyoto Protocol. Kyoto protocol to the united nations framework convention on climate change.
- M.A.D. Larsen, S. Petrović, A.M. Radoszynski, R. McKenna, and O. Balyk. Climate change impacts on trends and extremes in future heating and cooling demands over Europe. *Energy and Buildings*, 226:110397, November 2020. ISSN 03787788. doi: 10.1016/j.enbuild.2020.110397. URL <https://linkinghub.elsevier.com/retrieve/pii/S0378778820309737>.
- A. Lemonsu, V. Viguié, M. Daniel, and V. Masson. Vulnerability to heat waves: Impact of urban expansion scenarios on urban heat island and heat stress in Paris (France). *Urban Climate*, 14:586–605, December 2015. ISSN 2212-0955. doi: 10.1016/j.uclim.2015.10.007. URL <https://www.sciencedirect.com/science/article/pii/S2212095515300316>.
- Huan Li and Mei-Po Kwan. Advancing analytical methods for urban metabolism studies. *Resources, Conservation and Recycling*, 132:239–245, May 2018. ISSN 0921-3449. doi: 10.1016/j.resconrec.2017.07.005. URL <https://www.sciencedirect.com/science/article/pii/S0921344917301842>.
- Jochen Linssen, Peter Stenzel, and Johannes Fler. Techno-economic analysis of photovoltaic battery systems and the influence of different consumer load profiles. *Applied Energy*, 185:2019–2025, 2017. URL <https://ideas.repec.org/a/eee/appene/v185y2017ip2p2019-2025.html>. Publisher: Elsevier.
- Mengxue Lu and Joseph H.K. Lai. Building energy: a review on consumptions, policies, rating schemes and standards. *Energy Procedia*, 158:3633–3638, February 2019. ISSN 1876-6102. doi: 10.1016/j.egypro.2019.01.899. URL <http://dx.doi.org/10.1016/j.egypro.2019.01.899>.
- Jean-Pierre Lévy and Fateh Belaïd. The determinants of domestic energy consumption in France: Energy modes, habitat, households and life cycles. *Renewable and Sustainable Energy Reviews*, 81:2104–2114, January 2018. ISSN 1364-0321. doi: 10.1016/j.rser.2017.06.022. URL <https://www.sciencedirect.com/science/article/pii/S1364032117309632>.
- D. Majcen, L. C. M. Itard, and H. Visscher. Theoretical vs. actual energy consumption of labelled dwellings in the Netherlands: Discrepancies and policy implications. *Energy Policy*, 54:125–136, March 2013. ISSN 0301-4215. doi: 10.1016/j.enpol.2012.11.008. URL <https://www.sciencedirect.com/science/article/pii/S0301421512009731>.
- Georgios Martinopoulos, Konstantinos T. Papakostas, and Agis M. Papadopoulos. A comparative review of heating systems in EU countries, based on efficiency and fuel cost. *Renewable and Sustainable Energy Reviews*, 90:687–699, 2018. ISSN 1364-0321. doi: 10.1016/j.rser.2018.03.060. URL <https://www.sciencedirect.com/science/article/pii/S1364032118301333>.
- Bardia Mashhoodi and Arjan van Timmeren. Local determinants of household gas and electricity consumption in randstad region, netherlands: application of geographically weighted regression. *Spatial Information Research*, 26(6):607–618, July 2018. ISSN 2366-3294. doi: 10.1007/s41324-018-0203-1. URL <http://dx.doi.org/10.1007/s41324-018-0203-1>.
- Hicham Mastouri, Hicham Bahi, Hassan Radoine, and Brahim Benhamou. Improving energy efficiency in buildings: Review and compiling. *Materials Today: Proceedings*, 27:2999–3003, 2020. ISSN 2214-7853. doi: 10.1016/j.matpr.2020.03.270. URL <http://dx.doi.org/10.1016/j.matpr.2020.03.270>.
- Sandrine Mathy, Meike Fink, and Ruben Bibas. Rethinking the role of scenarios: Participatory scripting of low-carbon scenarios for france. *Energy Policy*, 77:176–190, February 2015. ISSN 0301-4215. doi: 10.1016/j.enpol.2014.11.002. URL <http://dx.doi.org/10.1016/J.ENPOL.2014.11.002>.
- Konstantinos Mavroyeoryos, Ioannis Engonopoulos, Hristos Tyralis, Panayiotis Dimitriadis, and Demetris Koutsoyiannis. Simulation of electricity demand in a remote island for optimal planning of a hybrid renewable energy system. *Energy Procedia*, 125:435–442, 2017. ISSN 18766102. doi: 10.1016/j.egypro.2017.08.095. URL <https://linkinghub.elsevier.com/retrieve/pii/S1876610217335786>.

- Allan Mazur. How does population growth contribute to rising energy consumption in america? *Population and Environment*, 15(5):371–378, May 1994. ISSN 1573-7810. doi: 10.1007/bf02208318. URL <http://dx.doi.org/10.1007/BF02208318>.
- Gary C. McDonald. Ridge regression. *WIREs Computational Statistics*, 1(1):93–100, July 2009. ISSN 1939-0068. doi: 10.1002/wics.14. URL <http://dx.doi.org/10.1002/wics.14>.
- Qinglong Meng, Chengyan Xiong, Monjur Mourshed, Mengdi Wu, Xiaoxiao Ren, Wenqiang Wang, Yang Li, and Hui Song. Change-point multivariable quantile regression to explore effect of weather variables on building energy consumption and estimate base temperature range. *Sustainable Cities and Society*, 53:101900, February 2020. ISSN 2210-6707. doi: 10.1016/j.scs.2019.101900. URL <https://www.sciencedirect.com/science/article/pii/S2210670719311552>.
- Zhifu Mi, Dabo Guan, Zhu Liu, Jingru Liu, Vincent Viguié, Neil Fromer, and Yutao Wang. Cities: The core of climate change mitigation. *Journal of Cleaner Production*, 207:582–589, 2019. ISSN 0959-6526. doi: 10.1016/j.jclepro.2018.10.034. URL <https://www.sciencedirect.com/science/article/pii/S0959652618330488>.
- Haleh Moghaddasi, Charles Culp, and Jorge Vanegas. Net zero energy communities: Integrated power system, building and transport sectors. *Energies*, 14(21):7065, October 2021. ISSN 1996-1073. doi: 10.3390/en14217065. URL <http://dx.doi.org/10.3390/en14217065>.
- I. Montero, MT. Miranda, F. Barrena, F. J. Sepúlveda, and J. I. Arranz. Analysis of photovoltaic self-consumption systems for hospitals in southwestern Europe. *Energy and Buildings*, 269:112254, August 2022. ISSN 0378-7788. doi: 10.1016/j.enbuild.2022.112254. URL <https://www.sciencedirect.com/science/article/pii/S037877882200425X>.
- Julián Moral-Carcedo and José Vicéns-Otero. Modelling the non-linear response of Spanish electricity demand to temperature variations. *Energy Economics*, 27(3):477–494, May 2005. ISSN 01409883. doi: 10.1016/j.eneco.2005.01.003. URL <https://linkinghub.elsevier.com/retrieve/pii/S0140988305000174>.
- Satyen Mukherjee. Opportunities and challenges with net zero energy buildings. In *2011 IEEE 23rd International Symposium on Power Semiconductor Devices and ICs*. IEEE, May 2011. doi: 10.1109/ispd.2011.5890776. URL <http://dx.doi.org/10.1109/ISPSD.2011.5890776>.
- Kevin P. Murphy. *Machine learning: a probabilistic perspective*. Adaptive computation and machine learning series. MIT Press, Cambridge, Mass., 4. print. (fixed many typos) edition, 2013. ISBN 978-0-262-01802-9.
- Frits Møller Andersen, Helge V. Larsen, and Trine Krogh Boomsma. Long-term forecasting of hourly electricity load: Identification of consumption profiles and segmentation of customers. *Energy Conversion and Management*, 68:244–252, 2013. ISSN 0196-8904. doi: 10.1016/j.enconman.2013.01.018.
- Paresh Kumar Narayan, Russell Smyth, and Arti Prasad. Electricity consumption in G7 countries: A panel cointegration analysis of residential demand elasticities. *Energy Policy*, 35(9):4485–4494, September 2007. ISSN 0301-4215. doi: 10.1016/j.enpol.2007.03.018. URL <https://www.sciencedirect.com/science/article/pii/S0301421507001061>.
- Nima Narjabadifam, Mohammed Al-Saffar, Yongquan Zhang, Joseph Nofech, Asdrubal Cheng Cen, Hadia Awad, Michael Versteeg, and Mustafa Gül. Framework for mapping and optimizing the solar rooftop potential of buildings in urban systems. *Energies*, 15(5):1738, 2022. ISSN 1996-1073. doi: 10.3390/en15051738. URL <https://www.mdpi.com/1996-1073/15/5/1738>. Number: 5 Publisher: Multidisciplinary Digital Publishing Institute.
- Jonathan Natanian, Or Aleksandrowicz, and Thomas Auer. A parametric approach to optimizing urban form, energy balance and environmental quality: The case of mediterranean districts. *Applied Energy*, 254:113637, 2019. ISSN 0306-2619. doi: 10.1016/j.apenergy.2019.113637. URL <https://www.sciencedirect.com/science/article/pii/S0306261919313248>.
- Angelos I. Nousdilis, Georgios C. Christoforidis, and Grigoris K. Papagiannis. Active power management in low voltage networks with high photovoltaics penetration based on prosumers’ self-consumption. *Applied Energy*, 229:614–624, November 2018. ISSN 0306-2619. doi: 10.1016/j.apenergy.2018.08.032. URL <https://www.sciencedirect.com/science/article/pii/S0306261918311875>.

- Renee Obringer, Roshanak Nateghi, Debora Maia-Silva, Sayanti Mukherjee, Vineeth Cr, Douglas Brent McRoberts, and Rohini Kumar. Implications of Increasing Household Air Conditioning Use Across the United States Under a Warming Climate. *Earth's Future*, 10(1):e2021EF002434, 2022. ISSN 2328-4277. doi: 10.1029/2021EF002434. URL <https://onlinelibrary.wiley.com/doi/abs/10.1029/2021EF002434>. _eprint: <https://onlinelibrary.wiley.com/doi/pdf/10.1029/2021EF002434>.
- Observatoire national de la rénovation énergétique ONRE. Les rénovations énergétiques aidées du secteur résidentiel entre 2016 et 2020 - résultats provisoire. URL <https://www.statistiques.developpement-durable.gouv.fr/media/6235/download?inline>.
- Giorgio Pagliarini, Carlotta Bonfiglio, and Pamela Vocale. Outdoor temperature sensitivity of electricity consumption for space heating and cooling: An application to the city of Milan, North of Italy. *Energy and Buildings*, 204:109512, December 2019. ISSN 03787788. doi: 10.1016/j.enbuild.2019.109512. URL <https://linkinghub.elsevier.com/retrieve/pii/S0378778819317360>.
- Paris Agreement. Paris agreement to the united nations framework convention on climate change. URL https://unfccc.int/sites/default/files/english_paris_agreement.pdf.
- Sebastian Petrick, Katrin Rehdanz, and Richard Tol. The Impact of Temperature Changes on Residential Energy Consumption. *Kiel Institute for the World Economy, Kiel Working Papers*, December 2010.
- Drobinski Philippe, Jordi Badosa, Bilger Isabelle, Crifo Benjamin, Brigaud Patricia, Esnos Antoine, Giraudet Louis-Gaëtan, Gosselin Marion, Guerineau Mathias, Guillemoles Jean-François, Habets Florence, Lévy Jean-Pierre, Mayer Julie, Quelin Bertrand, Raymond Florian, Suchet Daniel, Tao Qiqi, Tantet Alexis, and Viguié Vincent. Changement climatique et transition énergétique en région Île-de-france. Technical report, Groupe régional d'expertise sur le changement climatique et la transition écologique en Ile-de-France (GREC francilien), 11 2022. URL <https://grec-idf.eu/changement-climatique-et-transition-energetique-en-region-ile-de-france/>.
- S. T. A. Pickett, M. L. Cadenasso, E. J. Rosi-Marshall, K. T. Belt, P. M. Groffman, J. M. Grove, E. G. Irwin, S. S. Kaushal, S. L. LaDeau, C. H. Nilon, C. M. Swan, and P. S. Warren. Dynamic heterogeneity: a framework to promote ecological integration and hypothesis generation in urban systems. *Urban Ecosyst*, 20(1):1–14, February 2017. ISSN 1573-1642. doi: 10.1007/s11252-016-0574-9. URL <https://doi.org/10.1007/s11252-016-0574-9>.
- Karoliina Pilli-Sihvola, Piia Remes, Markku Ollikainen, and Heikki Tuomenvirta. Climate change and electricity consumption—witnessing increasing or decreasing use and costs? *Energy Policy*, 38:2409–2419, 05 2010. doi: 10.1016/j.enpol.2009.12.033.
- Stephanie Pincetl. Cities in the age of the anthropocene: Climate change agents and the potential for mitigation. *Anthropocene*, 20:74–82, 2017. ISSN 2213-3054. doi: 10.1016/j.ancene.2017.08.001. URL <https://www.sciencedirect.com/science/article/pii/S2213305417300413>.
- PVGIS. Pvgis photovoltaic geographical information system. https://joint-research-centre.ec.europa.eu/photovoltaic-geographical-information-system-pvgis_en, 2022. [Accessed 12-03-2024].
- Teresa Randazzo, Enrica De Cian, and Malcolm N. Mistry. Air conditioning and electricity expenditure: The role of climate in temperate countries. *Economic Modelling*, 90:273–287, August 2020. ISSN 0264-9993. doi: 10.1016/j.econmod.2020.05.001. URL <https://www.sciencedirect.com/science/article/pii/S0264999319308168>.
- Mohan Rawat and R. N. Singh. A study on the comparative review of cool roof thermal performance in various regions. *Energy and Built Environment*, 3(3):327–347, 2022. ISSN 2666-1233. doi: 10.1016/j.enbenv.2021.03.001. URL <https://www.sciencedirect.com/science/article/pii/S2666123321000209>.
- Florian Raymond, Albin Ullmann, Pierre Camberlin, Philippe Drobinski, and Carmela Chateau Smith. Extreme dry spell detection and climatology over the Mediterranean Basin during the wet season. *Geophysical Research Letters*, 43(13):7196–7204, 2016. ISSN 1944-8007. doi: 10.1002/2016GL069758. URL <https://onlinelibrary.wiley.com/doi/abs/10.1002/2016GL069758>. _eprint: <https://onlinelibrary.wiley.com/doi/pdf/10.1002/2016GL069758>.

- Florian Raymond, Albin Ullmann, Pierre Camberlin, Boutheina Oueslati, and Philippe Drobinski. Atmospheric conditions and weather regimes associated with extreme winter dry spells over the Mediterranean basin. *Clim Dyn*, 50(11):4437–4453, June 2018. ISSN 1432-0894. doi: 10.1007/s00382-017-3884-6. URL <https://doi.org/10.1007/s00382-017-3884-6>.
- Maxime Raynaud. Evaluation ex-post de l'efficacité de solutions de rénovation énergétique en résidentiel. 2014.
- A. Ribes, J. Boé, S. Qasmi, B. Dubuisson, H. Douville, and L. Terray. An updated assessment of past and future warming over France based on a regional observational constraint. *Earth System Dynamics*, 13(4):1397–1415, 2022. doi: 10.5194/esd-13-1397-2022. URL <https://esd.copernicus.org/articles/13/1397/2022/>.
- Mike B. Roberts, Anna Bruce, and Iain MacGill. Impact of shared battery energy storage systems on photovoltaic self-consumption and electricity bills in apartment buildings. *Applied Energy*, 245:78–95, 2019. URL <https://ideas.repec.org//a/eee/appene/v245y2019icp78-95.html>. Publisher: Elsevier.
- Girard Robin and Abdelouadoud Yassine. Estimation de la Performance Énergétique du Parc Résidentiel - Alternatives énergétiques, 2022. URL <https://www.energy-alternatives.eu/2022/03/16/DPE-open-data.html>.
- Johan Rockström, Owen Gaffney, Joeri Rogelj, Malte Meinshausen, Nebojsa Nakicenovic, and Hans Joachim Schellnhuber. A roadmap for rapid decarbonization. *Science*, 355(6331):1269–1271, March 2017. ISSN 1095-9203. doi: 10.1126/science.aah3443. URL <http://dx.doi.org/10.1126/science.aah3443>.
- Jesús Rosales Carreón and Ernst Worrell. Urban energy systems within the transition to sustainable development. A research agenda for urban metabolism. *Resources, Conservation and Recycling*, 132:258–266, May 2018. ISSN 0921-3449. doi: 10.1016/j.resconrec.2017.08.004. URL <https://www.sciencedirect.com/science/article/pii/S0921344917302434>.
- RTE. Futurs énergétiques 2050. principaux résultats. 4. la production d'électricité. Technical report, RTE Réseau de Transport d'Électricité, 2021. https://assets.rte-france.com/prod/public/2021-12/BP2050_rapport-complet_chapitre4_production-electricite.pdf.
- P. M. Ruti, S. Somot, F. Giorgi, C. Dubois, E. Flaounas, A. Obermann, A. Dell'Aquila, G. Pisacane, A. Harzallah, E. Lombardi, B. Ahrens, N. Akhtar, A. Alias, T. Arsouze, R. Aznar, S. Bastin, J. Bartholy, K. Béranger, J. Beuvier, S. Bouffies-Cloch e, J. Brauch, W. Cabos, S. Calmanti, J.-C. Calvet, A. Carillo, D. Conte, E. Coppola, V. Djurdjevic, P. Drobinski, A. Elizalde-Arellano, M. Gaertner, P. Gal an, C. Gallardo, S. Gualdi, M. Goncalves, O. Jorba, G. Jord a, B. L'Heveder, C. Lebeaupin-Brossier, L. Li, G. Liguori, P. Lionello, D. Maci as, P. Nabat, B.  onol, B. Raikovic, K. Ramage, F. Sevault, G. Sannino, M. V. Struglia, A. Sanna, C. Torma, and V. Vervatis. Med-CORDEX Initiative for Mediterranean Climate Studies. *Bulletin of the American Meteorological Society*, 97(7):1187–1208, July 2016. ISSN 0003-0007, 1520-0477. doi: 10.1175/BAMS-D-14-00176.1. URL <https://journals.ametsoc.org/view/journals/bams/97/7/bams-d-14-00176.1.xml>. Publisher: American Meteorological Society Section: Bulletin of the American Meteorological Society.
- J. R ais anen, U. Hansson, A. Ullerstig, R. D oscher, L. P. Graham, C. Jones, H. E. M. Meier, P. Samuelsson, and U. Will en. European climate in the late twenty-first century: regional simulations with two driving global models and two forcing scenarios. *Climate Dynamics*, 22(1):13–31, January 2004. ISSN 0930-7575, 1432-0894. doi: 10.1007/s00382-003-0365-x. URL <http://link.springer.com/10.1007/s00382-003-0365-x>.
- Perry Sadorsky. The effect of urbanization and industrialization on energy use in emerging economies: Implications for sustainable development. *The American Journal of Economics and Sociology*, 73(2):392–409, April 2014. ISSN 1536-7150. doi: 10.1111/ajes.12072. URL <http://dx.doi.org/10.1111/ajes.12072>.
- David J. Sailor and J. Ricardo Mu noz. Sensitivity of electricity and natural gas consumption to climate in the U.S.A.—Methodology and results for eight states. *Energy*, 22(10):987–998, October 1997. ISSN 0360-5442. doi: 10.1016/S0360-5442(97)00034-0. URL <https://www.sciencedirect.com/science/article/pii/S0360544297000340>.
- J. A. Santos, J. Corte-Real, U. Ulbrich, and J. Palutikof. European winter precipitation extremes and large-scale circulation: a coupled model and its scenarios. *Theor. Appl. Climatol.*, 87(1):85–102, January 2007. ISSN 1434-4483. doi: 10.1007/s00704-005-0224-2. URL <https://doi.org/10.1007/s00704-005-0224-2>.

- Simone Scapin, Francesco Apadula, Michele Brunetti, and Maurizio Maugeri. High-resolution temperature fields to evaluate the response of Italian electricity demand to meteorological variables: an example of climate service for the energy sector. *Theor Appl Climatol*, 125(3):729–742, August 2016. ISSN 1434-4483. doi: 10.1007/s00704-015-1536-5. URL <https://doi.org/10.1007/s00704-015-1536-5>.
- Sally Semple and David Jenkins. Variation of energy performance certificate assessments in the European Union. *Energy Policy*, 137:111127, February 2020. ISSN 0301-4215. doi: 10.1016/j.enpol.2019.111127. URL <https://www.sciencedirect.com/science/article/pii/S0301421519307141>.
- Susana Silva, Isabel Soares, and Carlos Pinho. Climate change impacts on electricity demand: The case of a Southern European country. *Utilities Policy*, 67:101115, December 2020. ISSN 0957-1787. doi: 10.1016/j.jup.2020.101115. URL <https://www.sciencedirect.com/science/article/pii/S0957178720301090>.
- Pawan Singh and Rakesh Verma. Zero-energy buildings-a review. *SAMRIDDHI: A Journal of Physical Sciences, Engineering and Technology*, 5(02):143–150, December 2014. ISSN 2229-7111. doi: 10.18090/samriddhi.v5i2.1532. URL <http://dx.doi.org/10.18090/samriddhi.v5i2.1532>.
- Jonathan Spinoni, Jürgen V. Vogt, Paulo Barbosa, Alessandro Dosio, Niall McCormick, Andrea Bigano, and Hans-Martin Füßel. Changes of heating and cooling degree-days in Europe from 1981 to 2100. *International Journal of Climatology*, 38(S1):e191–e208, 2018. ISSN 1097-0088. doi: 10.1002/joc.5362. URL <https://onlinelibrary.wiley.com/doi/abs/10.1002/joc.5362>. _eprint: <https://onlinelibrary.wiley.com/doi/pdf/10.1002/joc.5362>.
- Marc Stefanon, Fabio D’Andrea, and Philippe Drobinski. Heatwave classification over Europe and the Mediterranean region. *Environ. Res. Lett.*, 7(1):014023, February 2012. ISSN 1748-9326. doi: 10.1088/1748-9326/7/1/014023. URL <https://dx.doi.org/10.1088/1748-9326/7/1/014023>. Publisher: IOP Publishing.
- Marc Stéfanon, Philippe Drobinski, Fabio D’Andrea, Cindy Lebeau-pin-Brossier, and Sophie Bastin. Soil moisture-temperature feedbacks at meso-scale during summer heat waves over Western Europe. *Clim Dyn*, 42(5):1309–1324, March 2014. ISSN 1432-0894. doi: 10.1007/s00382-013-1794-9. URL <https://doi.org/10.1007/s00382-013-1794-9>.
- Minna Sunikka-Blank and Ray Galvin. Introducing the prebound effect: the gap between performance and actual energy consumption. *Building Research & Information*, 40(3):260–273, June 2012. ISSN 1466-4321. doi: 10.1080/09613218.2012.690952. URL <http://dx.doi.org/10.1080/09613218.2012.690952>.
- Alexis Tantet, Marc Stéfanon, Philippe Drobinski, Jordi Badosa, Silvia Concettini, Anna Cretì, Claudia D’Ambrosio, Dimitri Thomopoulos, and Peter Tankov. e4clim 1.0: The Energy for a Climate Integrated Model: Description and Application to Italy. *Energies*, 12(22):4299, November 2019. ISSN 1996-1073. doi: 10.3390/en12224299. URL <https://www.mdpi.com/1996-1073/12/22/4299>.
- Qiqi Tao, Marie Naveau, Alexis Tantet, Jordi Badosa, and Philippe Drobinski. Sub-regional variability of residential electricity consumption under climate change and air-conditioning scenarios in France. *Climate Services*, 33:100426, 2024a. ISSN 2405-8807. doi: 10.1016/j.cliser.2023.100426. URL <https://www.sciencedirect.com/science/article/pii/S2405880723000882>.
- Qiqi Tao, Alexis Tantet, Jordi Badosa, Sylvain Cros, and Philippe Drobinski. Multiple-scale distributed pv potential penetration in densely populated city: A case study of Grand Paris Metropolis. 2024b.
- R.H Taylor, S.D Probert, and P.D Carmo. French energy policy. *Applied Energy*, 59(1):39–61, January 1998. ISSN 0306-2619. doi: 10.1016/S0306-2619(97)00055-X. URL [http://dx.doi.org/10.1016/S0306-2619\(97\)00055-X](http://dx.doi.org/10.1016/S0306-2619(97)00055-X).
- The European Commission. Proposal for a directive of the European Parliament and of the Council on the promotion of the use of energy from renewable sources (recast). Technical report, Nov. 2016. URL <https://www.regeringen.se/contentassets/02db3703d7404d37872c36adc9076450/kommissionens-forslag-till-nya-co2-krav-for-latta-fordon.pdf>.
- Alba Torres-Rivas, Mariana Palumbo, Laureano Jiménez, and Dieter Boer. Self-consumption possibilities by rooftop PV and building retrofit requirements for a regional building stock: The case of Catalonia. *Solar Energy*, 238:150–161, May 2022. ISSN 0038-092X. doi: 10.1016/j.solener.2022.04.036. URL <https://www.sciencedirect.com/science/article/pii/S0038092X22002845>.

- Pradeebane Vaithinada Ayar, Mathieu Vrac, Sophie Bastin, Julie Carreau, Michel Déqué, and Clemente Gallardo. Intercomparison of statistical and dynamical downscaling models under the EURO- and MED-CORDEX initiative framework: present climate evaluations. *Clim Dyn*, 46(3):1301–1329, February 2016. ISSN 1432-0894. doi: 10.1007/s00382-015-2647-5. URL <https://doi.org/10.1007/s00382-015-2647-5>.
- Jeroen van der Heijden. Experimental governance for low-carbon buildings and cities: Value and limits of local action networks. *Cities*, 53:1–7, 2016. ISSN 0264-2751. doi: 10.1016/j.cities.2015.12.008. URL <https://www.sciencedirect.com/science/article/pii/S0264275115300317>.
- Bas J. Van Ruijven, Enrica De Cian, and Ian Sue Wing. Amplification of future energy demand growth due to climate change. *Nat Commun*, 10(1):2762, June 2019. ISSN 2041-1723. doi: 10.1038/s41467-019-10399-3. URL <https://www.nature.com/articles/s41467-019-10399-3>. Number: 1 Publisher: Nature Publishing Group.
- Anne-Lorène Vernay, Carine Sebi, and Fabrice Arroyo. Energy community business models and their impact on the energy transition: Lessons learnt from France. *Energy Policy*, 175:113473, April 2023. ISSN 0301-4215. doi: 10.1016/j.enpol.2023.113473. URL <https://www.sciencedirect.com/science/article/pii/S0301421523000587>.
- Vincent Vignié, Aude Lemonsu, Stéphane Hallegatte, Anne-Lise Beaulant, Colette Marchadier, Valéry Masson, Grégoire Pigeon, and Jean-Luc Salagnac. Early adaptation to heat waves and future reduction of air-conditioning energy use in Paris. *Environ. Res. Lett.*, 15(7):075006, July 2020. ISSN 1748-9326. doi: 10.1088/1748-9326/ab6a24. URL <https://dx.doi.org/10.1088/1748-9326/ab6a24>. Publisher: IOP Publishing.
- Lucas Vivier and Louis-Gaëtan Giraudet. Is france on track for decarbonizing its residential sector? assessing recent policy changes and the way forward. Preprint on HAL hal-04510798, 2024. URL <https://hal.science/hal-04510798>.
- Ilse M. Voskamp, Nora B. Sutton, Sven Stremke, and Huub H. M. Rijnaarts. A systematic review of factors influencing spatiotemporal variability in urban water and energy consumption. *Journal of Cleaner Production*, 256:120310, May 2020. ISSN 0959-6526. doi: 10.1016/j.jclepro.2020.120310. URL <https://www.sciencedirect.com/science/article/pii/S0959652620303577>.
- Adi Vulkan, Itai Kloog, Michael Dorman, and Evyatar Erell. Modeling the potential for PV installation in residential buildings in dense urban areas. *Energy and Buildings*, 169:97–109, 2018. ISSN 0378-7788. doi: 10.1016/j.enbuild.2018.03.052. URL <https://www.sciencedirect.com/science/article/pii/S0378778817339877>.
- Leonie Wenz, Anders Levermann, and Maximilian Auffhammer. North–south polarization of European electricity consumption under future warming. *Proceedings of the National Academy of Sciences*, 114:201704339, August 2017. doi: 10.1073/pnas.1704339114.
- Dominik Wiedenhofer, Manfred Lenzen, and Julia K. Steinberger. Energy requirements of consumption: Urban form, climatic and socio-economic factors, rebounds and their policy implications. *Energy Policy*, 63:696–707, December 2013. ISSN 0301-4215. doi: 10.1016/j.enpol.2013.07.035. URL <https://www.sciencedirect.com/science/article/pii/S0301421513006782>.
- Jonathan A. Wiley, Justin D. Benefield, and Ken H. Johnson. Green design and the market for commercial office space. *The Journal of Real Estate Finance and Economics*, 41(2):228–243, July 2008. ISSN 1573-045X. doi: 10.1007/s11146-008-9142-2. URL <http://dx.doi.org/10.1007/s11146-008-9142-2>.
- Sun Yan and Feng Lifang. Influence of psychological, family and contextual factors on residential energy use behaviour: An empirical study of china. *Energy Procedia*, 5:910–915, 2011. ISSN 1876-6102. doi: 10.1016/j.egypro.2011.03.161. URL <http://dx.doi.org/10.1016/J.EGYPRO.2011.03.161>.
- Madhura Yeligeti, Wenxuan Hu, Yvonne Scholz, Ronald Stegen, and Kai Von KrbeK. Cropland and rooftops: the global undertapped potential for solar photovoltaics. *Environmental Research Letters*, 18(5):054027, 2023. ISSN 1748-9326. doi: 10.1088/1748-9326/accc47. URL <https://iopscience.iop.org/article/10.1088/1748-9326/accc47>.

- Richard York. Demographic trends and energy consumption in european union nations, 1960–2025. *Social Science Research*, 36(3):855–872, September 2007. ISSN 0049-089X. doi: 10.1016/j.ssresearch.2006.06.007. URL <http://dx.doi.org/10.1016/J.SSRESEARCH.2006.06.007>.
- Youngsoo You and Saehoon Kim. Revealing the mechanism of urban morphology affecting residential energy efficiency in Seoul, Korea. *Sustainable Cities and Society*, 43:176–190, November 2018. ISSN 2210-6707. doi: 10.1016/j.scs.2018.08.019. URL <https://www.sciencedirect.com/science/article/pii/S2210670718302853>.
- Jihui Yuan, Craig Farnham, Kazuo Emura, and Siqiang Lu. A method to estimate the potential of rooftop photovoltaic power generation for a region. *Urban Climate*, 17:1–19, September 2016. ISSN 2212-0955. doi: 10.1016/j.uclim.2016.03.001. URL <https://www.sciencedirect.com/science/article/pii/S2212095516300128>.
- Geun Young Yun and Koen Steemers. Behavioural, physical and socio-economic factors in household cooling energy consumption. *Applied Energy*, 88(6):2191–2200, June 2011. ISSN 0306-2619. doi: 10.1016/j.apenergy.2011.01.010. URL <http://dx.doi.org/10.1016/J.APENERGY.2011.01.010>.
- Patrick X. W. Zou, Xiaoxiao Xu, Jay Sanjayan, and Jiayuan Wang. Review of 10 years research on building energy performance gap: Life-cycle and stakeholder perspectives. *Energy and Buildings*, 178:165–181, November 2018. ISSN 0378-7788. doi: 10.1016/j.enbuild.2018.08.040. URL <https://www.sciencedirect.com/science/article/pii/S0378778818309460>.
- Sheikh Zuhair, Senta Schmatzberger, Jonathan Volt, Zsolt Toth, Lukas Kranzl, Iná Eugenio Noronha Maia, Jan Verheyen, Guillermo Borragán, Cláudia Sousa Monteiro, Nuno Mateus, Rui Fragoso, and Jerzy Kwiatkowski. Next-generation energy performance certificates: End-user needs and expectations. *Energy Policy*, 161:112723, February 2022. ISSN 0301-4215. doi: 10.1016/j.enpol.2021.112723. URL <https://www.sciencedirect.com/science/article/pii/S0301421521005899>.
- Balázs Égert. *France’s Environmental Policies: Internalising Global and Local Externalities*. OECD Publishing, April 2011. doi: 10.1787/5kgdnp0n9d8v-en. URL <http://dx.doi.org/10.1787/5KGDPN0N9D8V-EN>.

Titre : Décarbonisation de la consommation d'énergie dans le secteur résidentiel en France dans le contexte du changement climatique

Mots clés : Consommation d'énergie résidentielle ; Changement climatique ; Décarbonisation ; Rénovation des bâtiments ; PV en toiture

Résumé : Le secteur résidentiel est important pour la transition énergétique afin de lutter contre le réchauffement climatique. Cette thèse vise à étudier l'évolution de la consommation d'énergie résidentielle dans le contexte des politiques climatiques en France sous l'effet du changement climatique. La première partie de l'étude projette la future consommation d'électricité résidentielle française (REC), en considérant des scénarios de changement climatique et de climatisation (AC) et en quantifiant leur variabilité spatiale. Un modèle linéaire de sensibilité à la température adapté aux données annuelles de consommation d'électricité observées et aux températures historiques est appliqué à l'échelle intrarégionale. Les REC futures sensibles à la température sont calculées en utilisant le modèle pour les projections de température dans le cadre du changement climatique RCP8.5. L'évolution des REC est modulée par l'évolution des besoins de refroidissement et le déploiement de systèmes de climatisation pour répondre à ces besoins. Après les projections futures, la décarbonisation de l'énergie résidentielle est étudiée selon deux axes principaux. Le premier axe vise à étudier les performances des rénovations.

Pour ce faire, le modèle linéaire de sensibilité à la température est modifié pour inclure les variables des âges de construction, de sorte que la consommation sensible à la température par groupes de périodes de construction est estimée pour chaque région administrative. Ces consommations thermosensibles estimées sur la base de la consommation réelle permettent de projeter les économies d'énergie futures grâce à la rénovation des bâtiments. Le deuxième axe consiste à décarboniser le secteur résidentiel en installant des panneaux photovoltaïques (PV) sur les toits. Cependant, en raison de la nature variable de l'énergie photovoltaïque, son intégration ajoute de la complexité à la gestion du réseau, nécessitant un examen minutieux du bilan énergétique. L'impact de l'intégration du photovoltaïque distribué sur les toits de la métropole du Grand Paris sur l'équilibre entre l'offre et la demande d'énergie est étudié à l'aide d'indicateurs de taux d'autoconsommation (SCR) et de taux d'autosuffisance (SSR). Les profils de consommation d'électricité en temps réel et les données de production d'énergie solaire sont utilisés pour explorer différentes échelles de complémentarité des acteurs.

Title : Decarbonizing energy consumption in the residential sector in France in the context of climate change

Keywords : Residential energy consumption ; Climate change ; Building retrofitting ; Rooftop PV

Abstract : The residential sector is important for the energy transition to combat global warming. This thesis aims to study the evolution of residential energy consumption in the context of climate policies in France under climate change. The first part of the study projects future French residential electricity consumption (REC), considering climate change and air-conditioning (AC) scenarios and quantifying their spatial variability. A linear temperature sensitivity model fitted by annual observed electricity consumption data and historical temperature is applied intraregionally. Future temperature-sensitive REC is computed using the model to temperature projections under the climate change pathway RCP8.5. The evolution of REC is modulated by the evolution of cooling needs and the deployment of AC systems to meet those needs. After future projections, the decarbonization of residential energy is studied via two principal axes. The first aims to study retrofitting performance. For this purpose, the linear temperature

sensitivity model is modified to include the variables of the construction ages so that the temperature-sensitive consumption by groups of construction periods is estimated for each administrative region. These temperature-sensitive consumptions estimated based on actual consumption allow the projection of future energy savings thanks to the building retrofitting. The second axis is to decarbonize the residential sector by installing photovoltaic (PV) panels on rooftops. However, due to the variable nature of PV, its integration adds complexity to grid management, requiring careful consideration of the energy balance. The impact of integrating distributed rooftop PV in the Grand Paris metropolis onto the balance between energy supply and demand is studied with indicators of self-consumption rate (SCR) and self-sufficiency rate (SSR). Real-time electricity consumption profiles and solar power generation data are used to explore different scales of complementarity of actors.